Faculty of Engineering and Science

A Comparative Study on the Seawater Quality of the Coral Environment between Miri (Sarawak) and Sipadan (Sabah)

Sun Veer Moollye

This thesis report is presented for the Degree of
Master of Philosophy in Chemical Engineering
of
Curtin University

June 2017

To the best of my knowledge and belief this thesis contains no material previously published by any other person except where due acknowledgment has been made. This thesis contains no material which has been accepted for the award of any other degree or diploma in any university.

Signature: 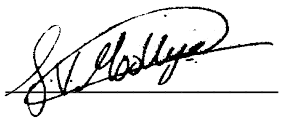 Date: 18/09/2017

To my parents…

Abstract

The coral reefs in the Southeast Asia region suffer from a number of impacts including turbidity, excess nutrients, and physical damage from sedimentation, dynamite fishing and human involvement. Borneo has one of the most internationally renowned and iconic dive sites in the world particularly, at Sipadan in Malaysia. On the other hand, Miri located in the state of Sarawak, North West of Borneo, Malaysia has shown signs of stress in its coral environment due to coastal development, logging, river runoff and fishing. Sarawak has many newly discovered reefs that collectively have been turned into a marine reserve in order to monitor and prevent from excessive harm to the water quality and corals at these sites. This study creates a baseline seawater quality data to understand the chemical nature of the seawater and its impact on the coral environment of Miri and compare to Sipadan Island reef system. The seawater samples were collected at three different sites (Eve's Garden (EG), Anemone Garden (AG) and North Siwa (NS)) of the Miri-Sibuti Coral Reef National Park (MSCRNP) at various depths for three seasons (beginning and end of southwest monsoon (SWM), and the transition to northeast monsoon (NEM)), and studied the spatial and temporal variations of water quality in the coral reefs. Collected samples were analysed for various physico-chemical parameters following standard procedures. At the beginning of SWM, a depth-wise increase in TDS was associated with the pH fluctuations, whereas at the end of SWM and transition to NEM, a combination of both EC and TDS were responsible for the variation of pH at MSCRNP. Ammonia-nitrogen concentration was highest during the start of SWM at the middle depth and a depth-wise decrease in phosphate was attributed to decreasing turbidity. The major ions, calcium and magnesium were inversely proportional from start of SWM to NEM transition as well as surface to seabed as increasing magnesium concentration was accompanied by a decrease in calcium. Sodium and chloride concentrations followed the pH values of the seawater from surface to seabed during the start of SWM, however, the trend was opposite during NEM transition. The concentration of Cd, Co Cu, Ni, Pb were higher during NEM transition period and that of Fe, Mn and Zn were lower, and their depth-wise concentration also varied at each site. However, it was observed that increasing turbidity was responsible for the variation of the trace metals from beginning of SWM to NEM transition. At MSCRNP, statistical analysis indicated strong anthropogenic activities derived from river runoff and coastal development during the end of SWM period and NEM transition. At Sipadan, the concentration of

ammonia-nitrogen and phosphate were generally higher, which were caused mostly by tourism. However, the other nutrients and major ions were part of the normal seawater chemistry. The higher concentration of Ni was attributed to fishing and recreational boats. Statistical analysis indicated that boat traffic around the island was mostly responsible for the variation in some parameters in the seawater quality at Sipadan. Photo-documentation showed signs of stress at all three sites of Miri, where the most affected area was EG. Strong presence of algae and coral bleaching was observed at EG, and AG was also showing similar stress signs. NS was better preserved but when comparing with Sipadan, the corals at MSCRNP were at higher risk of getting damaged.

Table of Contents

List of Figures

List of Tables

ACKNOWLEDGMENT

Many people were instrumental in the completion of this study. I would like to first thank Dr Lisa Marie King for developing the idea of the study. I would also like to acknowledge my thesis committee Dr Prasanna Mohan Viswanath for sculpting the backbone of the project and always encouraging me in my work, Dr Nagarajan Ramasamy for all his expertise and advices on how to detect and observe changes when going in-situ and Dr Chua Han Bing for guiding the project in the direction it needed.

Professor Marcus Lee deserves a special vote of thanks of his detailed reviews and corrections of my work.

My sincerest gratitude to Sarawak Forestry for issuing the permit (NCCD.907.4 (Jld.12)-150) which allowed me to collect samples at the Miri-Sibuti Coral Reef National Park.

Special thanks to the Sabah Police Department for completing the security clearance within less than half a day to obtain a research permit from Sabah Parks. Hence, my appreciations to Sabah Parks for supplying the permit (MKN.19[R].700-6/2/1 Jld.10[]) within the limited timeframe for the collection of samples at Sipadan Island Park.

My sincere appreciations to Jabatan Meteorologi Malaysia, Miri Airport Station for providing the rainfall and wind data required for the project.

My gratitude to Dr Eswaramoorthi Sellappa Gounder for his valuable input and support during my lab work.

My high regards to Dr Vijit Hamza for his immense help in creating and compiling the much required spatial maps through the GIS software.

I would like to thank the laboratory staff, Mrs Marilyn Andrew Anyi, Mrs Rassti Binti Serati, Miss Yuanna Anak Jubin and Miss Angeline Anak Jom for their continuous assistance in the laboratory before and during analyses. A great thanks to my friend and field trip assistant Stephan Ongetta for rarely getting seasick during data entry. I would also like to thank Claire Nixon, Aniqfizwa bin Akmalnizwa, DaisyJae Beresford-Slinn and all the staff at the Co.Co. Dive Shop for all their help and support during sampling periods at which would not have been the same without them.

My sincerest appreciations to the staff, especially Jamilah, at Uncle Chang's Resort in Sempurna, Sabah for sponsoring my stay on Mabul Island, as well as Sabah Parks Ranger, Mr Freddy Joliver, for bringing me to the sites for sampling at Sipadan Island Park.

My biggest thanks to my friends in HDR Room 8, Hong Hui, Sim, Rakesh, Nava, Ismail and Emmanuel with whom I shared the office and great conversations. Thanks to my friends Anand, Prabakaran, and Nadeen for helping whenever I needed assistance with a particular part of my study.

My sincere appreciations to the editors Vinodh Menon and Hanani Shukri for their valuable feedbacks.

Last but not least, my forever gratitude to my parents who have supported me, believed in me and their undying faith in my aptitude.

NOMENCLATURE

Symbol	Meaning
°C	Degrees Celsius
AG	Anemone Garden
BDL	Below Detection Limit
BP	Barracuda Point
DO	Dissolved Oxygen
Dir	Direction
E	East
EC	Electrical Conductivity
EG	Eve's Garden
ENE	East Northeast
ESE	East Southeast
Km	Kilometre
m	Meter
m/s	Meter per Second
mg/L	Milligram per Litre
mS/cm	Milli-Siemens per Litre
MSCRNP	Miri-Sibuti Coral Reef National Park
mV	Millivolts
N	North
NE	Northeast
NEM	Northeast Monsoon
NNE	North Northeast
NNW	North Northwest
NS	North Siwa
NTU	Nephelometric Turbidity Units
NW	Northwest
ORP	Oxidation Reduction Potential

pH	Power of Hydrogen
ppt	Parts per tonne
S	South
SE	Southeast
Spd	Speed
SIP	Sipadan Island Park
SP	South Point
SSE	South Southeast
SSW	South Southwest
SW	Southwest
SWM	Southwest Monsoon
TDS	Total Dissolved Solids
W	West
WNW	West Nortwest
WSW	West Southwest

CHAPTER 1 – INTRODUCTION

1.1 Background

The ocean's delicate ecosystem is resplendent with the most diverse forms of lives. Coral reefs are living networks that sustain most of those lifeforms which consist of one third of the marine fish in the world including the fish consumed by humans. The presence of coral reefs around the coastline of countries not only prevents sand erosion but also provides recreational activities such as snorkelling and diving (Lough and van Oppen, 2009; Lemke and Olech, 2011). The protection of coral reefs is paramount since it contributes to the livelihood of millions of people living by the sea. An assessment by Costanza et al. (2014) estimated the global value of coral reefs at 9.9 trillion USD constituting of tourism and recreational activities, coastal protection, fisheries and biodiversity. However, with mass coral bleaching on the rise, the global cost of severe bleaching scenarios has been calculated at 84 billion USD (C. International, 2008; Lough and van Oppen, 2009).

That bionetwork of marine life has been experiencing an exponential amount of extinctions in the last 50 years. This loss of species is a result of exploitation of the marine fauna which in turn kills the corals and forces the surviving species to migrate somewhere else (Dulvy, 2005). The loss of habitat and migration of species creates other problems where the migrating ones become invasive and start taking over the other surroundings in order to survive (Griffis and Howard, 2013). There are other causes, for example, global warming, pollution and diseases, that are equally responsible for marine defaunation (Briggs, 2011).

To avoid marine defaunation and extinctions of certain fish populations and species, Marine Protected Areas (MPAs) have been introduced around the world to help, monitor and protect the marine ecosystem. According to the National Oceanic and Atmospheric Association (NOAA), the characteristics of MPAs have to focus on conservation which includes level of protection, permanence of protection, constancy of protection and ecological scale of protection (National Oceanic and Atmospheric Administration, 2014). The number of these MPAs has been on the rise in developing countries. However, management have also been a problem. A number of those MPAs, mostly in the Indo-Pacific area, are where the corals and marine diversity are the highest (Dygico et al., 2013; Masud and Kari, 2015). A lot of those can be related to

lack of fund and enforcement. One of the main reasons why, non-profit and non-governmental organisations are being asked to help, is to provide funding in an attempt to enforce the protection of these marine ecosystems (Fabinyi, 2008; Teh et al., 2008).

1.1.1 Effect of Human Activities on Marine Life

There are many factors that tend to influence marine life: global warming, over-fishing, terrestrial runoff, boat and recreational activities to name a few. Global warming has been the biggest threat to marine life combined with the other factors (Griffis and Howard, 2013; Howard et al., 2013). Climate change has rapidly increased the temperature and acidity of the ocean which has led to large scale coral bleaching and an overall increase in coral diseases (Hobbs et al., 2013; Readman et al., 2013; Hoey, 2016). Corals, especially some parts of the Great Barrier Reef in Australia, have been deemed unrecoverable due to the thermal stress the corals have constantly been facing (Oliver et al., 2009; A. Thompson et al., 2014). Over-fishing, destructive fishing and trawling have contributed in coral reef destruction. These methods have shown to reduce the fish count dramatically, creating ecological imbalances by destroying habitats. Despite the ban of these practices by authorities, poor enforcement of the law means that these methods are still being used (Jakobsen et al., 2007; UNEP, 2007; Teh et al., 2008; Praveena et al., 2012). Terrestrial runoff has also caused much damage to marine life and have been linked to coastal development, increasing use of fertilisers and land clearing (Fabricius, 2005; UNEP, 2007; Jones et al., 2015). These practices have resulted in high turbidity levels carrying an excess of nutrients, most commonly known as eutrophication, which has eventually led to coral bleaching and the spread of coral diseases. The increasing ocean temperature coupled with eutrophication has caused an increase in algal growth at the reefs which then tends to smother the corals, eventually suffocating them (Fabricius, 2005; Burgin and Hardiman, 2015).

MPAs were introduced to restrict recreational activities for conservation purposes and have since become great attractions for divers. Statistically speaking, as for 2012, the estimated number of divers globally have been between 14.5 million to 15.5 million and rising yearly (Sykes, 2012). The Great Barrier Reef, for example, have been visited by around 150,000 divers per year as from 1980 to 450,000 up to 1987. By 2012 that number increased four times over to two million people yearly (Cairns, 2012; Tiedgen,

2012). Seeing the evolution of the diving industry, business-wise, the activity has proven to be a very lucrative business that asserts a good economic stand point since this activity is highly practiced as well as promoted by the media and other social means (Dimmock and Musa, 2015).

Divers travel to various dive destinations not only to look at corals, but also to see the diverse life forms indigenous to those sites. The divers vary in age, gender, income and experience which directly impact their behaviour (Lemke and Olech, 2011). It is the duty of tour operators to see the type of divers being brought and, a concise yet precise pre-dive briefing should be conducted, prior to a dive, about the importance of responsible diving, which comprises mainly of not touching anything under water. Pre-dive briefings have shown a decrease on the impact recreational divers have on corals and raising this awareness has made divers more cautious hence making them improve their skills (Mograbi and Rogerson, 2007; Chung et al., 2013; Krieger and Chadwick, 2013). One of the conservation structures put in place to avoid accidental harm have been to separate dive sites as harm-prone, fragile sites and pro-tourist sites (Uyarra et al., 2009). This manoeuvre has enabled scientists to do further research on the seawater; test the seawater at those sites and do a comparative study between the highly visited tourist site and the restricted area. This study has also enabled scientists to determine the cause of the rapid degradation of the corals at those different dive sites; being mainly, over-visitation, increase in ammonia-nitrogen concentration, and fuel leaks from the boats (Readman et al., 2013; Schintu et al., 2014). Monitoring those dive sites is crucial in order to allow preservation of species along with their proliferation (Kitchen-Wheeler et al., 2012; Hearn et al., 2014). A pilot survey between recreational and professional divers showed that the latter are less prone to touch the corals and/or collect dead corals as compared to the recreational divers. Professional divers are more likely to recognise and condemn improper behaviour of recreational divers. This protective behaviour towards the marine fauna helps to preserve reefs as well as promoting responsible diving (Salim et al., 2013).

Malaysia has seen the rise of dive tourism internationally since the famous Jacques Cousteau discovered Sipadan Island, Sabah in 1988 (Musa, 2002). Waheed and Hoeksema (2013) speak about the richness and diversity of the coral reef around the Semporna peninsula of Malaysia. Various sites were chosen and studies were carried out to document the various types of coral species present around the peninsula.

However, the rise of the tourism industry along with coastal developments and over-visitation of the dive sites, have had a negative impact on the marine fauna of Sipadan. As described by Teh et al. (2008), the lack of funds and personnel from the Malaysian Government resulted in a certain neglect of the reef leading to illegal fishing through the use of dynamite and cyanide. Miller et al. (2015) further reported a certain shortcoming of research on coral bleaching and diseases in the marine parks of Sabah, Borneo. In Miri, Sarawak, limited studies have been done about the corals and the seawater quality at the Miri-Sibuti Coral Reef National Park. The reports by Elcee-Instrumentation (2002) and UNEP (2007) both mention Miri to have the highest amount of sedimentation from the Miri and Baram rivers that have negative impacts on coral health. The problems outlined by both reports were coastal development, industrial discharge and over fishing from lack of enforcement from local authorities. This has shown a degradation in the coral health and an increase in algal growth at the marine park. The importance of the present study aims to create a baseline and establish a seawater quality monitoring system as well as continuing photo-documentation of the coral reefs in Miri marine park focusing on three highly visited sites namely, Anemone Garden, Eve's Garden and North Siwa Reef. The data will then be compared to the seawater quality of Sipadan Island Park to better understand the coral environment. This study will also raise awareness of the importance of seawater quality for the well-being of the coral reefs and the marine fauna.

1.2 Study Sites

Malaysia, located between 2º and 7º north of the equator, is roughly around 330,000km^2 with a population size close to 28 million. Two states, Sabah and Sarawak are located on the island of Borneo (Figure 1.2.1), which is east to the peninsula, in the South China Sea. These two states share borders with Brunei and Indonesia. Malaysia's primary forms of revenue are petroleum, palm oil, natural rubber and timber and very closely followed by tourism. The state of Sarawak is mostly known for its forests and caves whereas Sabah is famous for its diving sites like the world famous Sipadan dive site and Layang Layang (W. Malaysia, 2015). Bringing the lime light to this country, the iconic dive destination, Sipadan has implemented the 120 divers per day limit in order to protect the marine wildlife from the increasing interest of people. Sipadan is known worldwide as a "must dive" location because of its lavish

variety of fish and corals along with a high concentration of sea turtles around a dive site.

The focused area of the study in Miri, Sarawak, Malaysia is the Miri-Sibuti Coral Reef National Park (MSCRNP) (Figure 1.2.2) located in the Island of Borneo at latitude 4.383219º and longitude 113.969776º. Three dive sites, North Siwa, Anemone Garden and Eve's Garden, which are 20.96km, 19.36km and 9.45km respectively from the point of embarkation at the marina, located near Tanjung Lobang area (Figure 1.2.2), were chosen to collect the seawater samples. Miri, however, being an oil town, also has a number of oil rigs in the sea and that also have effect on the biodiversity of the marine ecosystem. Two rivers namely; Miri River and Baram River, located at 10.70km and 28.0km respectively from Eve's Garden and also have a certain impact on the reefs such as a large concentration of sedimentation from the Baram River as well as the presence of a port at the mouth of the river. Moreover, Miri River is considered as one of the most polluted rivers in Sarawak due to pollutants from timber processing industries as well as industrial discharge from the presence of harbours at the river mouth (Billah et al., 2016). Miri dive sites contain around 100 different species of corals at a depth of around 30 meters; the coral reefs are one the most well-preserved ecosystem. Most of the coral reefs in the Marine Reserve were only discovered around 5 years ago, and to try and keep the place as pollution free as possible, the Miri City Council has limited the daily number of divers to only 16 per day (Raphael, 2013; Rose, 2013; Malaysiaasia, 2014).

Sipadan Island Park in Sabah, Malaysia (Figure 1.2.3) also in Borneo Island is found at latitude 4.114937º and longitude 118.628584º, off the coast of Semporna, was chosen for the number of research done at the site (Abdullah et al., 1997; Musa, 2002; Abdullah et al., 2006; Jakobsen et al., 2007; Mokhtar et al., 2012; Praveena et al., 2012; Waheed and Hoeksema, 2013; J. Miller et al., 2015). The Island with a surface area of 0.135km^2, is located 40km south of the city Semporna in Sabah and is home to one of the top 10 dive sites in the world. The island is located in the western Pacific Ocean's Coral Triangle which is made up of the seas of Indonesia, Malaysia and the Philippines (World-Wildlife-Federation, 2015). That area of seawater is the epicentre of marine biodiversity and rising at 600 metres from the seabed, Sipadan boasts over a staggering 3000 species of fish. The hundreds of coral species that rest around the island accommodate 12 dive sites (Sabah, 2007; Teh et al., 2008; Vacation, 2015). The two

spots chosen for sampling were the northern-most site, named Barracuda Point situated at a latitude of 4.07151º, longitude 118.37355º, and the southern-most point aptly known as South Point at a latitude of 4.06151º and longitude of 118.37475º.

Some of the similarities between Miri-Sibuti Coral Reef National Park and Sipadan Island Park (Figures 1.2.2 and 1.2.3) are that both are located roughly on the same latitude, off the coast of Borneo Island. They are both MPAs, therefore the only common activities are diving and snorkelling. Some of the differences between both study areas are that Sipadan has been an iconic dive destination since the 1980s, whereas Miri discovered their corals only recently. Sipadan is also located much further from the coast of Semporna, Sabah than the corals in Miri.

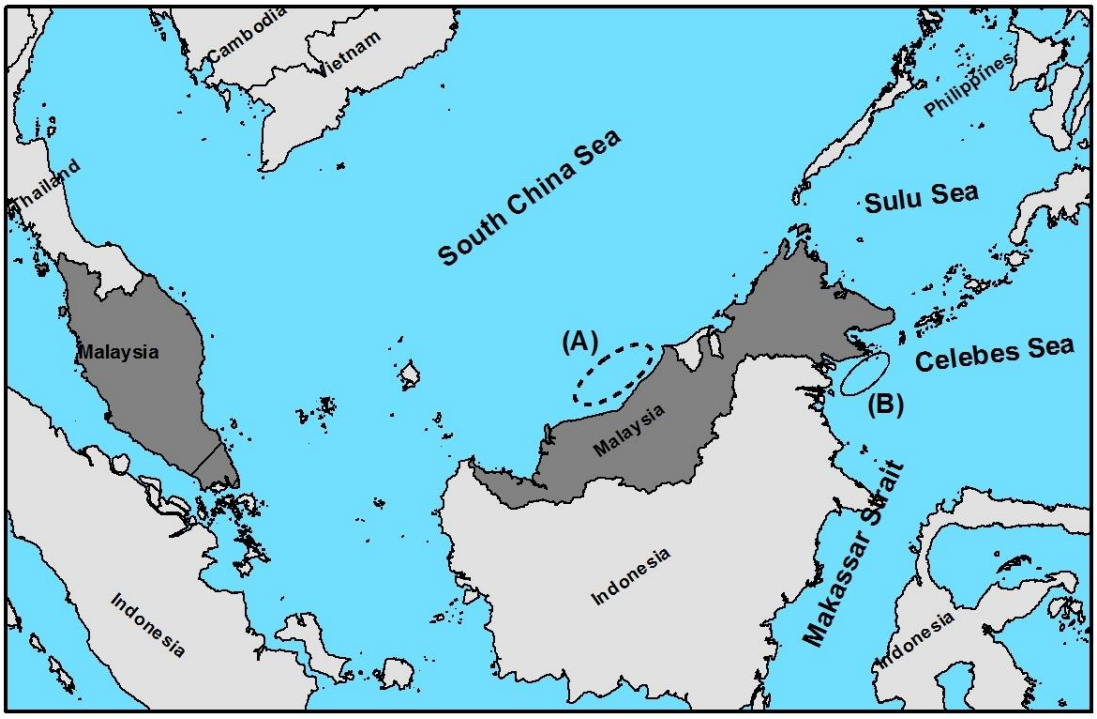

Figure 1.2.1 – (A): Miri-Sibuti Coral Reef National Park (lat:4.38321; long: 113.969776)
(B): Sipadan Island Park (lat:4.114937; long: 118.628584)

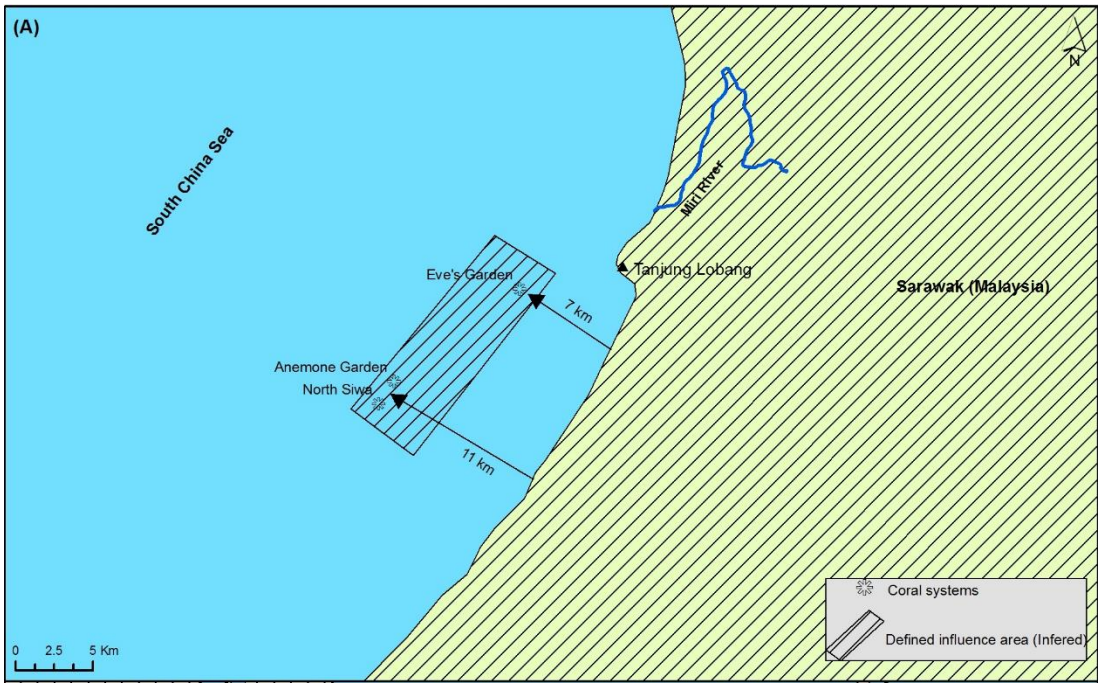

Figure 1.2.2 – Miri Study Sites

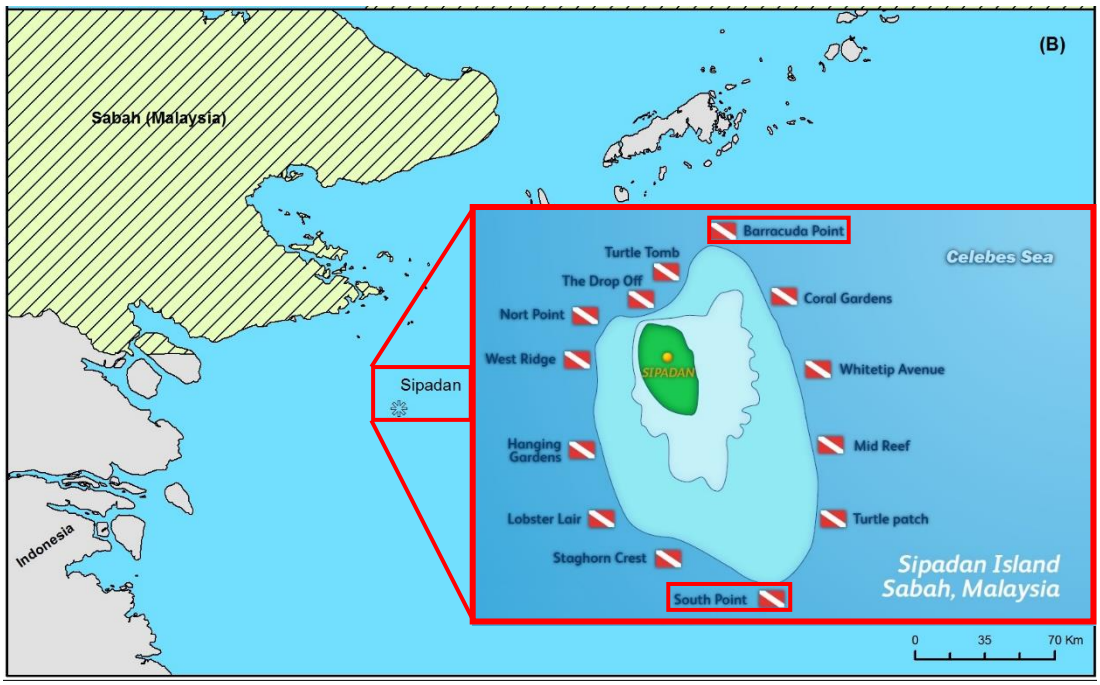

Figure 1.2.3 – Sipadan Island Study Sites
(sipadan.com, 2015)

1.3 Research Gap

The ocean has a delicate and fragile ecosystem. With the introduction of the human factor, in terms of tourism, coastal development, dynamite fishing and river runoff, that ecosystem can be disturbed. With an increase in the number of tourists, coastal accommodation is on the rise together with the business that surrounds it, which includes the dive industry. However, this does not work well for the marine fauna close to those coastal developments. Rapid growth of tourism has made businesses focus more on the income than on the preservation of the environment. In international cases, this has resulted in the complete annihilation of certain marine wildlife through waste water not being treated properly (Zakai and Chadwick-Furman, 2002; Atkins et al., 2011; Lamb et al., 2014).

In Miri, Sarawak, a sizeable amount of pollutants comes from the rivers which are then discharged in the ocean (Elcee-Instrumentation, 2002; UNEP, 2007; R. C. Malaysia, 2015a). Sarawak is also known for its heavy logging business. Soil erosion is known to be one of the most detrimental effects of deforestation. During the northeast monsoon season, a large amount of soil and solid waste from the villages nearby the Miri River gets washed and is found in the sea. Similarly, the Miri Port Authority is located near the mouth of Baram River and an aerial view of the mouth of the river shows the colour of the water being discharged in the ocean close to the marine reserve. This might cause a decline in the seawater quality and depending on the concentration of nutrients, major ions or dissolved trace metals from the rivers into the sea, the chances of coral bleaching is inflated. A lack of commitment and study are also present since the last study done was in 2002. However Elcee-Instrumentation (2002) was not equipped to practice any seawater quality analysis. In this scenario, a baseline of the seawater quality will be created. This proposed study will focus on the spatial and temporal variation of seawater quality and photo-documentation of the corals at the sites to determine their health.

Dive sites in Sipadan situated in the state of Sabah, have a much better monitoring system than Miri. In 2004, the Malaysian Government ordered all structures to be removed from the island and declared it a protected marine reserve in 2005. However, the number of divers allowed per day increased from 80 in 1998 to 120 at present date (D. International, 1997; Vacation, 2015). The figures do not include the people who go diving, fishing and stay over at the reserve illegally. This lack of control has caused

damage to the reefs and if continued, the effects might become irreversible. The numerous studies done and strategies implemented at Sipadan still makes it one of the best places to compare and contrast the studies that is being done in the Miri Marine Reserve (Abdullah et al., 1997; D. International, 1997; Toh, 1999; Joniston, 2004; Abdullah et al., 2006; Dive-The-World, 2014; J. Miller et al., 2015; sipadan.com, 2015).

1.4 Research Objectives

The aim of this project is to investigate the seawater quality of the Miri-Sibuti Coral Reef National Park and compare with Sipadan Island Park. The various tests, which include both in-situ analysis of seawater and laboratory experiments for nutrients, major ions and trace metals. This study will also be performed to have a better understanding of composition of the seawater in these regions. The objectives of the research have been enumerated below:

1. To analyse the physico-chemical parameters of seawater at Miri near-shore coral environment to determine the spatial and temporal variations of seawater quality and compare them to that of Sipadan.
2. To determine the physical changes in coral reefs over time through photo-documentation.
3. To investigate the varying water quality on the resilience of corals at Miri-Sibuti Coral Reef National Park and Sipadan Island Park.

CHAPTER 2 – LITERATURE REVIEW

2.1 International Overview

Seawater is prone to pollution from both natural and human assistances. There has been numerous seawater quality analysis done around the globe, with several parameters being studied. Most of the parameters were regionally focused, meaning, the investigations carried out were for various aspects specific to the areas chosen. Some examples are: heavy metal pollution such as lead and cadmium that was investigated at the Kepez harbour of Turkey (Yılmaz and Sadikoglu, 2011). The study hypothesised that the main heavy metal pollution source might have been from river runoffs, improper sewage disposal, industrial contamination as well as harbour related activities. In the Okinawa Island of Japan, red soil caused by the presence of iron along with surplus of hydrogen peroxide was the leading cause of seawater pollution (Arakaki et al., 2005). The study showed that the concentration of iron (II) was the main cause of pollution but did not disclose the reason behind the pollution. Krupp and Abuzinada (2008) focused their attention on the impact of oil pollution and sea surface temperatures in the Gulf region. The study explains the stressful effects of elevated temperatures on the species that live in shallow water. Human induced activities such as oil spills are mostly discussed since the study area is populated with oil companies. Mezhoud et al. (2016) did a study on the spatial and temporal variability of seawater in the south-eastern Arabian Gulf. Their research found that salinity and temperature were higher in summer and, pH and DO were higher during winter. A lower pH and a higher temperature were also noted in areas closer to the shore and oil platforms. Salinity was also higher closer to shorelines, which was attributed the presence of desalination plants (Mezhoud et al., 2016). A similar study was done by Tew et al. (2014) in the Nanwan Bay region of Taiwan; after experiencing a rapid degradation of their coral population, the team of researchers established “a continuous, real-time water quality monitoring system for the coral reef ecosystem” (Tew et al., 2014). The study found that the coral bleaching threshold was 29°C and that rapid changing temperatures affected corals and has even decreased the fish population in the past. Similarly, Naumann et al. (2015) began monitoring water quality in the region of Dahab located in the Gulf of Aqaba, Red Sea, to analyse the spatial and temporal impact of coastal development on corals of the Red Sea. The study observed a notable decrease in the hard coral cover because of the rise in algal cover

from the amount of nutrients, especially phosphate and ammonium (Naumann et al., 2015).

In regard to the presence of trace metals in seawater, Lü et al. (2015) did a pollution assessment of trace elements in Laizhou Bay, China. The study shows the different risk levels associated with the varied concentration of dissolved metals in seawater. The higher concentrations of trace metals, with Cd being the highest, were mostly found at the river estuaries caused by heavily polluted runoffs from industries and poor sewage control. Another study done by Hasan et al. (2013) at the ship breaking area of Sitakund Upazilla, Chittagong, Bangladesh found the highest concentration of Fe and Hg at the site than any other trace metals. The study was done to find the concentration of trace metals at the site and its contribution to the groundwater of the area. The team of researchers also performed tests for the concentration of major ions in their research. The conclusion drawn by the study explains the excessive amount of the two metals from the seawater, due mostly to the breaking of ships, mixing in the groundwater. The analysis of the major ions done by the team painted a better picture of the way the metals were getting mixed in the groundwater. Another study was done by Mackey et al. (1996) to investigate trace elements at Bathurst Harbour, South-western Tasmania. The results drawn from the experiments showed concentrations of copper and manganese to be 10 to 50 times higher, and cadmium and nickel concentrations to be 2 to 4 times more than previously recorded. The elevated levels of concentration from those elements were attributed to discharges from mining that was eventually mixed in a river over time.

The studies mentioned above employed various methods of sampling, including grab sampling and manual sampling as explained by APHA (2012). Yılmaz and Sadikoglu (2011) first collected seawater samples for analysis by using 250mL polyethylene bottles. Arakaki et al. (2005) used a more conventional approach with polypropylene 1000mL bucket for their sampling. Polyethylene (plastic) containers were the preferred material for sampling simply because this procedure prevents the loss of nutrients since they are the most volatile aspect of seawater quality analysis (APHA, 2012). In terms of storage, Grasshoff et al. (1999) explains the various ways of preserving samples by first filtering followed by acidifying the samples, then refrigerating them. Similar storage methods were adopted by many studies (Arakaki et al. (2005); Crompton (2006); Valdés et al. (2011); Yılmaz and Sadikoglu (2011)).

Based on the books by Strickland and Parsons (1972), Grasshoff et al. (1999), Crompton (2006), Keith et al. (2009) and APHA (2012), there are numerous techniques available for the analysis of trace metals. There are also multiple studies (Mentasti et al., 1989; L. A. Miller and Bruland, 1994; Komjarova and Blust, 2006; Noack et al., 2015), that compared some of those methods to determine the ease of practice, and accuracy of each of them. Liquid-liquid extraction (LLE) developed by Brooks et al. (1967) for the analysis of trace metals in seawater was chosen for the current study. The procedure makes use of ammonium pyrollidine dithiocarbamate (APDC) and isobutyl methyl ketone (IBMK) to separate the organic layer from the seawater leaving only dissolved trace metals. This procedure was adopted for its versatility and efficacy as explained by Mentasti et al. (1989), Komjarova and Blust (2006), Abdel Ghani (2015) and Noack et al. (2015). Two other methods, solid phase extraction and co-precipitation together with LLE were studied by Komjarova and Blust (2006). To the contrary of Brooks et al. (1967) who mentioned that the method was rapid and easy, the pair concluded that the method, however excellent it was coupled with very low experimental errors, was quite time consuming and the reagents used were unsafe for the environment. Noack et al. (2015) on the other hand, due to the nature of his study being slightly more specific, followed the same approach as outlined by Brooks et al. (1967) and the conclusion from that study still rated LLE to be more precise. Miller and Bruland (1994) evaluated the technique in their paper and further concreted LLE tends to filter out most of the organic matter leaving only dissolved metals in the sample for analysis. Another method for trace metal analysis, known as Acid Digestion Method (ADM) was mentioned in APHA (2012). This technique primarily used nitric acid which could be mixed with other acids such as hydrochloric acid, depending on the nature of the sample. Similar to LLE, the sample required filtration using a 0.45µm filter paper prior to digestion. ADM considerably reduced the interference with organic matter and converted the dissolved metals into a form detectable by the Atomic Absorption Spectrophotometer (APHA, 2012).

Other studies in relation to seawater quality analysis, are those of nutrients. Nutrients exist in seawater in the form of nitrate, sulphate, phosphate, ammonia-nitrogen, silicate and other trace elements such as sodium. Phytoplankton are the organisms in seawater that rely mostly on nutrients for photosynthesis, growth and reproduction. Studies have shown high concentration of nutrients favour algal growth over corals (Fabricius,

2005; Lough and van Oppen, 2009; Stanley and van de Schootbrugge, 2009; Naumann et al., 2015). Since algae absorb nutrients faster, they tend to grow quicker than corals. This leads to a bloom in algal growth which, over just a short period of time ends up blocking sunlight, thus restricting coral growth (Higuchi et al., 2015). Eutrophication is usually caused by river runoffs, which carry high amounts of phosphorus and nitrate to the ocean, which in turn favours algae growth to that of corals (Measurements, 2016a). High seawater temperature and strong to ultra-violet rays from the sun when mixed with excess nutrients cause coral degradation (Wagner et al., 2010). The authors also mention, in their study of the influences on coral bleaching, that the corals become darker in appearance first. This visual change makes them more susceptible to temperature variations, declining their health even further.

For the analysis of nutrients, the books mentioned (Strickland and Parsons, 1972; Grasshoff et al., 1999; APHA, 2012), above also provide numerous techniques that include digestion methods, copper-cadmium reduction method, colorimetric method and UV spectrophotometric methods that are specific to each nutrient. Naumann et al. (2015) used a simpler spectrophotometric method which made use of test kits for each nutrient to determine its concentration. The test kits results were reliable and a similar apparatus was used for the current study.

2.2 Malaysia Overview

The coast of Malaysia has one of the richest and most diverse marine fauna in the world. This richness and diversity tend to attract numerous tourists which in turn generates a substantial economic growth for the country. However, Malaysian Marine Protected Areas (MPA) are hampered by a restricted amount of resources coupled with the incapability of confronting challenges. These hindrances cascade to lack of enforcement, coordination, awareness and poor socio-economic status which tend to have immediate impacts on environmental conservation behaviour (Teh et al., 2008; Masud and Kari, 2015). Praveena et al. (2012) did a small review of most of the coral reef studies in Malaysia. The team explains that there are numerous studies done on the quality of the corals in the country, however, no spatial or temporal study has ever been done about seawater quality of the coral environment. The state of coral reefs was evaluated by comparing the percentage of live corals based on criteria from ASEAN – Australia Living Coastal Resources Project. Reef Check Malaysia is a NGO

that does yearly surveys of most of the coral reefs in Malaysia. In their 2015 report, it was noted that, over a five-year study, the live coral cover in the peninsular improved by 18.6% since 2011. Conversely, East Malaysia dropped by 2.75% from 2014 to 2015. This drop was caused mainly by the practice of dynamite fishing in the marine parks (R. C. Malaysia, 2015a). Reef Check Malaysia only does coral surveys through photo-documentation. Observation of the sites through identification of specific algae growth and crown of thorn starfish give the NGO an idea of the type of pollution occurring. However, with the absence of scientific data, the survey done is not enough to involve governmental bodies with the intention of maintaining the health of the corals.

A study by Miller et al. (2015) found common symptoms happening in three of Sabah's marine parks similar to those in other parts of the world, which were coral bleaching, diseases and pigmentation. Bleaching and pigmentation were more common and was accelerating at Sipadan Island Park. The proliferation of diseases at the three parks were attributed to human disturbances, pollution, sedimentation and habitat destruction. Pitkin (2011) wrote an article in Dive Magazine explaining the degradation of the coral environment taking over Sipadan. The government of Sabah relocated all the resorts formerly found on Sipadan Island, as a measure to preserve and protect the state of the reefs (Teh et al., 2008).

In a report released in 2002, issues concerning the declining state of the near-shore reefs of Miri in Sarawak, have been attributed to logging large areas of land for development, palm oil plantation, hill-slope clearing and sand dredging activities. Land clearing and construction completely destroyed one of the near-shore coral formation due to the heavy sedimentation that arose from those activities (Elcee-Instrumentation, 2002; Praveena et al., 2012). Another review was done by Praveena et al. (2012) explaining the various problems that Malaysia faces in terms of overfishing, sand mining, heavy sedimentation caused by land clearing, river runoffs, dynamite fishing to name a few. The latest report by Reef Check Malaysia (2015a) surveyed 6 coral reef sites at MSCRNP. The study mentions that 50% of the corals are in fair condition, 33% in good condition and 17% in poor condition. The main damage to the coral environment was attributed to warm water causing coral bleaching followed by boat anchors, fish net and solid wastes (R. C. Malaysia, 2015a). A report by UNEP (2007) claims that the reefs are being affected by the sediments from the

Miri and Baram rivers. The studies done at the Miri reefs only looked at the state of the corals but the seawater quality has never been analysed to investigate the parameters affecting or contributing to the health of the coral.

2.3 Summary

Internationally, numerous studies have been done to analyse and monitor the impact of human involvement on the corals and seawater. Several studies mentioned illustrate the effects of heavy metal pollution and the prevalence of diseases in coral from the contaminations (Mackey et al., 1996; Yılmaz and Sadikoglu, 2011; Hasan et al., 2013; Lü et al., 2015). In the case of nutrients, many studies mention that the impacts of eutrophication on seawater encourages algal bloom in coral environments while suffocating the corals and eventually causing coral bleaching. (Fabricius, 2005; Lough and van Oppen, 2009; Stanley and van de Schootbrugge, 2009; Wagner et al., 2010; Higuchi et al., 2015; Naumann et al., 2015). Authors such as Tew et al. (2014) and Mezhoud et al. (2016) highlight the effects of global warming through physico-chemical characteristics of the seawater. The authors together with Rakestraw (1943); APHA (2012); Praveena et al. (2012); Health (2016) also point out that industrial discharge and coastal runoffs largely affect the quality of the seawater causing rise in temperatures as well as a decrease in pH values. Lack of enforcement from local authorities contributes to coral death. The book "Coral Reefs of the United Kingdom Overseas Territories", describes that gaps in environmental legislations include seawater quality standards to control and monitor sedimentation (Readman et al., 2013).

Aforementioned works have designed methods; such as seawater sampling, analyses of trace metals and nutrient effects over time together with analyses of sediments around coral environments. The various methods utilised by the works have proven their efficacy as well as highlight the importance of monitoring the seawater quality and coral environment worldwide (Grasshoff et al., 1999; Crompton, 2006; APHA, 2012)

Environmental monitoring has been lacking in Malaysia, especially in Miri, since the last published report was released was in 2002. Reef Check Malaysia only does surveys once a year and based on photo-documentation, which gives neither a spatial

nor a temporal analysis of the marine reserve. Sipadan, even though studies are not done on a regular basis, has still had case studies that showed seawater quality assessments as well as coral health observations.

CHAPTER 3 – RESEARCH METHODOLOGY

3.1 Sampling

The sampling methods used in this study were a combination of 2 methods known as "Grab Sampling" and "Manual Sampling" (APHA, 2012). Grab Sampling requires single samples taken at specific locations at various depths and time. This form of sampling was done by using 5L polyethylene gallons. The maximum depth at each site varied, with the shallowest site being Eve's Garden at seven metres deep. Anemone Garden and North Siwa, both shared similar depths ranging from 15 to 18 metres. There were three depths of sampling at Anemone Garden and North Siwa; surface, middle depth and seabed, whereas samples at Eve's Garden were only taken at the seabed and surface layers.

Manual Sampling is more skilled-based and time consuming. However, while specific skills are required for this technique, less equipment is needed (APHA, 2012). This form of sampling might be tedious; however, the samples are well preserved. Each sampling container was washed thoroughly with concentrated nitric acid and rinsed with distilled water to ensure no foreign contaminants were present. Seawater was used to rinse the containers at least three times at each location as explained in the Standard Methods for the Examinations of Water and Wastewater (2012) prior to sampling.

Seawater samples were collected over three different seasons; start of southwest monsoon (SWM) (May 2016), end of SWM (September 2016) and transition to northeast monsoon (NEM) (October 2016), to determine the spatial and temporal variation of water quality. The samples at all three designated locations were retrieved by diving to the seabed first to find out the maximum depth of the site. A dive computer was used to measure the maximum depth at each site and the seawater samples were collected using polyethylene gallons. Once at the seabed, the bottom (third) layer seawater sample was taken before climbing to the middle or second layer. The second layer was calculated based on the maximum depth shown by the dive computer. After collecting samples at layer two and three, the samples were brought to the surface where the surface layer was collected at a depth of more than 0.2 metres as advised in the Methods of Seawater Analysis (1999).

Figure 3.1 – Sampling at North Siwa – Seabed

Figure 3.2 – Sampling at Anemone – Middle depth

3.2 Storage

After completing the on-site investigation, the samples were sealed and placed in a container with ice to maintain a low temperature after each field assessment. This helps preserve the nutrients in the seawater samples. In regards to major ions and trace

metals, the samples were stored in high density polyethylene containers to maintain the consistency of both the latter and the former for laboratory investigation (Grasshoff et al., 1999; Crompton, 2006). Except for nutrients (NH_3-N, SO_4^{2-}, PO_4^{3-} and NO_3^-) which were analysed immediately after reaching the laboratory, the remaining samples were separated for major ions (Ca, Na, Mg, K, Cl and HCO_3) and trace metals (Cu, Pb, Fe, Mn, Zn, Cd, Ni, Co, Cr).

Preservation of samples for trace metals analysis required filtering the samples using a 0.45µm (Millipore®) filter paper (Mentasti et al., 1989; Grasshoff et al., 1999; APHA, 2012; Mokhtar et al., 2012). Filtering helps to remove any suspended solids and/or interference present in the sample, after which the sample was acidified to pH<2.0 (Mentasti et al., 1989; Mokhtar et al., 2012).

3.3 Spatial Maps

The sampling points are spatially separated without a distinct boundary (limiting boundary). In order to generate the spatial surfaces of physico-chemical parameters measured at different depths, an arbitrary boundary was generated by 5km wide and 14km length covering all three sampling points (a total area of 70km^2). After generating the boundary, the parameter measurements were added as attributes of each sampling location. Further, using the spatial analyst extension of ArcGIS 9.3 was used to generate the surface maps corresponding to each parameter at different depths.

In order to get the representative distribution of phyico-chemical parameters analysed in the whole area (generated limiting boundary of 70km^2), considering the limited number of sampling points, in order to generate a more realistic spatial pattern, in the present research, the inverse distance weighted (IDW) interpolation method available in the spatial analyst extension was used. IDW is considered as the simplest and relatively accurate method of interpolation (Azpurua and Ramos, 2010; Setianto and Triandini, 2015) and it uses a weighted average value of surrounding locations during interpolation to calculate the values for non-measured locations (Burrough and Mcdonnell, 1998).

After selecting the interpolation method (IDW), attribute corresponding to the measured parameter was selected from the field to interpolate by keeping the analysis

mask as the boundary generated. Following this procedure, the spatial surface of each parameter analysed were generated and interpreted.

3.4 Chemical Analysis

Once the sample was retrieved, pH, temperature, electrical conductivity (EC), dissolved oxygen (DO), total dissolved solids (TDS), oxidation reduction potential (ORP) and salinity were measured in-situ using portable meters; Thermo Scientific's Orion Star, Hach® HQ40D and LaMotte 2020we Turbidimeter. For greater accuracy, the portable meters were calibrated prior to the test. The pH probe from Thermo Scientific's Orion Star, was calibrated using a pH 4.0 solution followed by a pH 7.0 solution and finishing the calibration with a pH 10.0 solution. The probe was then capped with a few drops of storage fluid to avoid any contamination. Another probe was used to measure the conductivity and was calibrated using a standard conductivity solution supplied by the manufacturer. The value being assessed was 1413µS/cm. DO was measured using the Hach® HQ40D meter and the calibration solution used was distilled water. The desired calibration value shown was 7.30mg/L. Turbidity of the samples were analysed using the LaMotte 2020we Turbidimeter. The apparatus was first calibrated using two standard solutions; 0.1NTU and 1.0NTU. Measurements were then performed by taking 10ml of each sample and placing them in the meter. Care was taken to avoid disturbances, such as fingerprints on the cuvette before placing it inside the apparatus or light entering the closed chamber of the equipment which could result in false readings.

Following the storage procedure explained in Section 3.2, the samples were brought to the Geochemistry Laboratory of Curtin University, Malaysia for further analysis. Nutrients being the most volatile were analysed first, followed by major ions and lastly trace metals. Table 3.1 gives a summary of the various methodologies involved in this study. Sections 3.3.1 to 3.4 elaborates on the different parameters and methods used to obtain the results.

Table 3.1 – Summary of Methodology		
Parameters	**Methods / Instruments**	**References**
Temperature, pH, EC, salinity, total dissolved solids, redox potential, dissolved oxygen and turbidity	Portable meters (Thermo Scientific's Orion Star, Hach® HQ40D and LaMotte 2020we Turbidimeter)	Scientific (2010); APHA (2012); HACH (2013)
Nutrients: SO_4^{2-}, PO_4^{3-}, NH_3-N, NO_3^-	Spectrophotometer (Hach® DR2800)	HACH (2007); APHA (2012)
Major ions: Ca^{2+}, Mg^{2+}, HCO_3^-, Cl^-	Titrimetric Method	Ramesh and Anbu (1996); APHA (2012)
Trace metals: Cu, Pb, Fe, Mn, Zn, Cd, Ni, Co, Cr, Na and K	Acid digestion and Liquid-liquid extraction followed by Atomic Absorption Spectrophotometer (AAS) (Perkin-Elmer AAnalyst 400)	Brooks et al. (1967); Mentasti et al. (1989); APHA (2012)
Photo-documentation	Diving using specialised underwater camera.	Aronson et al. (1994); R. C. Malaysia (2015a); Naumann et al. (2015)

3.4.1 Nutrients

The analysis of nutrients (Nitrate, Ammonia-Nitrogen, Phosphorus and Sulphate) required the use of the spectrophotometer by the Hach®. The company also supplies the reagents needed for the analysis of specific nutrient. The reagents come in the form of small packets called "Powder Pillows". Each method of analysis comes with a step by step guide required to prepare both the standard solution and samples. The powder reagents that were used for Nitrate, Ammonia-Nitrogen, Phosphate and Sulphate were Cadmium reduction method 8192 (HACH®, 2015a), Salicylate method 8155 (HACH®, 2015b), PhosVer 3® Ascorbic Method 8048 (HACH®, 2015c) and SulVer 4 Method 8051 (HACH®, 2015d). Each nutrient had a specific wavelength that was utilised by the program for the determination of the various nutrients. Nitrate was measured at 507nm, Ammonia-Nitrogen at 655nm, Phosphate at 880nm and Sulphate at 450nm.

3.4.2 Major Ions

The analysis of major ions was done using the titrimetric method. This method was chosen mostly due to the simplicity and availability of the various equipment and chemicals needed for the investigation. The visual changes at the endpoint also help in terms of accuracy of results. This particular method is also recommended by the Standard Methods for the Examination of Water and Wastewater (2012) and Ramesh and Anbu (1996).

3.4.2.1 Calcium and Magnesium

The reagents required to analyse the concentration of Calcium and Magnesium were; Ammonium Chloride – Ammonia buffer solution, Sodium Hydroxide 1N, Eriochrome Black-T indicator, Murexide Indicator, EDTA (Ethylenediaminetetraacetic acid) 0.02M and Standard Magnesium Sulphate solution 0.02M (for standardisation of EDTA solution).

7.44g of disodium salt of EDTA dihydrate was dissolved in 1000mL of distilled water to make EDTA (burette solution). After preparing the burette solution, measurements for the preparation of the other solutions were either halved or quartered. This was

done to minimise wastage, while maintaining the desired concentration, from the initial dilution from 1000mL distilled water.

Proceeding that, 0.02M magnesium sulphate was prepared by dissolving 1.48g of $MgSO_4$ salt in 250mL of distilled water. Ammonium chloride-ammonia buffer solution was prepared by dissolving 16.92g ammonium chloride salt in 143mL of concentrated ammonia solution. The solution was then diluted to 250mL with distilled water. Lastly, sodium hydroxide 1N was prepared by adding 10g of NaOH pellets and made up to 250mL with distilled water.

Standardisation of EDTA was done first to ascertain a 0.02M concentration. This procedure required 25mL of $MgSO_4$ to be pipetted in a conical flask. 2mL of ammonia-ammonium chloride buffer solution was added to the flask together with a pinch of Eriochrome Black-T indicator. Titration of $MgSO_4$ required 23mL EDTA to reach the endpoint which was a steel blue colour.

The steps involved in determining the concentrations of total Mg^{2+} and Ca^{2+} are as follows:

Total Calcium and Magnesium content required 10mL of sample to be pipetted in a clean 250mL conical flask and diluted using 12.5mL of distilled water. 1mL of ammonium chloride-ammonia buffer was added followed by 15-20mg of Eriochrome Black-T indicator. The solution was titrated with 0.02M EDTA until the colour changed from wine red to steel blue. It is important to titrate slowly close to endpoint and no trace of red should be present at the endpoint.

Total Calcium content was found by pipetting 10mL of sample in a 250mL clean conical flask. The sample was diluted using 12.5mL of distilled water followed by 1-2mL of sodium hydroxide. The basicity of the solution was tested by soaking red litmus paper in the solution until it turned blue. More sodium hydroxide was added when no change in colour was seen on the litmus paper. Finally, the solution was titrated with 0.02M EDTA until its colour changed from red to blue-violet.

The following calculation is used to find the concentration of Ca^{2+} and Mg^{2+} ions in mg/L:

Volume of sample	= 20 mL
Volume of EDTA for Ca^{2+} only	= *A* mL
Volume of EDTA for Calcium and Magnesium	= *B* mL
Volume of EDTA for Mg^{2+} only	= *(B – A)* mL

Calcium:

$$1mL\ EDTA = 0.0004g\ of\ Ca$$
$$A\ mL\ EDTA = (0.0004 \times A)g\ of\ Ca$$

$$\boldsymbol{Ca\ (mg/L) = \frac{0.0004 \times A\ mL}{20} \times 10^6}$$

Magnesium:

$$1mL\ EDTA = 0.00024g\ of\ Mg$$
$$A\ mL\ EDTA = (0.00024 \times (B - A)g\ of\ Mg$$

$$\boldsymbol{Mg\ (mg/L) = \frac{0.0004 \times (B - A)\ mL}{20} \times 10^6}$$

3.4.2.2 Carbonate and Bicarbonate

The various reagents needed for determining the presence of carbonate and bicarbonate were; Sulphuric Acid 0.02N, Sodium Carbonate solution 0.02N, Phenolphthalein indicator and Methyl Orange indicator.

Preparation of 0.02N sulphuric acid (burette solution) was done by diluting 0.72 mL of concentrated sulphuric acid with 1000mL of distilled water. 0.27g of sodium carbonate salt was diluted using 250mL of distilled water.

20mL of sample was pipetted in a conical flask. Phenolphthalein indicator was used to test for the presence of carbonate which would have turned the colour of the solution pink. No change of colour was seen, signifying the absence of carbonate. The experiment moved on to add 2 drops of methyl orange indicator. The straw yellow

coloured solution was then titrated against 0.02N sulphuric acid until the colour of the solution changed to pinkish red.

Calculation for the concentration of CO_3^{2-} and HCO_3^- in mg/L:

Volume of sample	*= 20 mL*
Volume of H_2SO_4 for phenolphthalein	*= X mL*
Volume of H_2SO_4 for Methyl Orange indicator	*= Y mL*
Volume of H_2SO_4 for CO_3^{2-} only	*= 2X mL*
Volume of H_2SO_4 for HCO_3^- only	*= (Y – 2X) mL*

Carbonate

$$\boldsymbol{CO_3^{2-}\ (mg/L) = \frac{(2X)mL \times 0.02 \times 30}{20} \times 1000}$$

Bicarbonate

$$\boldsymbol{HCO_3^-\ (mg/L) = \frac{(Y - 2X)mL \times 0.02 \times 61}{20} \times 1000}$$

3.4.2.3 Chloride

The titration method used to find the concentration of chloride is known as Argentometric or Mohr's Titration Method (Ramesh and Anbu, 1996). The reagents required for this experiment were: silver nitrate solution 0.05N, potassium chromate indicator and 0.05N sodium chloride solution to standardise $AgNO_3$ solution.

A 0.05N silver nitrate solution (burette solution) was prepared by dissolving 8.494g of $AgNO_3$ salt in 1000mL of distilled water. 0.05N sodium chloride solution was prepared by dissolving 0.7305g of NaCl salt in distilled water, which was then used to standardise the silver nitrate solution.

After pipetting 10mL of sample to a clean 250mL conical flask, around 1mL of potassium chromate indicator was added. The solution in the conical flask was titrated against silver nitrate until a red colour is formed. This colour change meant that most

of the chloride had been precipitated. The titration continued until the endpoint which was a persistent faint reddish brown tint.

The concentration (mg/L) of chloride ions in the sample was then calculated using the following information:

Volume of $AgNO_3$ for sample = *A mL*

Volume of $AgNO_3$ for blank = *B mL*

Normality of $AgNO_3$ = *N*

Chloride

$$\boldsymbol{Chloride\ (mg/L) = \frac{(A-B)mL \times N \times 35.45}{Vol.\ of\ Sample} \times 1000}$$

3.4.3 Trace Metals

3.4.3.1 Sample Preparation

The preparation of the seawater samples for the analysis of trace metal (Cu, Pb, Fe, Mn, Zn, Cd, Ni, Co, Cr, Na and K) first required at least 1000mL of each sample to be filtered using 0.45µm Millipore® filter paper. The samples were then acidified between pH 3 to 5 using concentrated HNO_3 for preservation purposes.

Two different methods: acid digestion and Liquid-Liquid Extraction (LLE), were used to analyse the concentration of trace metals in MSCRNP and Sipadan Island Park. Acid Digestion was used for the concentration of sodium and potassium only because the dilution process was much simpler to compute. This method favoured the two elements because there were practically no interferences due their high concentrations.

The LLE method, which was developed by Brooks et al. (1967), were chosen for the extraction of metals from the seawater. The method was further enhanced through back-extraction process using the method employed by Mentasti et al. (1989). This was the best method to obtain the concentration of the other eight metals to be analysed because of their low concentration values. The use of the organic and aqueous layers

and back extracting in nitric acid isolated the metals present in the samples without having interferences.

3.4.3.2 Liquid-Liquid Extraction (LLE)

Equipment and chemicals required for the LLE were:

- Isobutyl Methyl Ketone (IBMK)
- 1% Ammonium Pyrollidine Dithiocarbamate (APDC)
- Concentrated Nitric Acid (HNO_3)
- High Purity Water (HPW)
- 1000mL volumetric flask
- 1000mL separating funnel
- 5mL, 10mL and 25mL graduated pipettes
- 100mL and 1000mL beakers
- 200mL conical flasks
- Hot plate

The various literatures reviewed in Chapter 2 used less than 1000mL of sample. For this study, an amended procedure that followed the same principles was used but adjusted to the volume of sample being utilised.

1. Exactly 1000mL of sample was measured using a similar size volumetric flask and the sample was poured in the separating funnel.
2. 35mL of IBMK was added to the sample in the separating funnel.
3. 7mL of 1% APDC was then added to the sample.
4. The separating funnel containing all the solution was then shaken vigorously for 15 minutes.
5. After allowing the mixture to rest, an organic layer was formed on top of the sample.
6. The sample and the organic layer were removed in a 1000mL beaker and a conical flask respectively.
7. The conical flask containing the organic layer was kept closed to avoid evaporation.
8. The sample was added back to the separating flask.

9. 20mL of IBMK and 4mL of 1% APDC were added to the sample as explained in steps 2 and 3 followed by step 4.
10. The sample was then removed and the organic layer obtained from step 6 was added back to the separating funnel.
11. Back extraction of the dissolved trace metals was done by added 3mL of concentrated HNO_3 to the separating funnel and the mixture was shaken vigorously for 3minutes.
12. The aqueous layer formed was collected in the beaker.
13. 10mL of HPW was added to the organic layer. The mixture was again shaken vigorously for 3 minutes and the aqueous layer was collected in the same beaker.
14. Step 13 was repeated.
15. Steps 11 to 14 were done three times to remove all the trace metals that was extracted from the sample to the organic layer (IBMK).
16. The aqueous layer collected from steps 11 to 15 were then evaporated to dryness on a hot plate at a temperature not exceeding 70°C.

Once the aqueous layer was evaporated, 1% HNO_3 was used to make it up to 100mL. This final product was then brought to the Atomic Absorption Spectrophotometer for trace metal analysis.

Figure 3.3.3.1 – Step 13 of LLE: Addition of HPW to the organic layer

3.4.3.3 Acid Digestion

Another method employed to find the concentration of dissolved trace metals in the seawater samples was through acid digestion. This method simply required 10mL of concentrated HNO_3 to be added to 100mL of sample. The mixture was then allowed to evaporate until less than 20mL of sample remained. The sample was then made up to 100mL again using only HPW (APHA, 2012). The final product was then brought to the Atomic Absorption Spectrophotometer for trace metal analysis.

3.4.3.4 Atomic Absorption Spectrophotometer (AAS)

The PerkinElmer AAS (Figure 3.3.3.2) was used to analyse 10 different metals from 29 samples prepared as mentioned in sections 3.3.3.2 and 3.3.3.3. Prior to analysing the samples, standard solutions were prepared with high purity water (HPW) to calibrate the apparatus. Steps 1 to 13 below give a detailed explanation on setting up the equipment, preparation of the standard solutions and analysis of samples:

1. Air compressor was turned on.
2. Air dryer was turned on.
3. Blower was turned on.
4. Automatic voltage stabilizer was turned on.

5. AAS was turned on.
6. The desired lamp was inserted into one of four slots found in the hardware.
7. The lamp was switched on from the software on the computer connected to the equipment.
8. After switching on the lamp, which took approximately 15 minutes to reach nominal temperature, 1000ppm standard solutions by PerkinElmer was used to prepare 0.1ppm, 0.5ppm and 1.0ppm standard solutions for each element. These standards were used to determine the accuracy of the analyses done by the AAS.
9. The formula $M_1 V_1 = M_2 V_2$ was used to determine the dilution factor when creating the standard where M_1 and V_1 are the molarity of the concentrated solution, and M_2 and V_2 are the molarity and volume of the desired diluted solution.
10. A 100ppm solution of the standard was made using the following equation, which was then used to prepare the 0.1ppm, 0.5ppm and 1.0 ppm standard solutions.

$$M_1 V_1 = M_2 V_2$$

$$(1000ppm)(V_1) = (100ppm)(100mL)$$

$$V_1 = \frac{(100ppm)(100mL)}{1000ppm}$$

$$V_1 = 10mL$$

11. Using a pipette, 10mL of the prepared standard solution was made up to 100mL with high purity water (HPW) making a 100ppm standard solution.
12. Following the same formula used in step 10, the three standard solutions were prepared.
13. The AAS was then calibrated starting with a HPW blank to set the value to zero.
14. A quality control (QC) check was set for each of the prepared standards in the software which were then analysed at a 10% limit.
15. For samples that had a value less than 0.1mg/L after analysis, the 0.1ppm standard was used as QC to check for accuracy. If a value was closer to

0.5mg/L, the 0.5ppm standard was used as QC and the same process applied for values close to 1.0mg/L.

16. QC check was done after analysis of every 3 to 4 samples.
17. If QC failed after 3 tries, the equipment was calibrated again and analysis resumed from the last sample.
18. Steps 1 to 6 were done every day when switching on the AAS and steps 7 to 17 were done for each of the 10 elements analysed.

From the 10 different trace metals analysed, the concentrations that were below detection limit showed up as negative values.

Figure 3.3.3.2 - PerkinElmer Atomic Absorption Spectrophotometer

3.5 Photo-documentation

Photo-documentation is the use of photography to create a log of the various aspects of the project as well as documenting the state of corals at Eve's Garden, Anemone Garden and North Siwa. A specialised underwater camera was borrowed from the Corporate Communication department of Curtin University, Malaysia that helped with photo-documentation. Rather than setting a transect, pictures of corals were taken at each site in general to give an indication of their states as well as a comparison between a healthy reef and a reef that is undergoing coral bleaching. The pictures taken together

with the seawater quality assessment would give a better understanding of the reason behind the bleaching of corals.

Multiple field trips were done to take pictures of the corals whenever the underwater camera was available. Eve's Garden and Anemone Garden have more soft corals than North Siwa, and both were visited more than the latter. Pictures of both hard corals, such as Porites, Favia, Diploastrea, Echinopora, Acropora and soft corals were taken as well as healthy corals and bleached ones. The pictures would be used to identify the more resilient corals to the less resilient ones. The seawater quality would also provide information to what could be the cause of the degrading health of some of the coral species.

CHAPTER 4 – RESULTS

The average typical seawater quality (Table 4.1 – 4.3), has a pH of 8.1; EC is 35mS/cm; salinity value of 35ppt; TDS concentration of 34.48g/L; DO concentration of 8.5mg/L. Nutrients such as nitrate, phosphate and ammonia-nitrogen are highly dependent on their surroundings. However, average sulphate concentration is 2700mg/L. Major ions such as bicarbonate has an average concentration of 145mg/L; calcium is 416mg/L; magnesium content is 1295mg/L; potassium concentration is 390mg/L; sodium is 10752mg/L; chloride is 19345mg/L. The average availability of trace metal content in seawater is 0.00011mg/L for Cd; Co content is 0.00039mg/L; Cu is 0.0009mg/L; Fe concentration is 0.0034mg/L; Mn can be found at 0.0004mg/L; Ni is 0.0066mg/L; Pb is 0.00003mg/L and Zn is 0.005mg/L (Rakestraw, 1943; Lenntech, 2005; Anthoni, 2006).

Table 4.1 – Average Typical Seawater Quality Parameters (Physical)				
pH	**EC (mS/cm)**	**Salinity (ppt)**	**TDS (g/L)**	**DO (mg/L)**
8.1	35	35	34.48	8.5

Table 4.2 – Average Typical Seawater Quality Parameters (Major Ions)					
HCO_3^- (mg/L)	**Ca^{2+} (mg/L)**	**Mg^{2+} (mg/L)**	**K^+ (mg/L)**	**Na^+ (mg/L)**	**Cl^- (mg/L)**
145	416	1295	390	10752	19345

Table 4.3 – Average Typical Seawater Quality Parameters (Trace Metals)							
Cd (mg/L)	**Co (mg/L)**	**Cu (mg/L)**	**Fe (mg/L)**	**Mn (mg/L)**	**Ni (mg/L**	**Pb (mg/L)**	**Zn (mg/L)**
0.00011	0.00039	0.0009	0.0034	0.0004	0.0066	0.00003	0.005

4.1 In-Situ Parameters

4.1.1 Temperature

Temperature is the first parameter examined when taking in-situ data. This parameter affects nearly everything in the aquatic world, namely: metabolic rates, photosynthesis, seawater toxicity, concentration of dissolved gas, conductivity, salinity, oxidation reduction potential, pH and water density. Seawater temperature is the determining factor of various aquatic lives over both hemispheres together with all the mentioned attributes (Measurements, 2016d).

At the beginning of southwest monsoon (SWM), the highest temperature was recorded at the seabed of the shallowest site, Eve's Garden at 30.5°C, while the other sites all showed a decrease in temperature from surface to seabed. The lowest temperature was observed at North Siwa with a value of 28.5°C. The average temperature recorded at the start of SWM in all three sites was 29.69°C.

During the end of SWM, the highest temperature was recorded as 30.7°C at the surface of Eve's Garden while the lowest was 29.6°C at North Siwa, at a depth of seven meters. On average, the end of SWM showed a value of 30.14°C. The transition to NEM did not show any variations in temperature from surface to seabed maintaining a constant 30°C at all three sites. The same scenario was observed at Sipadan with 29°C recorded at all depths from both Barracuda Point and South Point.

The spatial map in Figure 4.1.1 clearly represents the variation of temperature across all three sites of MSCRNP. The map shows the increase in temperature at Anemone Garden when going from the surface to the seabed. The shallowest site, Eve's Garden can be seen to be the warmest while the temperature at North Siwa was only higher than Anemone Garden at the surface during the end of SWM. All three sites retained the same temperature during transition to northeast monsoon (NEM) as depicted in the third column of the map.

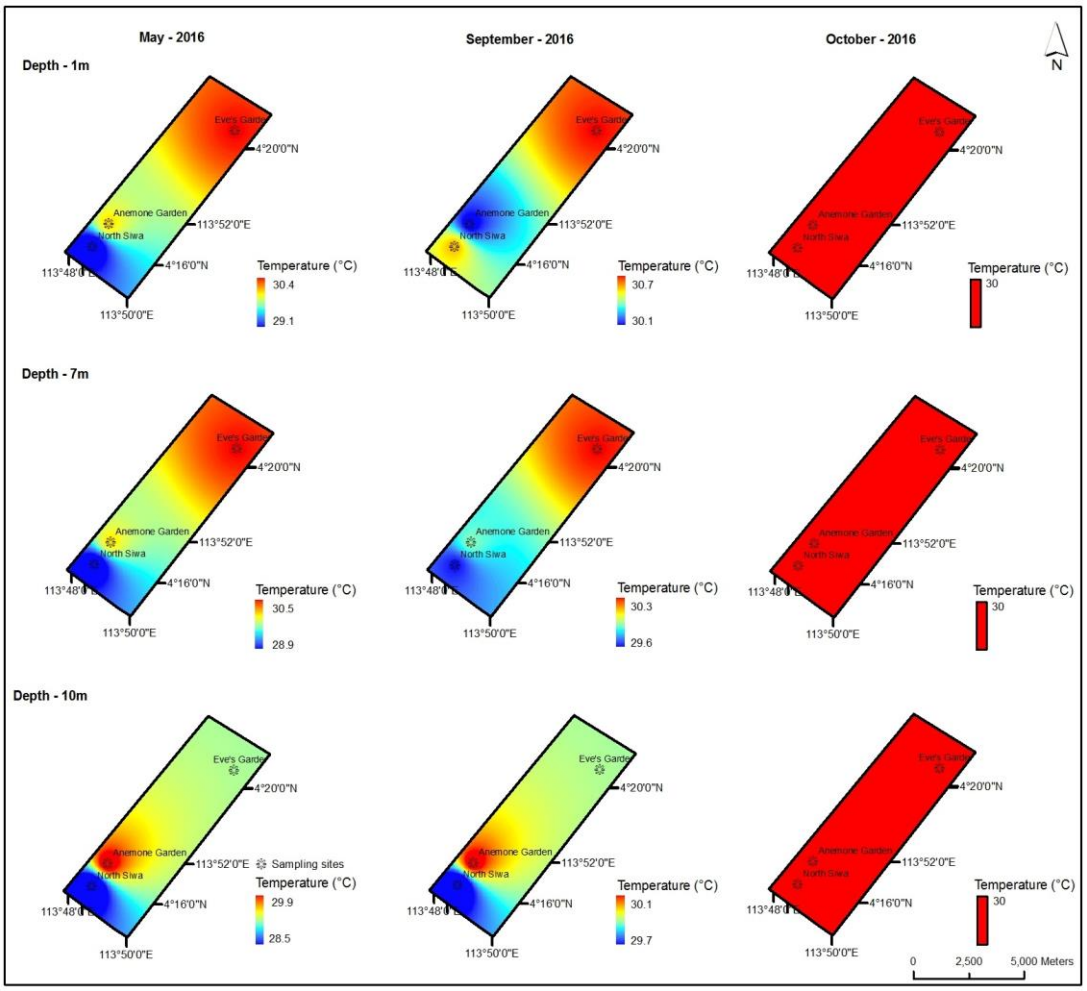

Figure 4.1.1 - Spatial Variation of Temperature at the MSCRNP

4.1.2 pH

pH abbreviated from "power of Hydrogen" (Toolbox, 2015), is the most important variable when investigating seawater. Mathematically, pH is expressed as the negative logarithmic value Hydrogen ion concentration; $pH = -\log[H^+]$. This equation, however, is closer to an approximation of a pH value than the exact value. Grasshoff (1999), speaks of the steps used to measure and calibrate a pH scale for the best value. Changes in pH can alter various characteristics, processes and chemical reactions, such as the concentration of nutrients and major ions since a low or high pH encourages certain chemical changes, even though minute.

The pH values, overall, were the highest in the start of SWM at all three sites in comparison to the end of SWM and NEM transition period. The maximum pH recorded during start of SWM was 8.41 at both the seabed and surface of North Siwa.

The minimum value of the same season was observed at the seabed of Anemone Garden. The average reading for the start of SWM from all three sites was 8.35.

The pH value decreased from the start of SWM to the transition to NEM with the lowest pH being during the end of SWM period. The maximum recorded value was 8.07 at the middle depth of North Siwa, while the minimum reached 7.76 at the surface of North Siwa. The average pH was observed as 8.00 for the end of SWM.

During the transition to NEM, the pH value increased slightly giving a maximum value of 8.15 at the seabed of North Siwa and a minimum of 8.00 at the seabed of Anemone garden. The average pH was 8.07 from all the sites studied during that period.

At Sipadan, a maximum pH of 8.17 was measured at the seabed of Barracuda point and a minimum of 8.10 was observed at the surface. The two pH values recorded at South Point were 8.09 at the seabed and 8.08 at the surface of the site.

Figure 4.1.2 shows the variation of pH spatially and temporally across all three sites. While the overall pH values experience a decrease from start of SWM to transition to NEM, the values among the sites were observed to fluctuate as in Figure 4.1.2. The pH at the surface layer of North Siwa observes a drop from beginning to end of SWM while only slightly increasing during NEM transition. The opposite event was observed at Anemone Garden with the pH value lower than North Siwa during start of SWM and higher during the end of SWM and transition to NEM. Eve's Garden observed a decreased value from beginning of SWM to transition to NEM, while the increased reading at the surface was noted.

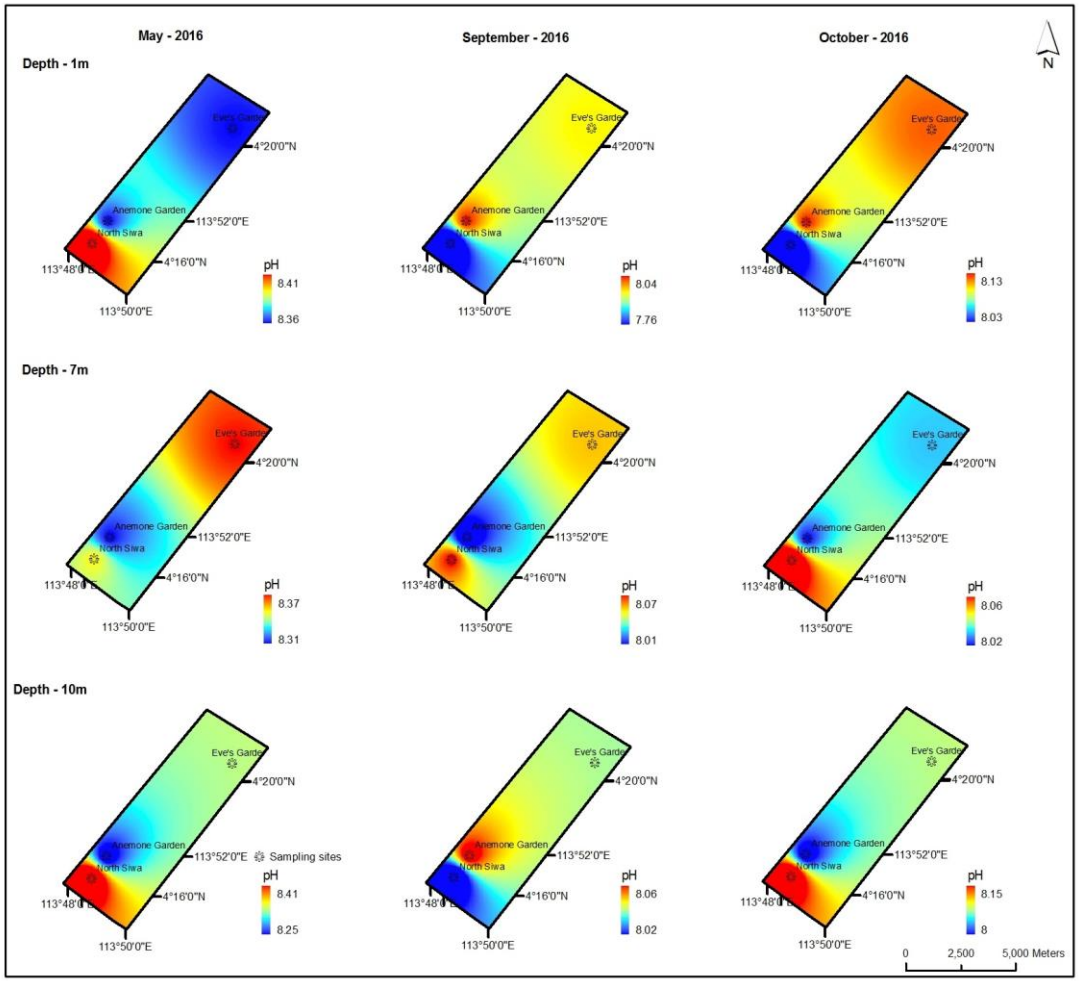

Figure 4.1.2 - Spatial Variation of pH at MSCRNP

4.1.3 Electrical Conductivity (EC)

EC in seawater is explained as the ability to pass electricity through it. The concentration of carbonates, chlorides, sulphides and other dissolved ions account for the degree of conductivity of seawater (Bradshaw and Schleicher, 1980; Measurements, 2016a). Conductivity is measured in Siemens per meter (S/m), however, for the samples that were taken, all the values were measured automatically in mS/cm by the portable meter.

The maximum conductivity reading for the start of SWM was recorded at the seabed of North Siwa with a value of 37.6mS/cm, while the minimum value was 36.80mS/cm at the surface of Eve's Garden. The average reading recorded across the start of SWM period was 37.30mS/cm.

The end of SWM had the highest average when compared to the other two seasons, with a value of 48.68mS/cm. The highest conductivity value was 49.3mS/cm at the seabed of both North Siwa and Anemone Garden. The lowest reading was noted at the surface of North Siwa with a value of 48.03mS/cm.

The highest value recorded during the transition to NEM was 48.9mS/cm at both Anemone Garden seabed and North Siwa Surface. The lowest value was noted at Eve's Garden surface with a value of 46.9mS/cm.

At Sipadan, not much variation was observed in the values. The maximum value at Barracuda Point was measured as 51.0mS/cm at the seabed, while the middle and surface maintained a value of 50.9mS/cm. South Point showed a slightly lower value of 50.7mS/cm at both seabed and surface.

The spatial maps (Figure 4.1.3) showcase the variations of EC at all three sites during all the sampling periods. The seabed of Anemone Garden and North Siwa had the same EC value at the end of SWM. At the surface, the maps show that during the end of SWM, North Siwa had the lowest EC. The seabed of Anemone Garden only had the lowest conductivity value at the start of SWM. During NEM transition, North Siwa was observed to have the lowest EC value.

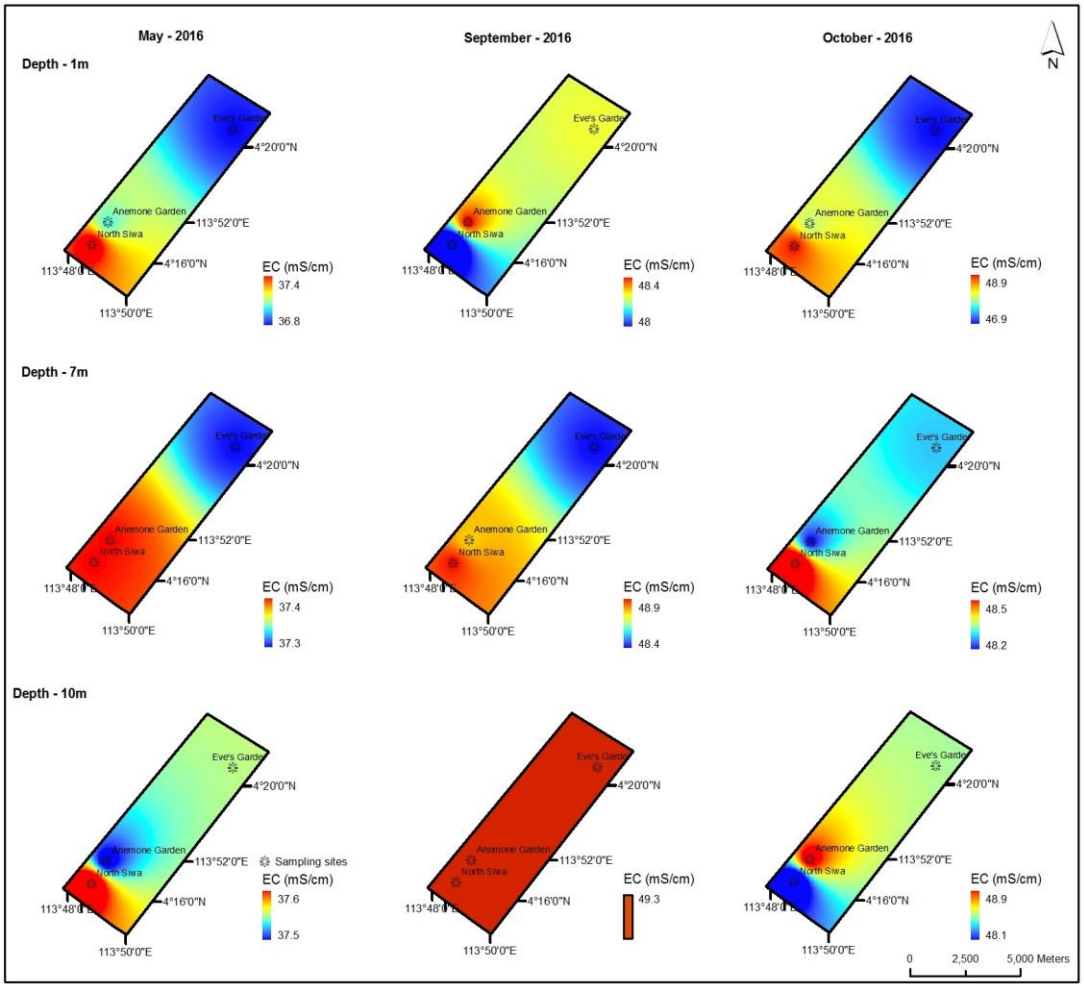

Figure 4.1.3 - Spatial Variation of EC at MSCRNP

4.1.4 Salinity

Salinity is defined as the amount of dissolved salt in seawater and is measured in parts per tons (ppt). Different major ions present in seawater (Section 3.3.2) are also major contributors of salinity of seawater. Salinity can also be calculated mathematically through conductivity values (Lewis and Perkin, 1978; Measurements, 2016a). However, salinity values were measured using the portable meters in this study.

The maximum salinity concentration at the beginning of SWM was 23.8ppt which was observed at the seabed of North Siwa. During the same season, the lowest value for salinity was 23.3ppt at the surface of Eve's Garden. The average value was 23.61ppt from all three locations.

The end of SWM showed an elevated concentration of salinity with a maximum value of 32.4ppt recorded at the seabed of North Siwa. In comparison, the lowest value

recorded during that period was 31.5ppt, still higher than the highest value from the beginning of SWM. The average value for that period was 31.93ppt.

Transition to NEM showed a maximum value of 31.6ppt at both the surface of North Siwa and the seabed of Anemone Garden. The lowest salinity value during this season was 30.2ppt at the surface of Eve's garden and the average of NEM transition period at all sites showed a reading of 31.10ppt.

Salinity values from Barracuda Point, at Sipadan registered a maximum salinity of 33.2ppt at the seabed and 33.1ppt at the surface and the middle depth. South Point measured the lowest salinity with a value of 32.97ppt at both surface and seabed.

Looking at the variations in the spatial maps (Figure 4.1.4), the site generally with the low salinity was Eve's Garden. Anemone Garden only had the highest value at the surface at the end of SWM, while North Siwa recorded the lowest salinity also at the surface. The salinity concentration also appeared to increase when the sites were further from the shoreline.

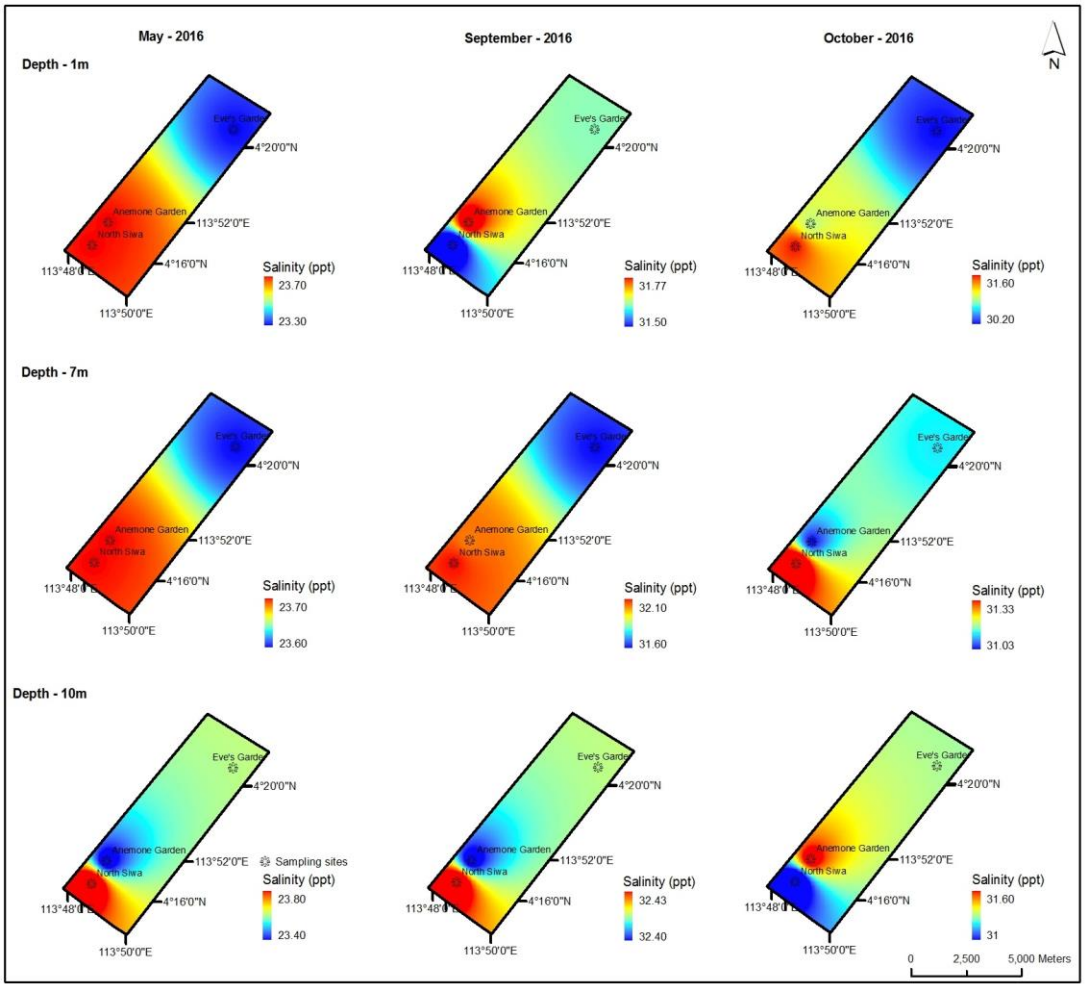

Figure 4.1.4 - Spatial Variation of Salinity at MSCRNP

4.1.5 Oxidation Reduction Potential (ORP)

ORP, also referred to as redox potential is defined as the measurement of an electrochemical reaction which allows the movement of electrons from one species to another (Francis and McIntyre, 2016). Oxidation is the process of receiving electrons, whereas reduction occurs when electrons are lost. Depending on the number of electrons lost or gained, the value for ORP can be either positive or negative respectively. ORP is measured in millivolts (mV).

The study showed that the ORP for seawater is only negative, therefore the maximum ORP registered within MSCRNP during the start of SWM was -55.3mV at the seabed of North Siwa. The minimum value was -63.9mV at Eve's Garden seabed. The average ORP was -60.18mV.

The end of SWM showed a higher disparity in readings than both beginning of SWM and NEM transition. The maximum ORP value for the end of SWM was recorded as -53.7mV at North Siwa surface. The minimum value was -68.6mV observed at North Siwa middle depth bringing the average value for the end of SWM to -65.19mV.

NEM transition had a maximum ORP value of -60.4mV recorded at the seabed of Anemone Garden. The lowest value of the season was -69.0mV measured at the seabed of North Siwa. The average of the transition period was -64.39mV.

Maximum redox value measured at Barracuda point in Sipadan was -66.9mV at the surface of the site. The minimum value of -70.93 was noted at the seabed. South Point values were -65.63mV at the surface and -66.67mV at the seabed.

As observed from Figure 4.1.5, ORP was most elevated at Eve's Garden at the commencement of SWM. The surface of North Siwa had the highest ORP value at the end of SWM and NEM transition. For the same periods, the middle depth of Anemone Garden was the highest value. During start and end of SWM, the seabed of North Siwa had the highest value while Anemone Garden had the lowest reading.

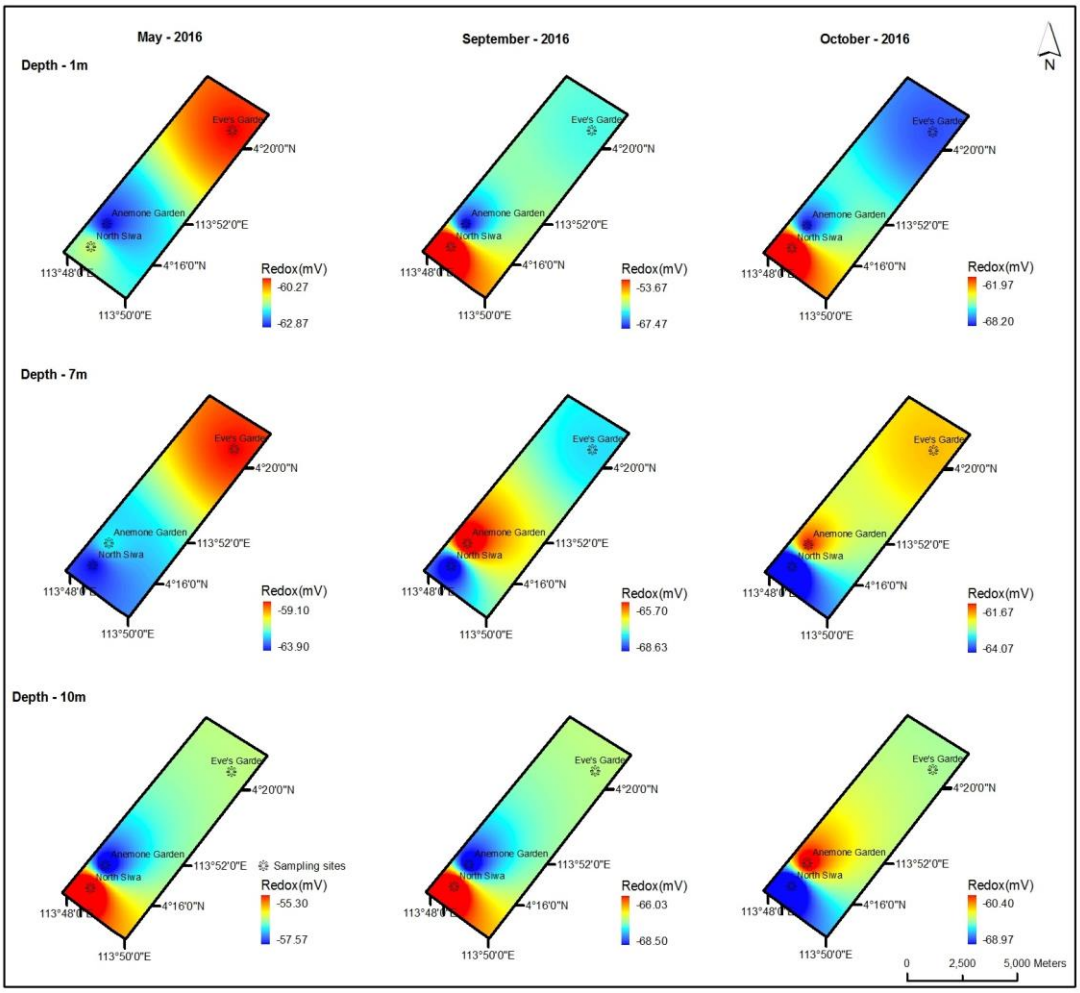

Figure 4.1.5 - Spatial Variation of ORP at MSCRNP

4.1.6 Turbidity

Turbidity is the determination of the clarity of the seawater. The clarity of seawater is disturbed by the amount of suspended solids present in the seawater. Usually, this is done visually with the use of a Secchi disk, however, a turbidity meter was used for this study. The apparatus used examined the amount of light that was scattered by the particles present in the water. The higher the turbidity, the more suspended particles present in the seawater. The unit of measure is Nephelometric Turbidity Unit (NTU) (APHA, 2012; Measurements, 2016b).

The maximum turbidity observed at the beginning of SWM was 0.26NTU at the seabed of Eve's Garden and the lowest value was noted aa 0.06NTU at the surface of both Anemone Garden and North Siwa. The average turbidity value of that period was 0.13NTU among all sites.

The end of SWM showed the value from the start of SWM increase by more than three folds giving a maximum value of 0.93NTU at Eve's Garden surface. The lowest value for that season was similar to the average from the previous period with a reading of 0.13NTU at the middle of both North Siwa and Anemone Garden. The average value for the end of SWM was 0.33NTU.

During NEM transition, the values were even higher than the end of SWM with a peak of 1.50NTU at the surface of Eve's Garden. The lowest value was noted at the surface of North Siwa with a value of 0.52NTU. The average for that season among the three sites was 0.98NTU.

Turbidity shows to be quite low both at Barracuda Point and South Point, in Sipadan. Barracuda Point's highest turbidity value was 0.30NTU at the seabed and lowest was 0.10NTU at the surface. At South Point 0.30NTU was recorded at the surface whereas the seabed value was 0.18NTU.

Eve's Garden always had the most turbid waters across all sampling periods and depths as noted in Figure 4.1.6. North Siwa and Anemone Garden had the least turbidity values at the middle depth except for Anemone Garden during NEM transition period. The seabed of North Siwa was the most turbid at the end of SWM and NEM Transition, while Anemone Garden had the lowest across all three sampling periods.

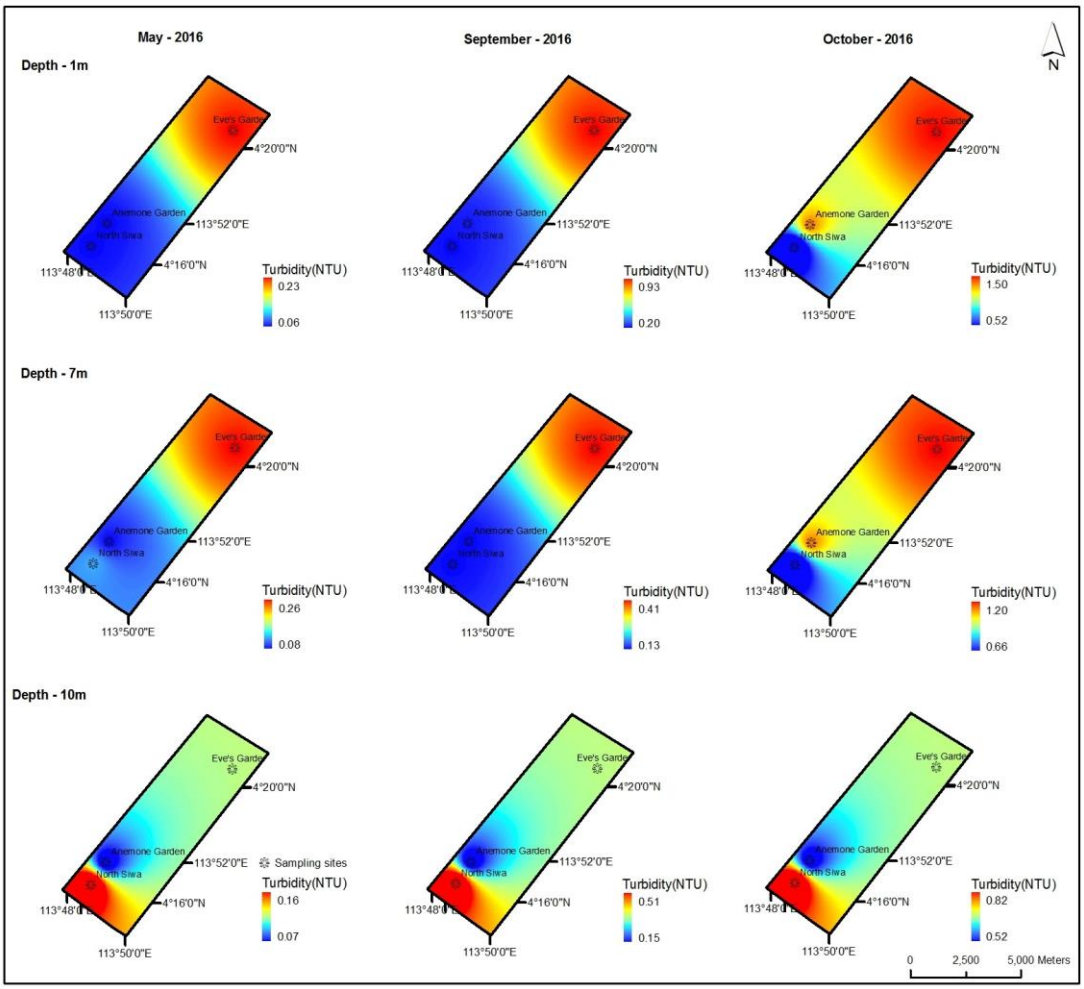

Figure 4.1.6 - Spatial Variation of Turbidity at MSCRNP

4.1.7 Total Dissolved Solids (TDS)

The analysis of trace metals required the samples to be filtered by a 0.45µm filter. In general, anything retained by a filter of size 2.0µm or smaller is taken as suspended solids and what goes through the filter is known as Total Dissolved Solids (TDS) (APHA, 2012; Measurements, 2016a). Furthermore, TDS is proportional to the salinity of seawater together with the concentration of dissolved organic matter. The unit of measurement is mg/L but in this study, the unit of measurement was g/L.

The maximum value observed in the beginning of SWM was 18.43g/L at the seabed of North seabed. The minimum value for the same season was found to be 18.02g/L at Eve's Garden surface. The average of all three sites was 18.28g/L.

The end of SWM showed the maximum value of 23.90g/L at North Siwa seabed, while the lowest value, 23.37g/L was noted at the surface of Eve's Garden. Combining all three sites, the average of that period was 18.28g/L.

NEM transition season did not differ from the end of SWM with a maximum value of 23.47g/L at the seabed of Anemone Garden and the surface of North Siwa. The minimum recorded value was 22.47g/L noted at the surface of Eve's Garden. The average for the season combining all three sites was 23.14g/L.

The concentration of TDS at Sipadan was mostly uniform at both Barracuda Point and South Point. The peak TDS value, 23.90g/L at Barracuda Point was noted at the seabed while the middle and surface, both show a value of 23.80g/L. South Point values were not very far from that of Barracuda Point with 23.83g/L at the seabed and 23.73g/L at the surface.

At the start and finish of SWM, the surface of North Siwa observed the highest concentrations of TDS while during NEM transition, Eve's Garden had the highest value. North Siwa, consistently, had the highest TDS value at the middle depth throughout all sampling periods. This was also the case at the seabed but only during the commencement and end of SWM. The highest TDS value at Anemone Garden was only observed at the middle depth during the end of SWM together with North Siwa, and at the seabed during NEM transition as shown in Figure 4.1.7.

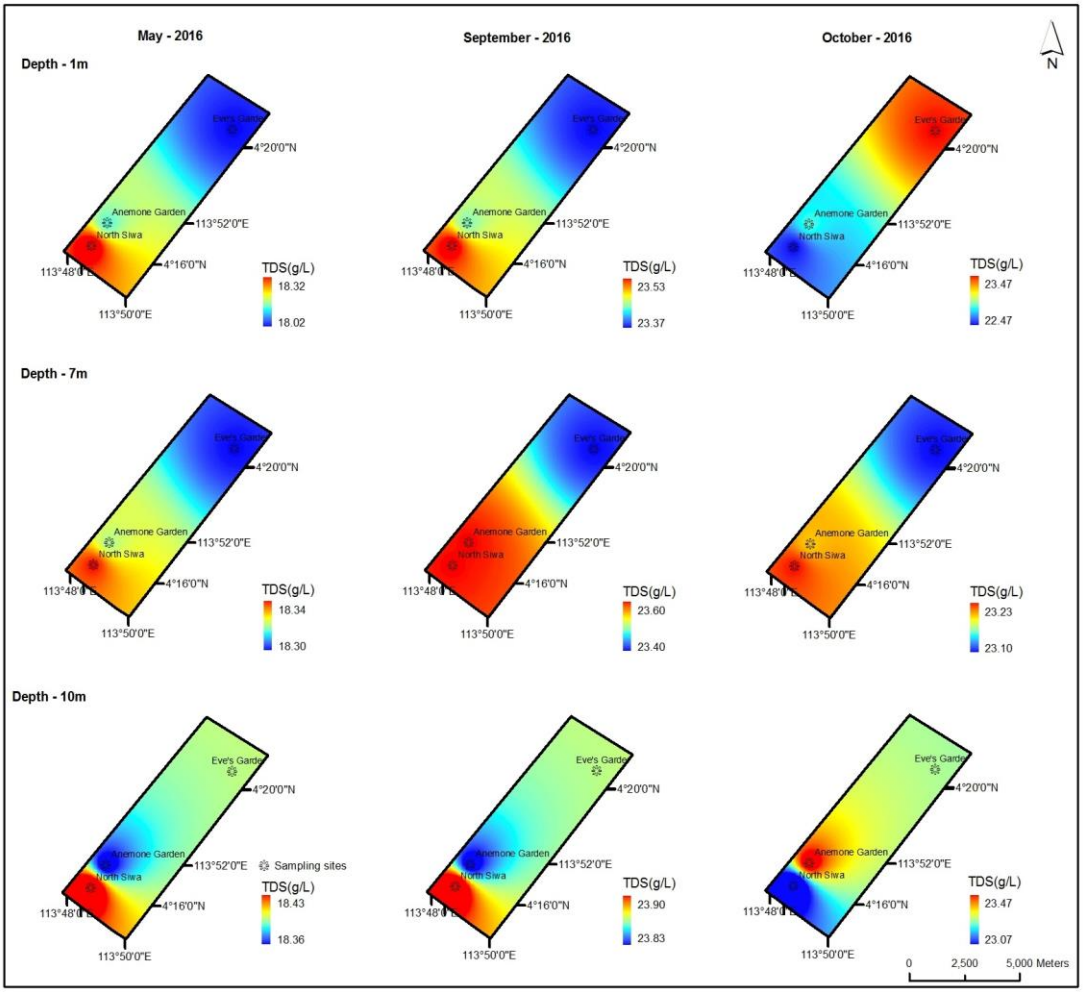

Figure 4.1.7 - Spatial Variation of TDS at MSCRNP

4.1.8 Dissolved Oxygen (DO)

DO refers to free oxygen molecules (O_2) present in seawater that has not reacted or bonded to any other element. The oxygen present in seawater is usually a by-product of photosynthesis from phytoplankton, algae, seaweed and other aquatic plants. The amount of oxygen present in seawater is important for the organisms living it in, and its quality (Measurements, 2016b).

During beginning of SWM, the highest recorded value for DO was 8.68mg/L at the middle of North Siwa. The lowest value for that season was observed at Eve's Garden surface with a value of 7.50mg/L and the average among all the sites was noted as 8.11mg/L.

The end of SWM showed a high value of 8.62mg/L at the middle of Anemone Garden. The minimum value was noted as 7.26mg/L at the seabed of North Siwa. The average value among all the sites during that period was 7.83mg/L.

The NEM transition period had a maximum value of 8.18mg/L measured at the surface of North Siwa, while a minimum value of 7.65mg/L was noted at the seabed of the same site. The average DO among all the sites was calculated as 7.92mg/L.

The maximum value for DO, at Sipadan, was measured at the surface Barracuda Point with a value of 9.63mg/L. The minimum value at the same site was 8.19mg/L at the seabed. South Point measured a high value of 8.27mg/L and a low value of 7.84mg/L.

The concentration of DO, as depicted in Figure 4.1.8, showed the high concentrations of DO being mostly at Anemone Garden and North Siwa and the low values at Eve's Garden. The surface of Anemone Garden only had the lowest DO reading during the NEM transition period. The seabed of North Siwa registered the lowest values throughout all sampling periods while Anemone Garden had the highest value at the same depth.

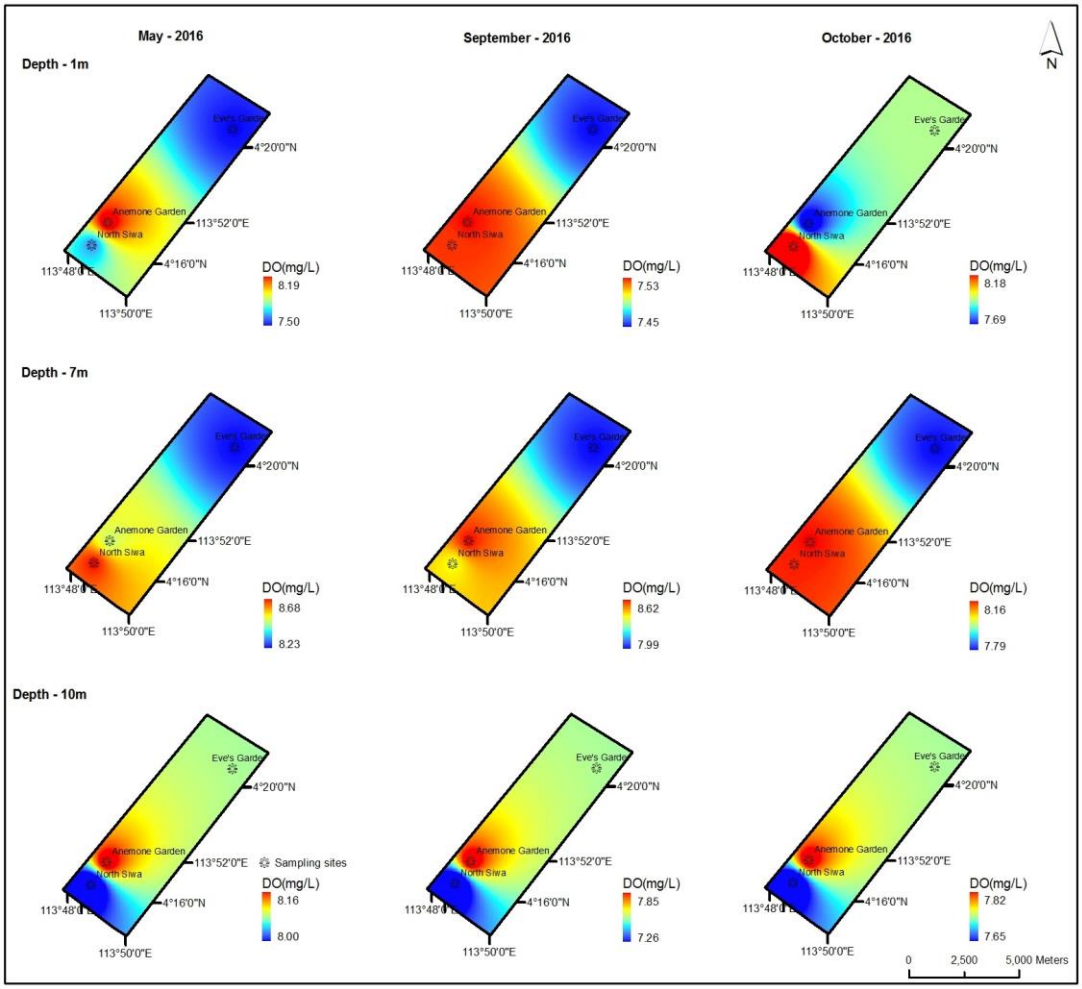

Figure 4.1.8 - Spatial Variation of DO at MSCRNP

4.1.9 Summary

Tables 4.1.1 to 4.1.3 summarise the in-situ parameters for all the sites in MSCRNP during start and end of SWM, and NEM transition. From the tables, it was observed that the values that showed an increase in their average from the beginning of SWM season to NEM transition period were temperature, EC, salinity, turbidity and TDS. North Siwa observed a depth-wise decrease in temperature at both beginning and end of SWM period, while Anemone Garden and Eve's Garden had the opposite pattern only for the start and end of SWM respectively. Eve's Garden noted an increase in temperature from surface to seabed at the start of SWM and Anemone Garden decreased towards the middle layer and then increased again at the seabed. EC noted a decrease from surface to seabed at North Siwa and Eve's Garden only during NEM transition period. During start and end of SWM, all the sites had increasing EC values

from surface to seabed, including Anemone Garden during the transition period. A decrease in salinity from surface to seabed was observed at Anemone Garden and North Siwa during start of SWM and NEM transition period respectively. All the other sites had increasing salinity from surface to seabed during the three seasons. Turbidity had the most variations both from surface to seabed and during the three seasons as compared to the other in-situ parameters. At the beginning of SWM, turbidity increased from surface to seabed at North Siwa and Eve's Garden but Anemone Garden had a higher turbidity value at the middle depth. During the end of SWM, lower turbidity values were observed at the middle layer of North Siwa and Anemone Garden. NEM transition period observed increasing turbidity only at North Siwa while the opposite occurred at Anemone Garden and Eve's Garden. TDS concentration increased from surface to seabed at all the sites from the beginning to the end of SWM. However, during NEM transition, TDS decreased depth-wise at North Siwa and Anemone Garden had a higher concentration at the middle layer. The parameters that experienced a decrease were pH, ORP and DO. These parameters noted a lower average at the end of SWM than NEM transition. The pH values were higher at the start of SWM as opposed to the other seasons; however, depth-wise, a decrease was observed at Anemone Garden only while North Siwa had the same pH reading at both surface and seabed but a lower reading at the middle layer and Eve's Garden did not differ much. During the end of SWM, the pH values was higher at the middle depth of North Siwa and that of Anemone Garden was lower at the same depth. During NEM transition, an increase in pH was observed at North Siwa but the opposite was noted at both Anemone Garden and Eve's Garden. ORP values were observed to be lower at the middle depth of Anemone Garden at the start of SWM while the values at North Siwa increased with depth and that of Eve's Garden, decreased. The end of SWM showed a higher ORP value at the middle layer of North Siwa but a lower value at Anemone Garden, though all three sites had a higher value at the surface than at the seabed. North Siwa was the only site to have a decreasing ORP value from surface to seabed during NE while that of Anemone Garden and Eve's Garden increased. The concentration of DO was observed to be higher at the middle depth during all three seasons except for North Siwa during NEM transition. Except for the middle layer, the DO value between the surface and seabed was observed to be higher at North Siwa and Eve's Garden during commencement of SWM; Anemone Garden and Eve's

Garden during end of SWM; Anemone Garden during the transition to NEM. Figures 4.1.1 to 4.1.8 help visualise the variations of the physico-chemical parameters in Miri.

The in-situ parameters from Sipadan Island (Table 4.1.4) that had a higher average than the three sites in Miri during northeast monsoon transition period were pH, EC, salinity, TDS and DO. The parameter with lower average than Miri were temperature, ORP and turbidity. At Barracuda Point, the parameters that had increasing values from surface to seabed were pH, EC, salinity, turbidity and TDS. The EC and salinity values at South Point were constant at both surface and seabed and the values that increased were pH and TDS. Turbidity decreased from surface to seabed at South Point while ORP and DO both had decreasing depth-wise values at Barracuda Point and South Point.

Table 4.1.1 – Physical Parameters Measured at MSCRNP

(Start of SWM)

Location	Depth (m)	Temperature (°C)	pH	EC (mS/cm)	Salinity (ppt)	ORP (mV)	Turbidity (NTU)	TDS (g/L)	DO (mg/L)
North Siwa	*1.0*	29.1	8.41	37.4	23.70	-61.7	0.06	18.32	7.63
	7.5	28.9	8.35	37.4	23.70	-59.1	0.12	18.34	8.68
	14.7	28.5	8.41	37.6	23.80	-55.3	0.16	18.43	8.00
Anemone Garden	*1.0*	30.1	8.36	37.0	23.70	-60.3	0.06	18.12	8.19
	6.0	30.1	8.31	37.4	23.70	-60.7	0.08	18.32	8.48
	9.5	29.9	8.25	37.5	23.40	-57.6	0.07	18.36	8.16
Eve's Garden	*1.0*	30.4	8.36	36.8	23.30	-62.9	0.23	18.02	7.50
	6.0	30.5	8.37	37.3	23.60	-63.9	0.26	18.30	8.23

Table 4.1.2 – Physical Parameters Measured at MSCRNP

(End of SWM)

Location	Depth (m)	Temperature (°C)	pH	EC (mS/cm)	Salinity (ppt)	ORP (mV)	Turbidity (NTU)	TDS (g/L)	DO (mg/L)
North Siwa	*1.0*	30.6	7.76	48.0	31.5	-53.7	0.20	23.53	7.53
	7.0	29.6	8.07	48.9	32.1	-68.6	0.13	23.60	8.41
	16.2	29.7	8.02	49.3	32.4	-66.0	0.51	23.90	7.26
Anemone Garden	*1.0*	30.1	8.04	48.4	31.8	-67.5	0.21	23.43	7.53
	5.0	29.9	8.01	48.8	32.0	-65.7	0.13	23.60	8.62
	10.0	30.2	8.06	49.3	32.4	-68.5	0.15	23.83	7.85
Eve's Garden	*1.0*	30.7	7.98	48.3	31.6	-63.8	0.93	23.37	7.45
	6.0	30.3	8.06	48.4	31.6	-67.7	0.41	23.40	7.99

Table 4.1.3 – Physical Parameters Measured at MSCRNP (NEM Transition)

Location	Depth (m)	Temperature (°C)	pH	EC (mS/cm)	Salinity (ppt)	ORP (mV)	Turbidity (NTU)	TDS (g/L)	DO (mg/L)
North Siwa	*1.0*	30.0	8.03	48.9	31.6	-62.0	0.52	23.47	8.18
	8.0	30.0	8.06	48.5	31.3	-64.1	0.66	23.23	8.16
	15.9	30.0	8.15	48.1	31.0	-69.0	0.82	23.07	7.65
Anemone Garden	*1.0*	30.0	8.13	48.0	30.9	-68.2	1.39	23.10	7.69
	6.3	30.0	8.02	48.2	31.0	-61.7	1.14	23.20	8.16
	12.3	30.0	8.00	48.9	31.6	-60.4	0.62	23.47	7.82
Eve's Garden	*1.0*	30.0	8.13	46.9	30.2	-67.8	1.50	22.47	7.90
	6.6	30.0	8.03	48.2	31.1	-62.1	1.20	23.10	7.79

Table 4.1.4 – Physical Parameters Recorded at Sipadan Island Park

Location	Depth (m)	Temperature (°C)	pH	EC (mS/cm)	Salinity (ppt)	ORP (mV)	Turbidity (NTU)	TDS (g/L)	DO (mg/L)
Barracuda Point	*1.0*	29.0	8.10	50.9	33.10	-66.9	0.10	23.80	9.63
	8.7	29.0	8.14	50.9	33.10	-69.5	0.27	23.80	8.70
	16.2	29.0	8.17	51.0	33.20	-70.9	0.30	23.90	8.19
South Point	*1.0*	29.0	8.08	50.7	32.97	-65.6	0.30	23.73	8.27
	6.0	29.0	8.09	50.7	32.97	-66.7	0.18	23.83	7.84

4.2 Major Ions

4.2.1 Bicarbonate (HCO_3^-)

The presence of carbon dioxide is what creates bicarbonate. Carbon dioxide molecules loosely bond with the water molecules to form bicarbonate. In the process, carbonic acid is also formed which is also responsible for the acidification of the ocean. (Anthoni, 2006; Drupp, 2015)

The data gathered in this study shows an increasing trend in the average concentration of bicarbonate from the start of SWM to NEM transition. At the start of SWM, the highest concentration of bicarbonate was 105.73mg/L at North Siwa seabed. The minimum concentration was noted at the middle depth of North Siwa with a value of 87.43mg/L. The average concentration from the three sites was 96.58mg/L.

The end of SWM shows a higher maximum value than NEM transition with a concentration of 146.40mg/L at the surface of Anemone Garden. The lowest value from this particular period was 101.67mg/L at the seabed of Anemone Garden. The average from all the three sites was 116.41mg/L.

During NEM transition period, a maximum value of 130mg/L for the concentration of bicarbonate at Anemone Garden's surface as well as Eve's Garden Seabed. The minimum value was 115.9mg/L, noted at the middle depth of North Siwa. The average from all three sites for that season was 123.02mg/L.

At Sipadan Island Park, bicarbonate levels show slightly more elevated concentrations than Miri during transition to NEM. The maximum concentration of bicarbonate noted at the surface and middle depth of Barracuda Point was 140.30mg/L and the lowest concentration of 132.17mg/L at the seabed. At South Point, a maximum value of 132.17mg/L was measured at the surface and a minimum of 130.13mg/L at the seabed.

Looking at Figure 4.2.1, the spatial maps show that, even though the concentration of bicarbonate varied at each site, the distribution however, remained quite similar over the sampling periods. North Siwa had the lowest concentration of bicarbonate at the surface and the middle depth from beginning of SWM to NEM transition, while the highest concentrations were found at the seabed of Eve's Garden. The lowest concentrations were found at the seabed of Anemone Garden at the start and end of SWM. The seabed of both North Siwa and Anemone Garden had the same concentration of bicarbonate.

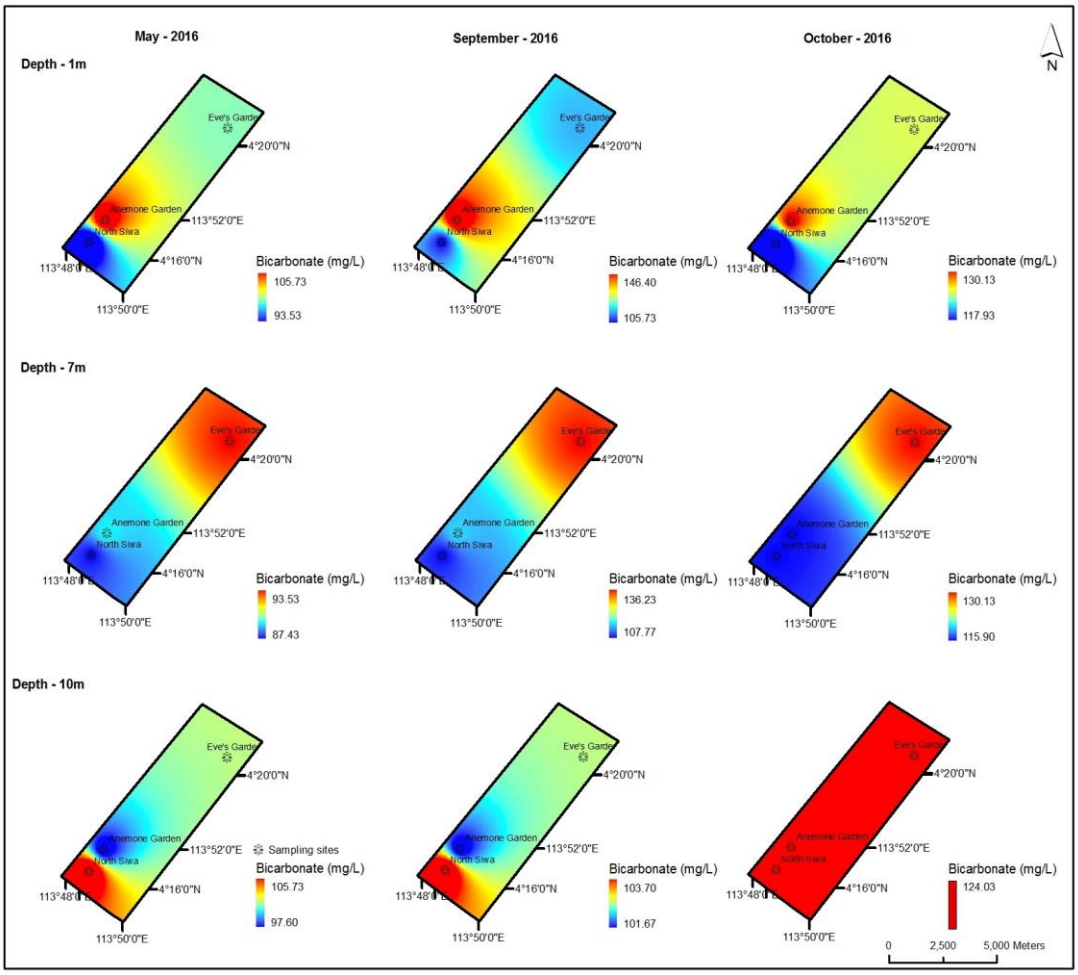

Figure 4.2.1 - Spatial Variation of Bicarbonate at MSCRNP

4.2.2 Calcium (Ca^{2+})

Based on the periodic table, calcium is found in the second group and it has a valence of 2, an atomic number of 20 and an atomic weight of 40. Calcium exists in the form of calcium carbonate and calcium-magnesium carbonate. The solubility of calcium carbonate is regulated by the pH and dissolved oxygen. Calcium is essential for the food of aquatic plants and animals. It is also a crucial component of corals, shells, limestone, bones and shell structures. Calcium also contributes to the total hardness of water (Rakestraw, 1943; APHA, 2012).

The concentration of calcium during beginning of SWM had a maximum value of 214.67mg/L at North Siwa Seabed. The lowest value among the three sites was noted

at the surface of Eve's Garden with a value of 193.33mg/L. The average value across the sites was 202.50mg/L.

The peak value measured at the end of SWM was 193.33mg/L at the seabed of Eve's Garden. The lowest value was 174.67mg/L measured at the seabed of Anemone Garden. The average of all the sites for that season was 184.50mg/L.

NEM Transition showed the highest concentration of calcium and the highest value measured at the surface of North Siwa was 237.33mg/L. The lowest value was 218.67mg/L at Anemone Garden seabed. Both the maximum and minimum value recorded during NEM transition period were higher than the beginning and end of SWM, therefore giving a higher average than the other two periods with a concentration of 226.83mg/L.

The concentration of calcium from Sipadan had a peak concentration of 392.00mg/L at the surface of Barracuda point. The lowest value was measured at the seabed with a concentration of 386.67mg/L. The values measured at South Point were 389.33mg/L at the surface and the 360.00mg/L at the seabed.

Figure 4.2.2 shows the variation in concentration of calcium both spatially and temporally. The figure shows that, at the surface, the concentration of calcium is highest at North Siwa during commencement of SWM and NEM transition, and Eve's Garden during the transition period. North Siwa also had the highest concentration of calcium from surface to seabed at the start of SWM, while Anemone Garden had the lowest concentration from surface to seabed at the end of it. The concentration of calcium was highest at the seabed of Eve's Garden and North Siwa. Anemone Garden recorded most of the lowest values throughout all the seasons and depths, for calcium.

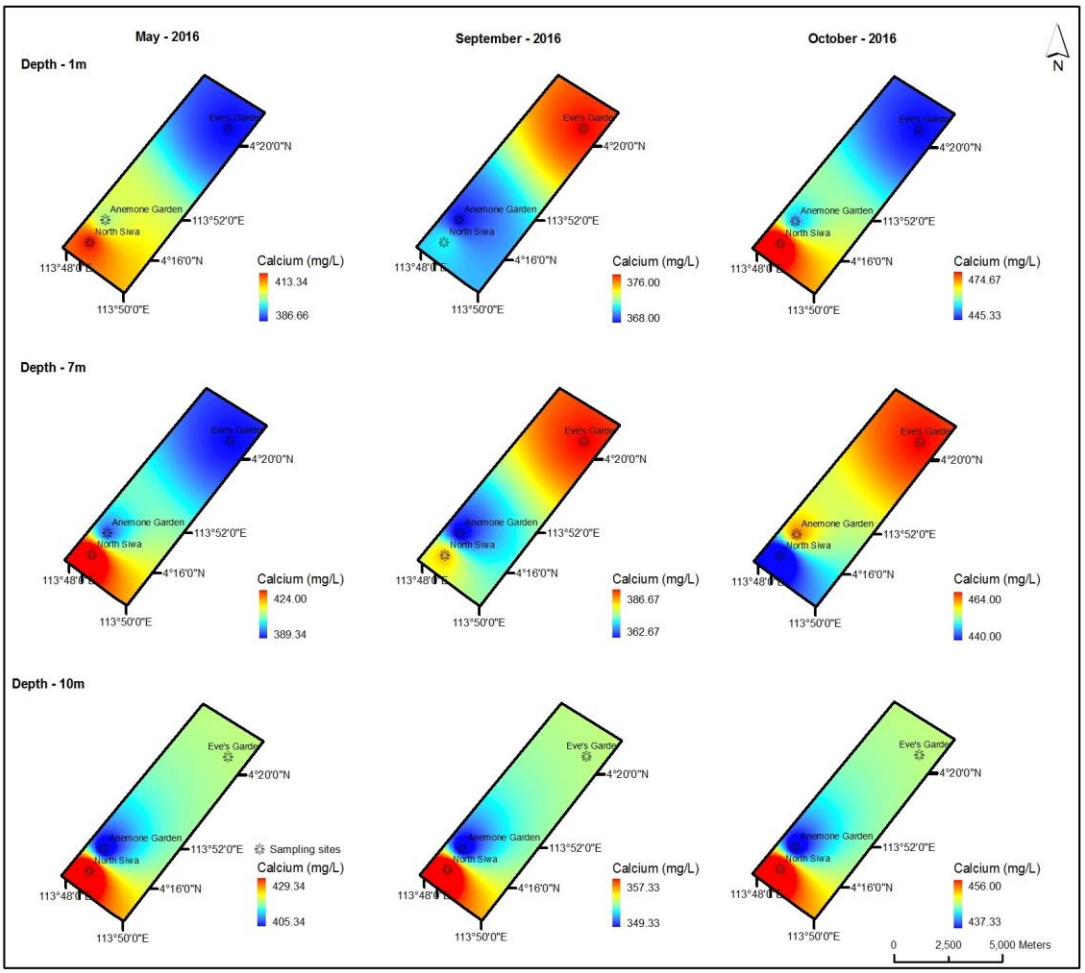

Figure 4.2.2 - Spatial Variation of Calcium at MSCRNP

4.2.3 Magnesium (Mg^{2+})

Magnesium is the second element in group two of the periodic table. It has a valence of 2, atomic number 12 and atomic weight of 24. This element can be found in natural water and similar to calcium, it is a contributor to water hardness. Magnesium usually occurs in minerals such as dolomite and magnesite. The ion is also a major constituent of marine sediments similar to calcium and is also more abundant than calcium (Rakestraw, 1943; APHA, 2012).

The concentration of magnesium during the beginning of SWM was found to be the highest at the middle depth of North Siwa with a value of 668.8mg/L. The minimum value was 626.4mg/L at the surface and middle of Anemone Garden. The average value from all three sites was 641.80mg/L.

During the end of SWM, the maximum magnesium concentration was found at the seabed of North Siwa with a value of 631.2mg/L. The lowest value registered was 553.6mg/L at the seabed of Anemone Garden. The average from all three sites was a concentration of 600.8mg/L.

NEM transition period showed a maximum concentration of 596.8mg/L at the seabed of Anemone Garden and a minimum value of 568.0mg/L at Eve's Garden surface. The average concentration of magnesium from all three sites was 584.1mg/L.

The concentration of magnesium was quite consistent at Sipadan with a highest concentration of 1297.60mg/L at the surface of Barracuda Point and the lowest being 1276.80mg/L at the seabed and middle depth. South Point values were quite close to Barracuda Point with concentrations of 1286.40mg/L measured at the surface and 1291.20mg/L at the seabed.

The concentration of magnesium had similarities to the concentration of calcium observed in the previous section. As seen in Figure 4.2.3, the highest concentration of magnesium was mostly observed at North Siwa during the beginning of SWM and throughout all the seasons at the middle depth of the site. The only high concentration observed at Eve's Garden was at the surface, during the end of SWM. Anemone Garden was the site with the lowest concentration of magnesium during beginning and end of SWM.

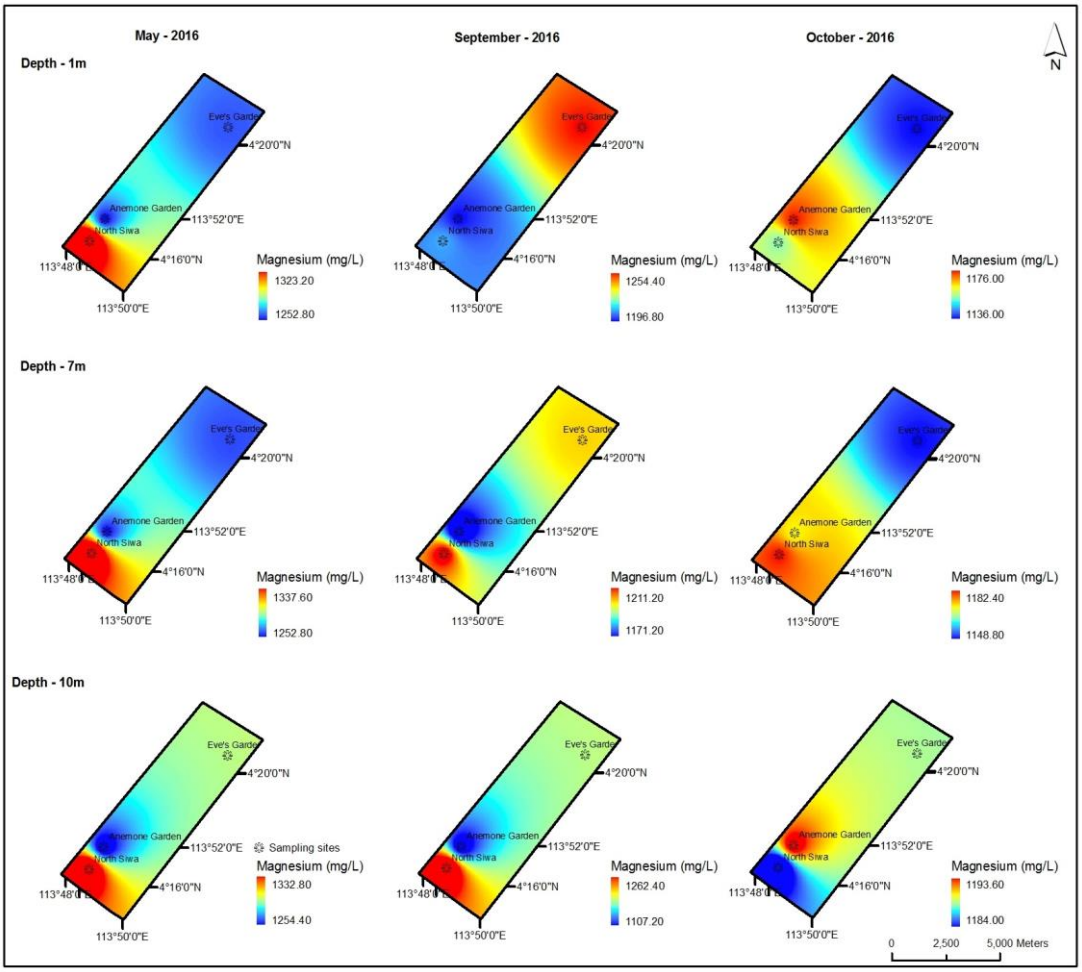

Figure 4.2.3 - Spatial Variation of Magnesium at MSCRNP

4.2.4 Potassium (K^+)

Potassium, located in Group 1A, is the fourth element in the periodic table. It only has a valence of 1, atomic number 19 and an atomic weight of 39.10 (APHA, 2012). Potassium is found abundantly in seawater and finds its way there in the form of minerals. It is a very important nutrient for most organisms and plays a pivotal role in the algal growth (Lenntech, 2017j)

The concentration of potassium during the start of SWM period was relatively stable with a peak value of 379.0mg/L observed at the middle layer of North Siwa and the seabed of Eve's Garden. The lowest concentration was 366.8mg/L measured at the middle depth of Anemone garden. The average concentration for that period was 373.85mg/L.

During the end of SWM, the highest concentration of potassium was 390.0mg/L, slightly higher than the beginning at the seabed of Eve's Garden. The lowest value was 248.6mg/L at the surface of Anemone Garden. The average concentration of 344.98mg/L was noted across all three sites for that sampling period.

The NEM transition period showed little variation in the concentration of potassium. The maximum reading measured 390.8mg/L at the surface of North Siwa and the lowest value of 361.4mg/L was noted at the surface of Eve's Garden. The average value for the transition period was 374.05mg/L which was close to the value observed during the beginning of SWM.

The maximum concentration of potassium measured at Barracuda Point in Sipadan Island was 392.0mg/L at the seabed. The lowest concentration at the surface was 368.2mg/L. South Point had a concentration of 376.4mg/L at the surface and 396.8mg/L at the seabed. The average concentration at Sipadan was 382.7mg/L which was slightly more than Miri.

Based on the spatial maps from Figure 4.2.4, North Siwa showed the highest concentration of potassium at the seabed throughout the seasons while Anemone Garden had the lowest reading. The seabed of the shallowest site, Eve's Garden observed a high value of potassium at the end of SWM and NEM transition, and for the same period, Anemone Garden had the lowest concentration at the middle depth. The figure also seems to indicate a transition in high concentration from the surface of Anemone Garden to the seabed of North Siwa during beginning of SWM.

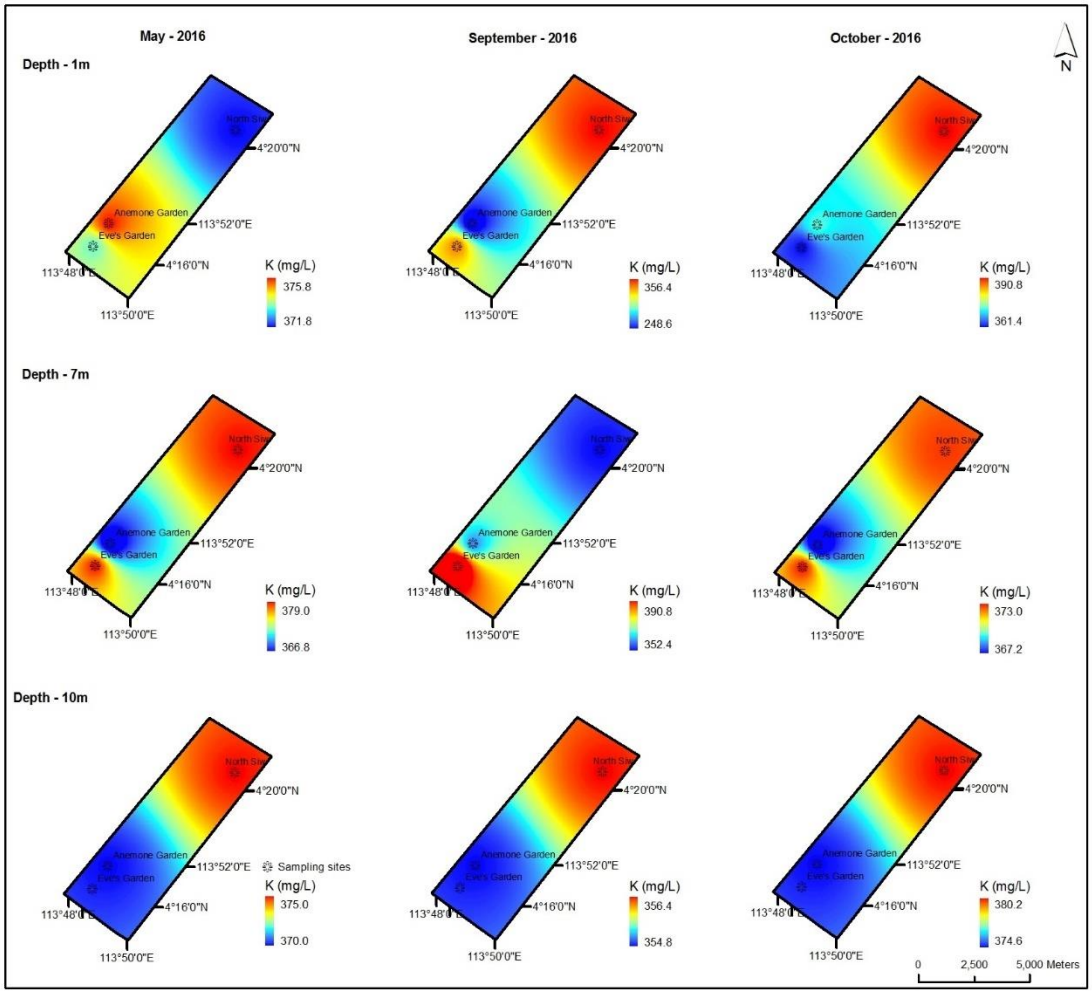

Figure 4.2.4 - Spatial Variation of Potassium at MSCRNP

4.2.5 Sodium (Na^+)

Sodium finds itself in Group 1A of the periodic table. This soft metal has an atomic number of 11, an atomic mass of 22.99 and a valence of 1 (APHA, 2012). With an approximate concentration of 10,000 mg/L, sodium is one of the most abundant elements in seawater and exists mostly as sodium chloride, also known as kitchen salt (Lenntech, 2017k).

The maximum concentration of sodium during beginning of SWM sampling was 15760.0mg/L at the surface of Anemone Garden. The lowest value was 10260.0mg/L at the middle depth of the same site. The average of all three sites was 11750.0mg/L as the concentration of sodium for this particular period.

The end of SWM shows a decrease in the concentration of sodium in Miri. The maximum value was 11360.0mg/L at the seabed of Eve's Garden. The lowest value

was 6620.0mg/L at the surface of Anemone Garden. The average concentration from all three sites was 9457.5mg/L.

The maximum concentration of sodium recorded during NEM transition was 11380.0mg/L at the bottom of Anemone Garden. The lowest concentration was 10000.0mg/L, which was observed at the middle layer of North Siwa. When comparing all the sites, the transition period also had a lower average concentration of 10400.0mg/L, when compared to beginning of SWM but was still higher than the end of SWM.

As per the spatial maps in Figure 4.2.5, higher concentrations of sodium were observed at the seabed of Eve's Garden and Anemone Garden during the end of SWM and NEM transition. North Siwa had the highest value for sodium at the middle depth and seabed during the start of SWM season while, Anemone Garden observed the lowest value.

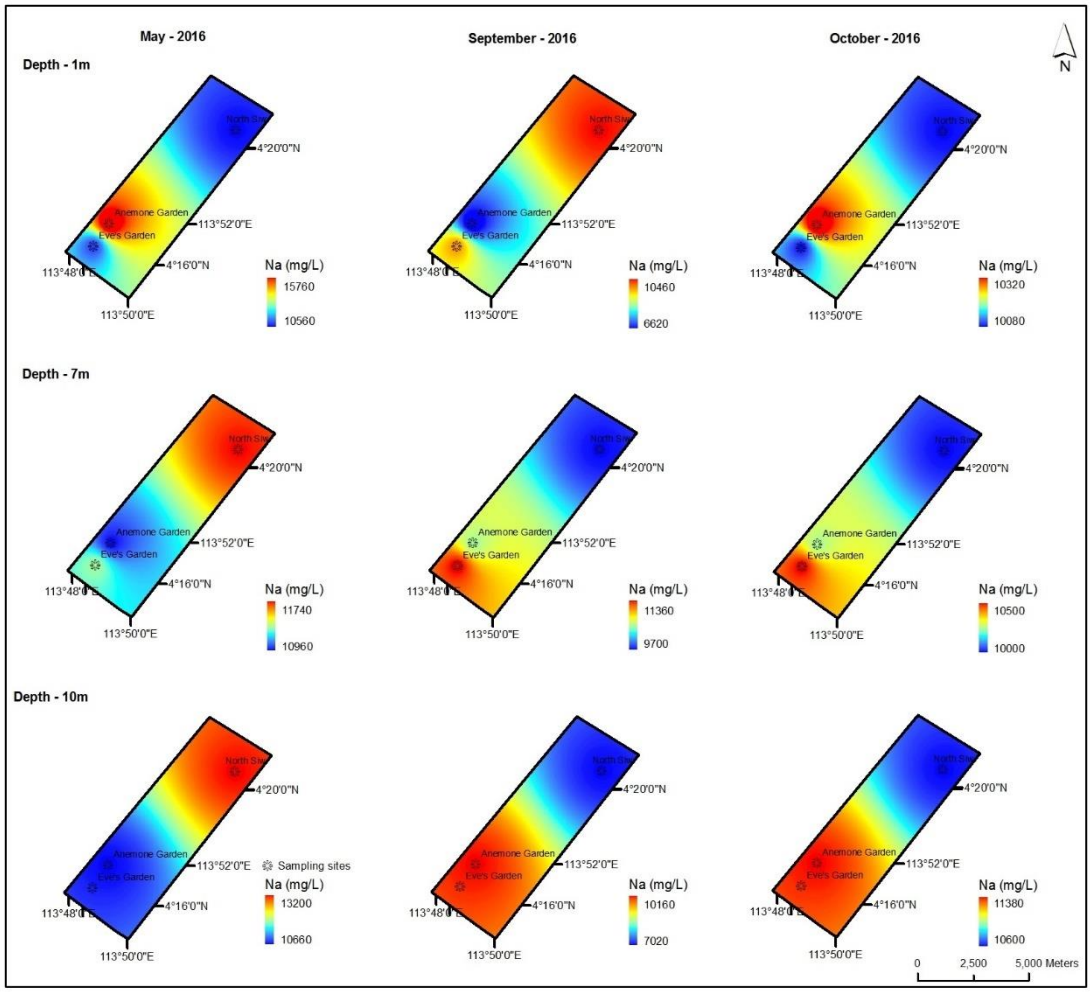

Figure 4.2.5 - Spatial Variation of Sodium at MSCRNP

4.2.6 Chloride (Cl^-)

The chloride ion present in seawater makes up to around 55% of the dissolved solids and are one of the major contributors of the ocean's salinity. Chloride ion are most commonly found in the form of sodium chloride or potassium chloride.

The concentration of chloride during the start of SWM showed a high concentration of 18342.4mg/L measured at the surface of Eve's Garden. The lowest concentration was measured at the surface of Anemone Garden with a value of 17905.2mg/L and the average among the three sites was 18103.887mg/L.

The end of SWM had a maximum chloride concentration of 17515.3mg/L found at the surface of Anemone Garden. The lowest value of that period was 16682.18mg/L, found at the seabed of Anemone Garden. The average value from all three sites was 17008.61mg/L.

NEM transition showed the lowest concentration when compared to the beginning and end of SWM with the highest value of 17403.00mg/L measured at the seabed of North Siwa. The lowest value was observed at the surface of Eve's Garden at 161.74mg/L. The average value of all three sites for the transition period was 16949.43mg/L.

Barracuda Point, in Sipadan maintained slight differences in chloride concentration from surface to seabed. South Point values were slightly lower than Barracuda Point. The highest concentration at Barracuda Point was 18454.68mg/L at the surface and lowest at the seabed with 18312.88mg/L.

From Figure 4.2.6, chloride concentration is only highest at the surface and seabed of Eve's Garden during the start of SWM. North Siwa had the highest concentration during the end of SWM and NEM transition. Anemone Garden had the lowest concentration of chloride only during the start of SWM at both the surface and the middle depth.

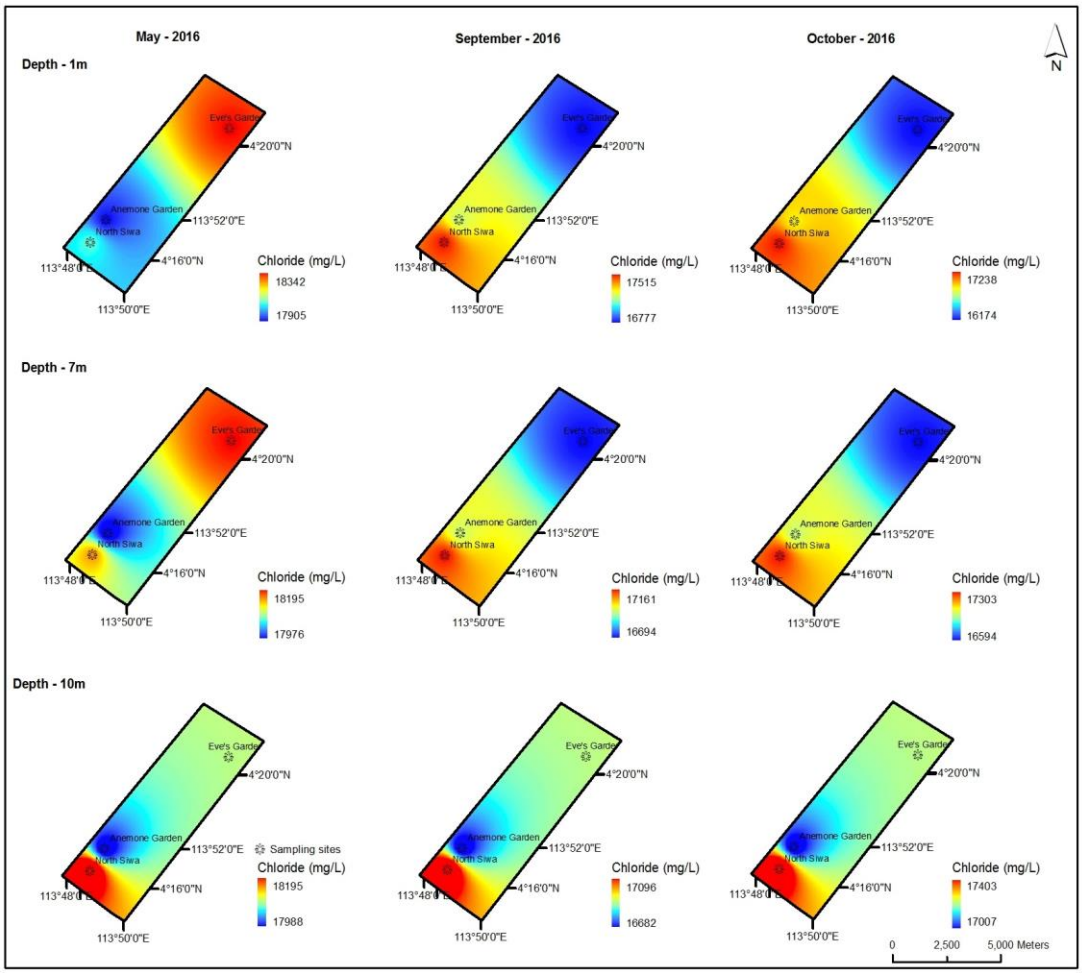

Figure 4.2.6 - Spatial Variation of Chloride at MSCRNP

4.2.7 Summary

In summary, all locations showed various concentrations that was spread among the sites. Higher concentrations of bicarbonate and calcium ion during the transition period, while the lowest concentrations were at the start of SWM. The concentration for magnesium and chloride were higher in beginning of SWM as compared to the transition period. The data gathered from the two sites at Sipadan had consistent values. Table 4.2.1 to 4.2.4 showcases the values discussed in the sections above. The spatial maps in Figures 4.2.1 to 4.2.6 indicate that higher concentrations of all ions were found at the seabed of North Siwa throughout the seasons except for magnesium during NEM transition. The lowest concentration of the ions was observed mostly at the seabed of Anemone Garden throughout all seasons as well. The major ions with the most fluctuations during the seasons were calcium and magnesium at the surface and the middle depth.

Table 4.2.1 – Concentration of Major Ions (mg/L) Analysed at MSCRNP (Start of SWM)

Location	Depth (m)	HCO_3^- (mg/L)	Ca^{2+} (mg/L)	Mg^{2+} (mg/L)	K^+ (mg/L)	Na^+ (mg/L)	Cl^- (mg/L)
North Siwa	*1.0*	93.53	413.34	1323.20	371.8	10560.0	18070.64
	7.5	87.43	424.00	1337.60	379.0	11740.0	18159.26
	14.7	105.73	429.34	1332.80	375.0	13200.0	18194.71
Anemone Garden	*1.0*	105.73	400.00	1252.80	375.8	15760.0	17905.20
	6.0	89.47	392.00	1252.80	366.8	10260.0	17976.10
	9.5	97.60	405.34	1254.40	370.0	10660.0	17987.92
Eve's Garden	*1.0*	99.63	386.66	1257.60	373.4	10860.0	18342.42
	6.0	93.53	389.34	1257.60	379.0	10960.0	18194.71

Table 4.2.2 – Concentration of Major Ions (mg/L) Analysed at MSCRNP (End of SWM)

Location	Depth (m)	HCO_3^- (mg/L)	Ca^{2+} (mg/L)	Mg^{2+} (mg/L)	K^+ (mg/L)	Na^+ (mg/L)	Cl^- (mg/L)
North Siwa	*1.0*	105.73	370.67	1209.60	356.4	10460.0	17515.25
	7.0	107.77	381.33	1211.20	352.4	9700.0	17160.75
	16.2	103.70	357.33	1262.40	356.4	7020.0	17095.76
Anemone Garden	*1.0*	146.40	368.00	1196.80	248.6	6620.0	17190.30
	5.0	115.90	362.67	1171.20	358.2	10480.0	16953.96
	10.0	101.67	349.33	1107.20	354.8	10160.0	16682.18
Eve's Garden	*1.0*	113.87	376.00	1254.40	342.2	9860.0	16776.71
	6.0	136.23	386.67	1200.00	390.8	11360.0	16694.00

Table 4.2.3 – Concentration of Major Ions (mg/L) Analysed at MSCRNP (NEM Transition)

Location	Depth (m)	HCO_3^-	Ca^{2+}	Mg^{2+}	K^+	Na^+	Cl^-
North Siwa	*1.0*	117.93	474.67	1153.60	390.8	10080.0	17237.56
	8.0	115.90	440.00	1182.40	372.8	10000.0	17302.55
	15.9	124.03	456.00	1184.00	380.2	10600.0	17403.00
Anemone Garden	*1.0*	130.13	450.67	1176.00	372.4	10320.0	16900.79
	6.3	115.90	461.33	1171.20	367.2	10240.0	16977.60
	12.3	124.03	437.33	1193.60	374.6	11380.0	17007.14
Eve's Garden	*1.0*	126.07	445.33	1136.00	361.4	10080.0	16174.06
	6.6	130.13	464.00	1148.80	373.0	10500.0	16593.55

Table 4.2.4 – Concentration of Major Ions (mg/L) Analysed at Sipadan Island Park

Location	Depth (m)	HCO_3^-	Ca^{2+}	Mg^{2+}	K^+	Na^+	Cl^-
Barracuda Point	*1.0*	140.30	392.00	1297.60	368.2	10640.0	18454.68
	8.7	140.30	389.33	1276.80	380.2	10800.0	18371.96
	16.2	132.17	386.67	1276.80	392.0	11100.0	18312.88
South Point	*1.0*	132.17	389.33	1286.40	376.4	11720.0	17993.83
	6.0	130.13	360.00	1291.20	396.8	10780.0	17987.92

4.3 Nutrients

4.3.1 Sulphate (SO_4^{2-})

Sulphate is a major constituent of seawater which is an indication of the presence of sulphur. It is a non-metallic element present from the precipitation of barium sulphate. Sulphate concentrations usually vary depending on the presence of river water which also contains a high concentration of sulphate (Rakestraw, 1943).

Sulphate concentration during the beginning of SWM was noted to have a maximum value of 2800mg/L measured at a depth of 6 meters at Anemone Garden. The lowest value recorded was 2000mg/L noted at North Siwa seabed and the average concentration of sulphate among all three sites was 2412.5m/L.

The end of SWM recorded a maximum sulphate concentration of 2350mg/L at the seabed and surface of North Siwa and Anemone Garden respectively. Anemone Garden recorded the lowest concentration of sulphate as 2100mg/L and the average from all sampled sites was 2281.2mg/L.

During the transition period, a maximum value of 6100mg/L for sulphate was found at the surface of Eve's garden. The lowest value was 1400mg/L at Anemone garden at a depth of 6.3m. All the sites together had an average concentration of 2712.5mg/L.

The two sites at Sipadan Island, showed consistent concentrations of sulphate. The maximum value at Barracuda Point was 2600mg/L at the seabed and minimum value of 2400mg/L at the surface and middle depth. The concentration of sulphate at South Point was 2400mg/L at the seabed and 2300mg/L at the surface.

Figure 4.3.1 shows the spatial and temporal distribution of the concentration of sulphate in the three sites. At the surface, the high sulphate concentration moves from North Siwa to Eve's Garden from beginning of SWM to NEM transition and the only period Eve's Garden had the highest concentration was during the end of SWM at the seabed. At the deeper sites, Anemone Garden had the highest value of sulphate during start of SWM and NEM transition. North Siwa had the highest concentration during the end of SWM.

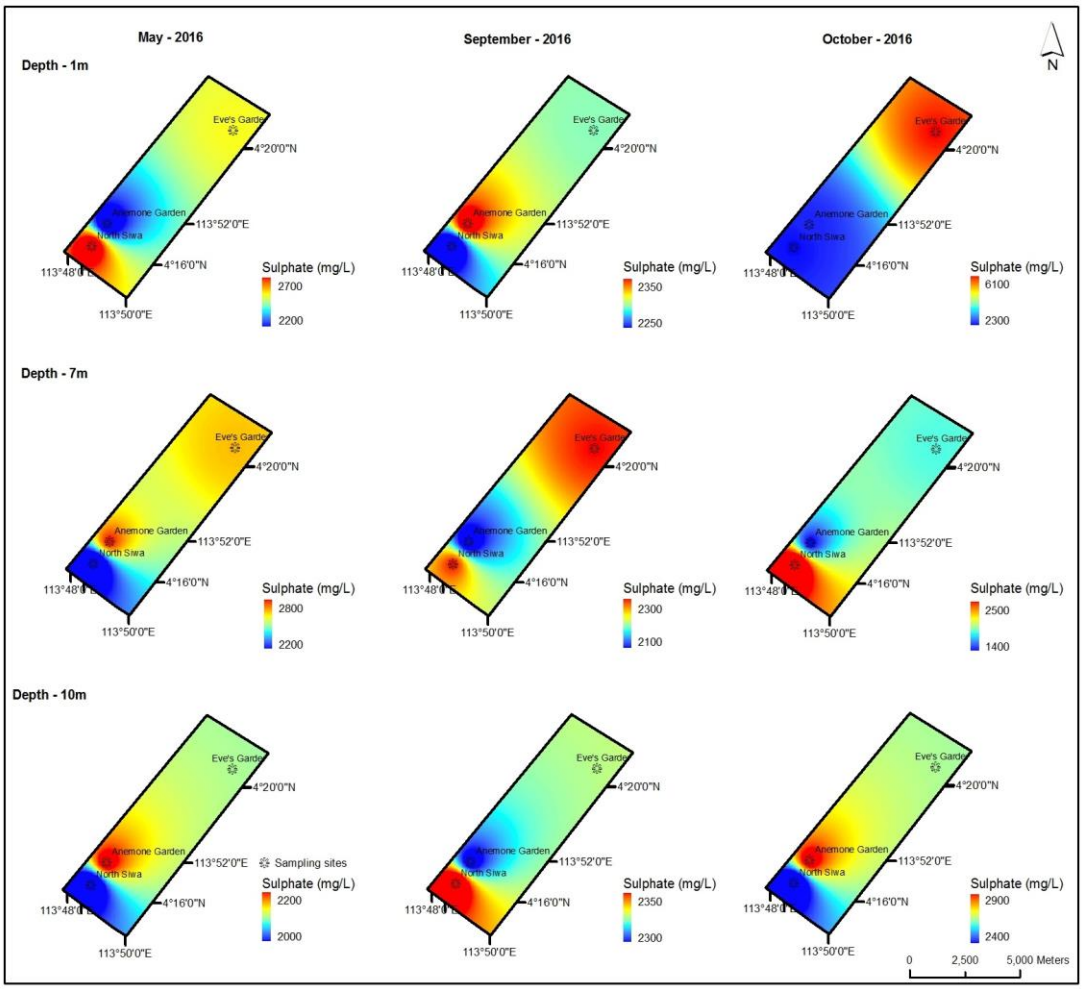

Figure 4.3.1 - Spatial Variation of Sulphate at MSCRNP

4.3.2 Phosphate (PO_4^{3-})

Phosphate is an important nutrient in seawater. It is needed by all organisms to produce food and usually bounds to planktons. Phosphate occurs in very low concentration in seawater. High concentrations of phosphate usually lead to an advance growth in plants.

The concentration of phosphate at the beginning of SWM was the highest at the seabed of Eve's Garden with a value of 0.04mg/L. A low value of 0.01mg/L was observed at all three sites starting at the surface of Eve's Garden, then at a depth of 6m at Anemone Garden and finally, at the seabed of North Siwa. The average value from all three sites was 0.02mg/L.

The end of SWM showed a maximum phosphate concentration of 0.14mg/L at the seabed of Eve's Garden. The lowest value was measured at the seabed of North Siwa with a value of 0.06mg/L, while the average from all three sites was 0.11mg/L.

The concentration of phosphate showed a dramatic increase from the beginning of SWM to NEM transition period. The highest concentration was 0.20mg/L at both the surface of Eve's Garden and North Siwa. The lowest value recorded was 0.09mg/L measured at the seabed of Eve's Garden. The overall average from the sites were higher than both the start and end of SWM with a value of 0.16mg/L.

Sipadan island showed a slight variation in the concentration of phosphate between Barracuda Point and South Point. The concentration of phosphate measured at Barracuda Point had a maximum value of 0.13mg/L at the surface and minimum of 0.08mg/L at the middle depth. South Point recorded a concentration of 0.02mg/L at both seabed and surface.

Figure 4.3.2 shows the variation of the concentration of phosphate spatially and temporally. The only consistency was found at the seabed of the deeper sites where the higher concentration was found at Anemone Garden and the lowest at North Siwa through all three sampling periods. North Siwa only had the highest phosphate concentration at the surface during the start of SWM. Eve's Garden maintained a maximum value at the surface during the end of SWM and transition period. The highest value was also observed at its seabed during start and end of SWM.

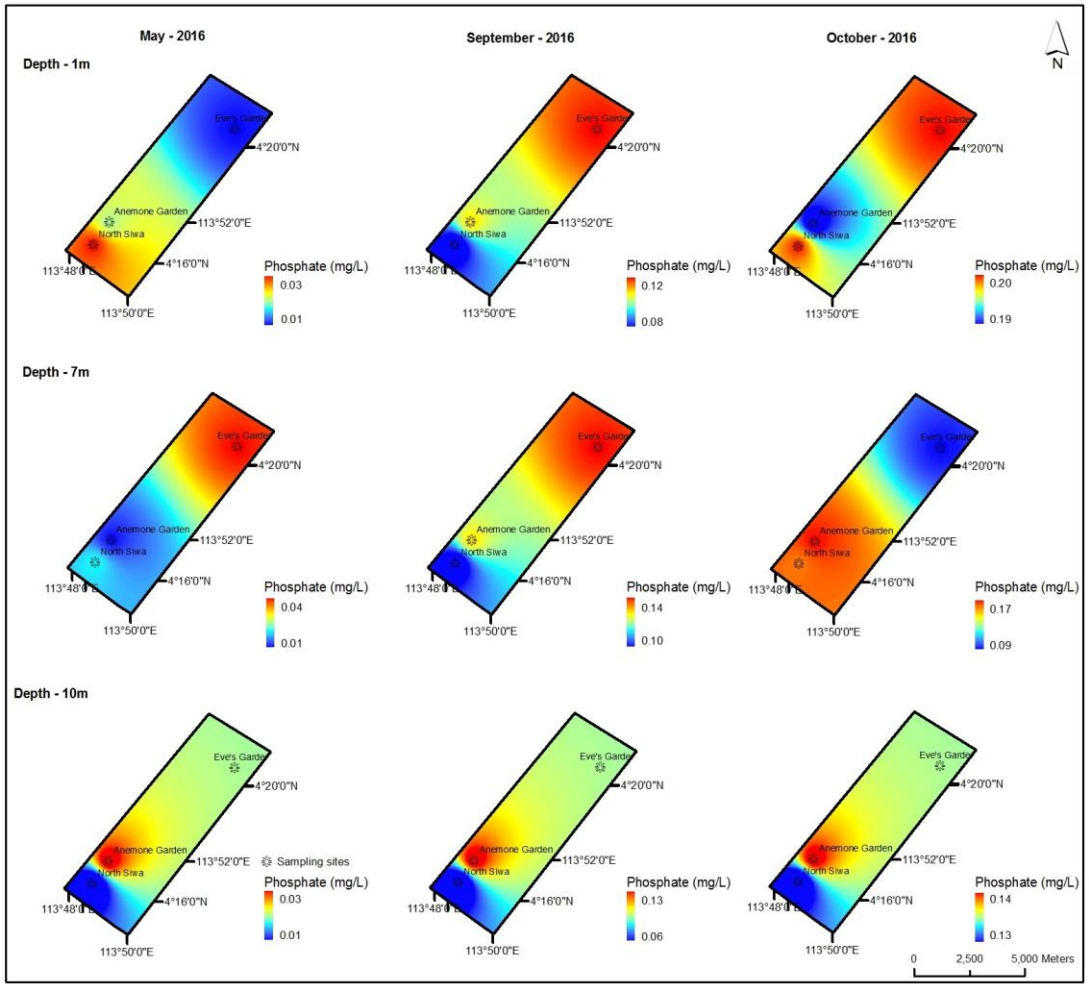

Figure 4.3.2 - Spatial Variation of Phosphate at MSCRNP

4.3.3 Ammonia-Nitrogen (NH_3^-N)

The study of ammonia-nitrogen is for the determination of ammonia in seawater. A high concentration of this compound would prove quite troublesome for the seawater due to its toxicity. Ammonia is one of the main causes of coral bleaching in seawater.

The highest concentration of Ammonia-Nitrogen was found during the start of SWM where the maximum value noted was 0.20mg/L at a depth of 6m at Anemone Garden. The surface of North Siwa had the lowest value of 0.06mg/L. The average from all three sites was 0.13mg/L during that period.

Eve's Garden surface had the highest concentration of Ammonia-Nitrogen at the end of SWM with a value of 0.09mg/L. The lowest value of 0.01mg/L was recorded at all three depths of North Siwa, surface and seabed of Anemone Garden and Eve's Garden respectively. The average concentration from all three sites was 0.03mg/L.

During NEM transition period, the highest concentration of Ammonia-Nitrogen was 0.11mg/L. This value was noted at both Anemone Garden and Eve's Garden at a depth of 6.3m at Anemone Garden, and the seabed of both sites. The average value from all three sites was 0.09mg/L.

Sipadan Island showed consistent values of Ammonia-Nitrogen concentration. Barracuda Point had a maximum concentration at the surface with a value of 0.12mg/L and a minimum concentration of 0.09mg/L at the middle level. The second site, South Point had the same concentration of 0.11mg/L at both seabed and surface levels.

Figure 4.3.3 shows the spatial and temporal variations of ammonia-nitrogen across all three sites. From the figure, it can be observed that the highest concentrations were generally at Anemone Garden during the transition period. Eve's Garden had the highest concentration at the surface at the start and end of SWM and at the seabed during transition period. North Siwa only experienced a high concentration at the seabed during the start of SWM.

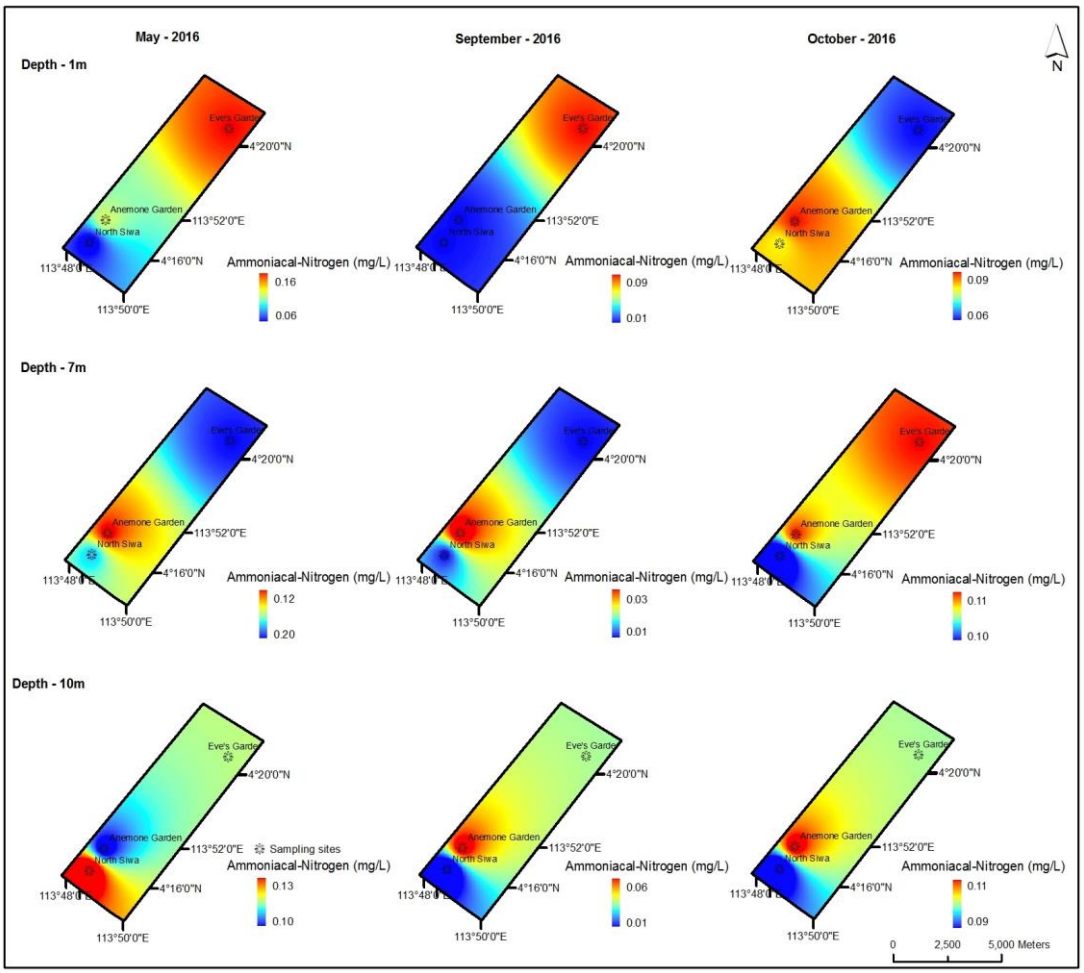

Figure 4.3.3 - Spatial Variation of Ammonia-Nitrogen at MSCRNP

4.3.4 Nitrate (NO_3^-)

Nitrates are usually found in low concentrations in seawater. When found in excess, nitrates can cause pollution and together with ammonia, is another cause of coral bleaching. Sources of this compound are usually from rivers washing up various kinds of nutrients and pollutants into the ocean.

The concentration of nitrate was relatively low throughout the beginning of SWM with a maximum value of 0.02mg/l measured at North Siwa seabed and mid depth, Anemone Garden surface and seabed and Eve's Garden surface and seabed. Similarly, the lowest concentration value of 0.01mg/L was measured at the surface of North Siwa and middle of Anemone Garden.

Similar to the start, the end of SWM showed a low concentration of nitrate with the only high value of 0.16mg/L at the surface of Eve's Garden. The lowest value

measured was 0.01mg/L at the seabed and surface of North Siwa. The average from all three sites showed a value of 0.04mg/L.

The transition period had a similar reading of maximum and minimum to that of the beginning of SWM where the peak concentration of 0.02mg/L was measured at the surface of Anemone Garden and North Siwa, and the seabed of all three sites. The average value for this season was 0.02mg/L with all sites combined.

Sipadan island had a uniform concentration of nitrate throughout both the investigated locations. The value measured at both Barracuda Point and South Point were 0.02mg/L at all depths.

As seen from the spatial maps in Figure 4.3.4, the concentration of nitrate at the three sites was quite erratic. The highest values were noted during the end of SWM at the surface of Eve's Garden and the seabed of Anemone Garden. The lower concentrations were noted at the seabed of North Siwa during beginning and end of SWM.

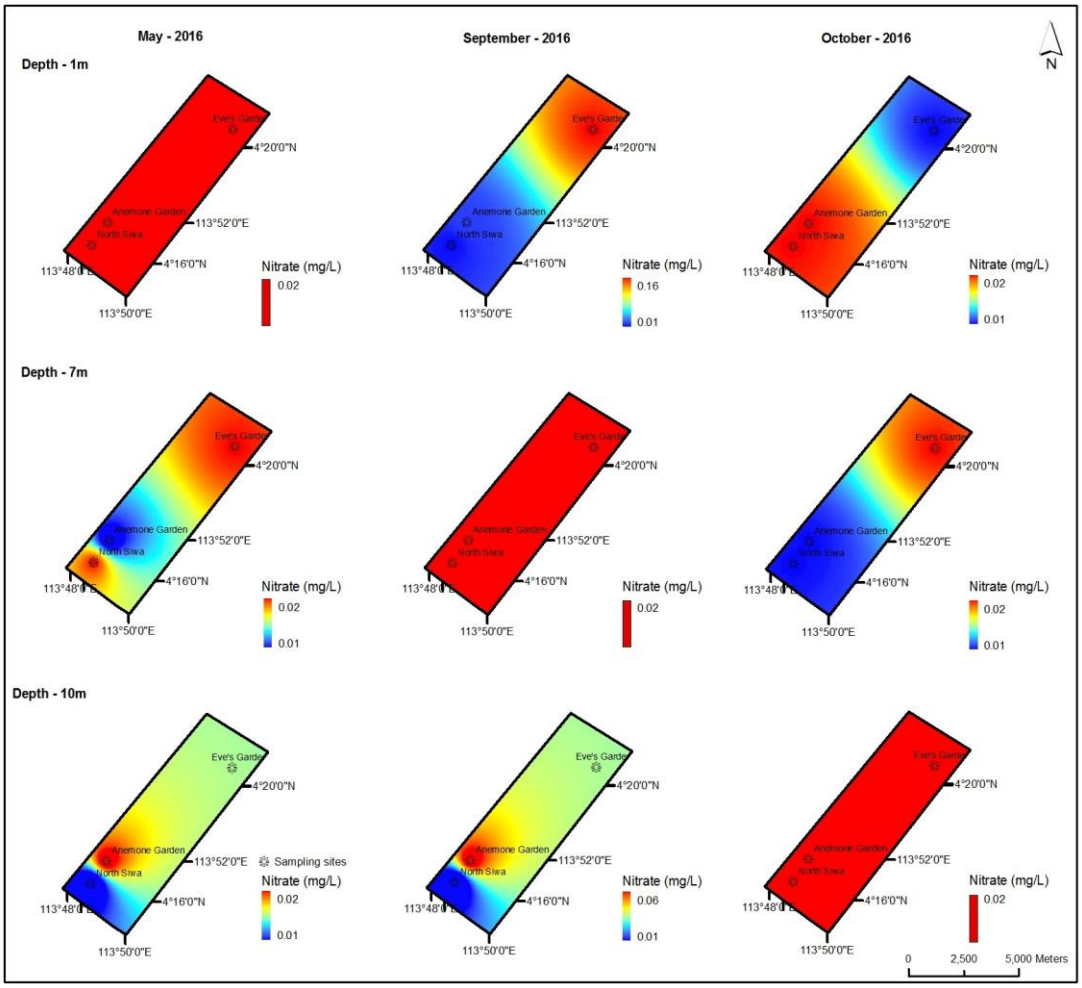

Figure 4.3.4 - Spatial Variation of Nitrate at MSCRNP

4.3.5 Summary

The concentration of nutrients throughout the three sites showed variations throughout the seasons (Tables 4.3.1 – 4.3.3). Higher concentrations of phosphate and nitrate were analysed during the end of SWM and NEM transition period rather than during beginning of SWM. The concentrations of ammonia-nitrogen and sulphate decreased from start of SWM to NEM transition. The concentration of nitrate peaked during the end of SWM where high values were noted at the surface of Eve's Garden and the seabed of Anemone Garden. Similar to nitrate, a high concentration of sulphate was noted at the surface of Eve's Garden and a very low value at the middle depth of Anemone Garden during the transition period. The data gathered at Sipadan Island (Table 4.3.7) had higher concentrations of phosphate, sulphate and ammonia-nitrogen at Barracuda Point than at South Point and a constant concentration of nitrate at both

sites. The spatial maps from Figures 4.3.1 to 4.3.4 show that higher concentration of sulphate was observed more at Anemone Garden and North Siwa. The concentration of phosphate detected was higher at Eve's Garden and Anemone Garden than North Siwa. Ammonia-nitrogen was observed at a higher concentration at Anemone Garden and the lowest concentration was found rather consistently at North Siwa. Nitrate concentration were highest at the seabed of Eve's Garden and Anemone Garden throughout the seasons.

Table 4.3.1 – Concentration of Nutrients (mg/L) Analysed at MSCRNP (Start of SWM)

Location	Depth (m)	Sulphate (SO_4^{2-})	Phosphate (PO_4^{3-})	Ammonia-Nitrogen (NH_3-N)	Nitrate (NO_3^-)
North Siwa	*1.0*	2700	0.03	0.06	0.02
	7.5	2200	0.02	0.14	0.02
	14.7	2000	0.01	0.13	0.01
Anemone Garden	*1.0*	2200	0.02	0.12	0.02
	6.0	2800	0.01	0.20	0.01
	12.0	2200	0.03	0.10	0.02
Eve's Garden	*1.0*	2500	0.01	0.16	0.02
	6.0	2700	0.04	0.12	0.02

Table 4.3.2 – Concentration of Nutrients (mg/L) Analysed at MSCRNP (End of SWM)

Location	Depth (m)	Sulphate (SO_4^{2-})	Phosphate (PO_4^{3-})	Ammonia-Nitrogen (NH_3-N)	Nitrate (NO_3^-)
North Siwa	*1.0*	2250	0.08	0.01	0.01
	7.0	2300	0.10	0.0.1	0.02
	16.2	2350	0.06	0.01	0.01
Anemone Garden	*1.0*	2350	0.11	0.01	0.02
	5.0	2100	0.13	0.03	0.02
	10.0	2300	0.13	0.06	0.06
Eve's Garden	*1.0*	2300	0.12	0.09	0.16
	6.0	2300	0.14	0.01	0.02

Table 4.3.3 – Concentration of Nutrients (mg/L) Analysed at MSCRNP NEM Transition

Location	Depth (m)	Sulphate (SO_4^{2-})	Phosphate (PO_4^{3-})	Ammonia-Nitrogen (NH_3-N)	Nitrate (NO_3^-)
North Siwa	*1.0*	2300	0.20	0.08	0.02
	8.0	2500	0.16	0.10	0.01
	15.9	2400	0.13	0.09	0.02
Anemone Garden	*1.0*	2400	0.19	0.09	0.02
	6.3	1400	0.17	0.11	0.01
	12.3	2900	0.14	0.11	0.02
Eve's Garden	*1.0*	6100	0.20	0.06	0.01
	6.6	1700	0.09	0.11	0.02

Table 4.3.4 – Concentration of Nutrients (mg/L) Analysed at Sipadan Island Park

Location	Depth (m)	Sulphate (SO_4^{2-})	Phosphate (PO_4^{3-})	Ammonia-Nitrogen (NH_3-N)	Nitrate (NO_3^-)
Barracuda Point	*1.0*	2400	0.13	0.12	0.02
	8.7	2400	0.08	0.09	0.02
	16.2	2600	0.11	0.10	0.02
South Point	*1.0*	2300	0.02	0.11	0.02
	6.0	2400	0.02	0.11	0.02

4.4 Trace Metals

4.4.1 Cadmium

Cadmium is found in the earth's crust, and in the periodic table, the metal is the second element in the Group 2B. the metal has an atomic number of 48, atomic weight of 112.41 and a valence of 2 (APHA, 2012). The presence of Cadmium in seawater is usually attributed to the use of phosphate fertilisers as well as industrial waste. The metal is also a by-product of zinc, lead and copper, and will also occur in small amounts as long as there are coastal developments (Lenntech, 2017a)

The concentration of cadmium during the start of SWM in Miri had a maximum value of 0.013mg/L measured at the surface and middle layer of Anemone Garden. The minimum value was 0.010mg/L at the middle layer of North Siwa. All the sites combined for that period gave an average concentration of 0.012mg/L.

The end of SWM had a maximum concentration of 0.021mg/L at the seabed of North Siwa. The lowest value was 0.012mg/L at the surface and seabed of Anemone Garden and Eve's Garden respectively. The average concentration from all the sites was 0.014mg/L, slightly more than the start of SWM.

The transition period sampling observed a maximum value of 0.052mg/L found at the middle depth of Anemone Garden. North Siwa surface and middle layer, and Anemone Garden's seabed had the lowest value with 0.049mg/L. The average concentration of cadmium from all three sites was 0.050mg/L.

The data observed from Sipadan Island showed that the concentration of cadmium at both Barracuda Point and South Point were below detection limit.

From Figure 4.4.1, Anemone Garden and North Siwa had the highest concentration of cadmium at the middle depth and the seabed respectively throughout all three seasons. The end of SWM shows the highest concentration of cadmium increasing from the surface of Eve's garden to the middle depth of both Anemone Garden and North Siwa and finally at the seabed of North Siwa.

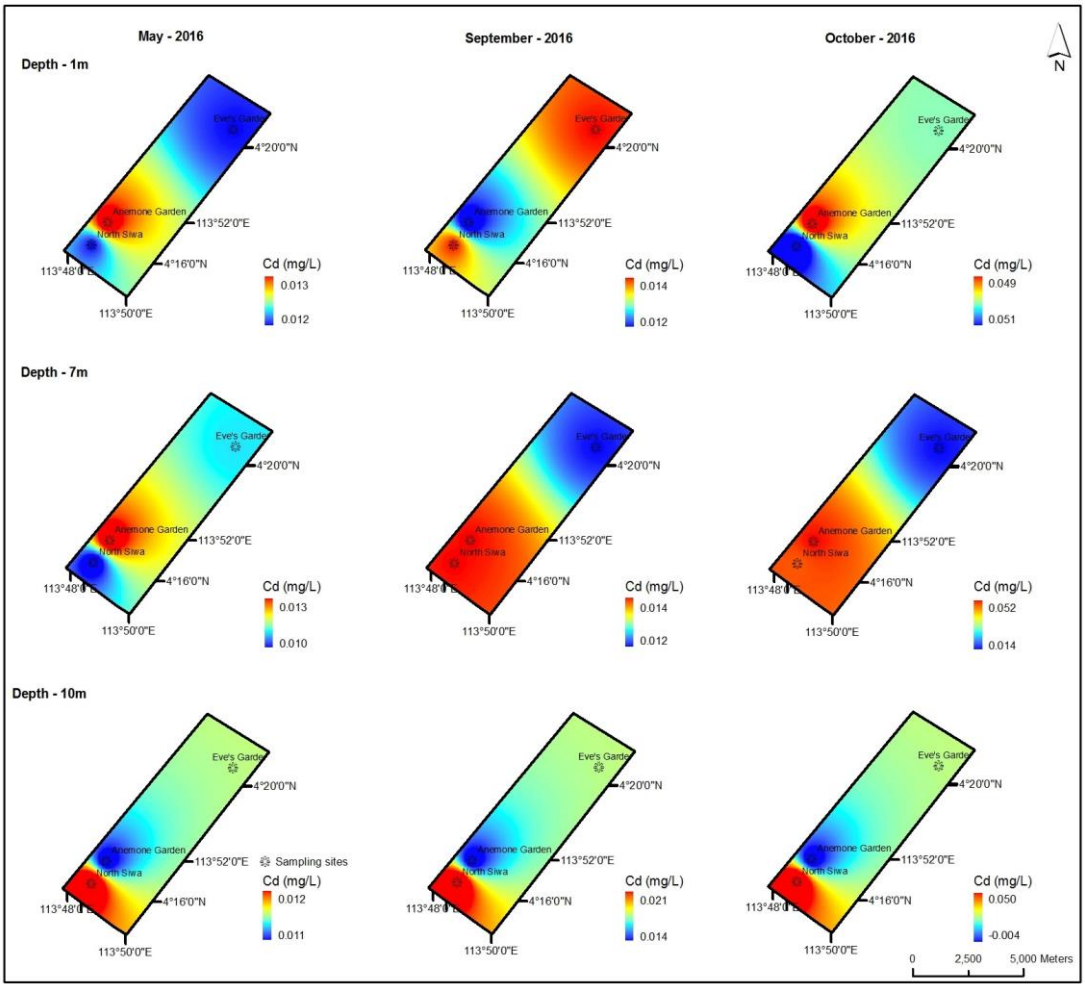

Figure 4.4.1 - Spatial Variation of Cadmium at MSCRNP

4.4.2 Cobalt

The second element in the Group 7 of the periodic table is Cobalt with an atomic number of 27, atomic weight of 58.93 and valences 1, 2 and 3 (APHA, 2012). Cobalt can be found naturally in the environment in soil but higher concentrations are found as waste from batteries, fertilisers, coal combustion and mining (APHA, 2012; Lenntech, 2017c)

The concentrations of cobalt observed were mostly below the detection limit of the Atomic Absorption Spectrophotometer (AAS) for the samples taken at North Siwa for both beginning and end of SWM. The only locations and depths that observed a small concentration of cobalt during start of SWM were Anemone Garden and Eve's Garden. A maximum value of 0.017mg/L was observed at the seabed of Anemone Garden while the lowest detected value was 0.002mg/L at the surface of Eve's Garden.

The end of SWM observed a maximum value of 0.016mg/L at the surface of Anemone Garden and a minimum of 0.005mg/L at the middle depth of the same location.

NEM transition period experienced an increase in the overall concentration of cobalt with a maximum reading of 0.232mg/L at the surface of North Siwa and a minimum value of 0.180mg/L at the seabed of Anemone Garden. The average concentration for the transition period was 0.206mg/L.

The concentration of cobalt at Sipadan Island was highest at the middle depth of Barracuda Point with a value of 0.011mg/L. The lowest value was observed at the same site with a value of 0.005mg/L. The seabed of South Point observed a concentration of 0.007mg/L while the seabed and surface of Barracuda Point and South Point respectively, had concentrations below the detection limit.

From the spatial maps in Figure 4.4.2, the maximum concentration of cobalt is observed from the surface of Eve's Garden to that of North Siwa from start of SWM to NEM transition. Anemone Garden had the highest concentration of cobalt at the middle depth for the start of SWM and the seabed for both beginning and end of SWM. During NEM transition, North Siwa observed highest value out of all the sites.

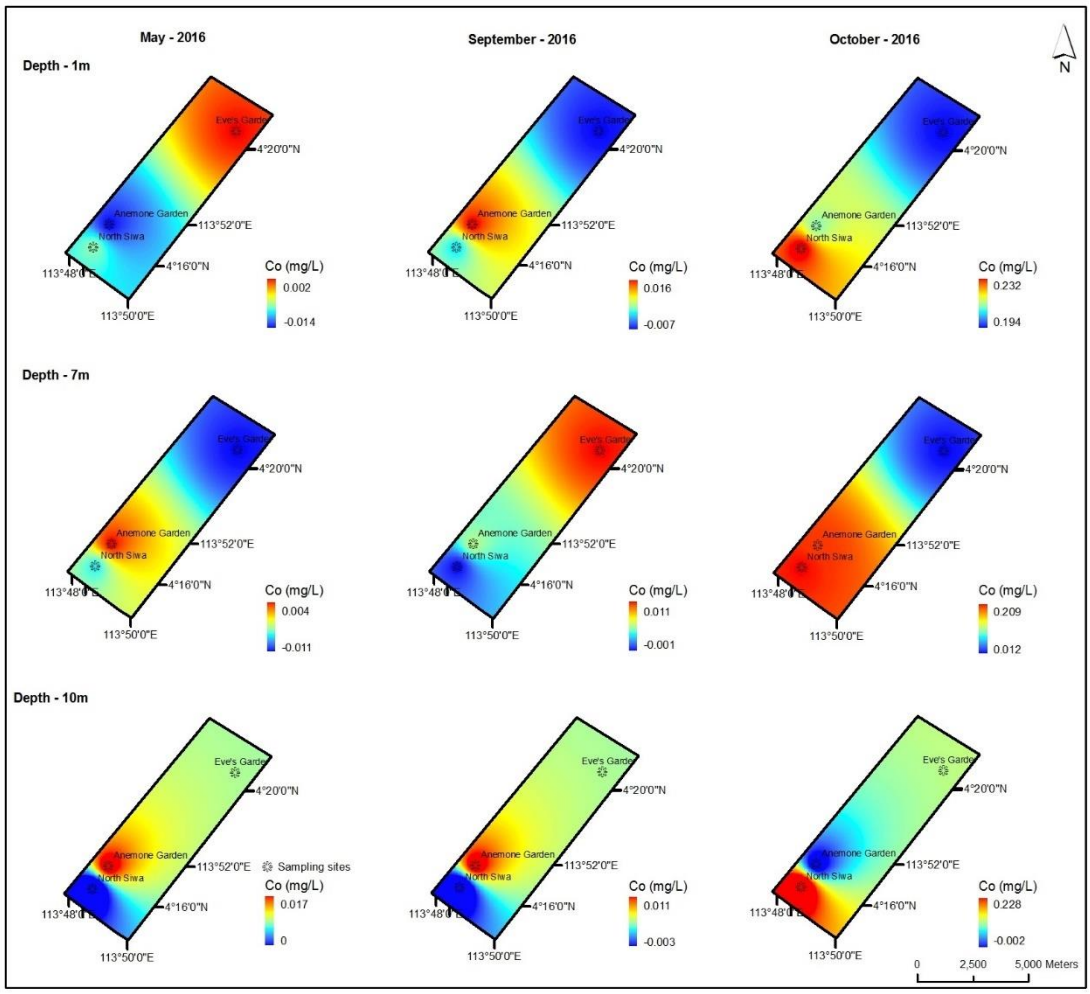

Figure 4.4.2 - Spatial Variation of Cobalt at MSCRNP

4.4.3 Copper

Copper exists in the environment in its natural state. The metal, first element in Group 1B in the periodic table, has an atomic number of 29, atomic weight of 63.54 and two valences, 1 and 2 (APHA, 2012). The presence of copper in seawater is mostly from natural phenomena but also from mining, metal production and sedimentation (Balls, 1985). Copper creates a strong bond with organic matter and mineral and similar to Cadmium, it is also associated with zinc (Lenntech, 2017d).

The concentration of copper during the beginning of SWM was the highest at North Siwa with a maximum of 0.060mg/L at the surface. The minimum concentration was at the seabed of Eve's Garden. The average concentration of copper measured for that period was 0.035mg/L.

The end of SWM observed a maximum value of 0.061mg/L at the surface of Eve's Garden and the minimum value was 0.037mg/L at the seabed of Anemone Garden. The average concentration of copper during the end of SWM was slightly higher than at the start with a value of 0.045mg/L.

The transition period measured the highest concentration of copper in MSCRNP with a maximum of 0.098mg/L at the surface of North Siwa. The minimum value was 0.083mg/L with an average concentration of 0.089mg/L during that period.

Sipadan Island showed lower values of copper concentration on average. The highest concentration was 0.054mg/L at Barracuda Point and the lowest was 0.023mg/L at the surface of the same site. The two values measured at South Point were 0.010mg/L at the surface and 0.011mg/L at the seabed of the site. On average, the concentration of copper was 0.024mg/L.

The variation of copper concentration both spatially and temporally as shown in Figure 4.4.2 was very similar to that of cadmium at the middle depth and the seabed of all three locations. The difference between the two trace elements was observed at the surface, where the concentration of copper was highest at North Siwa during beginning of SWM and NEM transition rather than at Anemone Garden. Figure 4.4.2 also indicate that the higher values of copper were observed at North Siwa and Anemone Garden.

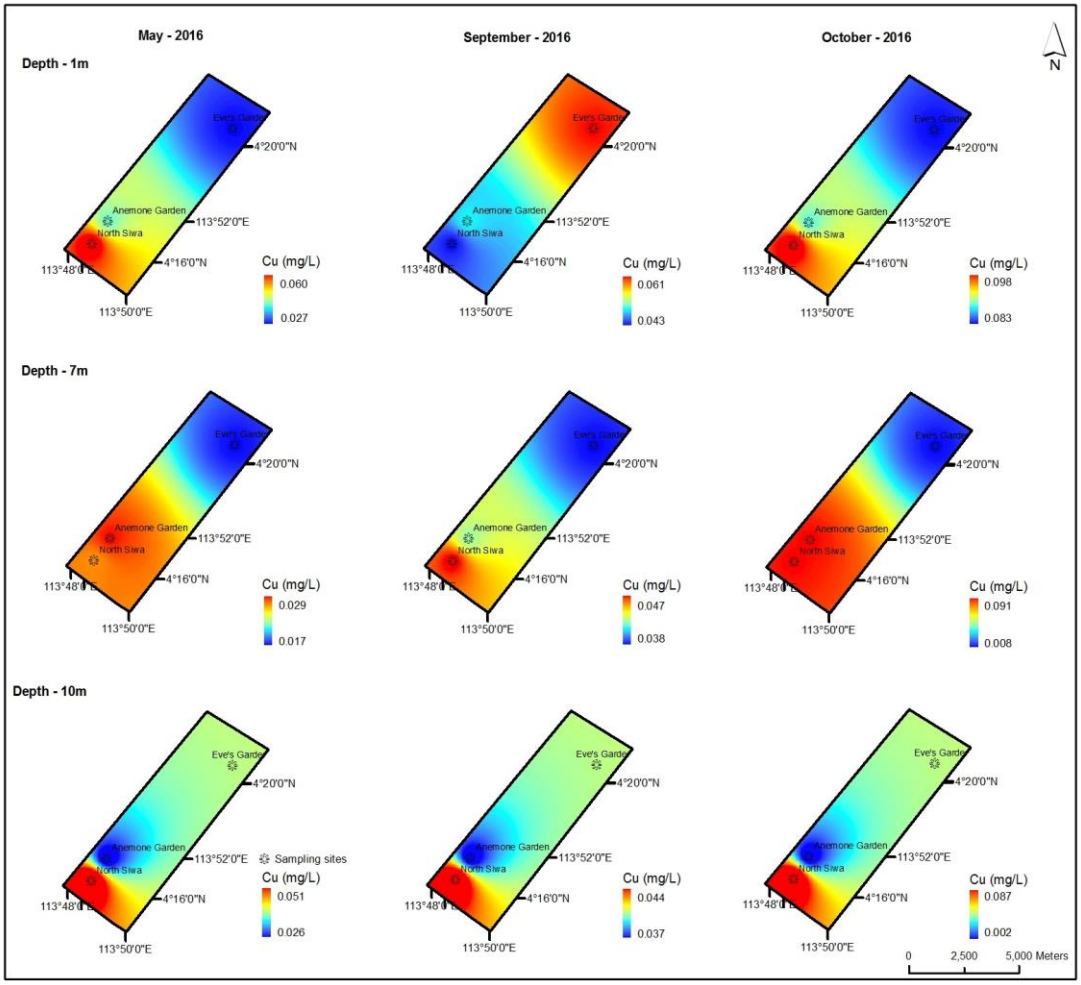

Figure 4.4.3 - Spatial Variation of Copper at MSCRNP

4.4.4 Iron

Iron is found in Group 8 of the periodic table with 26 as atomic number, atomic weight of 55.85 and valence 2 and 3. It is one of the most abundant metals on the planet (APHA, 2012). It is present in seawater in many forms, for example as iron carbonate. It is also present in algae and often, a brown colour algae would mean a higher concentration of iron in it (Lenntech, 2017e).

The maximum concentration of iron recorded during the start of SWM was 1.478mg/L at the seabed of North Siwa. The minimum value was 1.095mg/L at the surface of Anemone Garden and the average concentration for that period was 1.213mg/L.

The end of SWM showed similar values to that of the start, with a maximum concentration of 1.448mg/L. The lowest recorded value during that period was noted

at the middle depth of Anemone Garden with a value of 1.120mg/L. The average concentration during the end of SWM was 1.217mg/L.

There was a decrease in concentration during the transition period. The maximum value was 0.939mg/L at the surface of Eve's Garden, while the lowest value was noted at the seabed of North Siwa with a value of 0.789mg/L. The average concentration for that period was 0.857mg/L, which also noted less variations in the readings.

Barracuda Point, at Sipadan Island, observed a maximum value of 1.186mg/L for the concentration of iron at the surface and a minimum of 1.084mg/L at the middle depth. The values recorded at South Point were 1.415mg/L at the surface and 1.217mg/L at the seabed. The average concentration of iron at Sipadan was 1.214mg/L.

Figure 4.4.3 shows the spatial maps for the concentration of iron at the three sites. The high iron concentration during the start of SWM can be observed from the surface of Eve's Garden to the middle depth of Anemone Garden and finally at the seabed of North Siwa. The end of SWM had all the high values at North Siwa. Eve's Garden had the highest concentration of iron at both surface and seabed. Anemone Garden also had a high value at the seabed during the transition period, which was also the season when North Siwa had the lowest concentration from surface to seabed.

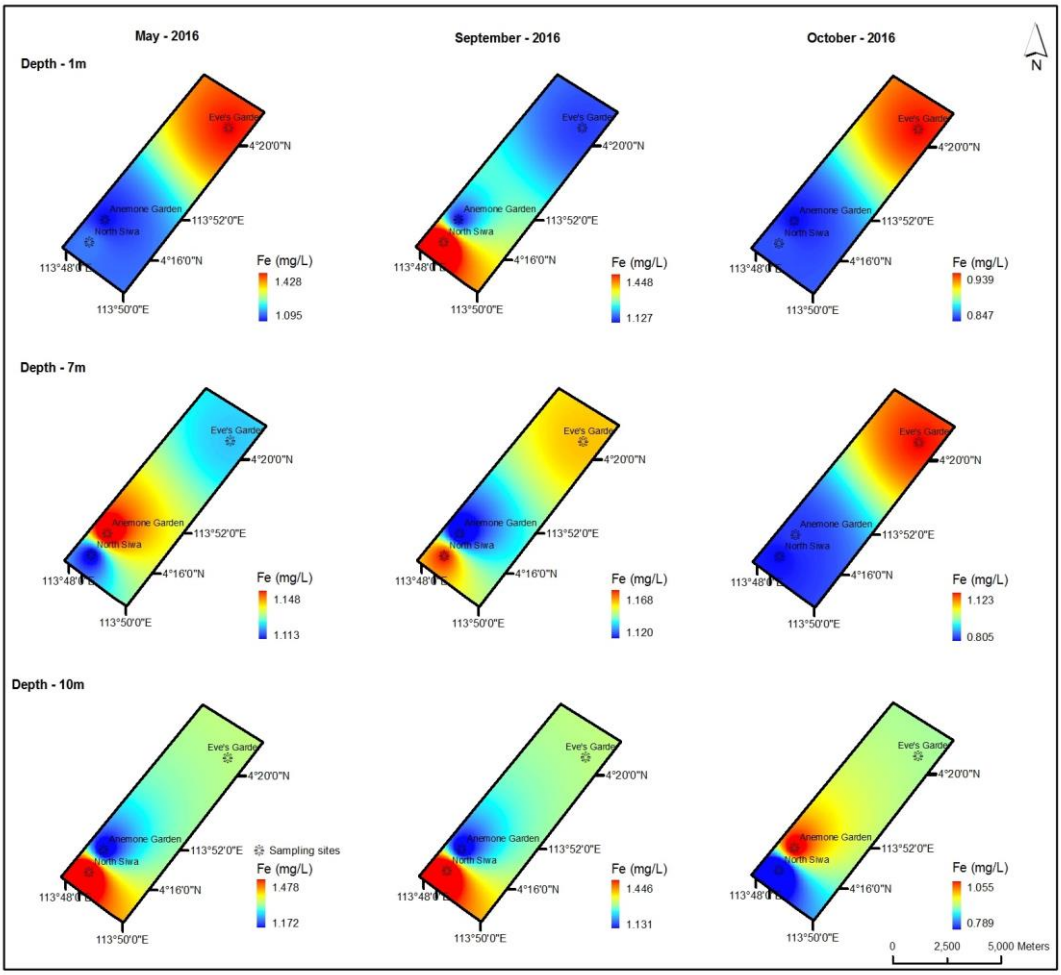

Figure 4.4.4 - Spatial Variation of Iron at MSCRNP

4.4.5 Manganese

Manganese, first element in Group 7B of the periodic table, has an atomic number of 25, atomic weight of 54.94 and has its most common valences are 2, 4 and 7 (APHA, 2012). Manganese can be found in seawater from groundwater discharge and sewage water and proliferates in lower pH water and is often a disturbance that affects plants (Lenntech, 2017h).

The concentration of manganese during the beginning of SWM had a maximum value of 0.087mg/L observed at the seabed of North Siwa. The minimum value was 0.070mg/L at both the middle depth of Anemone Garden and the surface of Eve's Garden. The average concentration of manganese for that period was measured as 0.078mg/L across all three sites.

A gradual decrease in the concentration of manganese was noted during the end of SWM. The maximum value was 0.079mg/L at the surface of North Siwa. The lowest value was 0.063mg/L measured at the surface of Eve's Garden. The average concentration from all three sites was 0.069mg/L.

The same gradual decrease was noticed from the end of SWM to the transition period. The highest concentration of manganese during the transition period was 0.063mg/L at the surface of Eve's Garden. The lowest value was 0.050mg/L at the surface of North Siwa. The average concentration during transition was measured as 0.055mg/L from all three sites.

Barracuda Point, in Sipadan measured a maximum concentration of manganese as 0.069mg/L at the surface and a minimum value of 0.059mg/L at the middle layer. At South Point, the concentration of manganese was 0.053mg/L at the surface and 0.058mg/L at the seabed. The average concentration was 0.060mg/L from both sites.

The spatial and temporal distribution of manganese as seen in Figure 4.4.4 show a higher concentration at the surface of Anemone Garden during the start of SWM. However, that high concentration shifts to North Siwa from the middle depth to the seabed. The seabed of North Siwa also has a high manganese concentration at the end of SWM. The seabed of the shallowest site, Eve's Garden, has the highest concentration of manganese during the end of SWM and NEM transition period. Anemone Garden also observed a high value at the seabed.

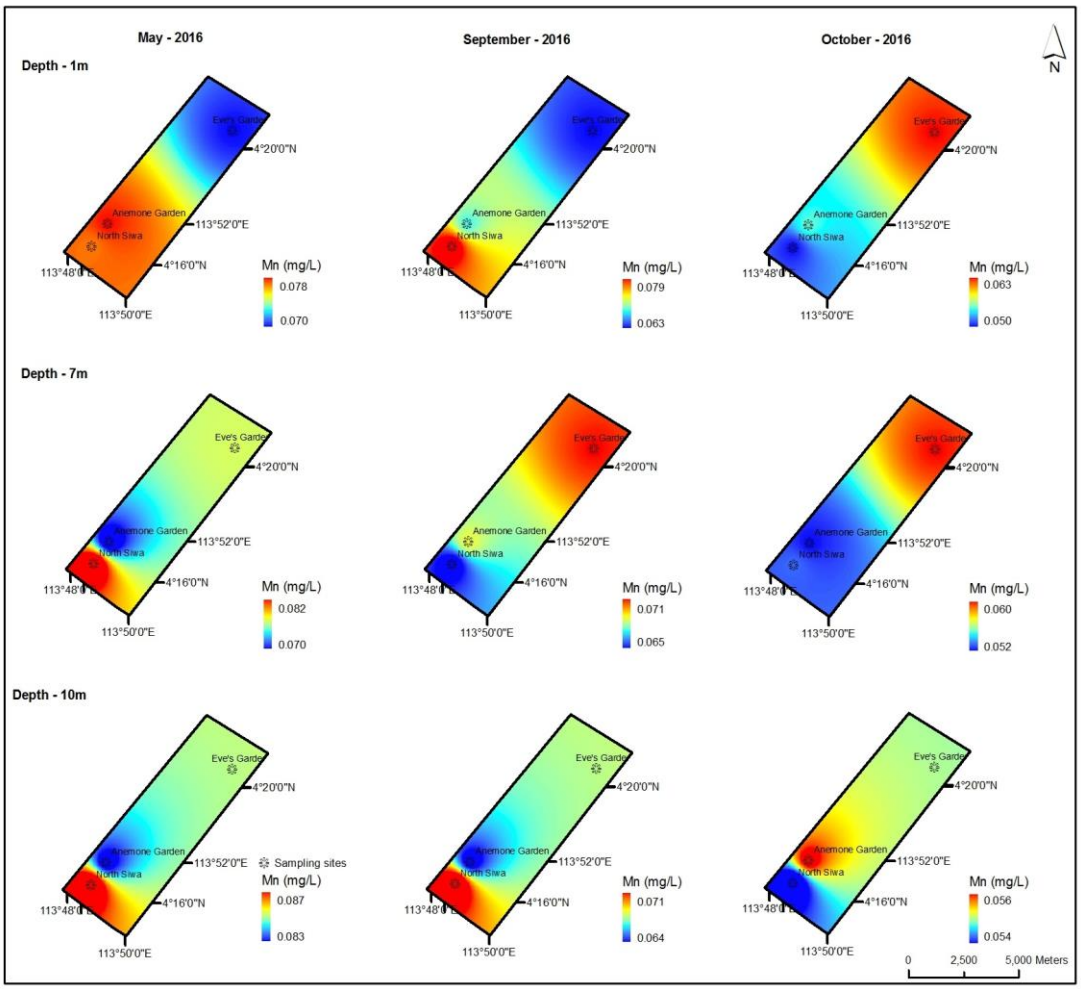

Figure 4.4.5 - Spatial Variation of Manganese at MSCRNP

4.4.6 Nickel

Nickel is the third element in Group 7 of the periodic table with an atomic number of 28, atomic weight of 58.69 and a valence of 2 (APHA, 2012). Nickel has a strong ability of being absorbed by organic matter which explains why coal and oil are some of the ways nickel finds its way to the ocean other than from poor wastewater control (Lenntech, 2017i).

The highest concentration of nickel for the beginning of SWM season was 0.212mg/L at the surface of Eve's Garden. The minimum value was 0.139mg/L at the seabed of Anemone Garden. The average for those samples were 0.165mg/L with all sites combined.

The concentration of nickel at the end of SWM showed a maximum of 0.187mg/L at the surface of North Siwa. The lowest value was at the middle of Anemone Garden

with a concentration of 0.136mg/L. The average from all three sites was 0.158mg/L, a lower value than that of the start of SWM.

NEM transition period had a maximum concentration of 0.397mg/L at the middle depth of North Siwa and Anemone Garden. The minimum value, which was still more than the start and finish of SWM value combined, was 0.366mg/L, at the surface of Eve's Garden. The average concentration from all the sites was 0.388mg/L.

Barracuda Point, at Sipadan Island measured a maximum concentration of Nickel at the surface with a value of 0.158mg/L. The minimum value at the same location was 0.147mg/L at the seabed. South Point had a nickel concentration of 0.173mg/L at the surface and the value at the seabed was 0.150mg/L. The average concentration at Sipadan Island was 0.155mg/L.

Based on Figure 4.4.5, the concentration of nickel was highest at both depths of Eve's Garden during commencement of SWM and again at the seabed during the end of SWM. The seabed of North Siwa also had the highest concentration of nickel throughout all seasons. Anemone Garden only had a high concentration of nickel at the middle depth, which was also common with North Siwa. during the transition period.

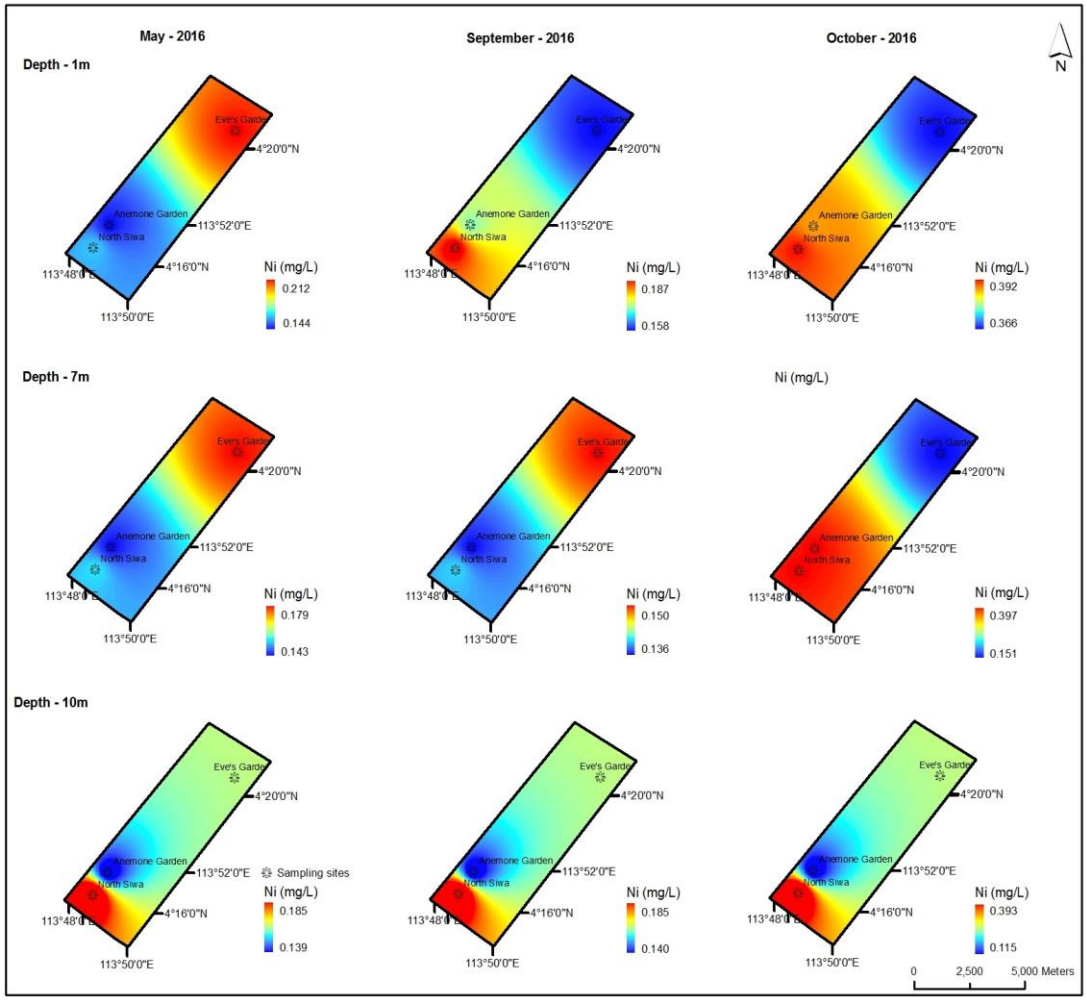

Figure 4.4.6 - Spatial Variation of Nickel at MSCRNP

4.4.7 Lead

Lead belongs in group 14 of the periodic table, has an atomic number of 82 and an atomic mass of 207.2 (APHA, 2012). Lead finds itself in seawater through old water pipes that partially dissolved pipes. Lead can also be found in car batteries and oil (Lenntech, 2017f).

From the beginning to the end of SWM, the lead concentration was below detection limit by the AAS. The metal was detected during the transition period with the highest value of 0.420mg/L observed at the seabed of North Siwa. The lowest value was 0.396mg/L, observed at the surface of Eve's Garden.

Sipadan Island observed traces of lead at the seabed of Barracuda point with a value of 0.036mg/L. A value of 0.031mg/L was detected at the surface of South Point and a concentration of 0.032mg/L was observed at the seabed of the same site.

Observing only the 'October-2016' section of the spatial maps in Figure 4.4.7, it is noted that the concentration of lead was the highest at the surface of Anemone Garden and slowly transitioning to the seabed of North Siwa.

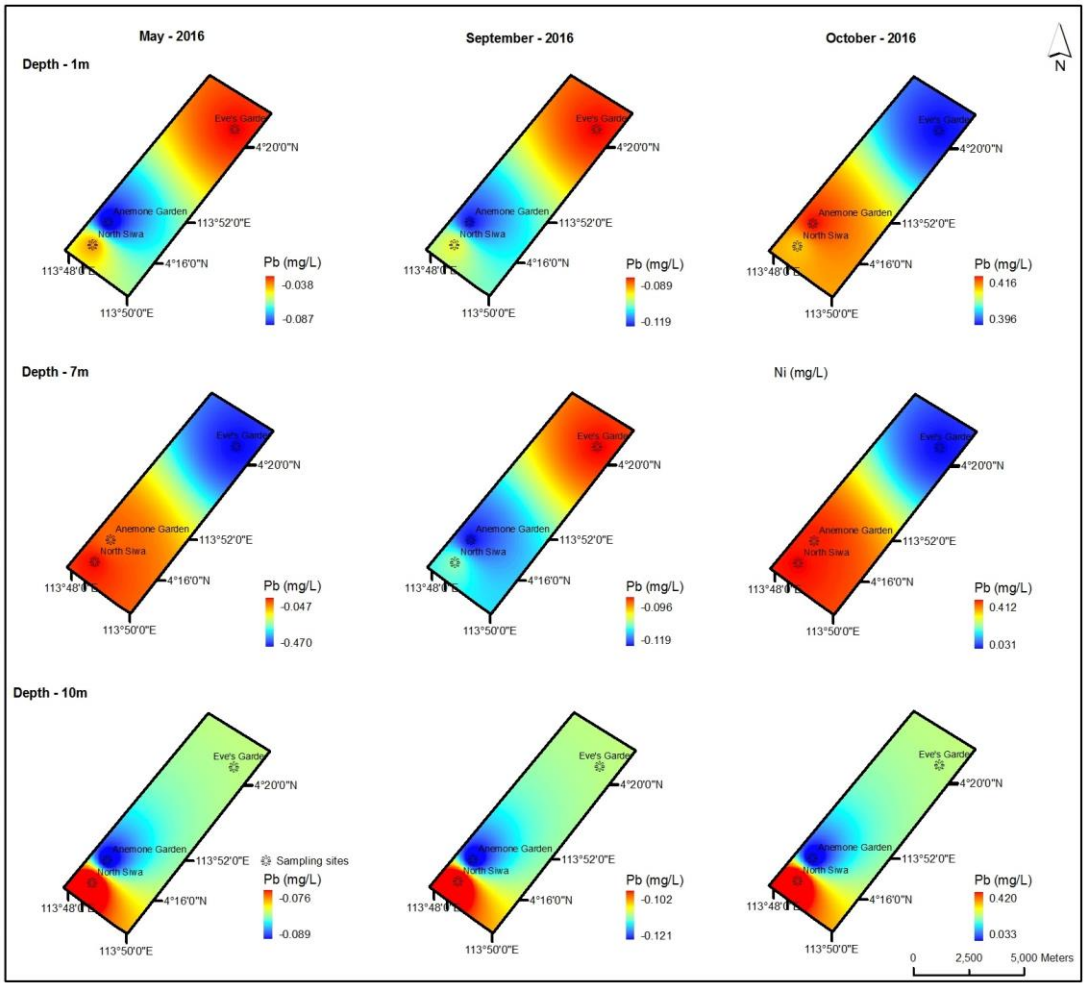

Figure 4.4.7 – Spatial Variation of Lead at MSCRNP

4.4.8 Zinc

Zinc, the first element in Group 2B, has an atomic number of 30 and an atomic mass of 65.38. The element also has a valence of 2 (APHA, 2012). Zinc occurs naturally in

seawater but also comes from human induced activities such as coastal development, mining, burning of waste and coal (Lenntech, 2017l).

During the start of SWM, the samples had a maximum zinc concentration of 0.180mg/L at the surface of Eve's Garden. The minimum value was 0.046mg/L noted at the surface of North Siwa. The average vaue was 0.091mg/L from all the sites.

The maximum concentration of zinc obtained at the end SWM was 0.132mg/L at the surface of North Siwa. The minimum concentration was 0.037mg/L at the middle layer of the same site. The average amount of zinc during that period was 0.063mg/L.

The transition period had a maximum concentration of zinc at the seabed of Eve's Garden with a value of 0.090mg/L. The seabed of North Siwa had the lowest concentration of 0.076mg/L. The average concentration for this metal was 0.082mg/L from all sites.

Barracuda Point, at Sipadan Island had a maximum zinc concentration of 0.134mg/L obtained at the middle layer, while the minimum concentration was observed at the surface. South Point had a surface and seabed concentration of 0.051mg/L. The average zinc concentration for the Sipadan Island was 0.079mg/L.

The spatial maps from Figure 4.4.8 help to explain the variation of the concentration of zinc at all three sites for the start and finish of SWM, and NEM transition period. The values observed were quite similar to that of nickel. The more noticeable exceptions at Anemone Garden were the lower concentrations of zinc at the surface during the end of SWM and NEM transition period. The other difference was the higher value at the seabed during the start of SWM.

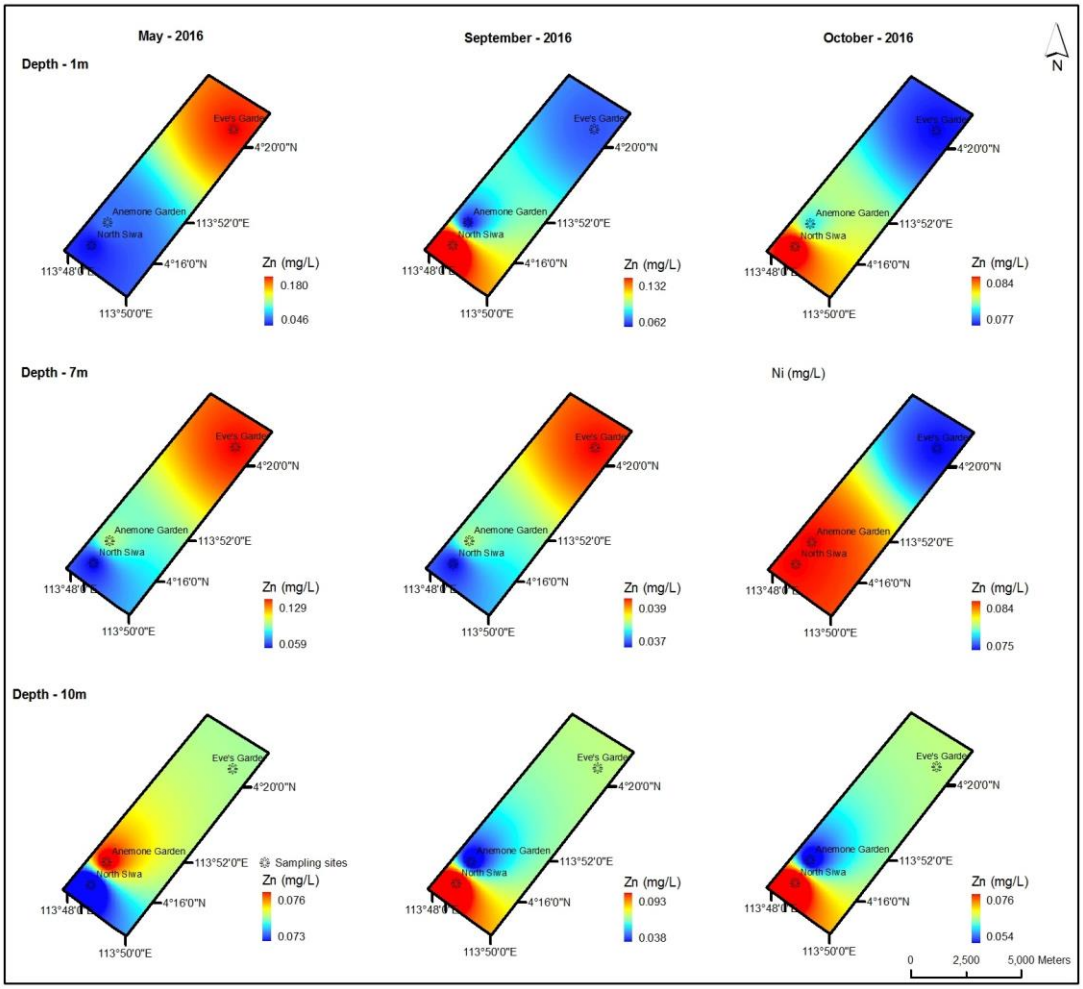

Figure 4.4.8 - Spatial Variation of Zinc at MSCRNP

4.4.9 Summary

Eight different metals (Cd, Co, Cu, Fe, Mn, Ni, Pb, Zn) were chosen to be analysed within the Miri-Sibuti Coral Reef National Park and Sipadan Island Park (Tables 4.4.4 – 4.4.7). From the analyses, the results for the concentration of Pb were negative, meaning that the amount of Pb present in the ocean were below detection limit except for NEM transition where high Pb concentrations were observed at the Miri sites. The trace metals cadmium, cobalt, copper, nickel and zinc show a rise in their average value in MSCRNP from the start of SWM to NEM transition. Cobalt and nickel had the most drastic increase where the concentration almost doubled from commencement of SWM to NEM transition. The average concentration of iron and manganese decreased when compared to their average from the beginning SWM.

The spatial maps from Figures 4.4.1 to 4.4.8 indicate that the high concentration of trace metals was mostly found at Eve's Garden and North Siwa throughout all three seasons. At the seabed of Eve's Garden, Fe, Mn, Ni and Zn observed a higher concentration during the end of SWM except Cu and Cd. Ni and Zn had the highest concentration at both depths of Eve's Garden during the start of SWM. Cd was the only metal that had the highest value at the middle of depth of Anemone Garden through all the seasons.

Table 4.4.1 – Trace Metals Concentrations (mg/L) at MSCRNP (Start of SWM)

Location	Depth (m)	Cd	Co	Cu	Fe	Mn	Ni	Zn
North Siwa	*1.0*	0.012	BDL	0.060	1.149	0.077	0.162	0.046
	7.5	0.010	BDL	0.027	1.113	0.082	0.154	0.059
	14.7	0.012	BDL	0.051	1.478	0.087	0.185	0.073
Anemone Garden	*1.0*	0.013	BDL	0.039	1.095	0.078	0.144	0.066
	6.0	0.013	0.004	0.029	1.148	0.070	0.143	0.095
	9.5	0.011	0.017	0.026	1.172	0.083	0.139	0.076
Eve's Garden	*1.0*	0.012	0.002	0.027	1.428	0.070	0.212	0.180
	6.0	0.011	BDL	0.017	1.122	0.076	0.179	0.129

Table 4.4.2 – Trace Metals Concentrations (mg/L) at MSCRNP (End of SWM)

Location	Depth (m)	Cd	Co	Cu	Fe	Mn	Ni	Zn
North Siwa	*1.0*	0.014	BDL	0.043	1.448	0.079	0.187	0.132
	7.5	0.014	BDL	0.047	1.168	0.065	0.140	0.037
	14.7	0.021	BDL	0.044	1.446	0.071	0.185	0.093
Anemone Garden	*1.0*	0.012	0.016	0.049	1.127	0.068	0.170	0.062
	6.0	0.014	0.005	0.042	1.120	0.069	0.136	0.038
	9.5	0.014	0.011	0.037	1.131	0.064	0.140	0.038
Eve's Garden	*1.0*	0.014	BDL	0.061	1.141	0.063	0.158	0.067
	6.0	0.012	0.011	0.038	1.158	0.071	0.150	0.039

Table 4.4.3 – Trace Metals Concentrations (mg/L) at MSCRNP (NEM Transition)

Location	Depth (m)	Cd	Co	Cu	Fe	Mn	Ni	Pb	Zn
North Siwa	*1.0*	0.049	0.232	0.098	0.856	0.050	0.392	0.411	0.084
	7.5	0.049	0.209	0.091	0.805	0.053	0.397	0.412	0.084
	14.7	0.050	0.228	0.087	0.789	0.054	0.393	0.420	0.076
Anemone Garden	*1.0*	0.051	0.210	0.088	0.847	0.055	0.387	0.416	0.079
	6.0	0.052	0.201	0.091	0.824	0.052	0.397	0.406	0.084
	9.5	0.049	0.180	0.088	0.868	0.056	0.376	0.412	0.081
Eve's Garden	*1.0*	0.050	0.194	0.083	0.939	0.063	0.366	0.396	0.077
	6.0	0.050	0.196	0.086	0.929	0.060	0.393	0.412	0.090

Table 4.4.4 – Trace Metals Concentrations (mg/L) at Sipadan Island Park

Location	Depth (m)	Co	Cu	Fe	Mn	Ni	Pb	Zn
Barracuda Point	*1.0*	0.005	0.023	1.186	0.069	0.158	BDL	0.071
	7.5	0.011	0.054	1.084	0.059	0.148	BDL	0.134
	14.7	BDL	0.024	1.169	0.060	0.147	0.036	0.088
South Point	*1.0*	BDL	0.010	1.415	0.053	0.173	0.031	0.051
	6.0	0.007	0.011	1.217	0.058	0.150	0.032	0.051

4.5 Rainfall Data

Rainfall data for 11 years, shown in Tables 4.5.1 to 4.5.3 were obtained from the Miri Meteorological Centre. Tables 4.5.1 and 4.5.2 illustrate the amount of rainfall from 2006 to 2016 for each month and the number of rain days from those months respectively. Table 4.5.3 gives the daily rainfall amount for 2016 and indicates that the data is taken every 24hrs beginning at 0800MST.

In 2006, the total rainfall was 2985.7mm, where December noted the most rainfall with 428.8mm, the lowest was in March with 45.4mm and the average was 248.8mm. The total number of rain days in that year was 204days where January had the maximum with 24days, of rain and the minimum was March with had 9 days of rain. The average for that year was 17days.

In 2007, a total of 3266.8mm of rain was recorded for the whole year. The month with the highest amount of rain was June with 648.8mm and the month with the lowest rainfall was August with 102.0mm. The average rainfall for that year was 272.2mm. The total number of rain days was 228days with a maximum of 28days in January and the least rain days was in March with 12days of rain. The mean number of rain days for that year was 19days.

The total amount of rain in 2008 was 2986.0mm, where October had the most rain at 389.8mm and April was the lowest at 82.4mm. The average rainfall for that year was 248.8mm, similar to 2006. It rained for 212days and the maximum number of rain days was observed in December at 24days and the months with the lowest rain days were May and June at 13days. The average number of rain days for that year was 17.7days.

2009 had a total rainfall of 3252.2mm and January at 928.2mm was the maximum and May was the minimum with 65.6mm. The mean amount of rain for that year was 271.0mm. The total number of rain days was 191days and January had the most rain days at 27days. The least number of rain days was May with 9days and the mean for 2009 was 15.9days.

In 2010, the total amount of rain observed was 3086.5mm. At 407.2mm, July had the highest amount of rain and February had the lowest with 7.8mm. The mean for that year was 257.2mm. During that year, it rained for a total of 205days where December had the maximum rain days at 26days and February with 3days was the lowest month. The average number of days rained was 17.1days.

2011 noted a total of 3246.4mm of rain, where January with 669.9mm, had the most rainfall and October with 118.2mm was the lowest. The average amount of rain for the year was 270.5mm, which was close to the years 2007 and 2009. It rained for a total of 199days in 2011 and the months with the maximum rain days was March and December with 21days. The month with the least rain days was July with 8days and the average rain days for the year was 16.6days.

The annual rainfall for 2012 was 2695.8mm and the month with the most rainfall was November at 463.2mm. The least rainfall of 80.8mm was recorded in September and the average amount of rain for that year was 224.7mm. The sum of all rain days for 2012 was 203days, where the month with the most rain days was November. The least number of rain days was June with 8days. The average number of rain days in 2012 was 16.9days.

In 2013, the annual rainfall was 3125.0mm, where the highest amount of rainfall was in December at 694.0mm and the lowest was in June at 101.8mm. The average rainfall observed was 260.4mm. It rained for a total of 198days in 2013 and the month of December with 24days had the most number of rain days. June, with 6days was the least days it rained and the average for year was 16.5days.

The total amount of rainfall for 2014 was 2373.2mm, where the maximum amount of rain of 506.2mm was noted in January and a minimum of 29.0mm was observed during September. The average amount of rain for the year was 197.8mm. The sum of all the rain days for 2014 was 171days and the month with the most days of rain was November at 24days. February and March had 8days of rain each, which was the least it rained during that year. The average number of rain days observed in 2014 was 14.3days.

In 2015, the total rainfall for the year was 2634.8mm. The month with the most rainfall was January at 652.8mm and the month with the lowest amount of rain was March at 15.8mm. The average rainfall for 2015 was 219.6mm. That year it rained for a total of 194days, where January, at 27days was the month with the most rain days, and March was the lowest at 6days of rain. The mean number of rain days during 2015 was 16.2days.

In 2016, from January to October, the amount of rain observed was 1607.5mm. During that period, October had the most rainfall with 310.9mm and January the least with

70.6mm. The average rainfall was 160.8mm for these ten months. The total number of rain days during that period was 127days whereas, May, with 19 days of rain was the maximum and January was the least with 6days of rain. The mean number of rain days for the ten months of 2016 was 12.7days.

Figures 4.5.1 and 4.5.2 highlight the fluctuations in the monthly and yearly rainfall for those 11 years respectively. Figure 4.5.1 shows the amount of monthly rainfall, which indicates high rainfall records of January and December. Figure 4.5.2 clearly shows alternating years of high rainfall and the amount has been decreasing in 2014. The total rainfall for 2016 does not include November and December since the data was requested before the end of November (Table 4.5.3).

In May 2016, a total of 228.8mm of rain was recorded near the Miri study sites. The years with higher rainfall than that May 2016 were 2006 (377.0mm), 2010 (332.7mm) and 2014 (248.4mm). During the time of sampling on 31 May 2016, no rainfall was observed, however, 12mm of rain was recorded later that day.

The month of September 2016 recorded 108.4mm of rain (Table 4.5.1). That month had the third lowest rainfall recorded in 2016 with 2012 (80.8mm) and 2014 (96.0mm). No rain was recorded on 14 September 2016 which was the day the samples were collected.

The last samples were collected on 27 October 2016. From Table 4.5.1, the total rainfall recorded for that month was 310.9mm, which was the third highest in comparison to 2008 (389.8mm) and 2012 (339.4mm). Similar to May 2016, no rainfall was observed during sampling but 1.6mm of rain was recorded later that day.

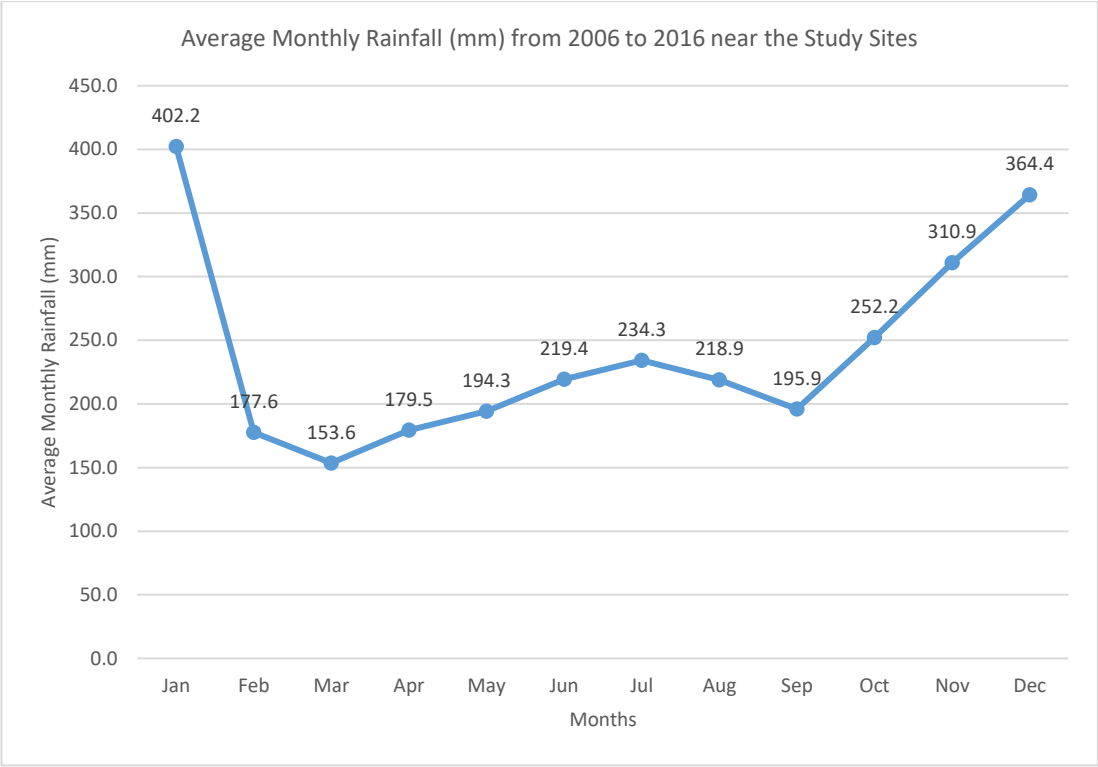

Figure 4.5.1 – Average Monthly Rainfall (mm) from 2006 to 2016 near the Study Sites

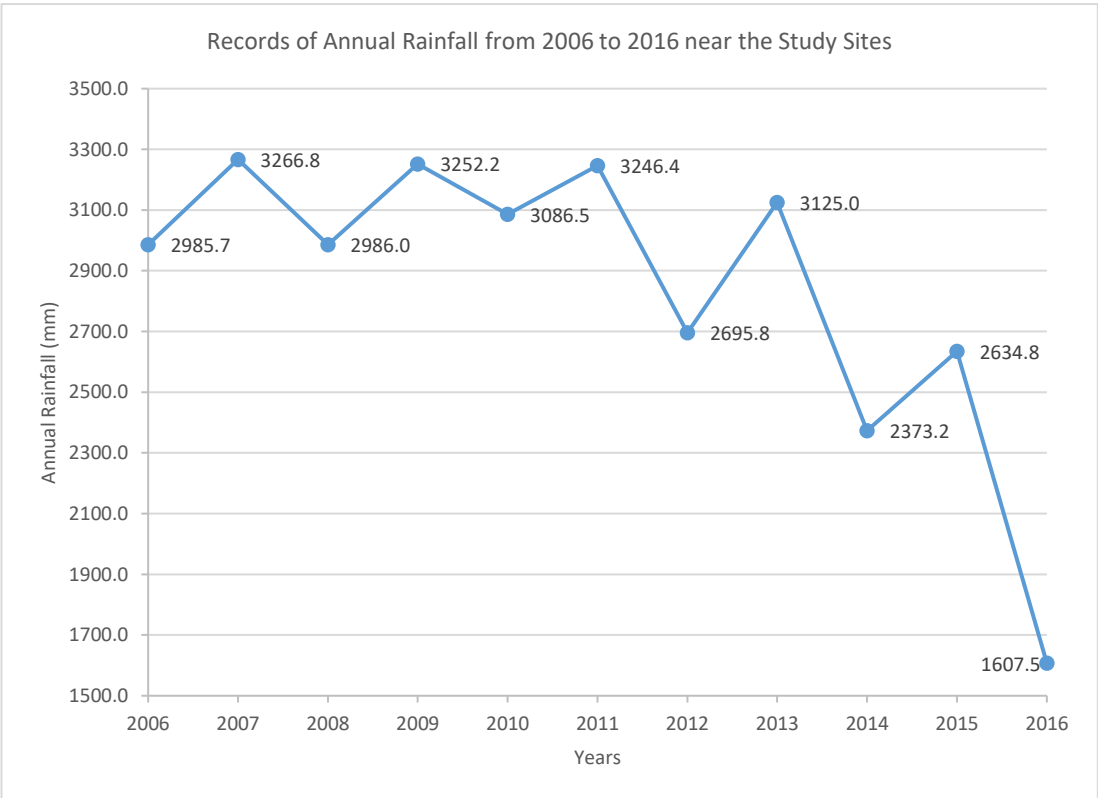

Figure 4.5.2 – Records of Annual Rainfall from 2006 to 2016 near the Study Sites

Table 4.5.1 – Records of Monthly Total Rainfall Amount near the Study Sites													
Unit: Millimeter			**Latitude: 04 Deg. 20' N**			**Longitude: 113 Deg. 59' E**			**Height Above Mean Sea Level (MSL): 17.0 M**				
Month/ Year	**Jan**	**Feb**	**Mar**	**Apr**	**May**	**Jun**	**Jul**	**Aug**	**Sep**	**Oct**	**Nov**	**Dec**	**Annual**
2006	340.6	105.8	45.4	307.1	377.0	120.6	254.0	380.4	238.8	180.2	207.0	428.8	2985.7
2007	351.6	260.8	108.2	211.8	114.0	648.8	426.0	102.0	167.8	173.0	398.0	304.8	3266.8
2008	159.6	252.6	286.8	82.4	106.6	304.4	297.4	321.6	265.8	389.8	219.6	299.4	2986.0
2009	928.2	241.2	197.4	255.6	65.6	123.6	124.0	162.0	189.6	262.2	249.2	453.6	3252.2
2010	273.4	7.8	45.4	159.8	332.7	211.0	407.2	342.6	404.8	287.8	338.0	276.0	3086.5
2011	669.9	308.7	330.4	175.6	225.6	282.2	157.8	165.8	120.4	118.2	313.4	378.4	3246.4
2012	280.8	204.4	316.4	141.0	136.6	168.0	160.8	170.6	80.8	339.4	463.2	233.8	2695.8
2013	191.0	339.0	131.8	197.0	220.8	101.8	168.0	249.0	317.9	254.3	260.4	694.0	3125.0
2014	506.2	29.0	126.0	97.2	248.4	66.2	101.4	179.8	96.0	307.4	354.2	261.4	2373.2
2015	652.8	122.6	15.8	182.2	81.4	259.4	216.0	169.4	164.8	150.6	306.2	313.6	2634.8
2016	70.6	81.4	85.8	164.8	228.8	127.6	265.0	164.2	108.4	310.9			

Table 4.5.2 – Records of Number of Rain Days Per Month near the Study Sites													
Unit: Millimetre			**Latitude: 04 Deg. 20' N**			**Longitude: 113 Deg. 59' E**			**Height Above Mean Sea Level (MSL): 17.0 M**				
Month/ Year	**Jan**	**Feb**	**Mar**	**Apr**	**May**	**Jun**	**Jul**	**Aug**	**Sep**	**Oct**	**Nov**	**Dec**	**Annual**
2006	24	19	9	20	21	13	11	16	18	14	18	21	204
2007	28	20	12	17	16	23	16	13	18	20	22	23	228
2008	16	16	23	16	13	13	21	16	16	22	16	24	212
2009	27	16	21	13	9	13	10	11	11	16	23	21	191
2010	17	3	6	18	21	22	21	14	20	18	19	26	205
2011	20	19	21	17	16	17	8	15	12	16	17	21	199
2012	19	23	16	19	14	8	14	9	12	22	24	23	203
2013	14	18	12	22	17	6	15	14	17	19	20	24	198
2014	20	8	8	13	19	11	10	17	10	17	24	14	171
2015	27	13	6	13	14	15	15	17	12	14	25	23	194
2016	6	7	14	11	19	16	15	13	9	17			

Table 4.5.3 – Records of Daily Total Rainfall Amount (0800-0800MST) near the Study Sites (2016)											
Unit: Millimetre			**Latitude: 04 Deg. 20' N**				**Longitude: 113 Deg. 59' E**				
Height Above Mean Sea Level (MSL): 17.0m							**T: <0.2mm**				
Month/ Date	**Jan**	**Feb**	**Mac**	**Apr**	**May**	**June**	**Jul**	**Aug**	**Sep**	**Oct**	**Nov**
1	0.0	0.0	0.0	0.0	16.8	0.2	2.2	9.4	2.8	0.0	74.6
2	0.0	0.0	10.0	7.2	0.2	0.0	0.0	82.0	0.0	0.0	17.0
3	5.0	3.6	16.0	0.0	0.4	4.4	0.0	0.0	49.2	4.0	17.2
4	T	57.2	0.6	0.0	1.4	3.4	0.0	0.0	0.0	0.0	0.0
5	0.0	0.0	0.0	0.2	10.6	0.0	0.0	14.4	0.0	0.0	1.4
6	0.0	0.4	0.0	10.6	1.0	0.2	0.0	0.0	5.6	0.0	4.2
7	0.0	5.8	0.2	0.0	66.2	0.0	0.0	0.0	1.0	0.4	0.0
8	0.0	4.8	0.0	0.0	0.6	0.0	0.0	0.0	13.6	53.6	0.0
9	T	1.8	0.0	3.4	0.0	0.0	0.0	0.0	0.0	7.8	10.8
10	17.6	7.8	0.0	T	0.0	0.0	0.0	7.2	0.0	0.0	0.0
11	41.2	0.0	1.4	0.0	50.4	3.4	0.0	21.2	0.0	0.0	4.0
12	0.0	0.0	0.0	0.0	0.8	0.0	0.0	1.0	17.4	0.0	2.0
13	0.0	0.0	0.0	2.4	22.4	2.8	0.0	0.0	0.0	9.8	2.0
14	0.0	0.0	0.0	T	0.0	0.2	0.8	0.0	0.0	35.2	27.2
15	0.0	0.0	2.2	0.0	23.0	0.0	0.4	0.0	0.0	1.0	3.0
16	0.0	0.0	0.0	0.0	14.2	3.2	2.4	0.2	T	10.6	8.8
17	0.0	0.0	9.8	0.0	0.0	22.2	20.4	T	0.0	59.6	17.0
18	0.0	0.0	1.6	0.0	0.0	4.8	0.0	0.0	0.0	T	1.0
19	0.0	0.0	0.0	0.0	0.4	5.2	0.0	0.0	0.0	0.0	0.0
20	1.4	0.0	0.0	0.0	0.0	0.0	13.8	0.2	0.0	2.3	0.0
21	0.2	0.0	0.0	6.4	0.0	20.8	114.8	T	T	0.0	0.2
22	5.2	0.0	0.0	0.0	0.8	0.2	0.0	0.0	3.0	10.8	89.4
23	0.0	0.0	0.0	12.8	2.4	T	30.4	0.0	0.6	27.8	45.0
24	0.0	0.0	11.8	9.8	0.0	0.0	7.8	10.4	0.0	8.0	1.2
25	0.0	0.0	0.4	0.0	0.0	18.2	3.6	1.6	0.0	T	0.0
26	0.0	0.0	0.0	18.2	0.0	0.0	11.4	0.0	0.0	0.0	0.0
27	0.0	0.0	27.2	0.0	0.0	25.6	1.4	0.0	0.0	1.6	4.8
28	0.0	0.0	0.8	36.0	0.0	0.0	0.0	0.6	0.0	19.8	0.0
29	0.0	0.0	0.0	57.8	5.0	0.0	7.4	0.0	15.2	0.0	
30	0.0		3.4	0.0	0.2	12.8	8.4	15.6	0.0	25.6	
31	0.0		0.4		12.0		39.8	0.4		33.0	
Total	70.6	81.4	85.8	164.8	228.8	127.6	265.0	164.2	108.4	310.9	
Total Rain days	6	7	14	11	19	16	15	13	9	17	

4.6 Wind Data

Similar to rainfall data (Section 4.5), wind speed data was also obtained from the Miri Meteorological Centre. Tables 4.6.1 and 4.6.2 illustrate the daily mean and daily maximum wind speed in 2016, whereas Tables 4.6.3 and 4.6.4 show the monthly mean and maximum from 2006 to 2016 respectively.

The highest mean wind speed recorded from 2006 to 2016 was observed in February with a value of 2.31m/s while the lowest mean value was 2.03m/s recorded during May as shown in Figure 4.6.1. Based on Figure 4.6.2, 2006 and 2007 were the least windy years from the eleven-year period at a mean surface speed of 2m/s. The windiest year was observed in 2016 with a value of 2.4m/s.

Figure 4.6.3 show the monthly wind distribution and speed from 2006 to 2016. During the eleven-year period, it was observed that January till April had the strongest winds measured from S to WSW directions. April had strongest winds from the NW regions while June and July registered the strongest winds between SW and WNW directions. August and September registered strong winds from W to SSW directions. The highest recorded winds were observed from WSW to a more southern direction from October to December.

In 2016, as seen in Figure 4.6.4, most of the winds registered between 10m/s and 16m/s from January till March were within the NNE and NE directions. In April, 8m/s to 10m/s winds measured from the S to SSW and, WNW to N directions. May observed winds at 10m/s to 13m/s from the S to SSW and NNW directions. June recorded wind speeds between 13m/s to 16m/s from W to WNW directions and July from WSW to W directions. August registered the same wind speed from SW and WNW directions. September and October recorded those wind speeds from WSW to W and SW to W directions respectively. November measured the 13m/s to 16m/s wind speed from a WNW direction.

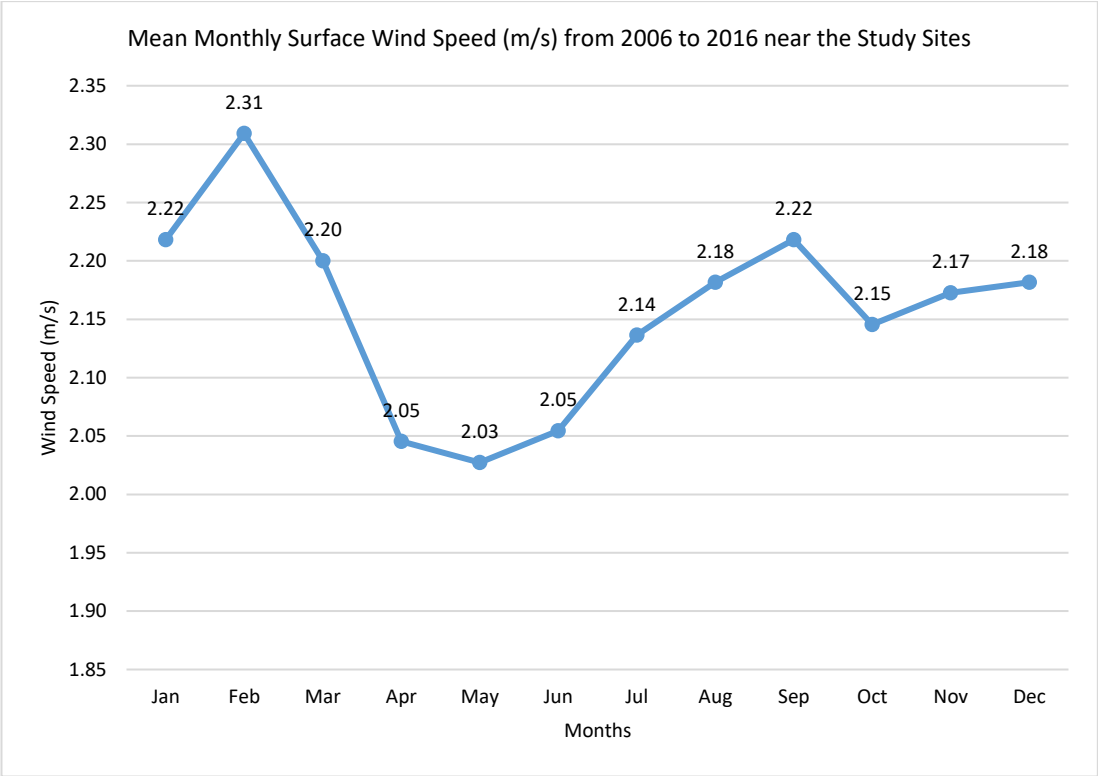

Figure 4.6.1 – Mean Monthly Surface Wind Speed (m/s) from 2006 to 2016 near the Study Sites

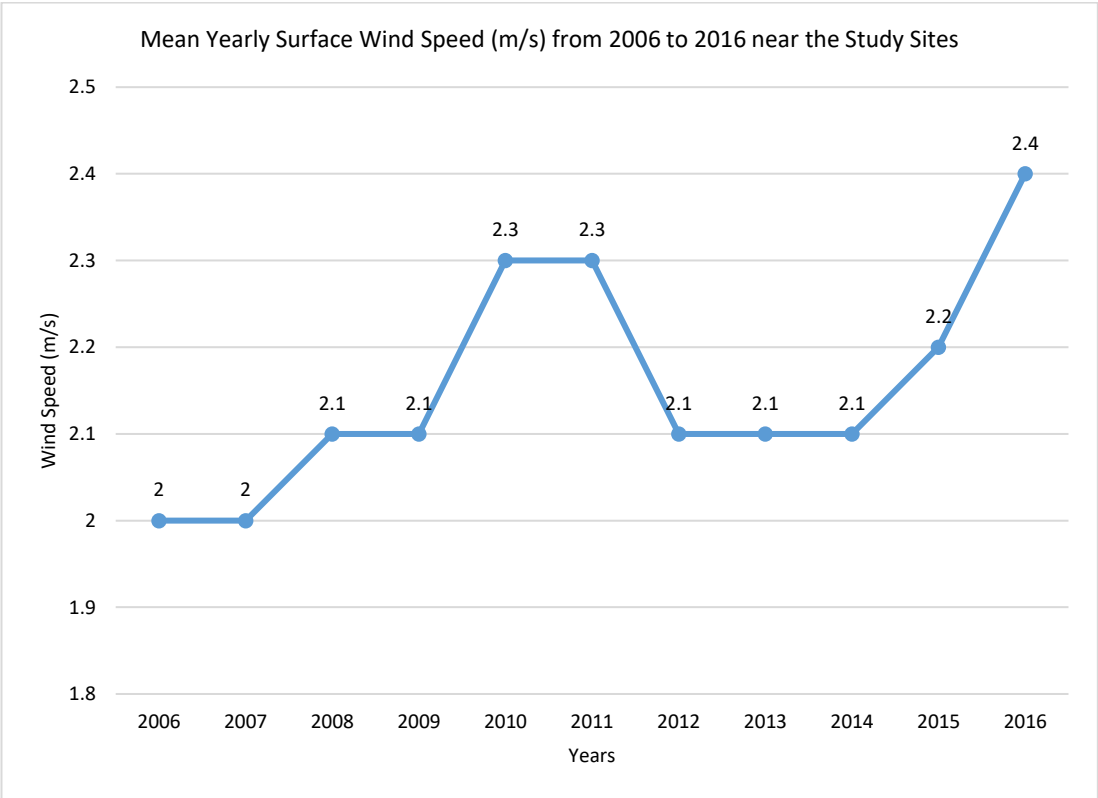

Figure 4.6.2 – Mean Yearly Surface Wind Speed (m/s) from 2006 to 2016 near the Study Sites

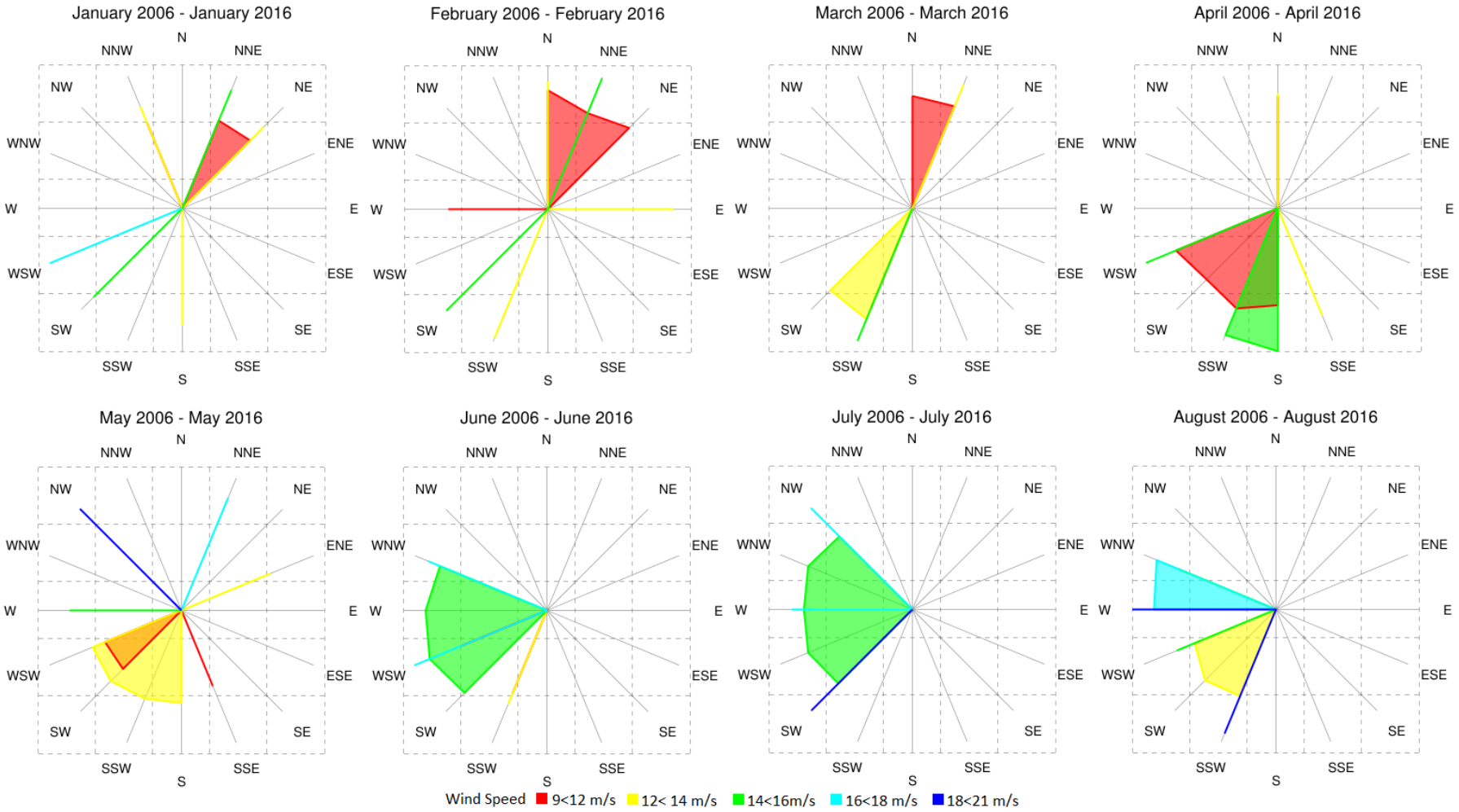

Figure 4.6.3 – Monthly Wind Distribution Diagrams (2006 – 2016) and Speed near the Study Sites (Enviroware, 2017)

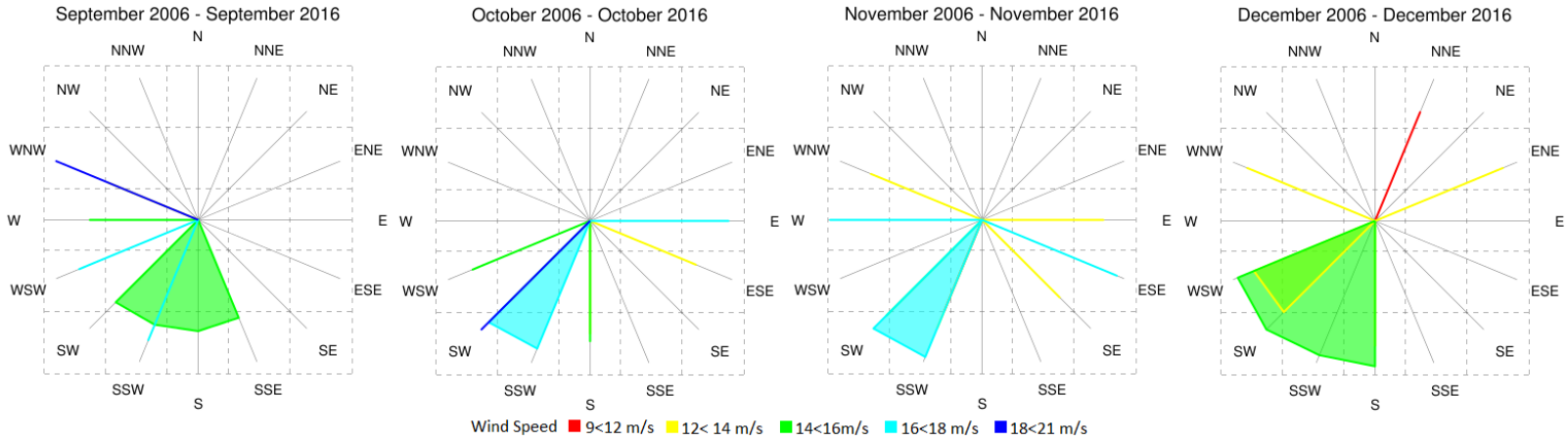

Figure 4.6.3 - Monthly Wind Distribution Diagrams (2006 – 2016) and Speed near the Study Sites (contd.)
(Enviroware, 2017)

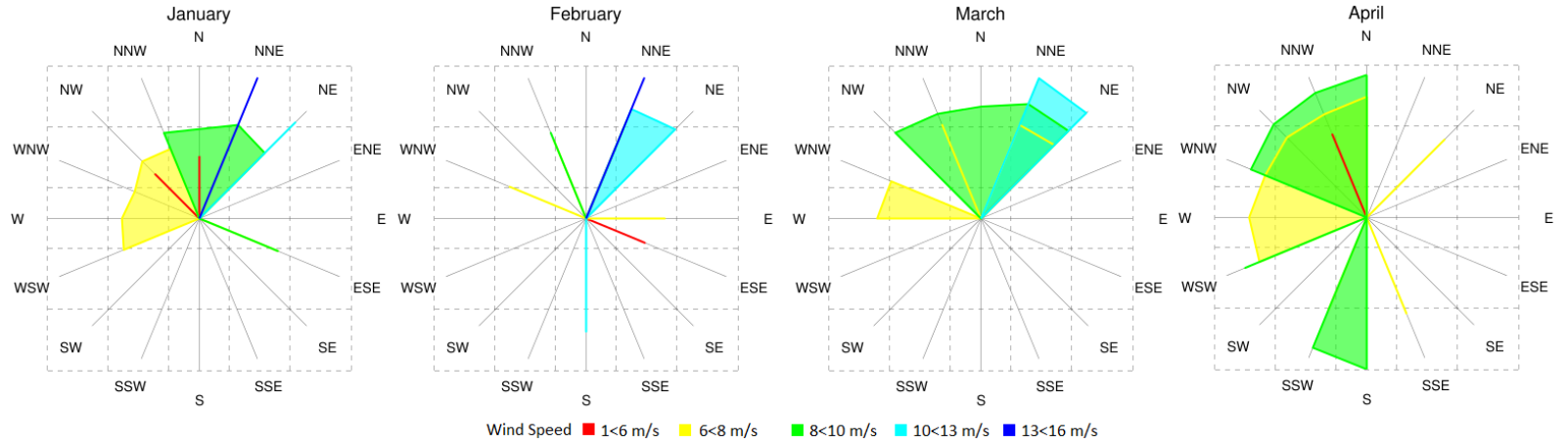

Figure 4.6.4 – Daily 2016 Wind Distribution Diagrams (January – April) and Speed near the Study Sites
(Enviroware, 2017)

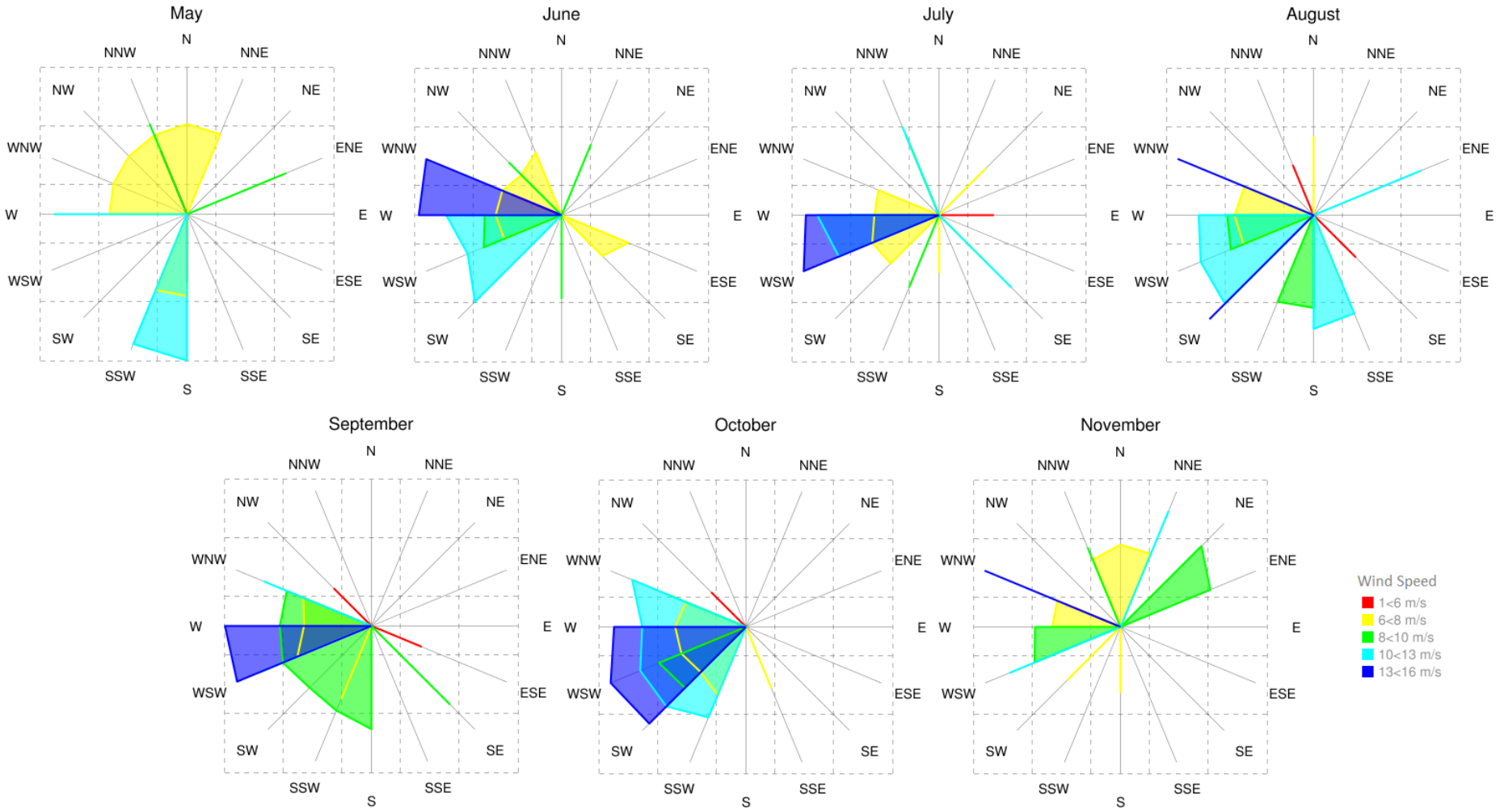

Figure 4.6.4 – Daily 2016 Wind Distribution Diagrams (May – November) and Speed near the Study Sites (contd.) (Enviroware, 2017)

Table 4.6.1 – Records of Daily Mean Surface Wind Speed near the Study Sites (2016)											
Unit: (m/s)			**Latitude: 04 Deg. 20' N**				**Longitude: 113 Deg. 59' E**				
Height Above Mean Sea Level (MSL): 17.0m							**N.A: Not Applicable**				
Month/ Date	**Jan**	**Feb**	**Mar**	**Apr**	**May**	**June**	**Jul**	**Aug**	**Sep**	**Oct**	**Nov**
1	3.3	3.3	4.8	2.8	1.9	1.6	1.4	3.4	2.8	1.9	2.2
2	2.1	4.1	4.1	2.3	2.0	2.2	1.6	2.6	2.8	2.6	3.8
3	1.6	2.5	2.8	2.1	2.0	2.0	1.9	2.8	2.8	2.7	4.2
4	1.7	2.4	2.4	2.2	2.4	2.4	2.7	1.6	2.6	2.6	2.3
5	2.1	2.6	3.0	1.9	2.6	2.4	2.2	1.9	2.5	1.9	1.2
6	1.8	3.8	2.8	2.1	2.7	1.8	1.8	1.8	2.0	3.0	1.8
7	2.6	5.4	3.0	1.9	1.9	2.2	1.7	2.6	3.1	2.4	2.0
8	3.0	3.2	2.6	2.4	2.5	1.8	2.4	1.9	2.2	2.4	3.3
9	2.7	2.6	2.0	1.9	2.5	2.0	2.4	2.3	2.6	3.0	1.4
10	2.0	1.6	2.3	2.4	1.8	2.1	2.2	2.2	1.9	1.8	1.7
11	1.9	2.6	2.9	2.1	1.6	2.4	1.9	2.2	1.6	1.9	1.8
12	2.1	1.8	3.2	2.1	1.7	2.3	1.9	1.6	2.0	2.5	2.0
13	2.0	2.2	2.1	2.4	1.9	2.8	2.9	2.0	2.1	2.6	1.8
14	2.3	2.4	2.0	1.8	1.5	2.0	2.6	2.1	1.6	2.4	2.1
15	2.3	3.1	2.5	2.1	1.9	2.9	2.2	2.2	2.1	1.6	2.0
16	2.3	3.2	2.7	2.7	2.2	2.0	2.0	2.3	2.2	1.9	1.8
17	1.9	2.4	1.6	2.3	2.1	2.3	2.1	2.3	2.6	3.0	1.7
18	2.2	4.0	2.3	2.4	2.3	1.9	2.5	2.1	2.1	2.8	1.8
19	2.8	4.3	2.2	2.0	1.9	4.1	2.2	2.3	2.3	2.0	1.8
20	2.7	5.4	2.2	2.2	2.4	2.2	2.0	2.5	2.3	1.7	1.9
21	1.8	4.6	2.2	2.1	1.9	2.2	2.7	2.4	2.2	1.9	2.1
22	2.0	2.7	2.0	2.1	2.9	2.5	1.8	2.8	2.8	1.3	1.6
23	3.4	2.6	2.2	2.6	2.8	2.0	1.7	2.3	2.8	3.5	2.4
24	5.0	4.9	2.5	2.2	2.1	2.2	2.3	2.0	2.8	3.4	2.0
25	4.6	4.3	2.7	2.4	1.7	2.5	2.7	2.1	1.8	3.4	1.3
26	2.8	3.6	2.3	1.6	2.0	2.2	3.2	3.3	2.0	1.8	1.8
27	2.2	4.5	4.1	2.5	2.3	2.4	2.8	2.1	2.6	2.2	1.9
28	2.1	4.6	4.2	2.3	2.1	2.2	1.9	2.5	2.9	2.3	2.1
29	2.1	4.4	3.5	1.8	2.4	1.7	1.8	2.6	2.3	1.7	2.1
30	2.1		2.7	1.8	2.4	1.9	2.6	2.3	2.1	2.3	3.5
31	2.8		2.3		2.3		3.1	2.2		2.3	
Mean	2.5	3.4	2.7	2.2	2.2	2.2	2.2	2.3	2.4	2.3	2.1

Table 4.6.2 – Records of Daily Maximum Surface Wind Direction and Speed near the Study Sites																						
Unit: Dir (Degrees) Spd (m/s)					**Latitude: 04 Deg. 20' N**						**Longitude: 113 Deg. 59' E**						**Height Above Mean Sea Level (MSL): 17.0 M**					
Month	**Jan**		**Feb**		**Mar**		**Apr**		**May**		**Jun**		**Jul**		**Aug**		**Sep**		**Oct**		**Nov**	
Date	**Dir**	**Spd**	**Dir**	**Spd**	**Dir**	**Spd**	**Dir**	**Spd**	**Dir**	**Spd**	**Dir**	**Spd**	**Dir**	**Spd**	**Dir**	**Spd**	**Dir**	**Spd**	**Dir**	**Spd**	**Dir**	**Spd**
1	030	9.2	330	9.3	030	10.9	350	9.2	310	6.6	250	6.5	210	8.2	300	13.9	290	9.2	230	7.1	300	13.7
2	280	6.7	020	10.7	040	9.2	290	7.9	280	6.1	300	6.9	140	11.3	220	11.6	250	9.9	270	10.3	250	10.6
3	340	8.4	330	8.2	030	7.6	180	9.8	290	7.5	260	8.4	260	5.8	190	10.8	270	8.7	150	6.8	240	10.3
4	350	5.8	170	10.5	010	8.4	320	8.8	360	7.7	240	8.9	140	7.2	330	5.1	200	8.8	200	7.6	20	11.7
5	310	7.4	340	7.9	030	9.8	290	6.3	340	8.5	240	7.2	260	7.1	260	10.9	260	6.4	230	6.1	300	5.1
6	290	6.5	020	10.2	340	8.1	290	7.2	190	7.3	320	6.2	290	6.8	140	5.6	130	10.5	250	9.8	260	8.0
7	340	8.4	020	14.1	330	8.5	330	7.2	270	6.1	250	6.6	300	6.2	190	8.2	300	6.9	210	10.1	030	7.4
8	030	9.5	030	8.4	340	8.1	280	7.6	170	7.7	290	5.8	300	6.6	250	7.3	300	11.0	250	11.8	040	10.7
9	120	7.9	330	8.5	340	8.5	210	9.1	310	7.3	290	6.7	300	6.3	260	8.3	260	9.1	220	12.4	300	5.9
10	320	5.8	330	8.0	300	7.3	250	7.5	280	6.1	300	7.4	280	6.9	180	9.2	110	4.6	240	7.0	350	7.5
11	310	7.1	080	7.3	340	9.1	280	7.3	200	7.0	300	7.7	170	6.0	260	7.1	250	8.2	270	7.9	330	6.7
12	350	8.3	300	7.6	030	9.6	350	7.6	020	7.4	240	9.5	300	6.8	350	7.5	250	13.8	250	7.3	340	7.0
13	340	6.9	110	5.9	270	7.9	150	6.7	300	6.6	260	12.6	130	10.0	240	6.6	120	5.6	270	7.4	070	9.1
14	050	7.8	300	7.8	340	8.1	340	5.8	070	9.1	270	8.3	340	8.3	240	8.5	280	14.3	260	11.1	340	6.6

15	330	7.8	030	10.8	050	9.4	330	7.5	290	7.0	290	6.5	330	10.0	240	7.4	250	7.7	230	10.8	300	6.4
16	380	7.7	040	10.2	330	9.6	330	8.7	170	12.5	300	7.4	300	7.1	270	7.9	230	8.3	270	13.9	220	6.7
17	330	7.2	340	8.8	050	5.2	290	7.5	280	6.5	030	8.3	260	9.5	160	10.1	210	7.7	250	15.1	230	7.2
18	310	7.8	040	12.1	330	8.1	300	8.1	260	7.1	320	8.1	290	7.7	270	8.1	290	8.2	230	14.1	290	6.2
19	050	9.0	030	11.3	340	8.2	350	7.9	190	5.8	220	13.4	340	6.9	170	9.	250	7.6	300	6.0	260	6.7
20	030	9.1	020	12.8	330	9.2	050	7.1	290	6.5	240	11.1	230	7.2	250	111.6	250	7.4	240	4.5	300	6.1
21	340	6.1	030	11.2	320	8.5	240	8.2	300	6.3	300	6.7	290	7.7	250	7.4	240	12.0	290	12.7	340	8.0
22	240	7.6	330	8.6	340	7.5	280	7.8	210	12.0	170	9.1	040	6.9	230	11.6	250	11.2	310	5.0	280	6.0
23	020	9.9	340	9.1	280	7.6	310	8.1	270	11.3	340	7.7	280	6.5	210	8.9	280	13.4	270	13.3	350	7.9
24	030	14.1	040	12.9	340	7.7	310	7.2	190	6.1	140	6.3	330	9.9	260	7.4	310	5.0	250	9.6	340	7.4
25	040	12.6	050	11.4	030	8.1	310	7.4	330	5.8	260	15.6	240	7.6	230	13.9	290	7.0	220	9.7	300	6.5
26	040	8.1	030	10.1	040	7.8	210	6.5	300	6.4	280	7.2	270	12.8	230	12.4	200	8.7	270	6.7	190	6.1
27	320	7.7	030	9.7	030	11.9	240	8.2	340	7.3	300	16.0	280	14.0	290	7.5	210	8.5	250	7.2	250	8.7
28	310	7.7	030	11.0	040	11.2	290	6.5	260	6.4	110	7.9	090	5.7	270	8.3	270	8.4	290	6.7	300	6.9
29	340	8.1	020	9.8	030	9.7	240	9.2	330	8.1	330	7.3	340	7.5	150	6.8	210	7.0	220	8.0	340	6.2
30	330	8.5			320	9.7	340	6.8	290	7.1	330	7.2	240	11.4	060	11.0	170	9.8	290	7.4	240	12.7
31	340	9.7			340	8.5			260	7.8			250	15.4	300	6.7			300	8.8		
Max	030	14.1	020	14.1	030	11.9	180	9.8	170	12.5	300	16.0	250	15.4	300 230	13.9 13.9	280	14.3	250	15.1	300	13.7

Table 4.6.3 – Records of Mean Monthly Surface Wind Speed near the Study Sites													
Unit: m/s			**Latitude: 04 Deg. 20' N**			**Longitude: 113 Deg. 59' E**			**Height Above Mean Sea Level (MSL): 17.0 M**				
Month/ Year	**Jan**	**Feb**	**Mar**	**Apr**	**May**	**Jun**	**Jul**	**Aug**	**Sep**	**Oct**	**Nov**	**Dec**	**Annual**
2006	2.0	2.2	2.1	1.9	1.9	2.1	1.9	2.1	2.0	1.9	2.0	1.9	2.0
2007	2.3	1.8	1.7	1.7	1.8	1.8	2.0	2.1	2.2	2.3	2.4	2.2	2.0
2008	1.8	2.4	2.0	2.0	2.1	1.9	2.1	1.9	2.3	2.1	2.1	2.1	2.1
2009	2.5	2.0	2.0	2.0	2.0	2.0	2.0	2.1	2.2	2.2	2.1	1.9	2.1
2010	2.1	2.3	2.2	2.2	2.2	2.3	2.4	2.3	2.4	2.5	2.3	2.4	2.3
2011	2.3	2.3	2.4	2.4	2.1	2.1	2.1	2.3	2.5	2.1	2.3	2.3	2.3
2012	2.2	2.2	2.3	2.0	2.0	2.2	2.3	2.2	2.1	2.1	2.1	2.1	2.1
2013	2.3	2.3	2.1	2.0	2.0	2.0	2.1	2.2	2.1	2.1	2.1	2.2	2.1
2014	2.1	2.3	2.4	2.0	2.0	2.0	2.0	2.1	2.1	1.9	2.2	2.1	2.1
2015	2.3	2.2	2.3	2.1	2.0	2.0	2.4	2.4	2.1	2.1	2.2	2.4	2.2
2016	2.5	3.4	2.7	2.2	2.2	2.2	2.2	2.3	2.4	2.3	2.1	2.4	2.4

Table 4.6.4 – Records of Monthly Maximum Surface Wind Speed near the Study Sites													
Unit: Dir (Degree) / Spd (m/s)			**Latitude: 04 Deg. 20' N**			**Longitude: 113 Deg. 59' E**			**Height Above Mean Sea Level (MSL): 17.0 M**				
Month/ Year	**Jan**	**Feb**	**Mar**	**Apr**	**May**	**Jun**	**Jul**	**Aug**	**Sep**	**Oct**	**Nov**	**Dec**	**Max**
2006	050/11.2	210/13.9	210/14.9	180/10.3	030/16.1	300/14.4	270/13.6	280/19.8	160/14.0	190/13.2	130/12.5	250/13.5	280/19.8
2007	210/14.6	360/11.9	220/12.1	160/12.0	210/12.7	210/12.6	290/15.4	300/14.7	290/20.3	240/14.7	200/13.3	250/12.0	290/20.3
2008	020/11.1	230/14.3	210/11.2	210/14.3	320/19.0	290/14.0	260/14.2	200/13.9	220/15.4	180/14.1	220/15.4	180/14.2	320/19.0
2009	190/13.6	020/10.4	210/11.2	200/11.3	230/13.3	220/11.2	230/14.3	240/14.8	210/15.0	220/16.8	220/17.5	210/14.2	220/17.5
2010	340/12.8	350/12.8	350/11.7	010/12.0	070/12.8	240/11.6	280/16.4	290/14.6	300/12.5	210/16.2	200/16.9	230/12.6	200/16.9
2011	030/15.7	080/12.5	210/12.5	240/11.5	170/12.0	300/15.1	280/15.4	210/12.0	240/16.5	230/13.4	260/17.3	220/15.0	260/17.3
2012	020/11.1	270/9.9	030/11.9	230/10.6	280/14.8	240/17.9	310/14.1	310/17.9	190/14.7	120/13.4	110/16.6	020/11.5	310/17.9
2013	040/13.3	040/11.4	030/13.9	190/14.9	160/10.8	250/15.9	230/19.4	210/18.5	250/17.5	230/18.0	080/13.8	170/12.2	230/19.4
2014	340/10.8	030/14.0	020/11.0	360/11.7	250/11.0 220/11.0	230/14.6	270/13.3	240/12.2 250/12.2	290/13.2	240/14.9	210/11.2	060/13.5	240/14.9
2015	240/16.7	050/11.5	030/11.1	250/14.8	250/12.8	270/15.2	320/19.5	260/16.9	200/17.2	100/16.2	210/11.1	290/13.5	320/19.5
2016	030/14.1	020/14.1	030/11.9	180/9.8	170/12.5	300/16.0	250/15.4	300/13.9 230/13.9	280/14.3	250/15.1	300/13.7	240/14.5	300/16.0

CHAPTER 5 – DISCUSSION

This research work gives a detailed understanding of the seawater quality of the Miri-Sibuti Coral Reef National Park, spatially and temporally, and compares it to that of Sipadan Island Park. The field measurements were taken from three sites; North Siwa, Anemone Garden and Eve's Garden. Those measurements and results from the laboratory analysis of the major ions, nutrients and trace metals help to describe the state of both marine reserves.

5.1 Field Condition during Sampling

While heading to the first site, North Siwa, at the start of southwest monsoon (SWM) (May), there was a slight swell in the waves, which did not exceed a height of one meter present. Once at the site, an ocean current from south to north was noted. The maximum surface wind speed was 7.8m/s from the west direction. Visibility at the surface was better than at the seabed, which was also observed in the turbidity readings. Anemone Garden had better weather conditions where the visibility was better than North Siwa and the current was also less strong. Eve's Garden had similar weather conditions as Anemone Garden. However, even though the ocean current was still from south to north, the visibility was noticeably less than the other two locations, which indicated that the two main rivers; Baram river and Miri river still had an influence on the site.

The second sampling was at the end of SWM (September). A strong North to South current was noted. The maximum surface wind speed that day was 14m/s from a westerly direction. The seawater was green in colour and turbidity was much higher than the start of SWM. Suspended particles could be seen in the water when samples were being collected. The weather was cloudy and windy, and the conditions did not improve even at Eve's Garden, the last sampling site. The seawater temperature was warmer than the atmospheric temperature measured at 27°C.

The last sampling performed in Miri during northeast monsoon (NEM) transition period was the most challenging. A strong persistent north to south current was present at all three sites and the water was brownish-green in colour. The maximum surface

wind speed recorded that day was 7.2m/s from a westerly direction. Visibility in the water, was less than 1m and the wind at the surface was stronger and the waves higher.

Seawater from Sipadan Marine Park was retrieved on 21st October 2016. There was a light but persistent current going from east to west, and even though it rained a day before sampling, visibility was not affected. The small town of Semporna is roughly 40km away and Mabul Island, where most of the divers and resorts are, is approximately 14km from Sipadan Island, which meant that the marine park was mostly affected by human and boat activities.

5.2 Miri-Sibuti Coral Reef National Park

5.2.1 In-Situ Parameters

Temperature and pH are the first two parameters measured to ascertain the quality of seawater since variations in temperature can modify the number of ions present, which incidentally also changes its pH (Measurements, 2016d). At the Miri-Sibuti Coral Reef National Park, the average temperatures of all three sites observed a decrease of 0.45°C from commencement to end of SWM and a 0.14°C increase from the end of SWM to transition period. Figures 5.2.1 to 5.2.3, spatially and temporally compares the temperature against the pH at each site. Studies have been done to show the relationship between pH and temperature such as the absorption of carbon dioxide from the atmosphere, which is then converted to carbonic acid, thereby decreasing the pH of seawater (M. Lee et al., 2008; Edzwald and Haarhoff, 2011; Howard et al., 2013). However, the variation of temperature in Miri was too small to have a direct effect on the pH of the seawater. North Siwa was the only site that showed a small correlation between increasing temperature and decreasing pH from beginning of SWM to NEM transition. Anemone Garden and Eve's Garden did not exhibit the same correlations as North Siwa since no clear trend was observed (Figures 5.2.2 and 5.2.3). Therefore, in Miri, pH and temperature were not dependent on each other but pH was governed by other parameters as shown in Figures 5.2.4 – 5.2.9.

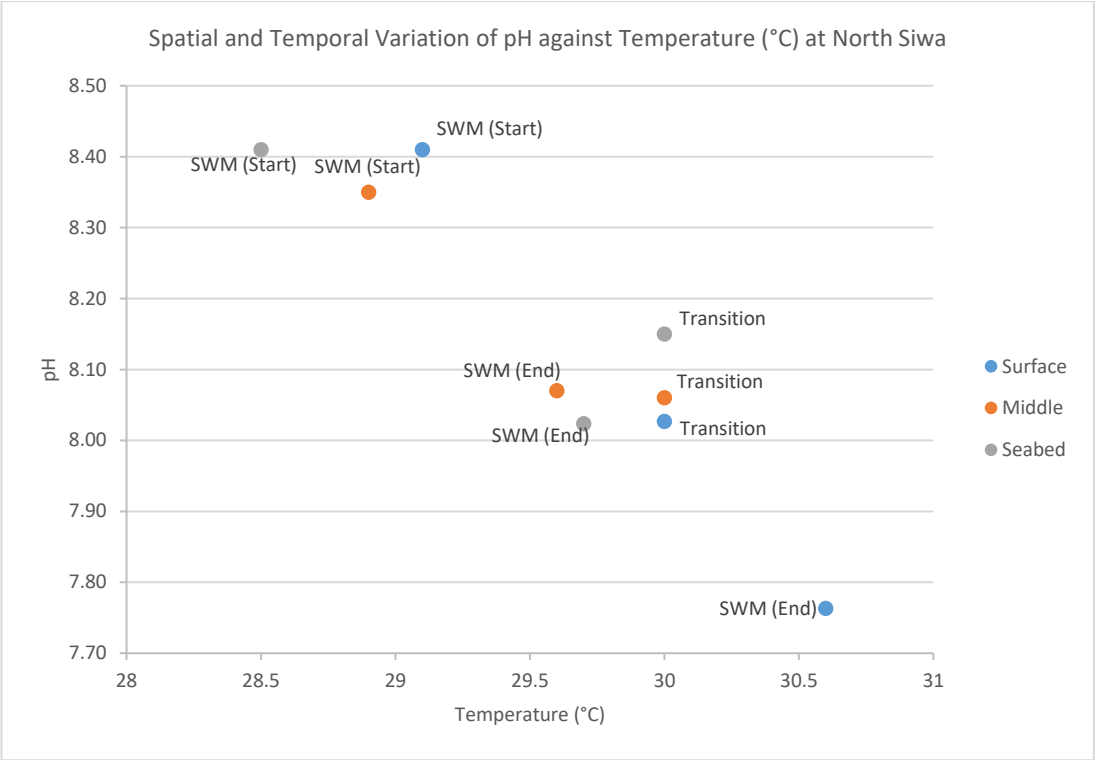

Figure 5.2.1 – pH against Temperature (°C) at North Siwa

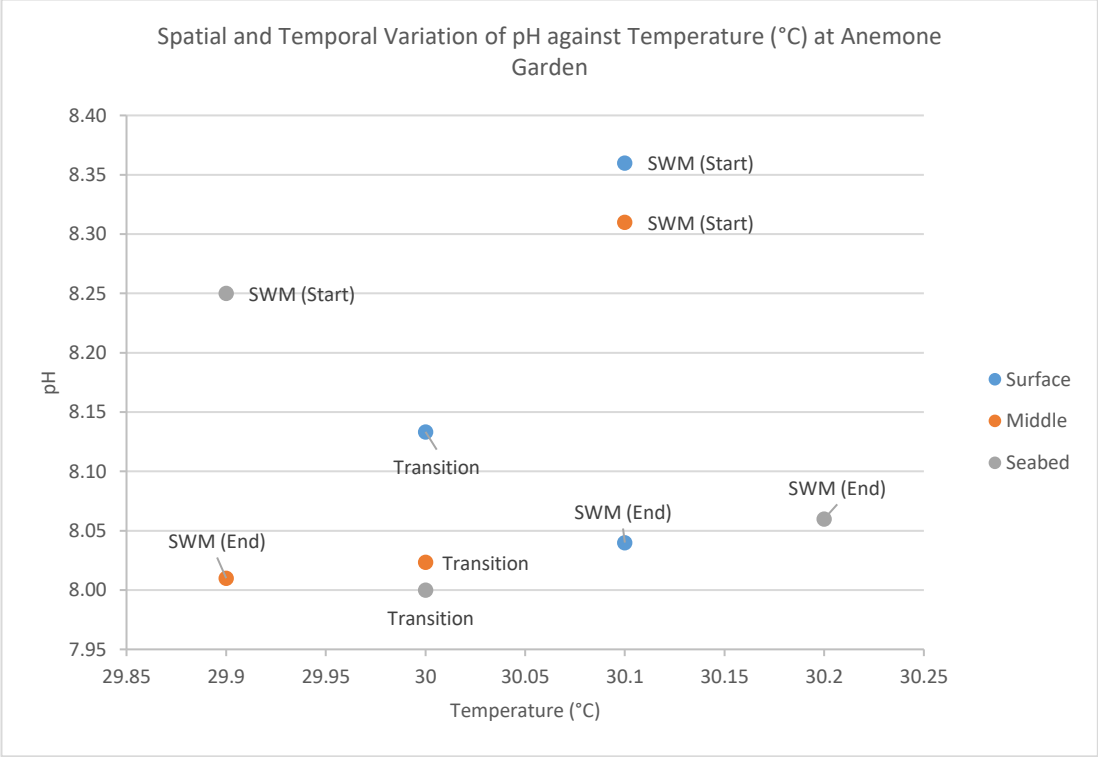

Figure 5.2.2 – pH against Temperature (°C) at Anemone Garden

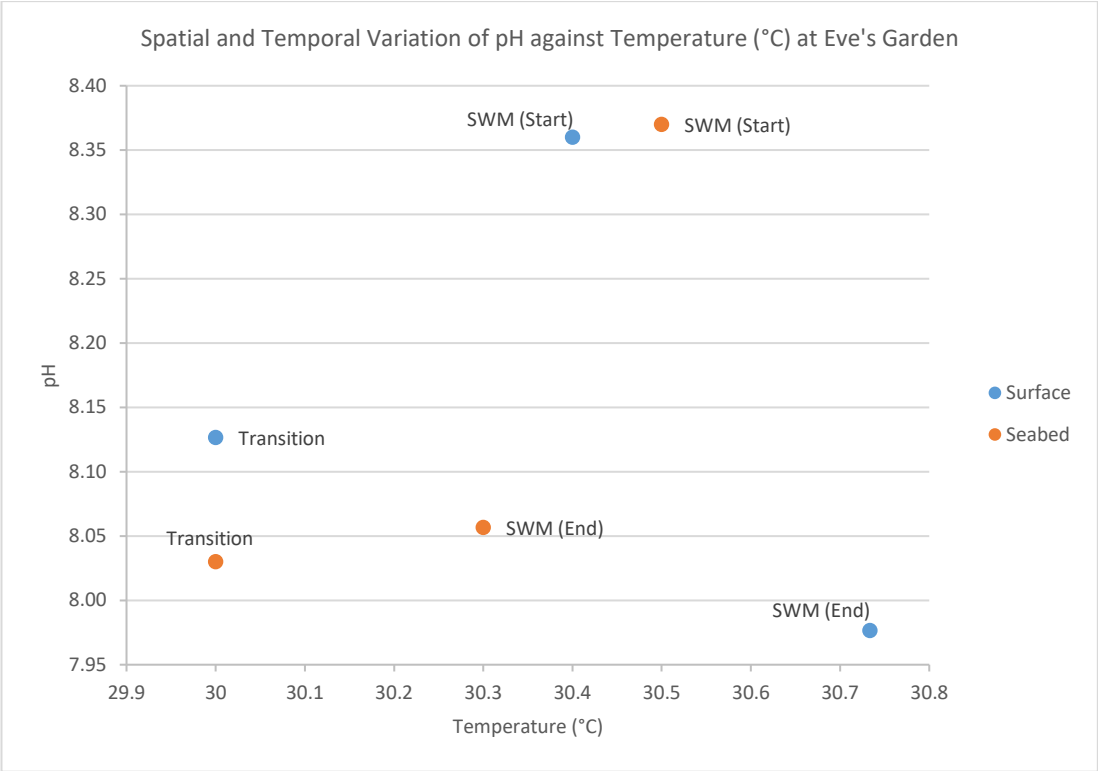

Figure 5.2.3 - pH against Temperature (°C) at Eve's Garden

Electrical conductivity (EC) is also known as the measure of the salinity of the water since the measure of salt from evaporating the seawater was deemed tedious and inaccurate (Health, 2016). The average EC during start of SWM was 37.30mS/cm, which was 11.38mS/cm lower than the end of SWM at an average conductivity of 48.68mS/cm. The average value during NEM transition was 48.21mS/cm, which was a decrease of 0.47mS/cm from the end of SWM. The variations in EC and pH in seawater could be linked to anthropogenic activities such as fertilisers and sewage from river runoffs (Edzwald and Haarhoff, 2011; Tew et al., 2014; Drupp, 2015; Measurements, 2016a). Figures 5.2.4 to 5.2.6 clearly indicate a higher conductivity with a lower pH during the end of SWM and NEM transition. Sections 4.3 and 4.4 also show that the concentration of nutrients and trace metals are higher during those two seasons as compared to the start of SWM.

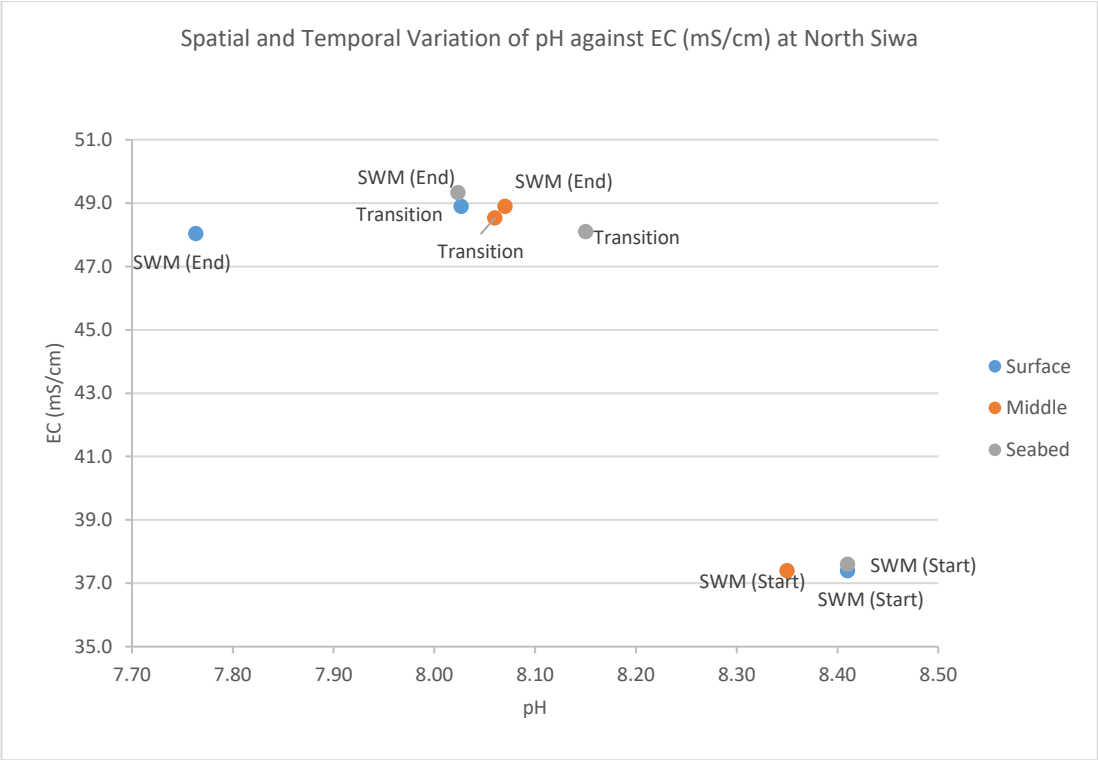

Figure 5.2.4 – EC (mS/cm) against pH at North Siwa

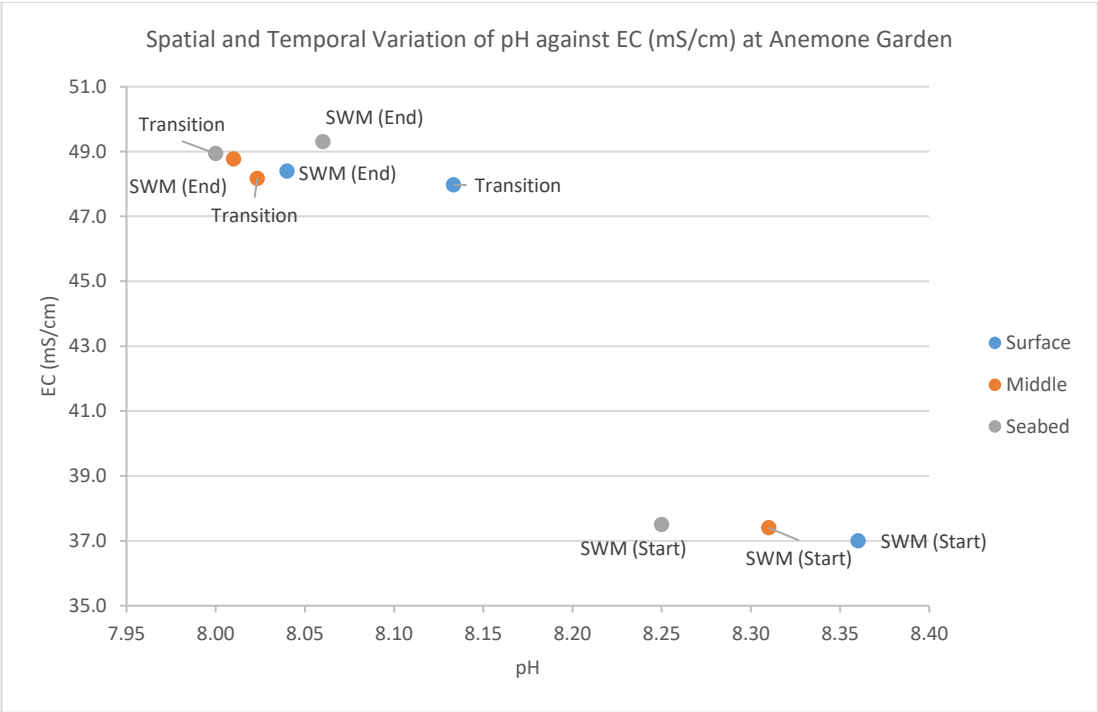

Figure 5.2.5 – EC (mS/cm) against pH at Anemone Garden

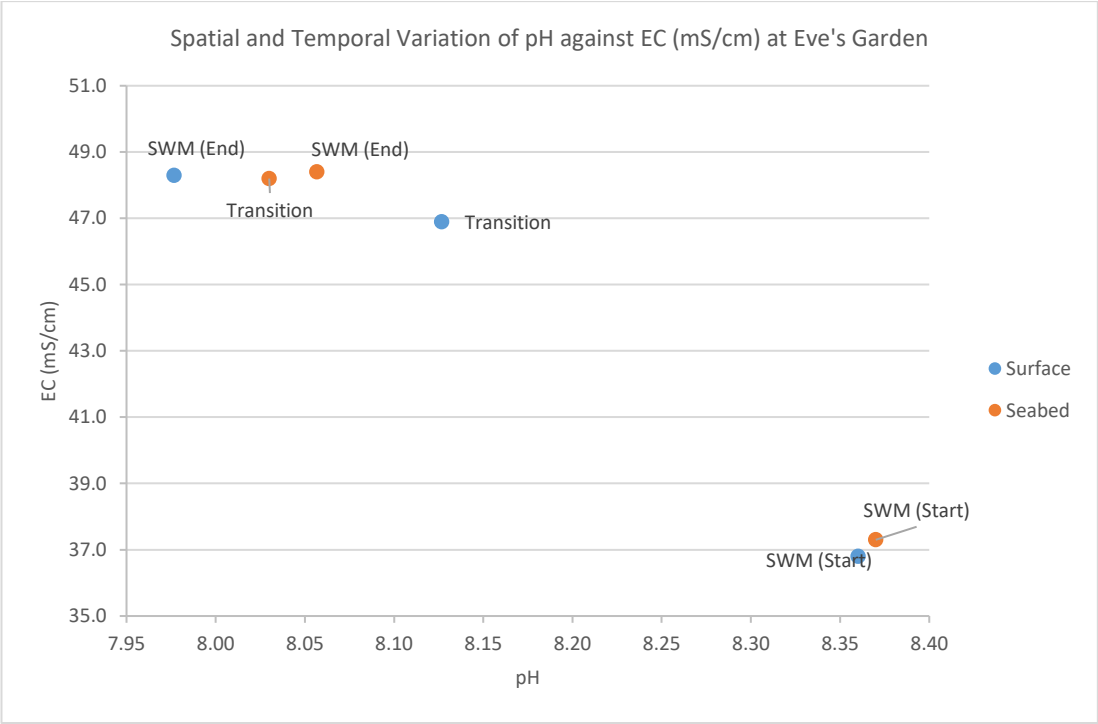

Figure 5.2.6 - EC (mS/cm) against pH at Eve's Garden

The highest average of ORP was measured at the beginning of SWM at -60.18mV and at a difference of -5.01mV, the lowest average was -65.19mV at the end of SWM. The average during the transition period was -64.39mV which was -0.8mV more than the end of SWM. Based on the observations of Rakestraw (1943), ORP is relative to the concentration of DO in the seawater and its pH. However, the author also explains the difficulty in identifying the sources of ORP species in-situ. In Figures 5.2.7 to 5.2.8, the lower pH values from the end of SWM and NEM transition had lower ORP values at North Siwa and Anemone Garden respectively and the high pH values during commencement of SWM also correlated to high ORP values. During the start of SWM, higher ORP values were observed at the seabed of North Siwa and Anemone Garden but Eve's Garden had a higher value at the surface and lower at the seabed. The correlation between ORP and pH was more erratic at Eve's Garden making it difficult to pinpoint the relationship between the two parameters, thus confirming the observations made by previous authors (Rakestraw, 1943; Measurements, 2016d).

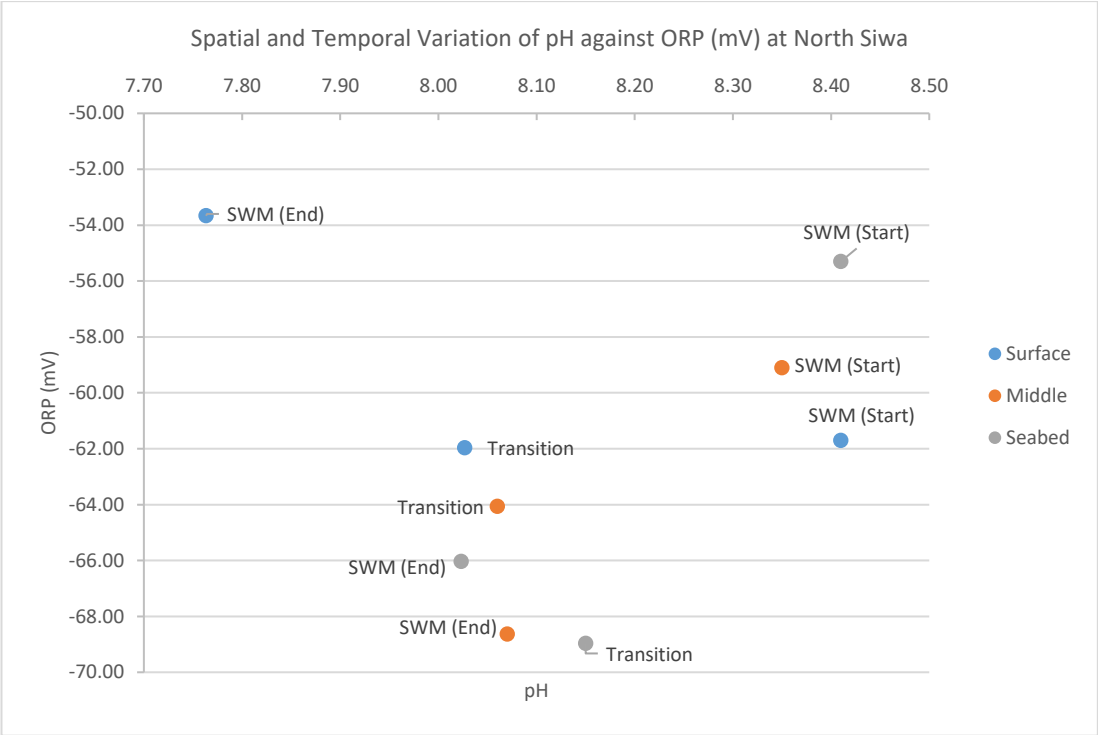

Figure 5.2.7 – ORP (mV) against pH at North Siwa

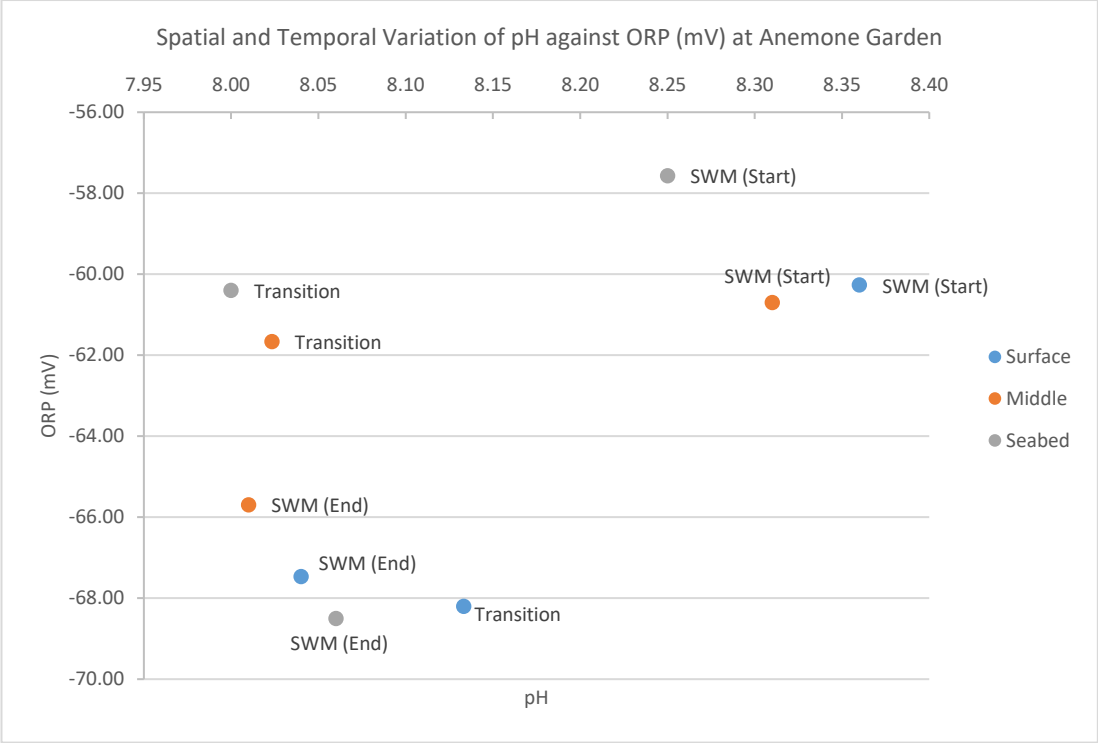

Figure 5.2.8 – ORP (mV) against pH at Anemone Garden

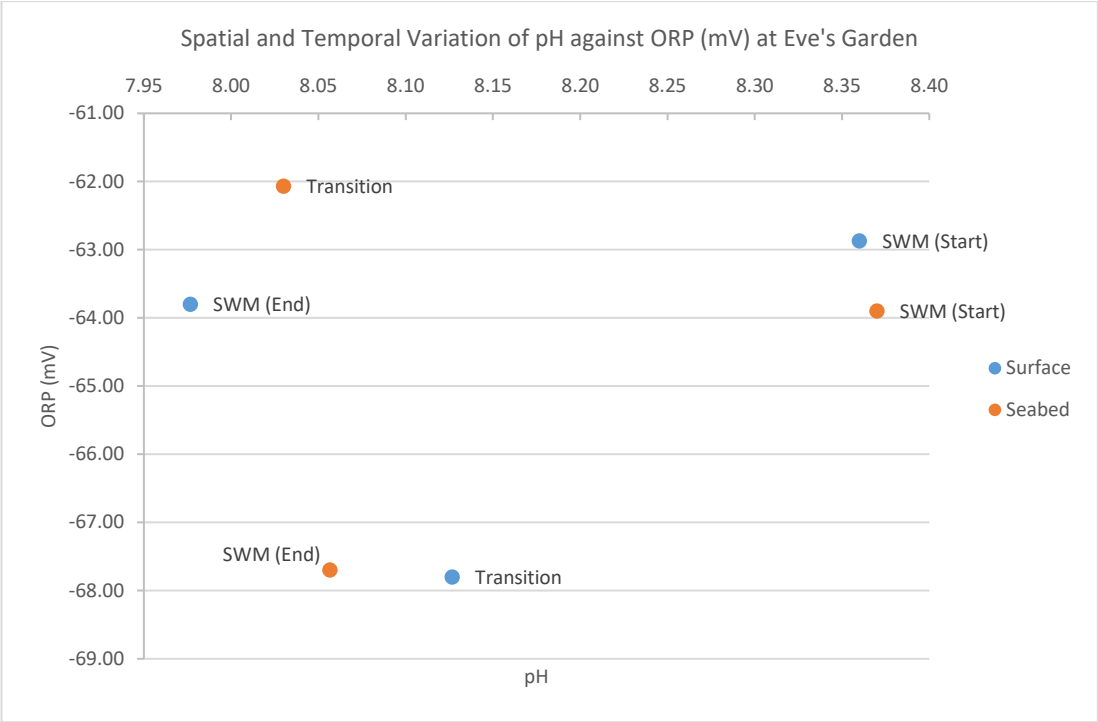

Figure 5.2.9 – ORP (mV) against pH at Eve's Garden

The average concentration of TDS was highest during the end of SWM with a value of 23.58mg/L as compared to the lowest average of 18.28mg/L in the beginning of SWM, and 23.14mg/L for the transition period. That is 5.30mg/L more than the start of SWM and 0.44mg/L higher than NEM transition. A higher concentration of TDS is also responsible for the increase in conductivity, since TDS is made up of ions from various types of salts such as the ones in this study (Rakestraw, 1943; Measurements, 2016a). Figures 5.2.10 to 5.2.12 represent the relationship between EC and TDS which shows that a higher input of ions was observed during the end of SWM and transition period at all three sites indicated by the increase in EC. Figures 5.2.13 to 5.2.15 illustrate that an increase in the concentration of TDS had a direct impact on the pH of the seawater at the three sites. Those increase in concentrations could be due to the influence of river runoffs and coastal development (Rakestraw, 1943; Edzwald and Haarhoff, 2011; Measurements, 2016a).

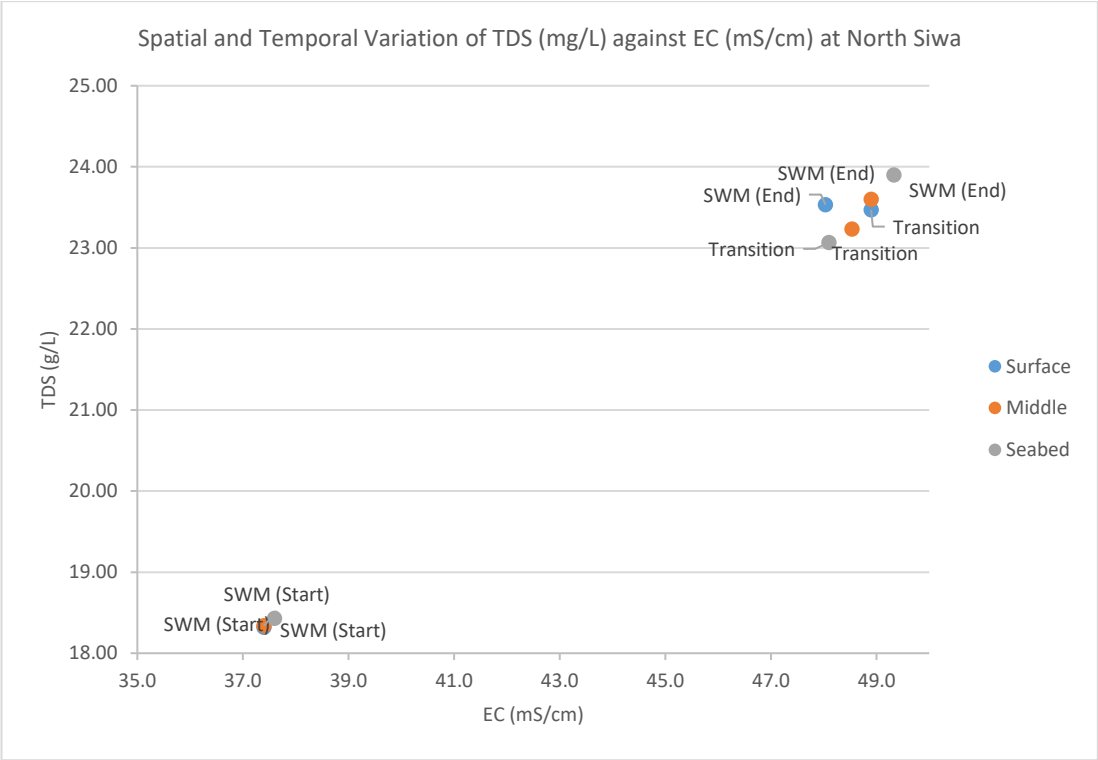

Figure 5.2.10 - TDS (g/L) against EC (mS/cm) at North Siwa

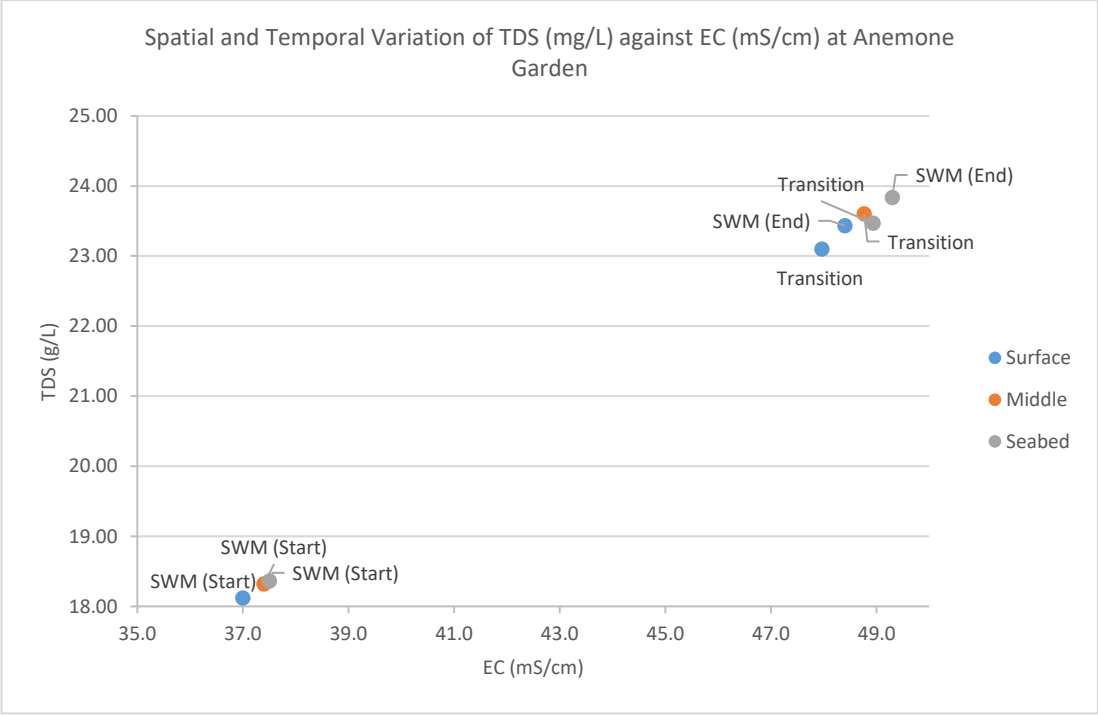

Figure 5.2.11 - TDS (g/L) against EC (mS/cm) at Anemone Garden

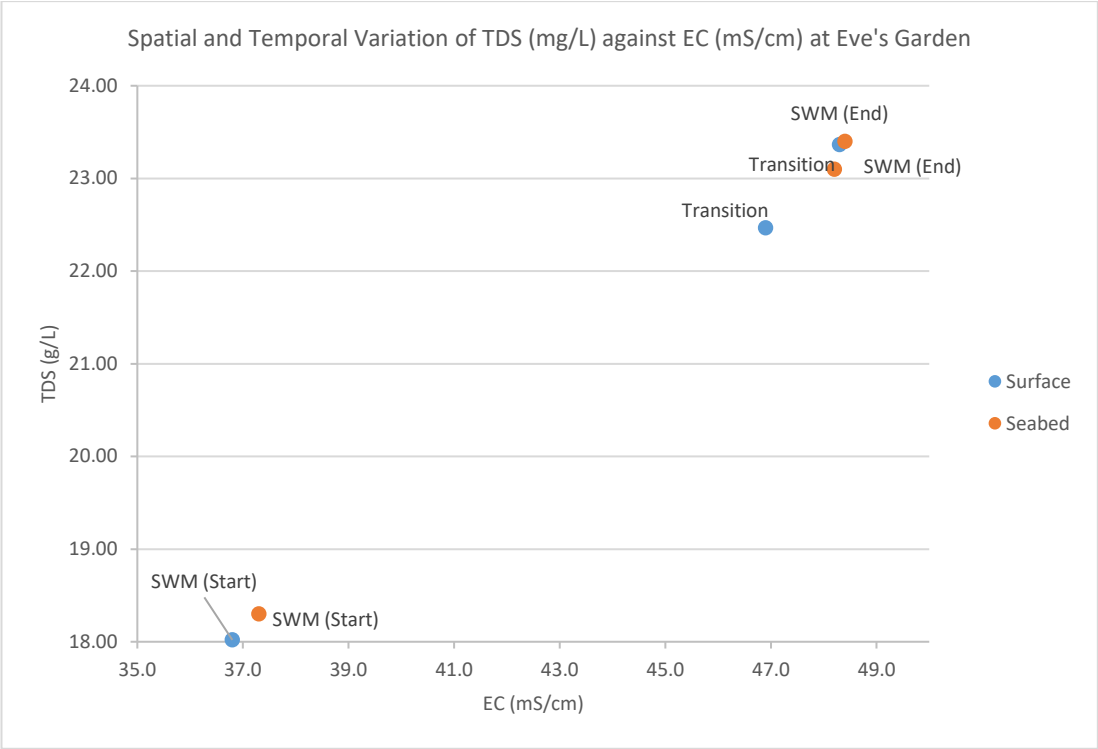

Figure 5.2.12 - TDS (g/L) against EC (mS/cm) at Eve's Garden

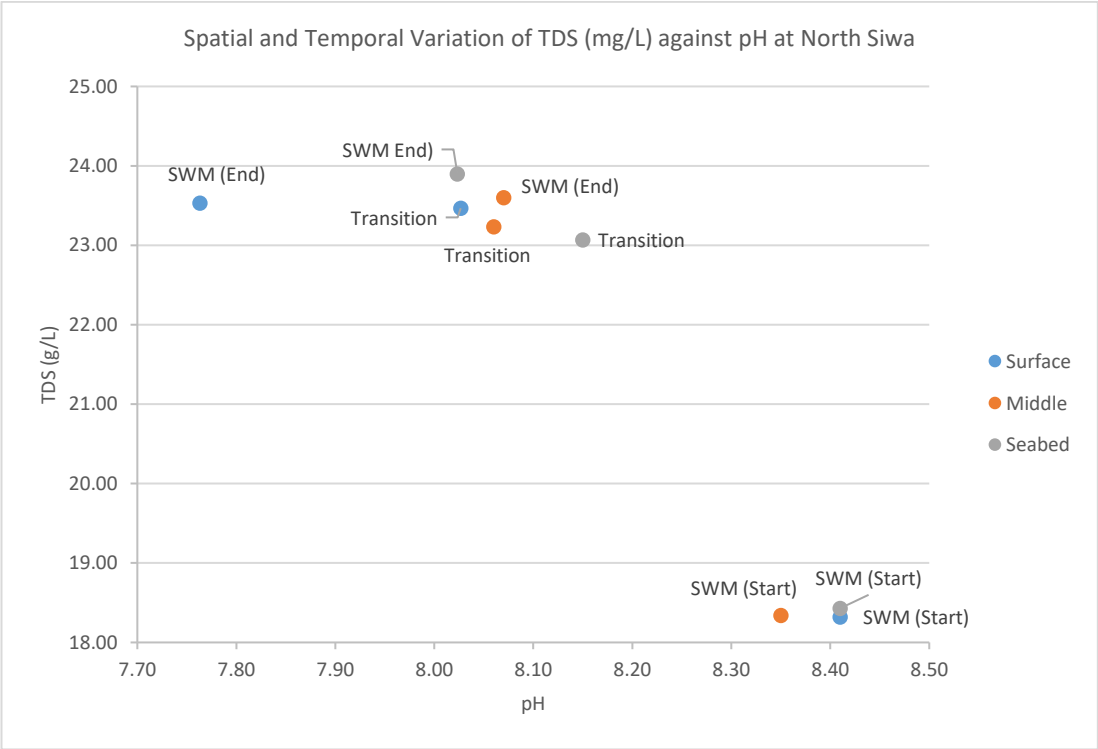

Figure 5.2.13 – pH against TDS (g/L) at North Siwa

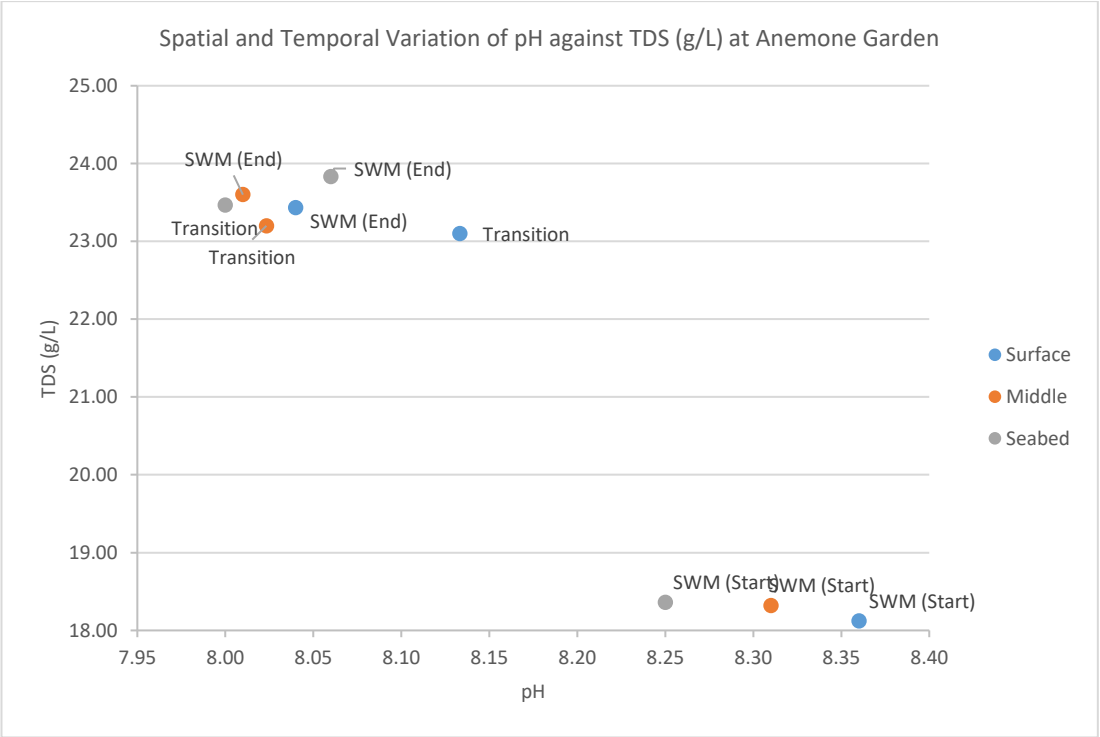

Figure 5.2.14 – pH against TDS (g/L) at Anemone Garden

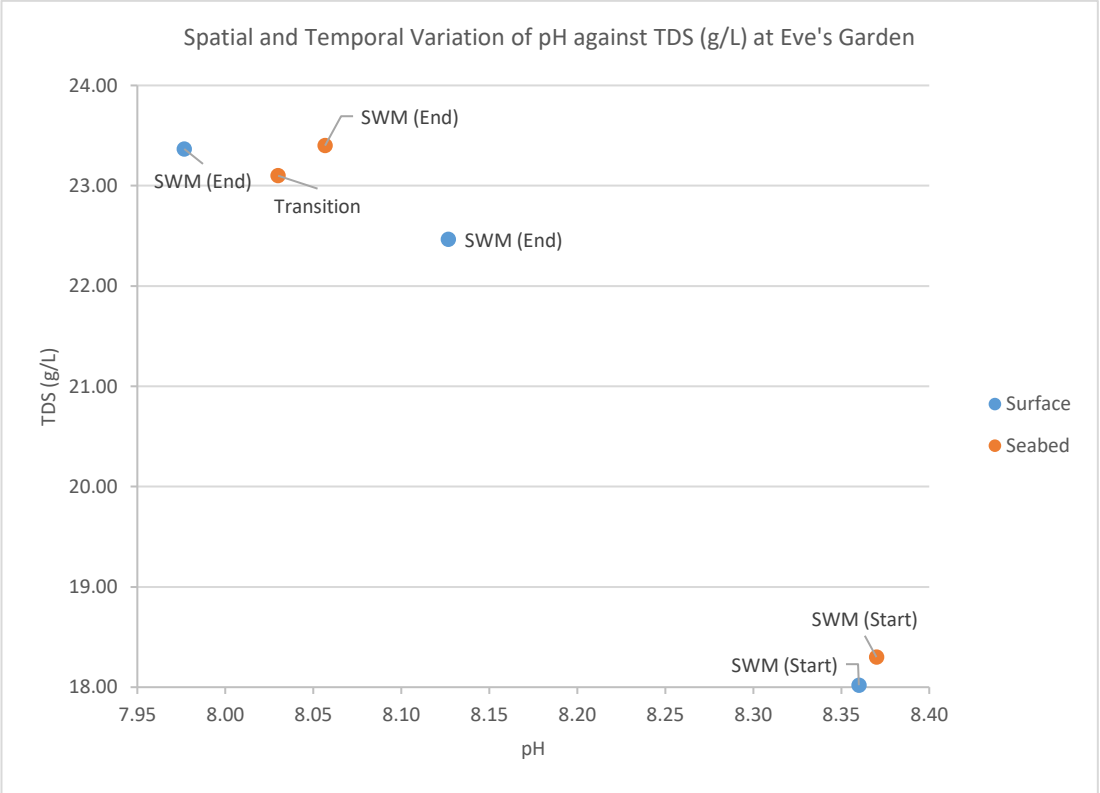

Figure 5.2.15 – pH against TDS (g/L) at Eve's Garden

The average concentration of DO was highest during the start of SWM season at 8.11mg/L. This value was 0.28mg/L more than the 7.83mg/L, which was the lowest average observed during the end of SWM. The transition period average was 0.09mg/L more than the average value of 7.92mg/L during the end of SWM. During the study, it was observed that the concentration of DO was much higher at the middle depths (5 to 8 meters) than at the surface or the seabed, except for Eve's Garden, where the seabed was at 6 meters on average. This phenomenon can be explained through stratification, which is defined as the separation of a body of water into layers based on temperature or other dissolved constituents (Rakestraw, 1943; Measurements, 2016b). The distribution of density, also known as pycnocline, is responsible for the concentration of DO to be higher at depths of 5 to 7 meters than at the surface or seabed (Paraskevopoulou et al., 2014; Measurements, 2016b). The surface temperature at all three sites are higher than the middle depth and seabed, causing that layer of the ocean to sink. However, there are more fish at the slightly lower temperature seabed causing the DO to be used up, hence leaving a higher concentration at the middle depth. The direction of the wind (Figure 4.6.4) also adds to the effects of ocean stratification (NOS, 2017). The relationship between temperature and DO can be seen in Figures 5.2.16 to 5.2.18.

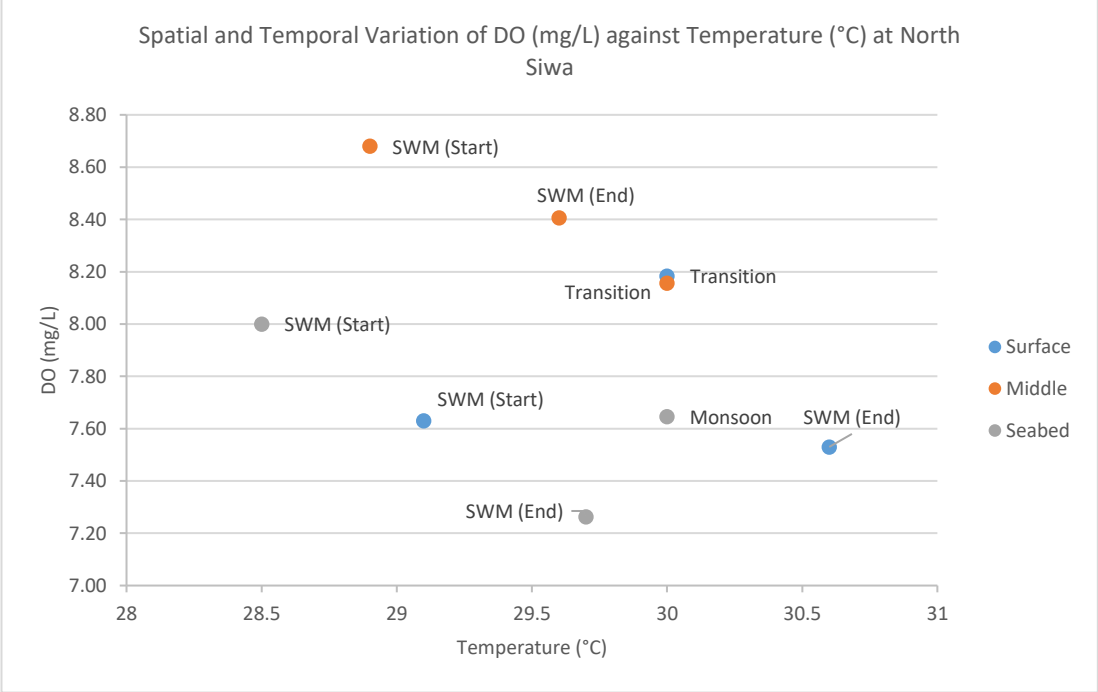

Figure 5.2.16 – DO (mg/L) against Temperature (°C) at North Siwa

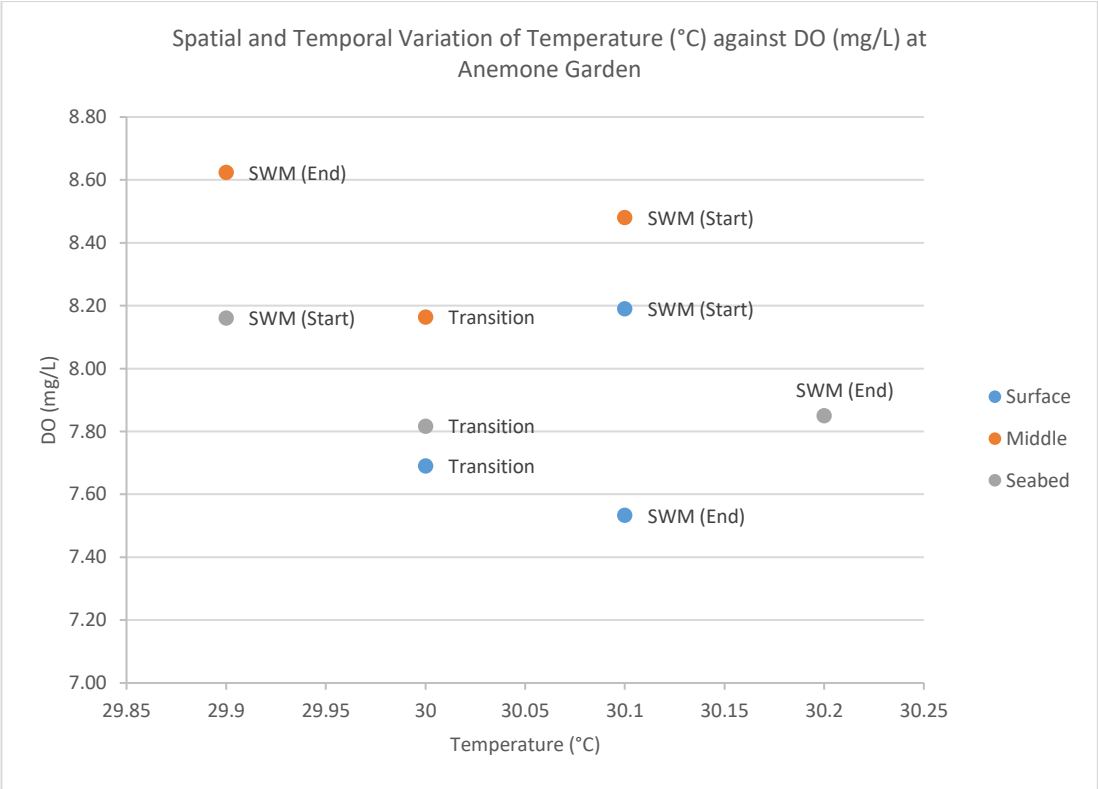

Figure 5.2.17 – DO (mg/L) against Temperature (°C) at Anemone Garden

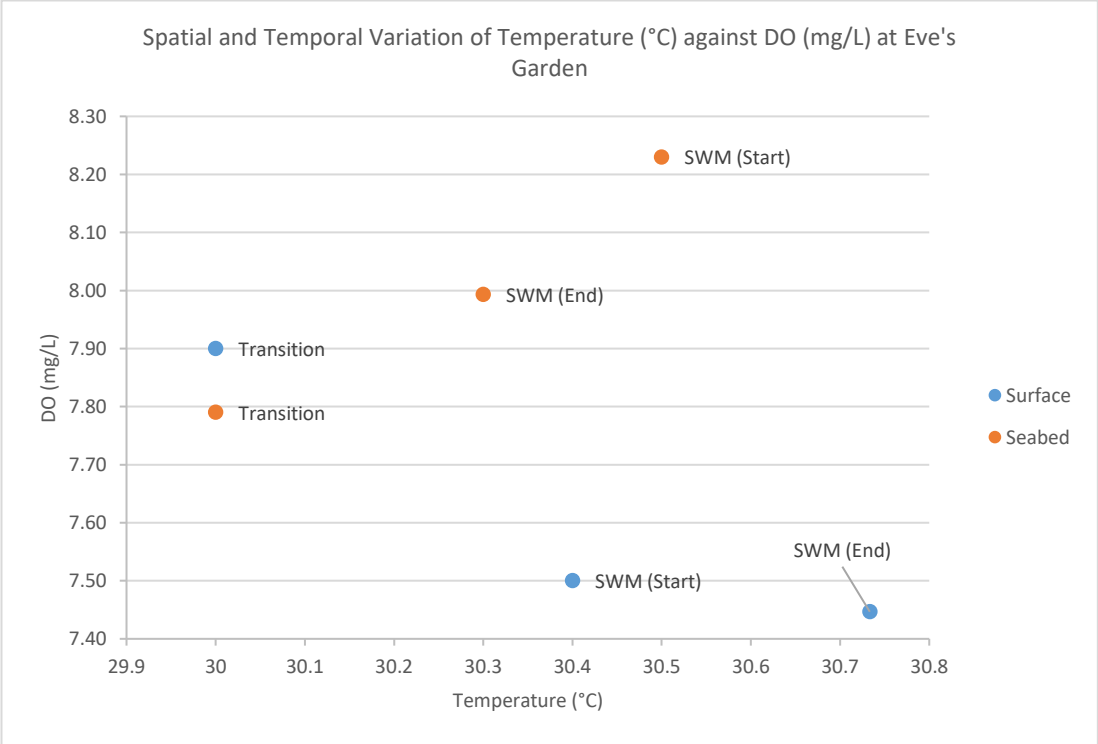

Figure 5.2.18 – DO (mg/L) against Temperature (°C) at Eve's Garden

5.2.2 Nutrients

The concentration of each nutrient gives a basis of the seawater quality of the Miri-Sibuti Coral Reef Marine Park. As explained in Chapter 2, coral bleaching happens due to high concentrations of nutrients in seawater, specific weather conditions and human involvement (Praveena et al., 2012; Tew et al., 2014; Higuchi et al., 2015; J. Miller et al., 2015; Zawada et al., 2015; Hoey, 2016; Manikandan et al., 2016). Among the four different nutrients analysed, the concentration of nitrate was noted to have the least variations as compared to phosphate, sulphate and total ammonia-nitrogen content. However, the higher nitrate concentrations were mostly found at Eve's Garden. Being the closest to the mouth of the Miri river, Eve's Garden experiences the immediate impacts of pollutants from river runoffs (Higuchi et al., 2015). This site has also observed the highest coral bleaching effects as well as prominent algal growth which are suffocating the corals. The only two highest values recorded were during the transition period at the surface of Eve's Garden and at the seabed of Anemone Garden. The low concentration of nitrate allows for planktons to proliferate which then invites marine animals such as whale sharks to visit MSCRNP (Hall et al., 1996). Nitrate as such does not cause coral bleaching, however, high concentrations coupled with the elevated temperature of the sea makes for a lethal combination to the coral environment (Fabricius, 2005; Higuchi et al., 2015).

The concentration of sulphate in the ocean is normally around 2700mg/L (Rakestraw, 1943; Anthoni, 2006). Most of the concentrations recorded at MSCRNP remained below that amount with the average being the lowest during the transition period (Table 4.3.2). The intrusion of fresh water, which generally have a lower concentration of sulphate ion, could be the cause of the fluctuations experienced by the concentrations of the ion together with the presence of fertilisers (Prasanna et al., 2010). The high concentration of sulphate observed at the surface of Eve's Garden indicated the practice of dynamite fishing at the site close to the date of sampling since the site is known for such activities (M. Abdullah, 2017). The current direction during NEM transition which was observed to be from North to South also indicates that the high sulphate concentration detected at the surface of Eve's Garden is slowly diffusing since the value registered at the seabed of Anemone Garden was slightly less than half of Eve's Garden (Table 4.3.1 – 4.3.3).

As observed in Figures 5.2.19 to 5.2.21, the concentration of ammonia-nitrogen was highest during start of SWM. The middle depth of both Anemone Garden and North Siwa had higher concentrations of ammonia-nitrogen followed by the second highest at the surface of both sites. Eve's Garden also observed similar situations but the highest concentration was noted at the surface. The population of tourists was observed to be much higher than the end of SWM and NEM transition periods, and recreational activities such as diving and snorkelling would account for the higher concentration of ammonia-nitrogen (Ilter. et al., 2012; Lamb et al., 2014). The high amount of rainfall, strong north to south ocean current and close to two meter waves during the end of SWM and transition period caused the number of tourists and water activities to drop which also observed a drop in the concentration of ammonia-nitrogen. While tourists still influenced the concentration of the nutrient, anthropogenic sources such as fertilisers from river runoff and coastal development were the main sources of ammonia-nitrogen (Naumann et al., 2015; Singaraja et al., 2015).

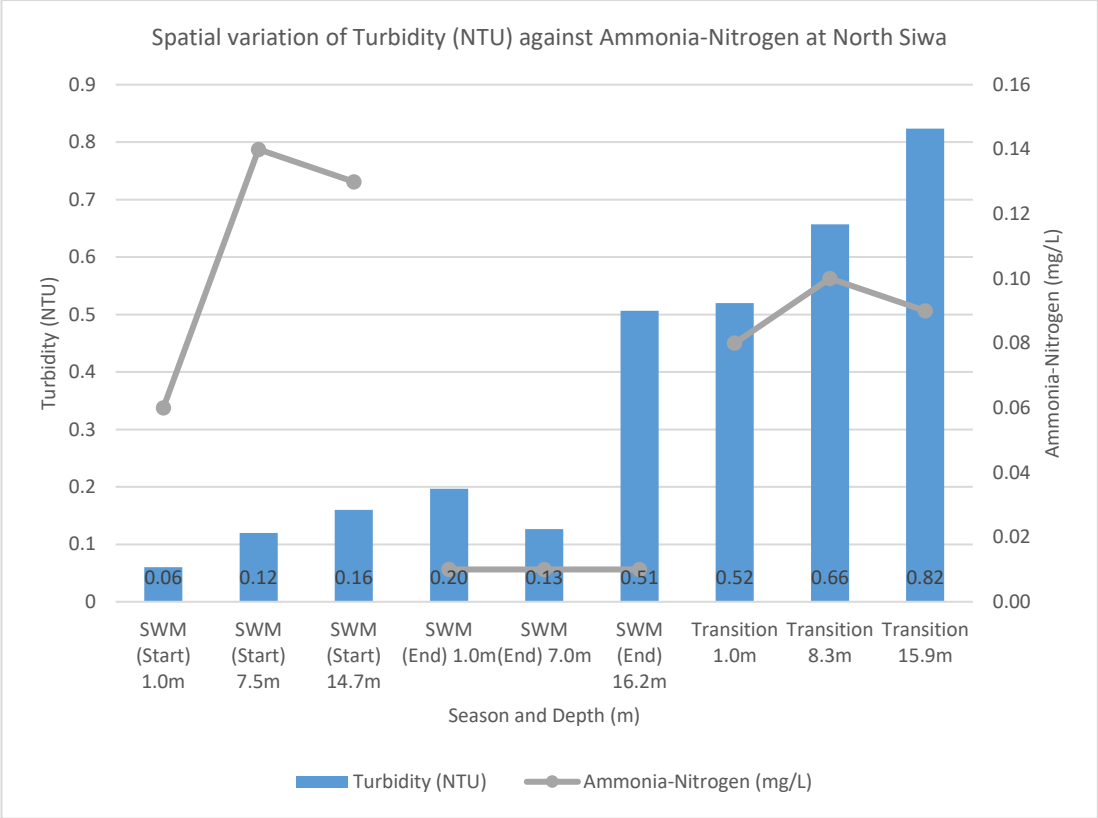

Figure 5.2.19 – Turbidity (NTU) against Ammonia-Nitrogen at North Siwa

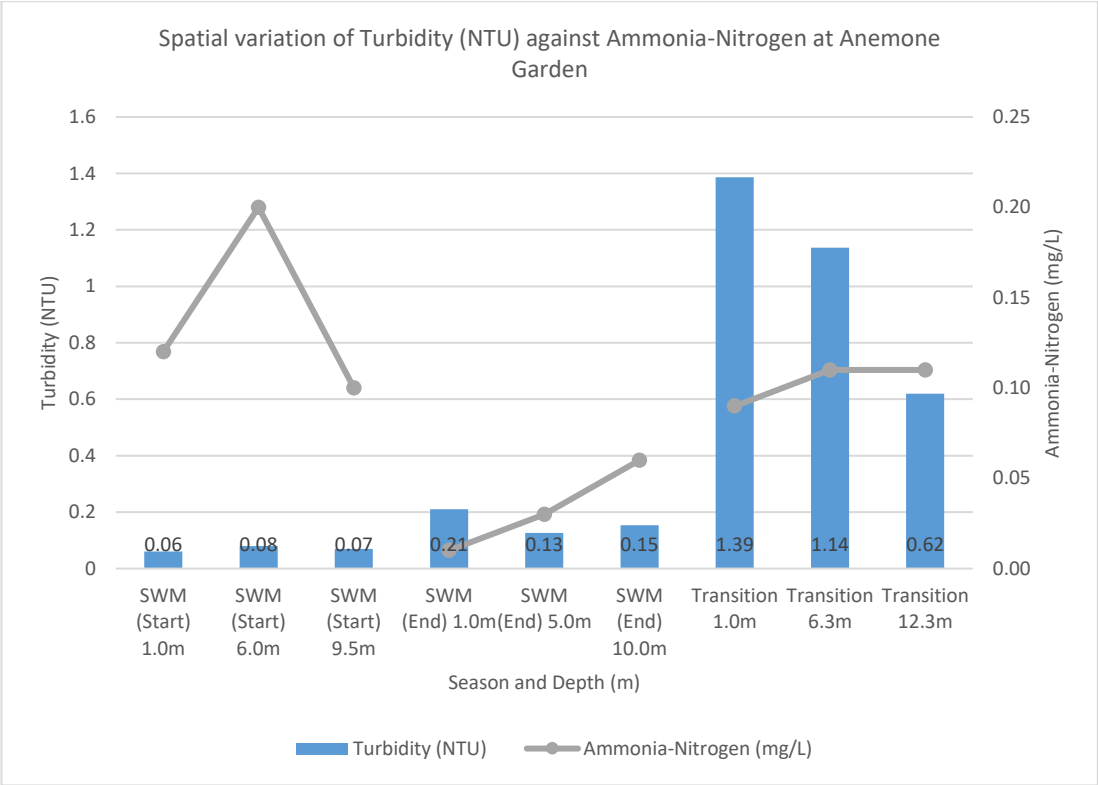

Figure 5.2.20 – Turbidity (NTU) against Ammonia-Nitrogen at Anemone Garden

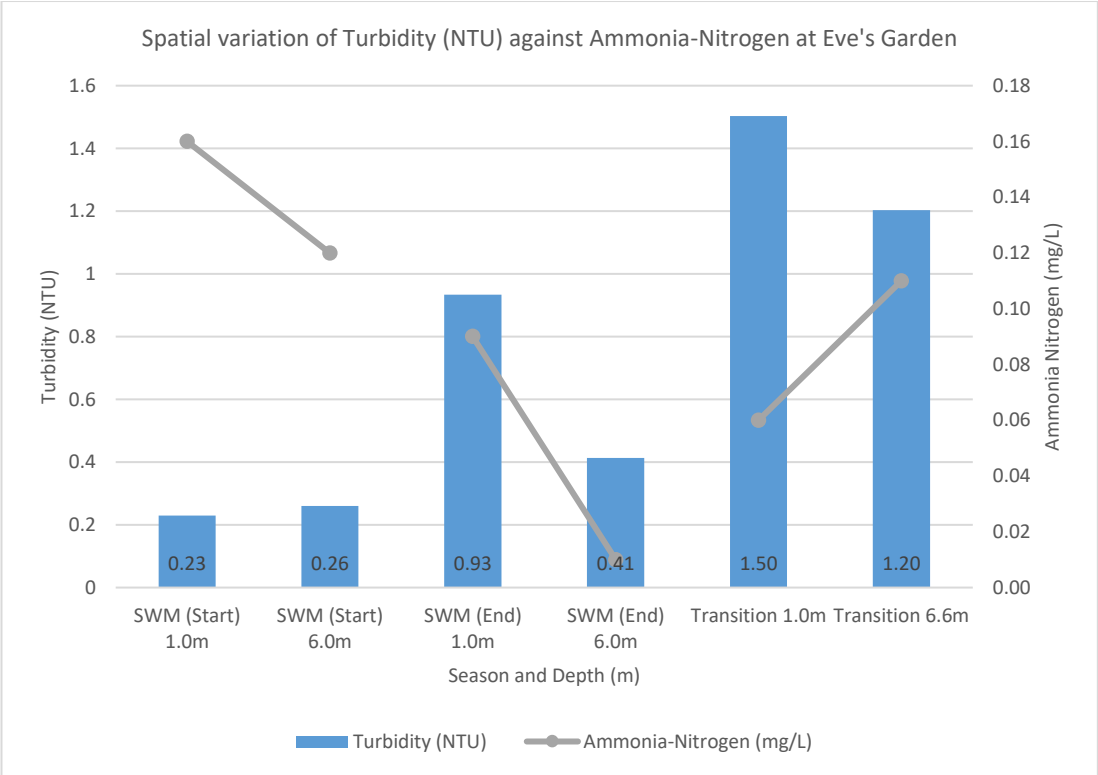

Figure 5.2.21 – Turbidity (NTU) against Ammonia-Nitrogen at Eve's Garden

The combination of high temperatures, low turbidity and the high concentrations of ammonia-nitrogen during the start of SWM can create conditions where the coral environment becomes at risk. Referring to the satellite image from NOAA (Figure 5.2.22) and based on the thermal stress of the date for the beginning SWM sampling (31-05-16), it can be observed that coral bleaching alert was at its highest during week 5 – 8 starting from May 2016. The turbidity of the seawater was one of the lowest recorded from all the sampling periods. Looking at the rainfall data for the week before the 31st May 2016, (Section 4.5), very little rainfall was recorded that could have perturbed the seawater. Combining the thermal stress, the above average ammonia-nitrogen concentration and the very low turbidity of the water, the coral environment starts to get affected (Lough and van Oppen, 2009; Readman et al., 2013; Browne et al., 2015; Higuchi et al., 2015; Manikandan et al., 2016).

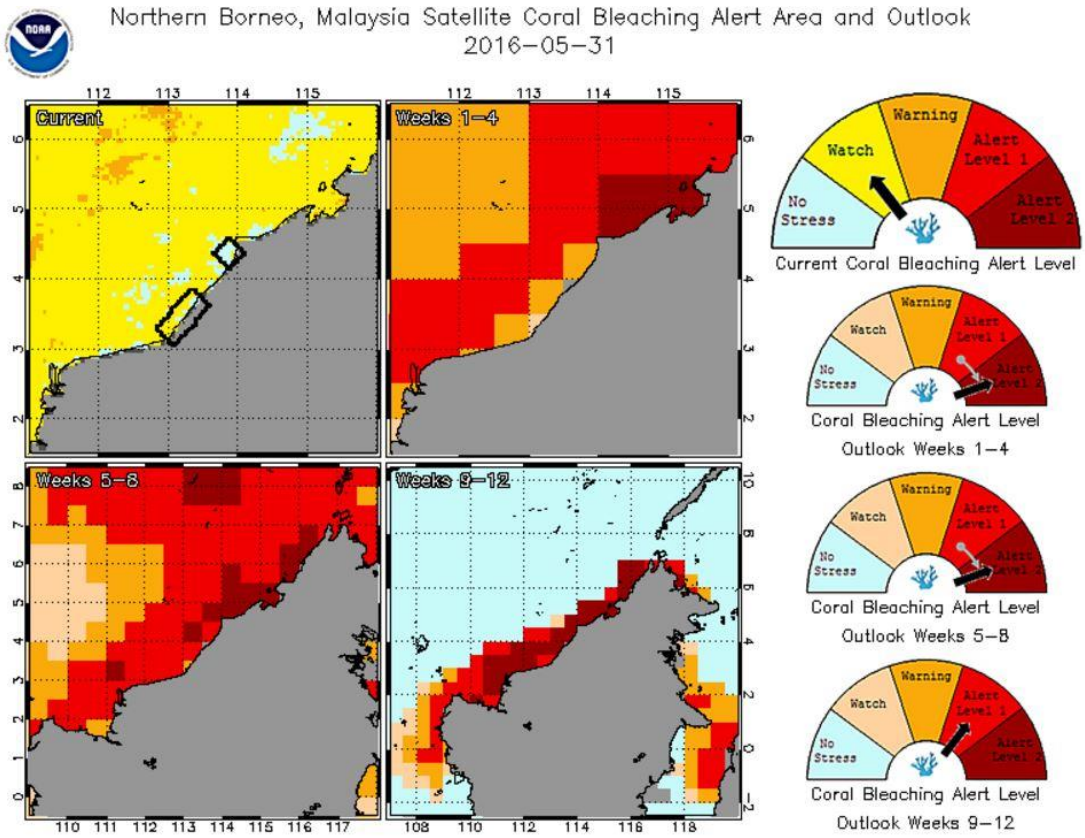

Figure 5.2.22 – Coral Bleaching Alert for 31-05-16

From Tables 4.3.1 to 4.3.3, the phosphate levels increased from the beginning to the end of SWM (14-09-16) and was the highest during the transition period (27-10-16). Figures 5.2.23 to 5.2.25, indicate a rise in the concentration of phosphate with the seasonal increase in turbidity. The figures also show that during the end of SWM, the concentration of phosphate increases quickly at Anemone Garden and Eve's Garden which are closer to the shore, than at North Siwa. Comparing these values with the amount of daily rainfall from Table 4.5.3, the source of the increase in the concentration of phosphate as well as the increase in turbidity can be linked to anthropogenic activities such as fertilisers from river runoffs. Phosphate is also a nutrient which promotes algal growth. High turbidity and excessive algae found at Eve's Garden would prevent sunlight from reaching the corals thereby suffocating them (Rakestraw, 1943; Fabricius, 2005; Gerhard, 2009).

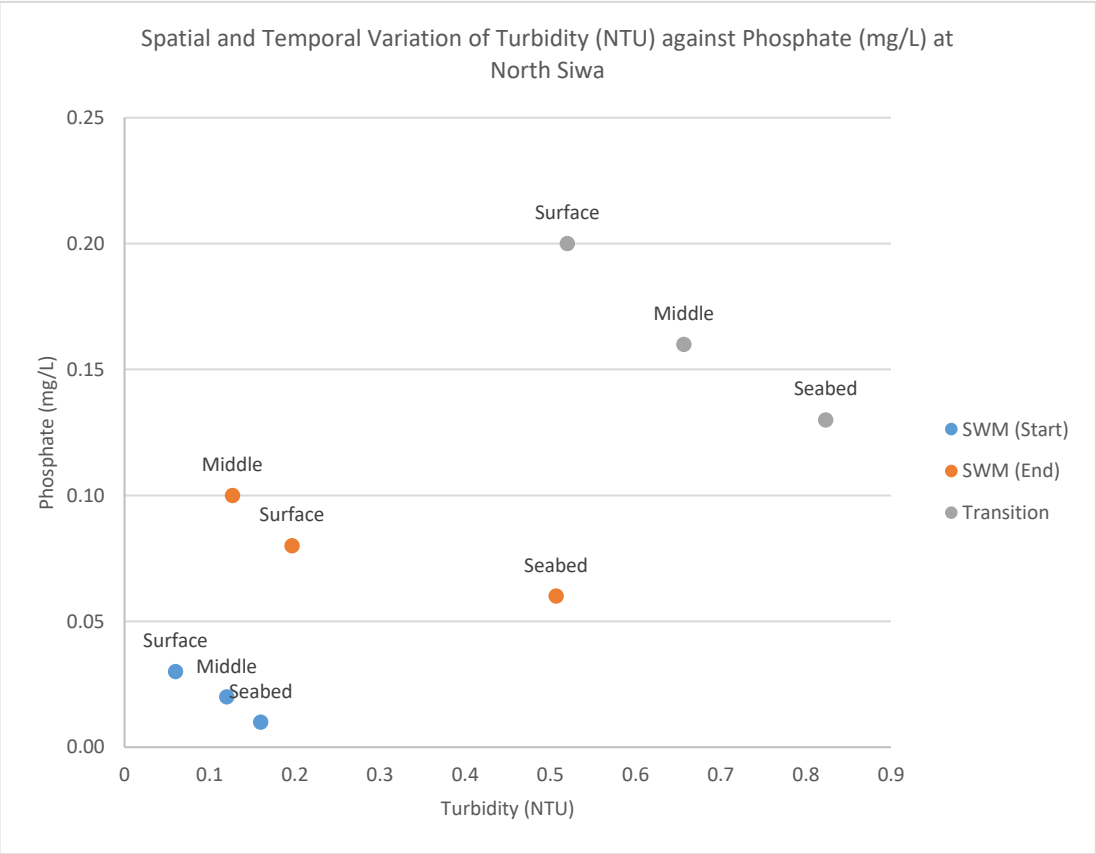

Figure 5.2.23 – Phosphate (mg/L) against Turbidity (NTU) at North Siwa

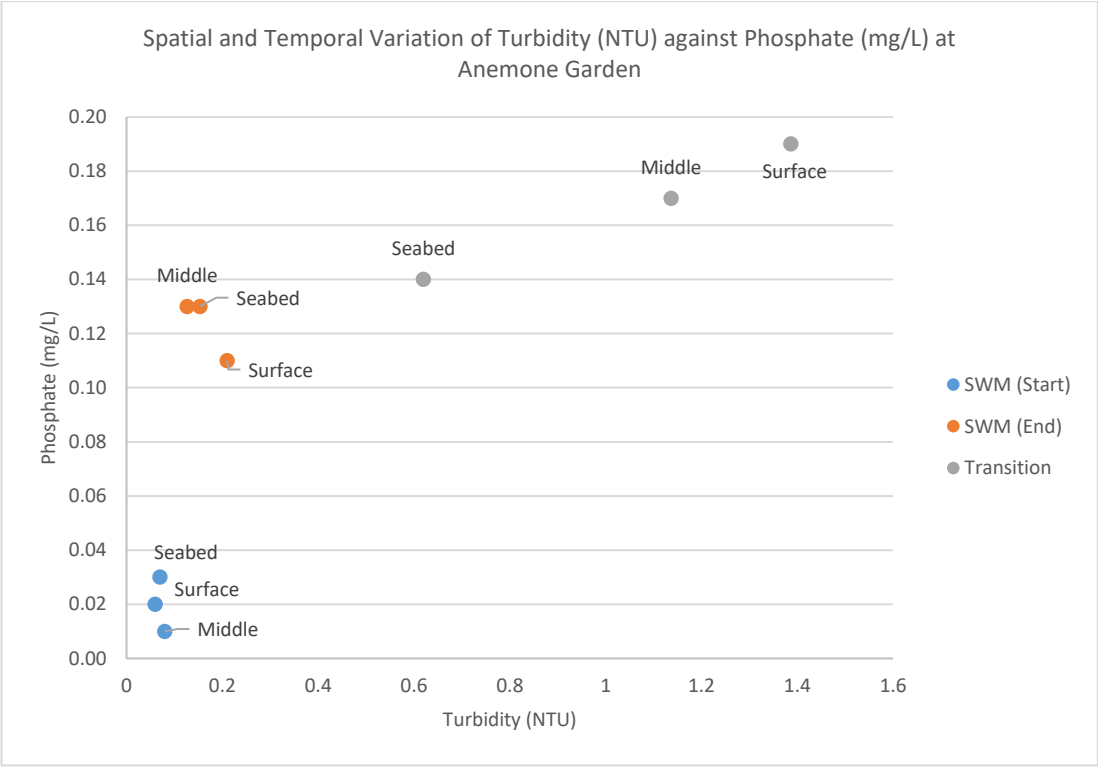

Figure 5.2.24 – Phosphate (mg/L) against Turbidity (NTU) at Anemone Garden

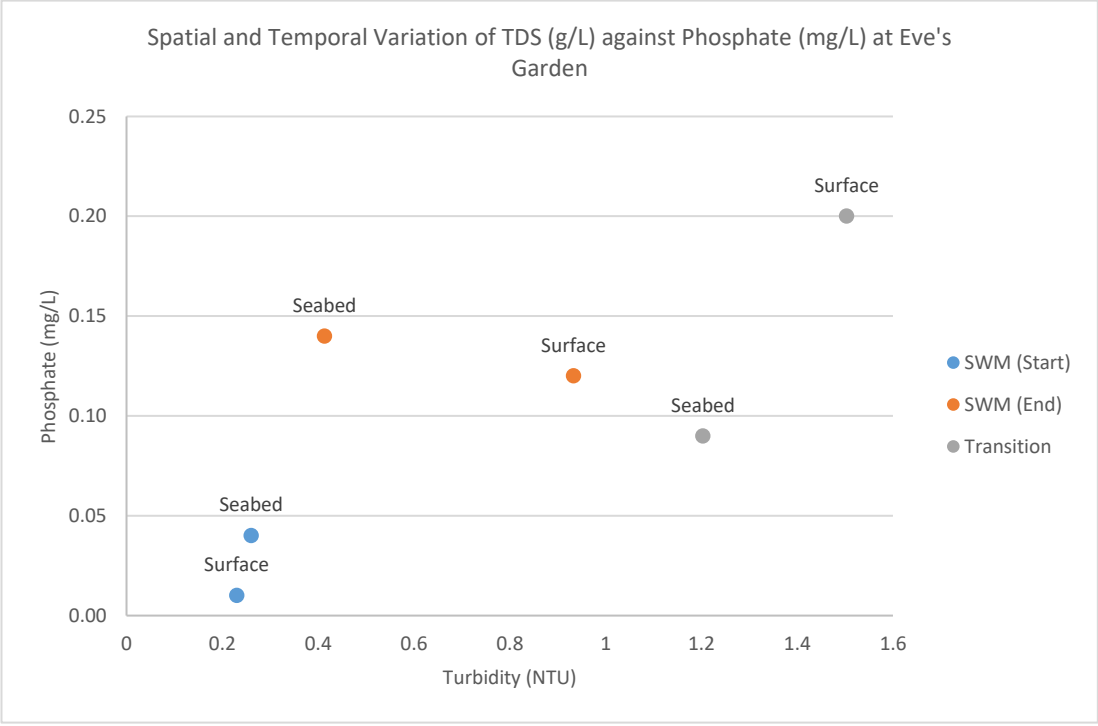

Figure 5.2.25 - Phosphate (mg/L) against Turbidity (NTU) at Eve's Garden

5.2.3 Major Ions

The major constituents in seawater are mostly present in the form of ions. The concentration of those elements usually varies upon the regions, its surroundings as well as the physico-chemical attributes of the seawater during the sampling period (Rakestraw, 1943; Lenntech, 2005; Anthoni, 2006). The absorption of carbon dioxide, described in Section 5.2.1 contributes to the acidification of the ocean. As explained by Anthoni (2006), carbon dioxide is only loosely bonded with seawater to produce bicarbonate. Carbonic acid is first created and only after an atom of hydrogen detaches from carbonic acid, that bicarbonate is formed as represented by the equation;

$$CO_2 + H_2O \leftrightarrow H_2CO_3 \leftrightarrow H^+ + HCO_3^- \leftrightarrow H^+ + H^+ + CO_3^{2-} \quad [1]$$

Figures 5.2.26 to 5.2.28 show the relationship between the concentration of bicarbonate and the pH at each site during all three sampling periods. North Siwa observed a relatively constant pH while having a fluctuating bicarbonate concentration similar to Anemone Garden, while experiencing a decrease in pH when going deeper. Both the pH and bicarbonate concentration appeared relatively constant. The ocean current during beginning of SWM was from south to north and while there were no other divers present at North Siwa and Eve's Garden during sampling, Anemone Garden had some divers present. The maximum wind speed recorded during that day was 7.8m/s from a westerly direction. The current during the end of SWM was observed to go from north to south and the highest wind speed of 14m/s was noted blowing from the west. The two big rivers that meet the ocean, north to the study sites are the Miri and Baram Rivers. North Siwa observed a constant concentration of bicarbonate while seeing a rise in pH from surface to seabed. Anemone Garden observed a decrease in bicarbonate concentration from surface to seabed, while the pH values remained quite constant. Both the pH and the concentration of bicarbonate at Eve's Garden experienced an increase during the end of SWM. The direction of the ocean current during the transition period was the same as the end of SWM, however, a 7.2m/s maximum wind speed was observed coming from a WSW direction. The pH and the bicarbonate concentration at North Siwa increase from the surface to the seabed during that period similar to Eve's Garden except for the decreasing value in pH. Anemone Garden had fluctuating concentrations from surface to seabed but had a definite decrease in pH.

Based on Figures 5.2.26 to 5.2.28, the concentration of bicarbonate increased when the direction of the ocean current changed from south to north (start of SWM) to north to south (End of SWM). Eve's Garden, being closest to the shore observed a higher increase in bicarbonate concentration from surface to seabed as opposed to Anemone Garden and North Siwa which are much further from the shore. This increase is due to coastal development and pollution (Makkaveev, 2009; Howard et al., 2013). The westerly surface wind direction being the strongest during the SWM season (Figure 4.6.4) was also a contributing factor to the high values of bicarbonate at the surface of the sites.

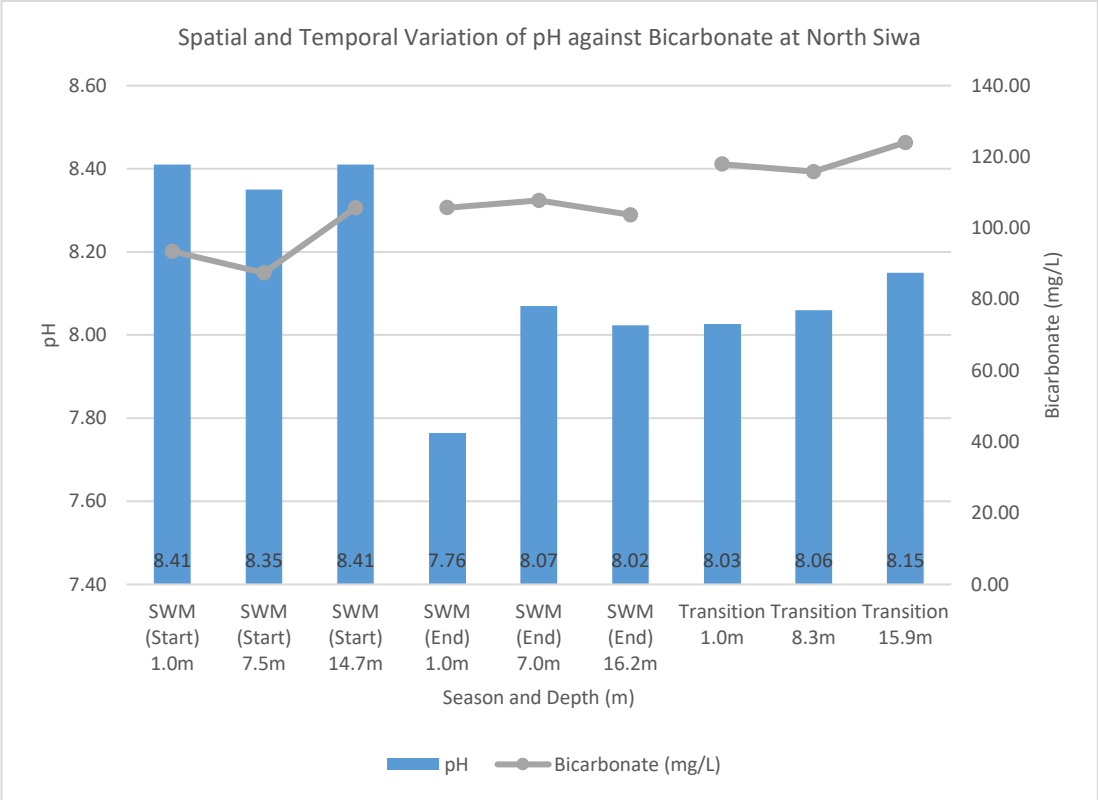

Figure 5.2.26 – Spatial and Temporal Variation of pH against Bicarbonate (mg/L) at North Siwa

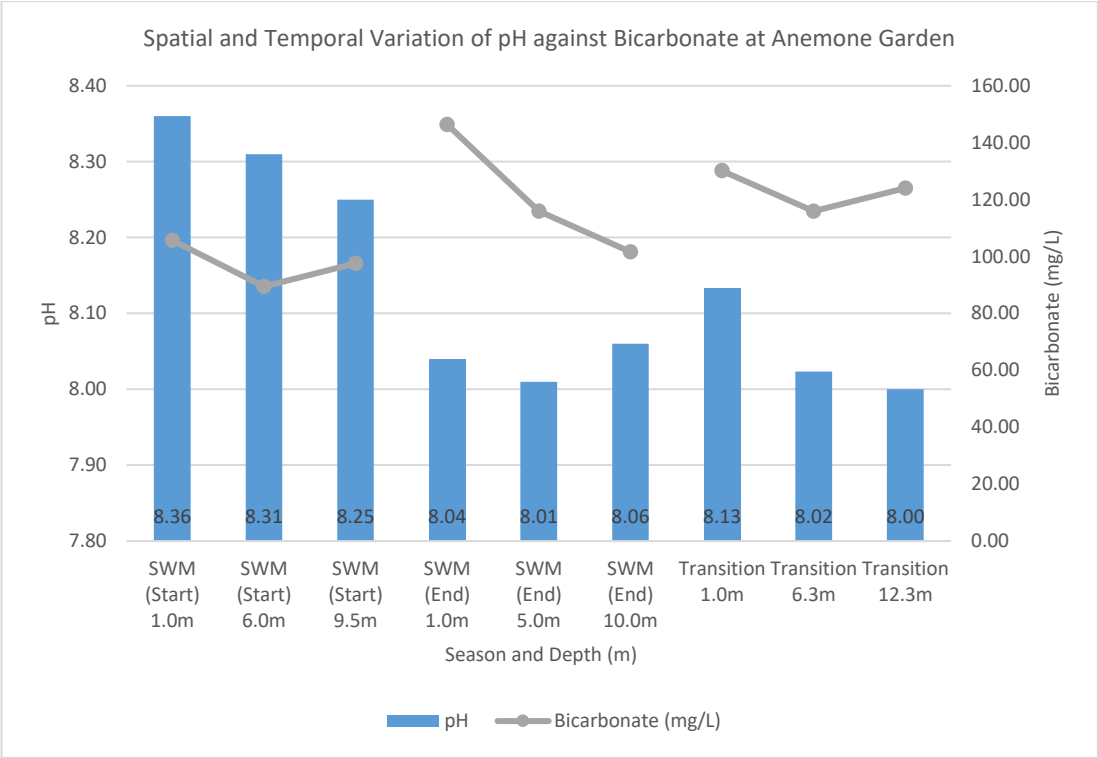

Figure 5.2.27 – Spatial and Temporal Variation of pH against Bicarbonate (mg/L) at Anemone Garden

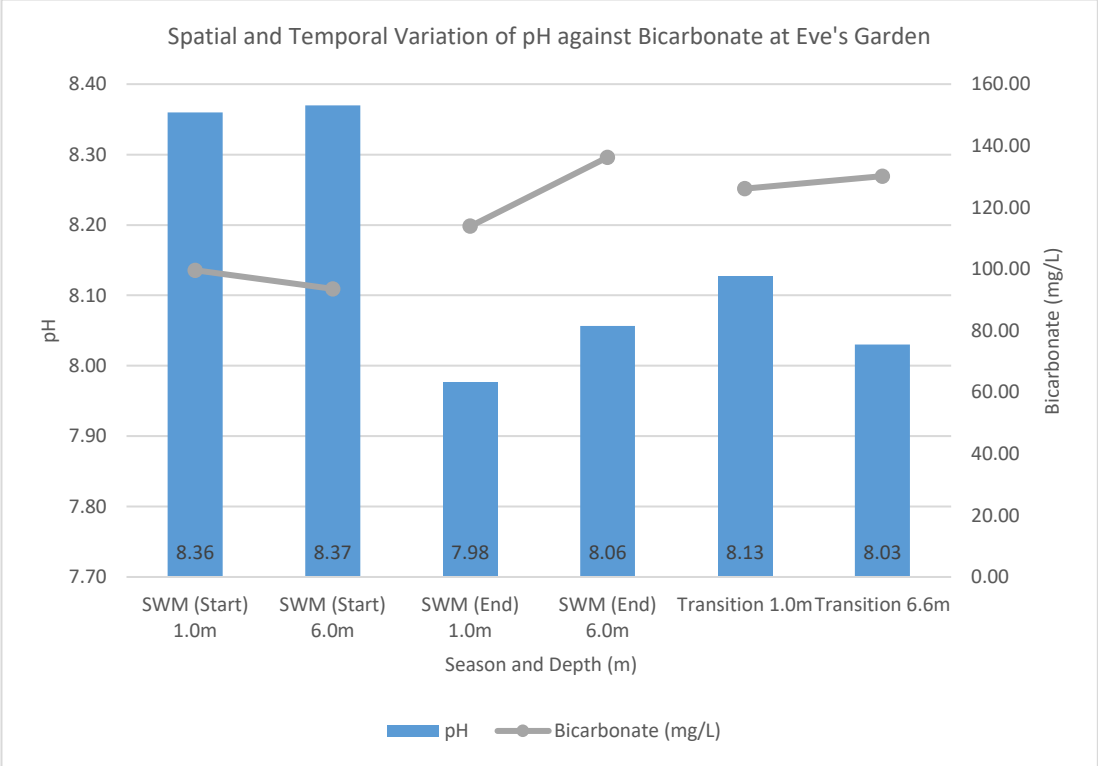

Figure 5.2.28 – Spatial and Temporal Variation of pH against Bicarbonate (mg/L) at Eve's Garden

Calcium exists mostly in the form of calcium carbonate ($CaCO_3$) in seawater. This means a lower pH helps to dissolve $CaCO_3$. Calcium therefore also acts as a buffer preventing the accelerated acidification of the ocean. However, this happens at the expense of the corals. The dissolution of calcium in seawater can be summarised through the equations [2], [3] and [4] (Readman et al., 2013; Lenntech, 2017b);

$$H_2O + CO_2 \rightarrow H_2CO_3 \quad [2]$$

$$CaCO_3 + H_2CO_3 \rightarrow Ca(HCO_3)_2 \quad [3]$$

$$CaCO_{3\,(s)} + CO_{2\,(g)} + 2H_2O_{\,(l)} \rightarrow Ca^{2+}{}_{(aq)} + 2\,HCO_3^{-}{}_{(aq)} \quad [4]$$

Based on Figures 5.2.29 to 5.2.31, the concentration of calcium was observed to remain consistent during beginning of SWM, when the pH values were still higher than the end of SWM and the transition period. A depth-wise decrease in calcium was observed during the end of SWM period, which would indicate a high amount of rain during that period causing dilution of the concentration. Eve's Garden, being the closest site has seen a depth-wise increase in the concentration of calcium from the start of SWM to NEM transition indicating coastal development activities since calcium is found in limestone, cement and concrete (Lenntech, 2017b).

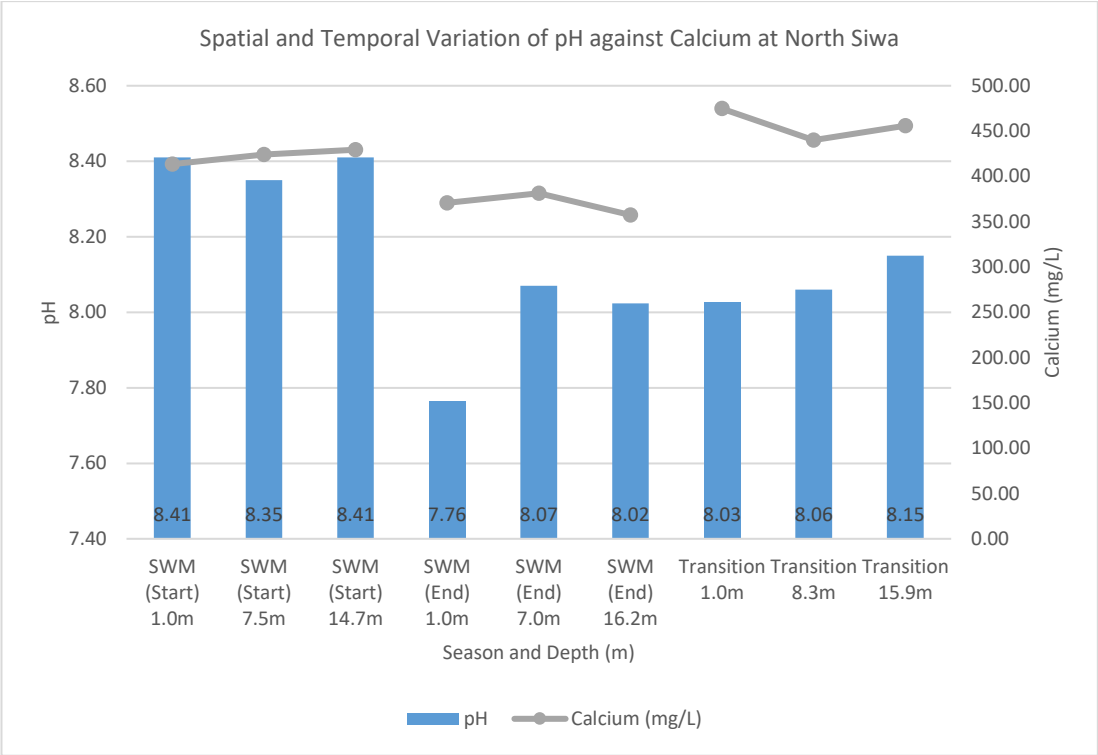

Figure 5.2.29 – pH against Calcium (mg/L) at North Siwa

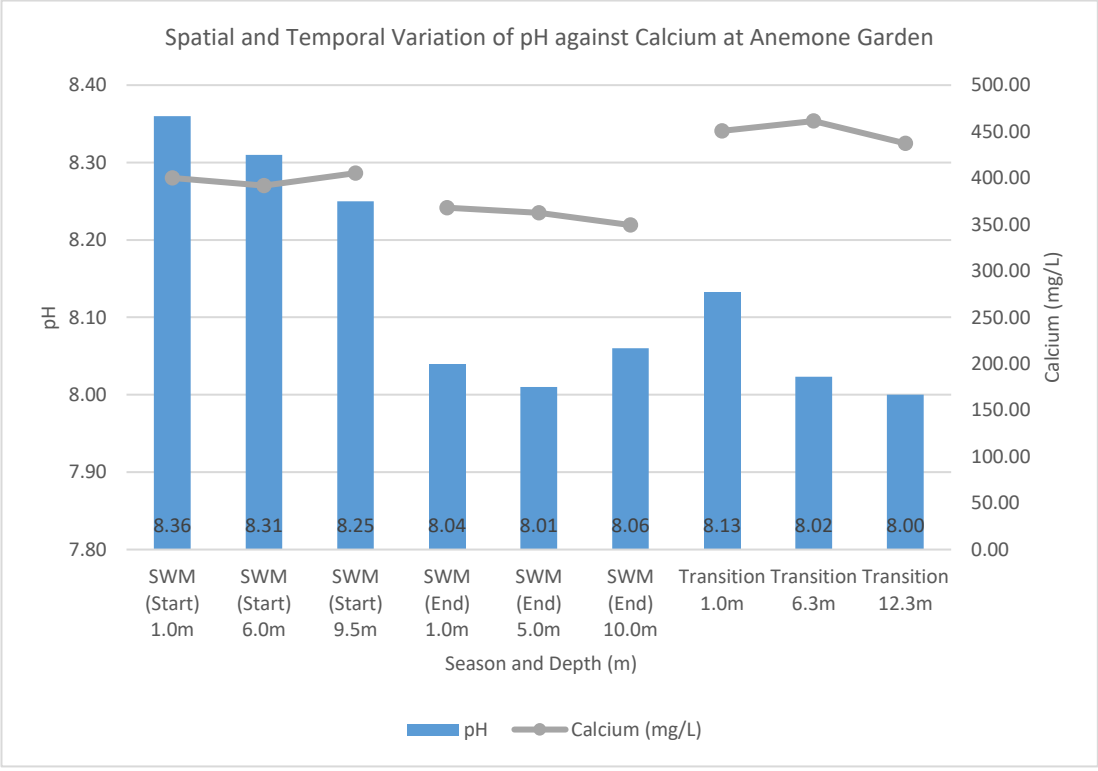

Figure 5.2.30 – pH against Calcium (mg/L) at Anemone Garden

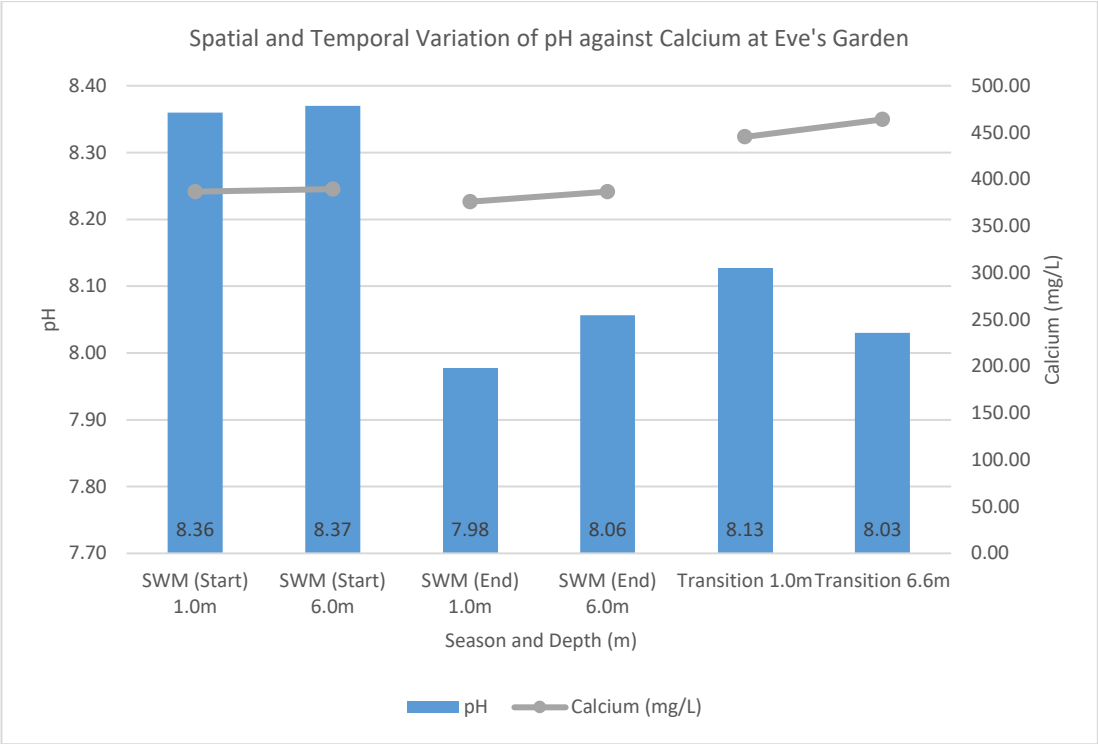

Figure 5.2.31 – pH against Calcium (mg/L) at Eve's Garden

Among all the sites investigated at the beginning of SWM, the concentration of magnesium showed a depth-wise consistency together with a high pH value. At North Siwa, the concentration of magnesium increased with depth at the end of SWM and transition period as noted in Figure 5.2.32. However, the opposite was observed at both Anemone Garden and Eve's Garden (Figures 5.2.33 – 5.2.34) as the concentration of magnesium decreased with increasing pH, and increase with decreasing pH during the end of SWM and NEM transition respectively. This change in dynamics is attributed to the presence of river runoffs and coastal development (Cabon et al., 2007; Drupp, 2015). This effect is more visible when the concentration of magnesium and calcium are compared together as noted in Figures 5.2.35 to 5.2.37. During commencement of SWM, the concentrations of both calcium and magnesium varied very little from surface to seabed at all three sites. However, Anemone Garden and Eve's Garden clearly showed a decrease in concentration of magnesium from surface to seabed and a general increase in calcium during the end of SWM period respectively. The gap in concentration was further enhanced during the transition period, where Eve's Garden observed the highest disparity between these two ions (Lenntech, 2017b, 2017g).

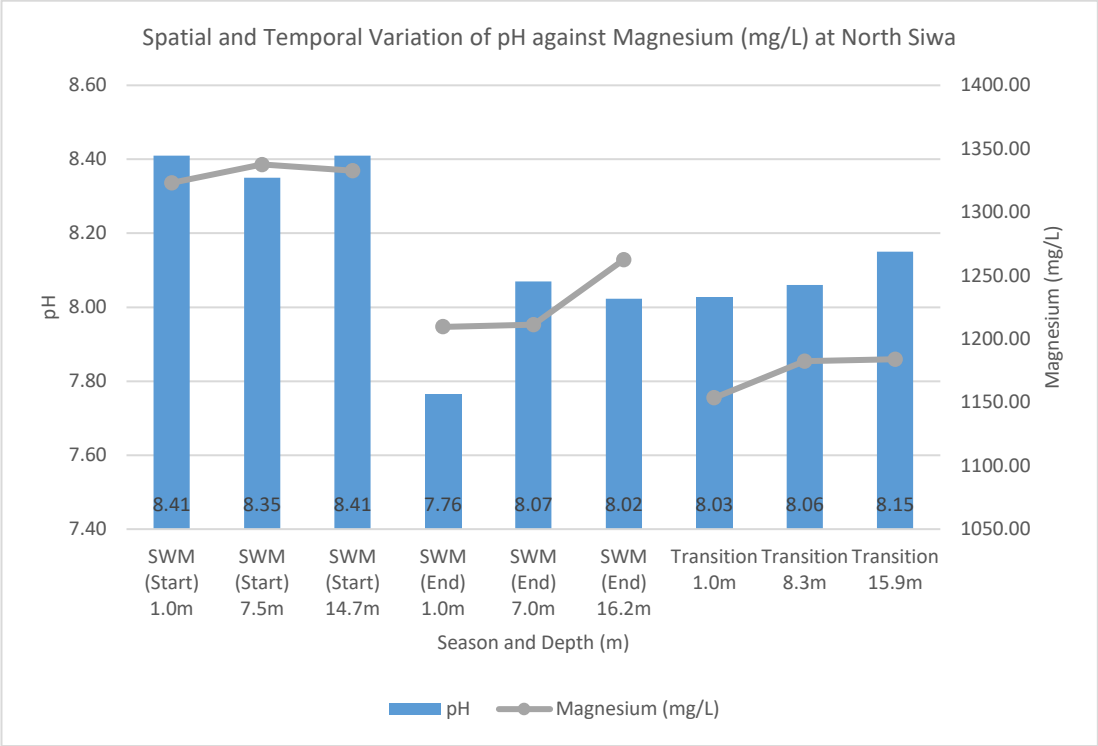

Figure 5.2.32 – pH against Magnesium (mg/L) at North Siwa

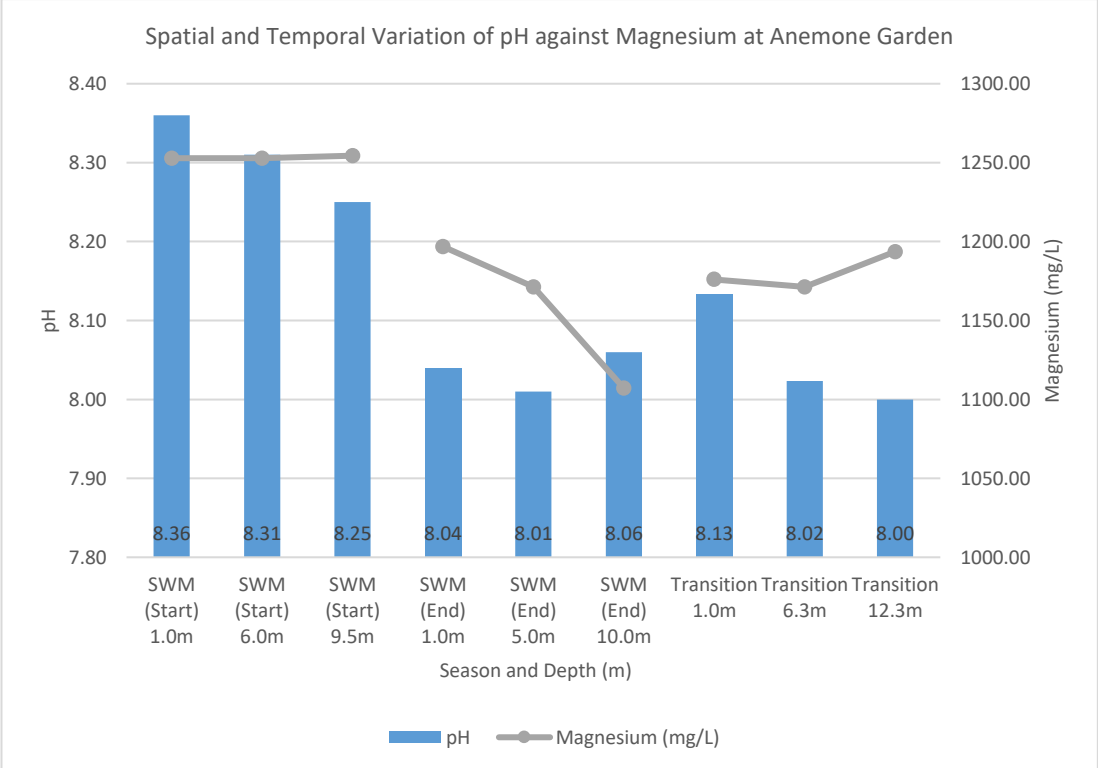

Figure 5.2.33 – pH against Magnesium (mg/L) at Anemone Garden

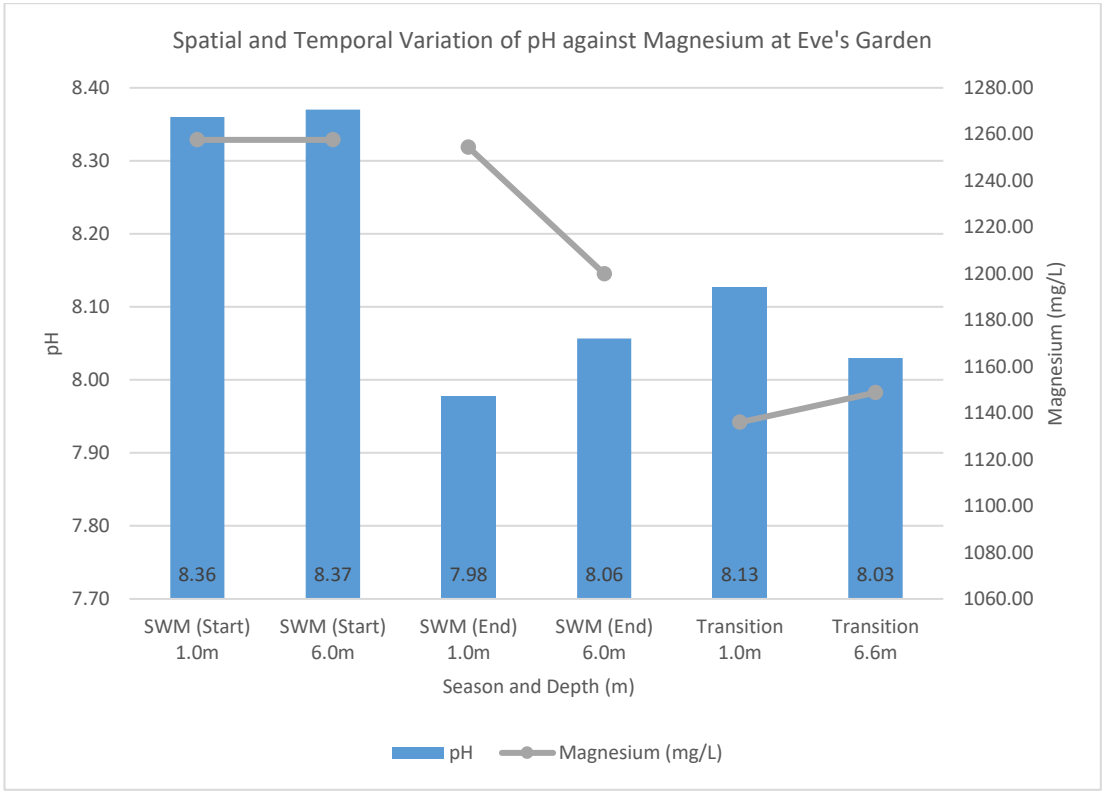

Figure 5.2.34 – pH against Magnesium (mg/L) at Eve's Garden

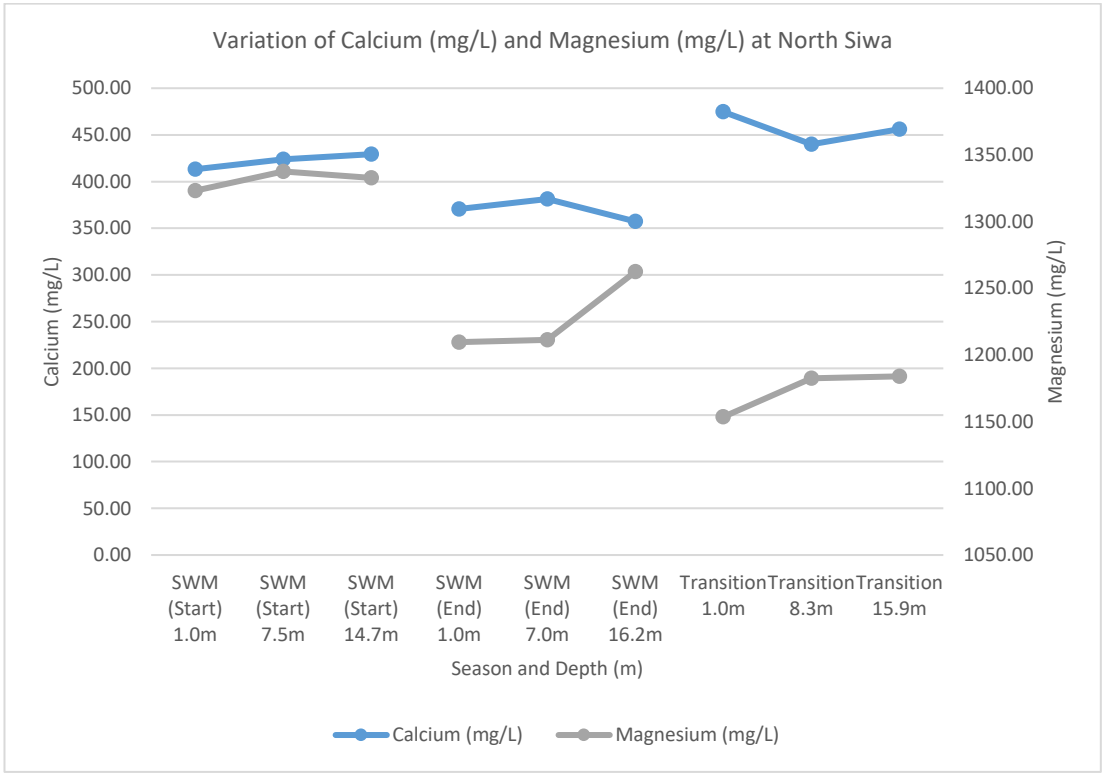

Figure 5.2.35 – Calcium (mg/L) and Magnesium (mg/L) at North Siwa

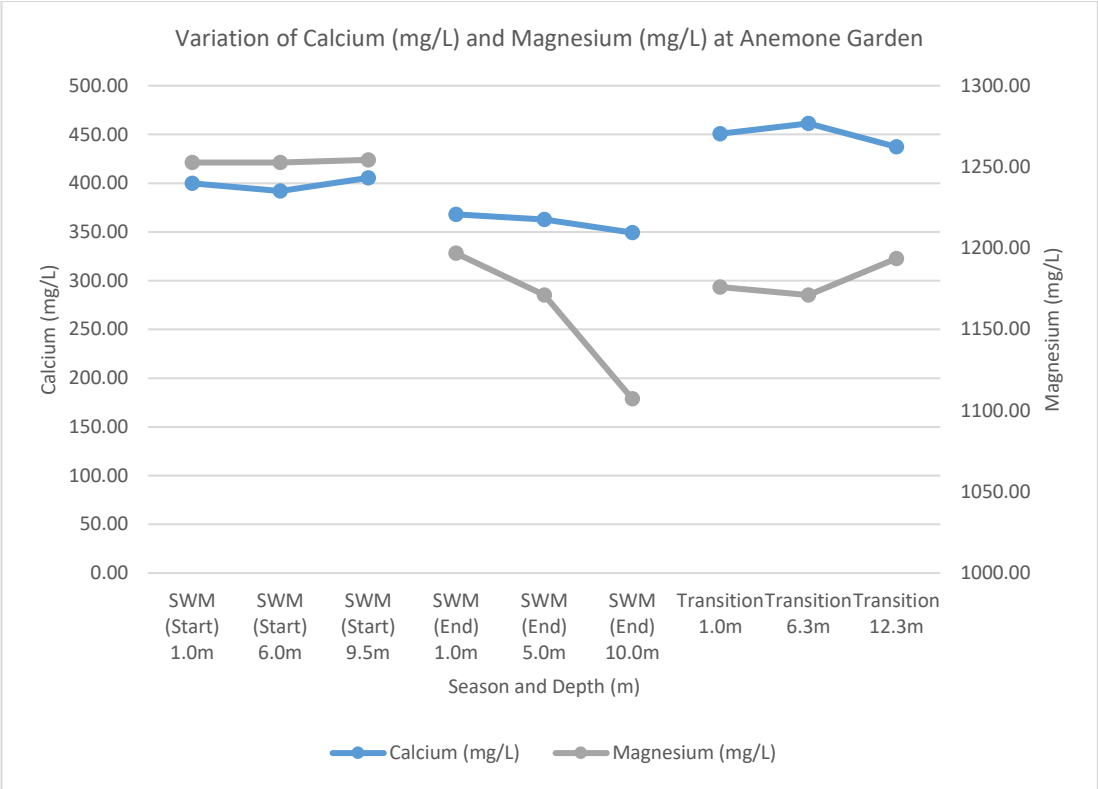

Figure 5.2.36 – Calcium (mg/L) and Magnesium (mg/L) at Anemone Garden

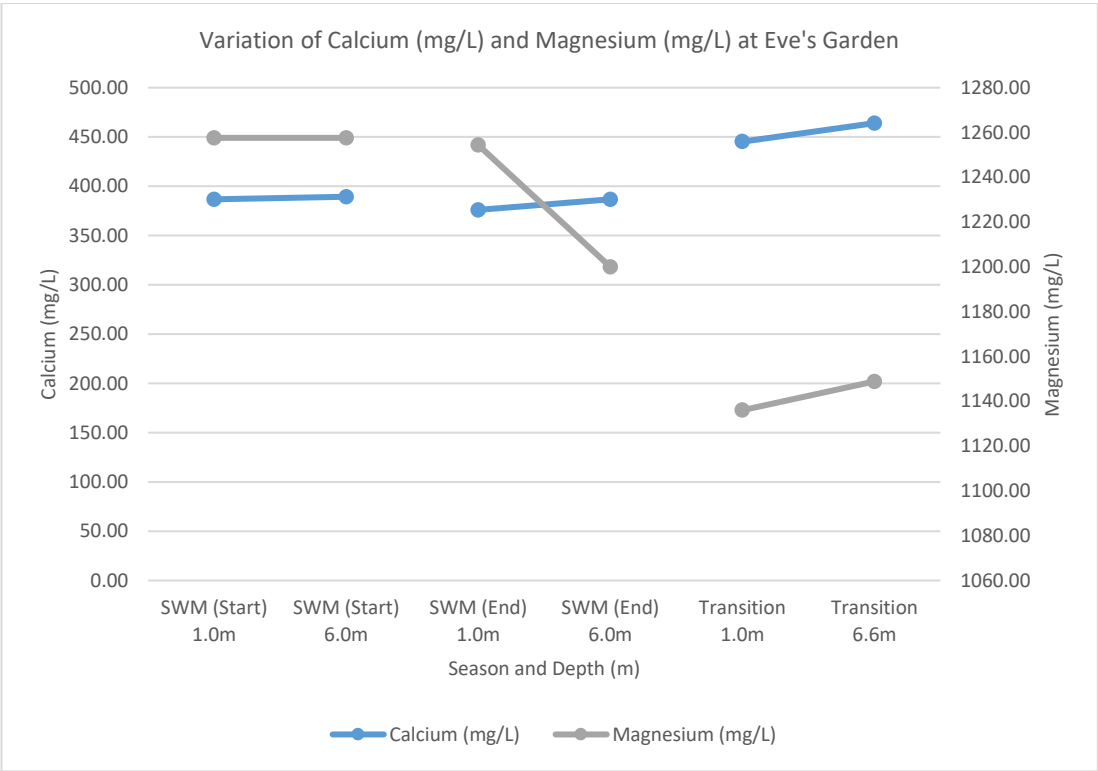

Figure 5.2.37 – Calcium (mg/L) and Magnesium (mg/L) at Eve's Garden

Figures 5.2.38 to 5.2.40 show the variation in the concentration of potassium with pH, spatially and temporally at each site. At the start of SWM, slight variations in the depth wise concentration of potassium was observed. However, Eve's Garden noted an increase in the concentration of potassium from surface to seabed for all seasons. The rise in concentration was sharper during the end of SWM because of the proximity of the site to the shoreline as well as the presence of the Miri river mouth which would have diluted the seawater at the surface (Lenntech, 2017j). The direction of the ocean current, which was from north to south, also helped carry the water from the rivers to the site. Anemone Garden too experienced a sharp increase in the concentration of potassium from the surface to the middle depth indicating the presence of river water and coastal development similar to Eve's Garden (Rakestraw, 1943; Lenntech, 2017j). North Siwa had little variation in the concentration of potassium as compared to Eve's Garden and Anemone Garden indicating less influence of the river runoffs and rainfall at the site.

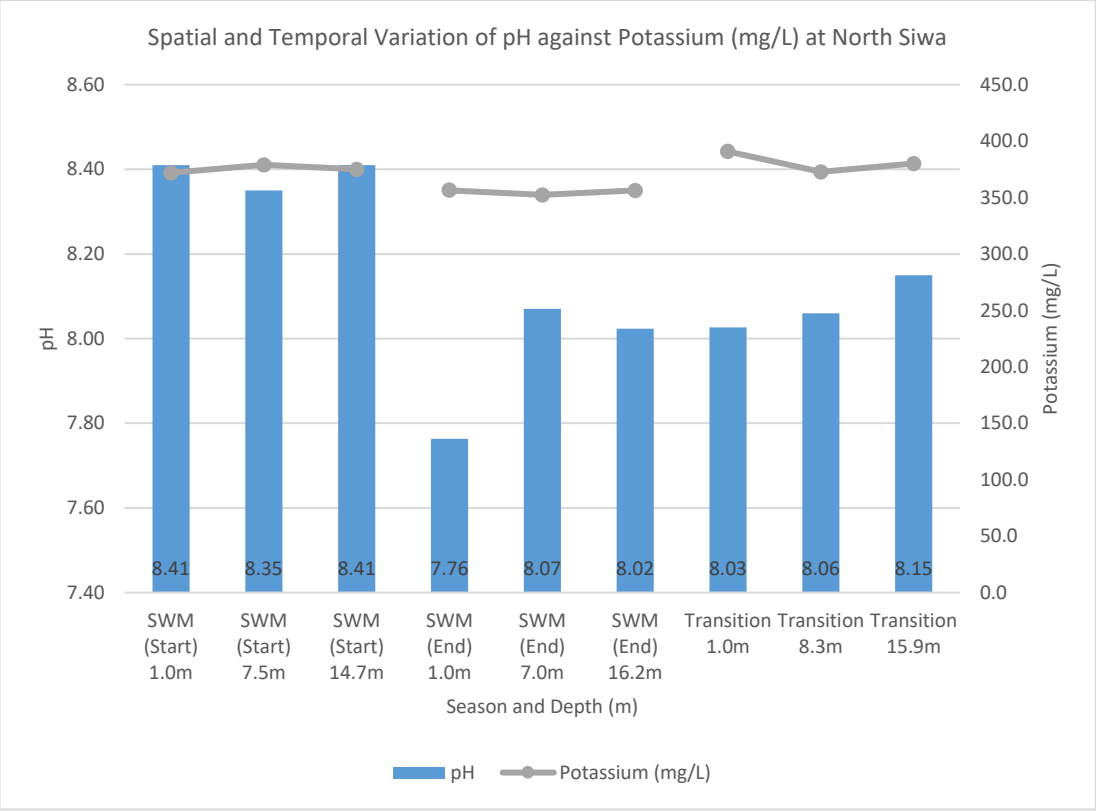

Figure 5.2.38 – pH against Potassium (mg/L) at North Siwa

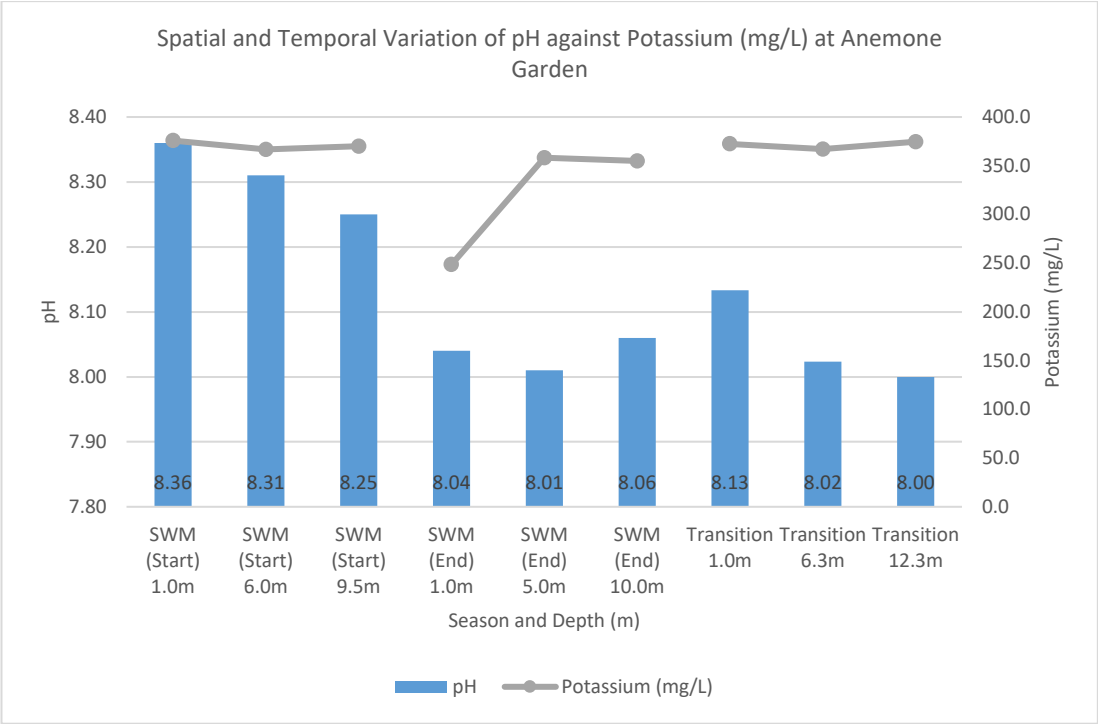

Figure 5.2.39 – pH against Potassium (mg/L) at Anemone Garden

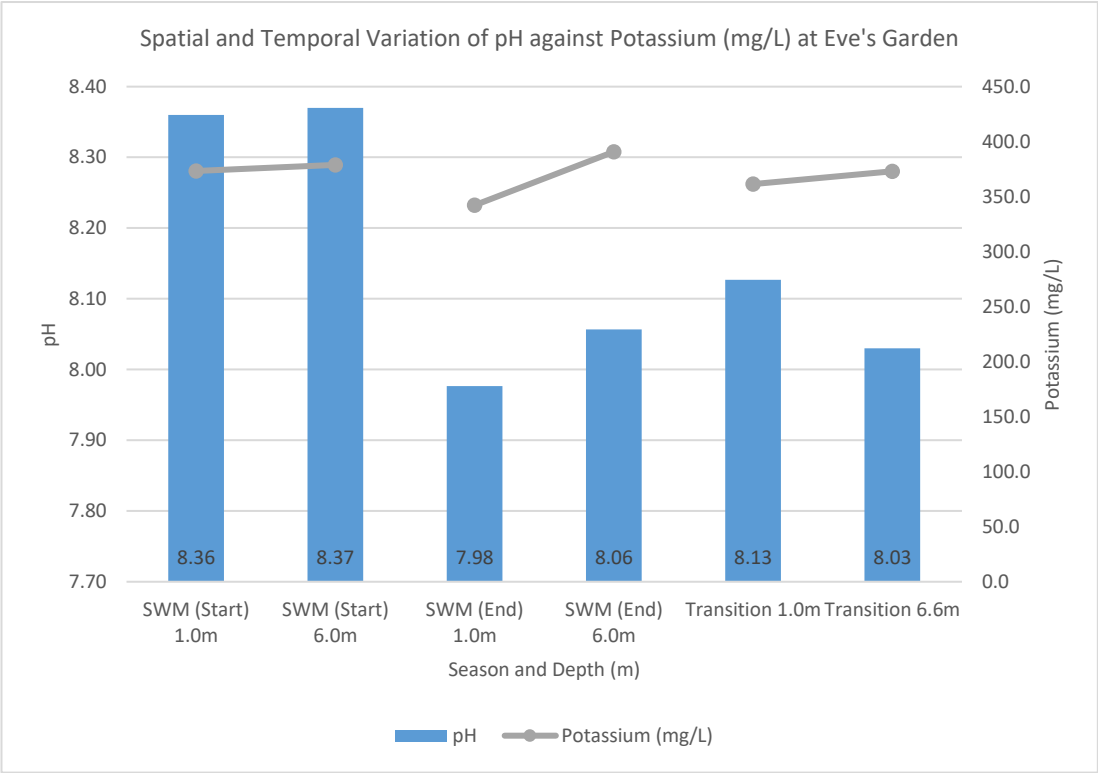

Figure 5.2.40 – pH against Potassium (mg/L) at Eve's Garden

The concentration of sodium and chloride had very similar patterns from surface to seabed at both Eve's Garden and Anemone Garden throughout all the seasons (Figures 5.2.41 – 5.2.43). Similar factors which affected potassium also affected the concentration of sodium and chloride at those two sites, which include the presence of the Miri river mouth, the proximity to the shoreline as well as dilution from rainfall (Rakestraw, 1943; Lenntech, 2017j). At North Siwa (Figure 5.2.41), the concentration of sodium and chloride increased from surface to seabed at the start of SWM. The opposite was observed during the end of SWM where both sodium and chloride concentrations decreased from surface to seabed. The change in current direction from south-north in the beginning of SWM, to north-south during the end of SWM and transition period could be the reason behind the small variations of sodium and chloride at North Siwa. The concentrations of the ions indicate very little to negligible influence of river runoffs and rainfall affecting that site.

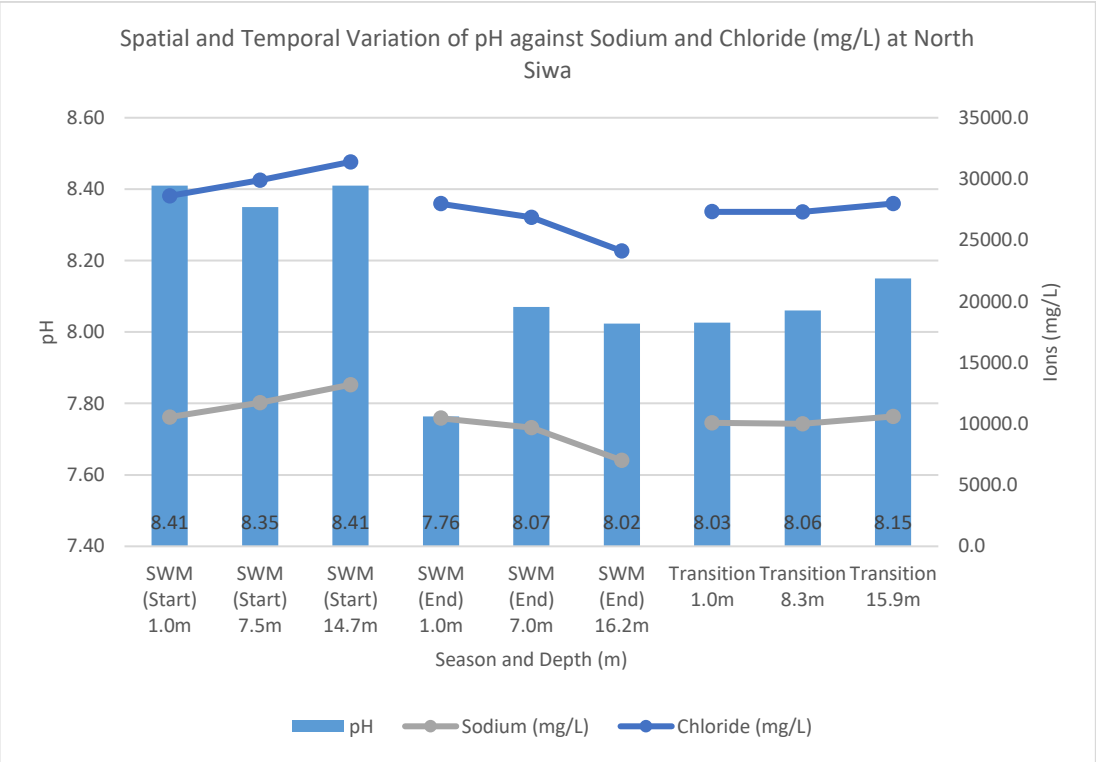

Figure 5.2.41 – pH against Sodium (mg/L) and Chloride at North Siwa

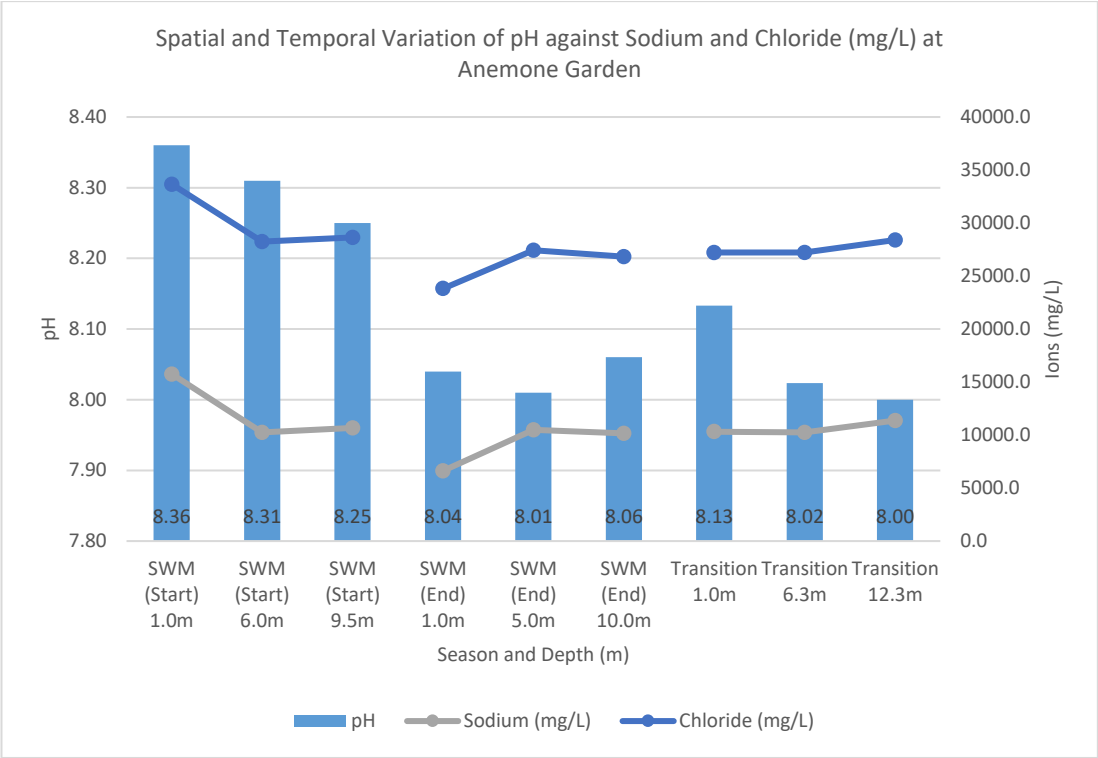

Figure 5.2.42 – pH against Sodium (mg/L) and Chloride at Anemone Garden

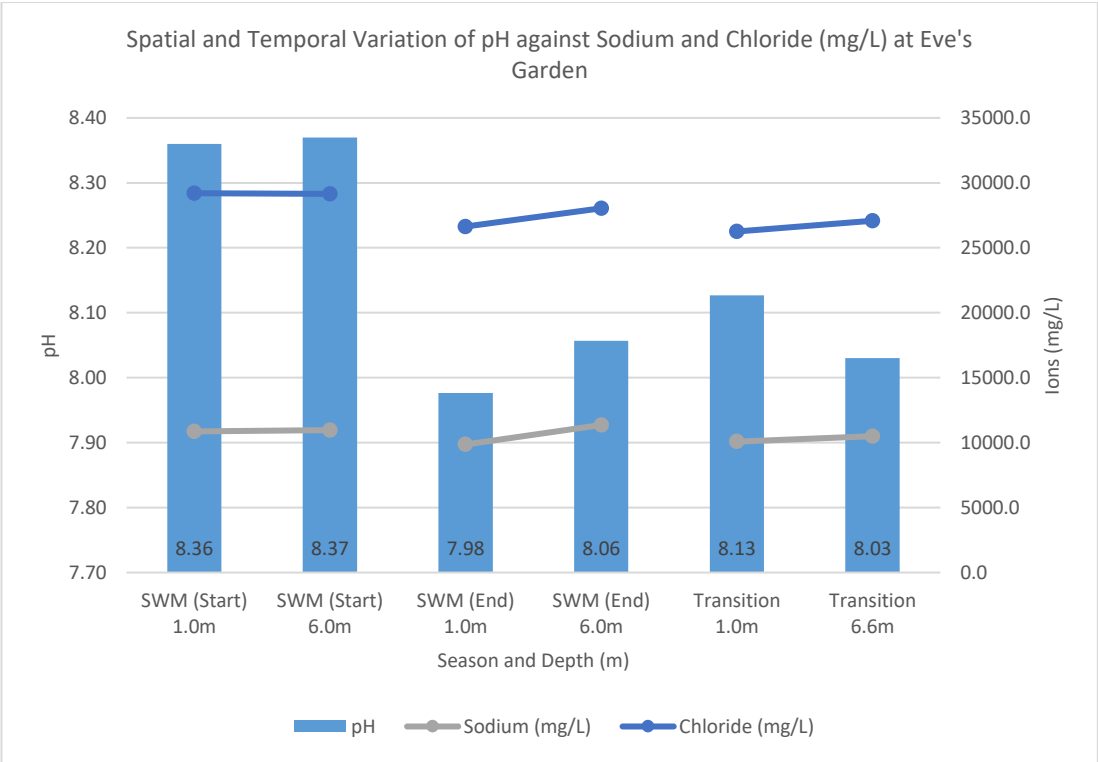

Figure 5.2.43 – pH against Sodium (mg/L) and Chloride at Eve's Garden

5.2.4 Trace Metals

The average concentration of cadmium in seawater according to Anthoni (2006) is 0.00011mg/L. The concentrations observed at all three locations for this study showed much higher values. As seen in Tables 4.4.1 to 4.4.4, there is slight variations in the concentration of cadmium during the start of SWM at all three locations, however during the end of SWM, elevated concentration can be observed at the seabed of North Siwa and generally through all sites during the transition period. The concentrations, which fall within 0.01mg/L to 0.02mg/L indicate the presence of anthropogenic activities such as industrial waste, use of fertilisers as well as coastal development (Balls, 1985). The more elevated concentrations which ranged from 0.049mg/L to 0.052mg/L were linked to the presence of soil at the sites from river runoffs. During the transition period sampling, the colour of the water was also observed to be more towards brown-green than blue. Figures 5.2.44 to 5.2.46 show the relationship between turbidity and the concentration of cadmium indicating river runoff and industrial discharge (Balls, 1985; Lenntech, 2017a).

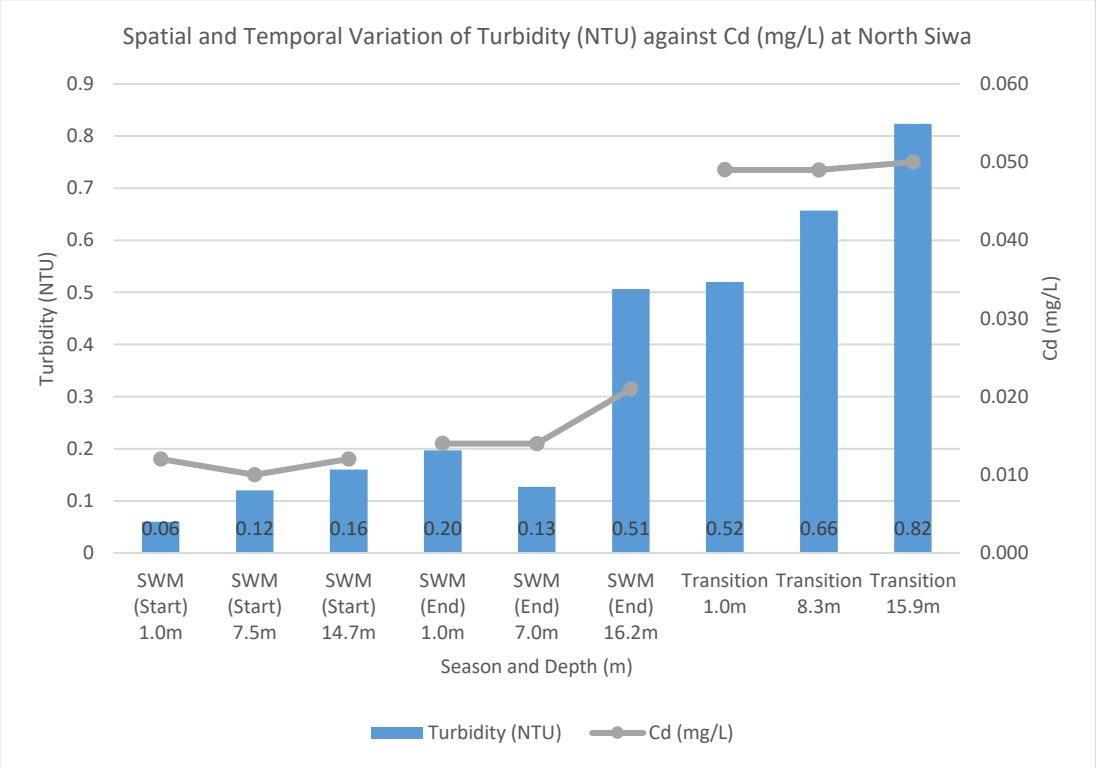

Figure 5.2.44 –Turbidity (NTU) against Cd (mg/L) at North Siwa

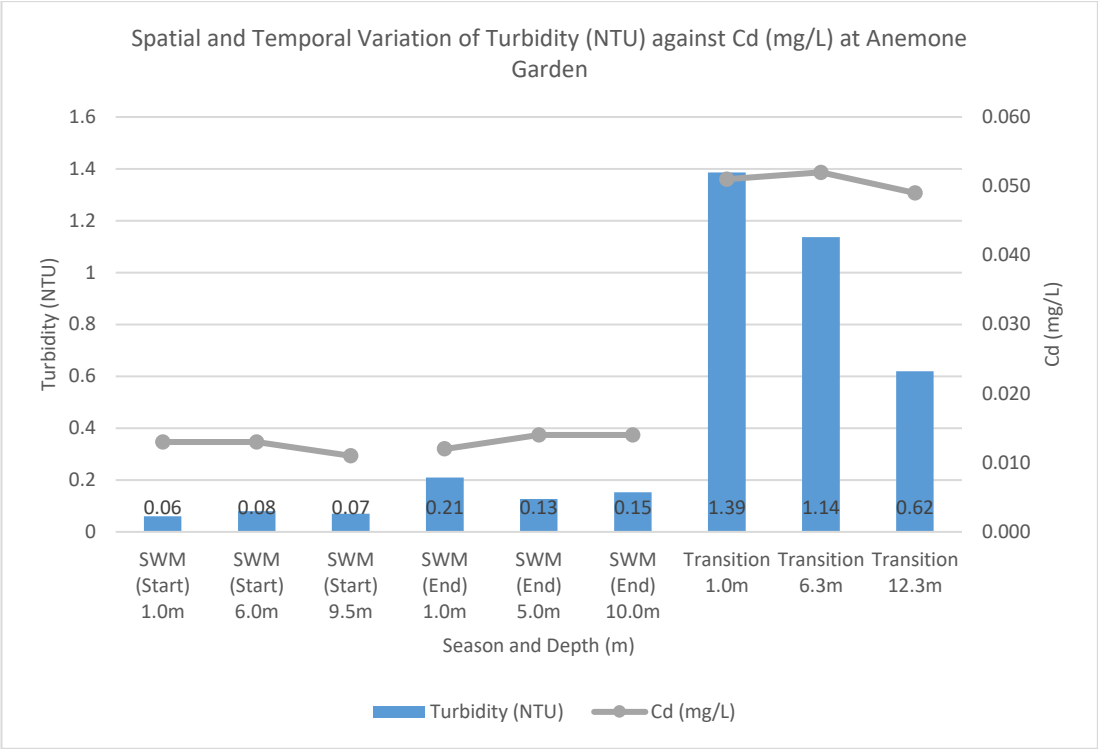

Figure 5.2.45 –Turbidity (NTU) against Cd (mg/L) at Anemone Garden

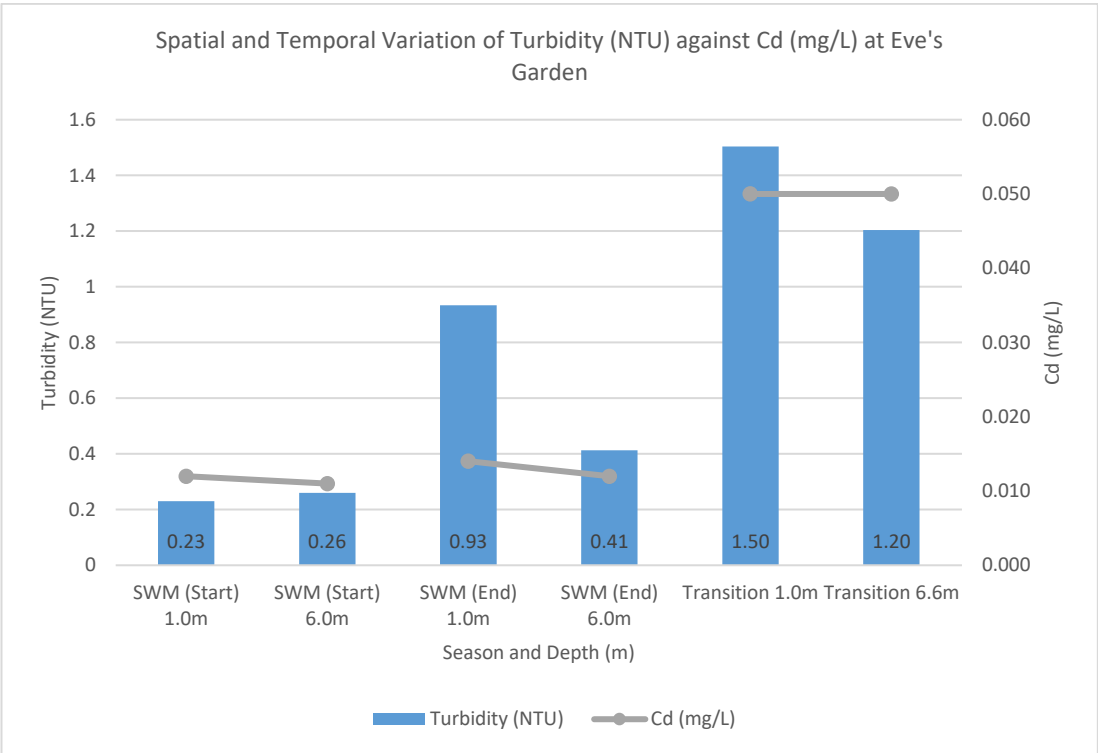

Figure 5.2.46 –Turbidity (NTU) against Cd (mg/L) at Eve's Garden

The concentrations of cobalt, copper and nickel followed a similar trend to that of cadmium as noted in Figures 5.2.47 to 5.2.49. The concentration of cobalt was mostly below detection limit during the beginning and end of SWM at North Siwa and then experiencing a spike during the NEM transition period. The same observations were made for copper and nickel where their concentrations were increased close to double the amount in the transition period. The reason behind the increase in concentration of cobalt and copper are due to coastal development, industrial activities, input from Miri-river and the use of fertilisers (Rakestraw, 1943; Balls, 1985; APHA, 2012; Mokhtar et al., 2012). The depth-wise variance in copper concentration is also attributed to the biological uptake and remineralisation explaining the decrease at the seabed. Whereas the decomposition of organic particles at Anemone Garden during the start of SWM indicates more coral damage as noted by the slight increase in copper concentration from the decomposing organic particles (J.-M. Lee et al., 2011). The increase in the concentration of nickel observed from start of SWM to NEM transition indicates heavy boat activity, a nearby harbour and the presence of crude oil and solid waste (Mokhtar et al., 2012; Lenntech, 2017i).

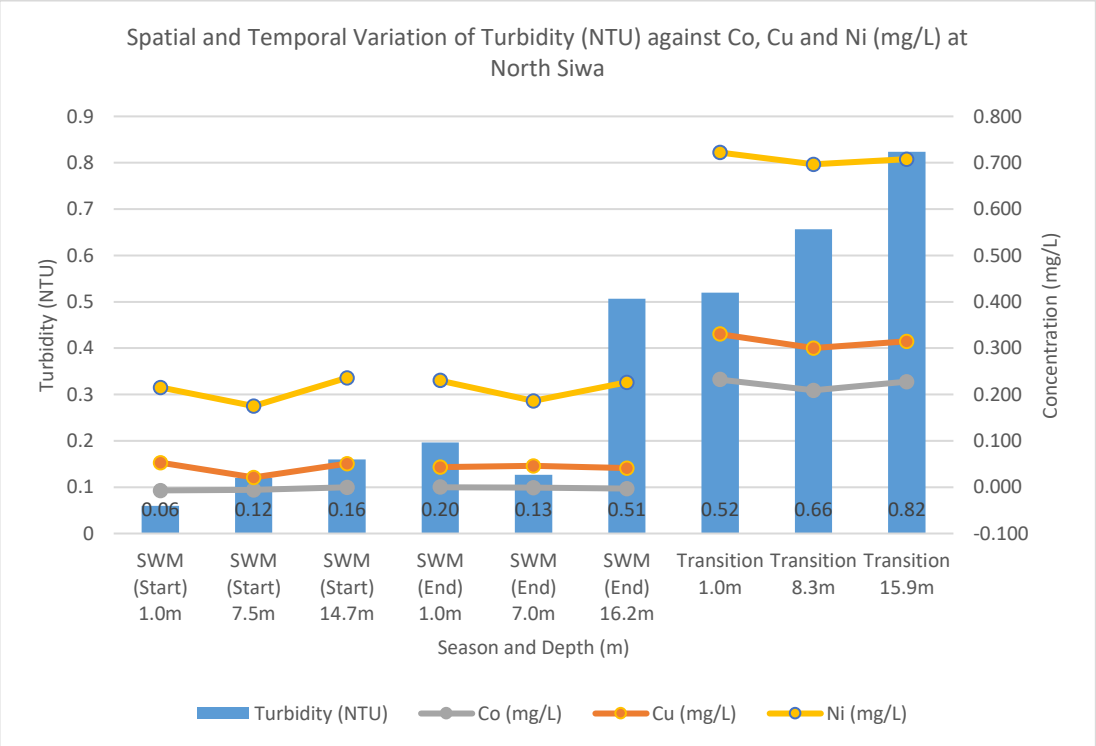

Figure 5.2.47 - Turbidity (NTU) against Co, Cu and Ni (mg/L) at North Siwa

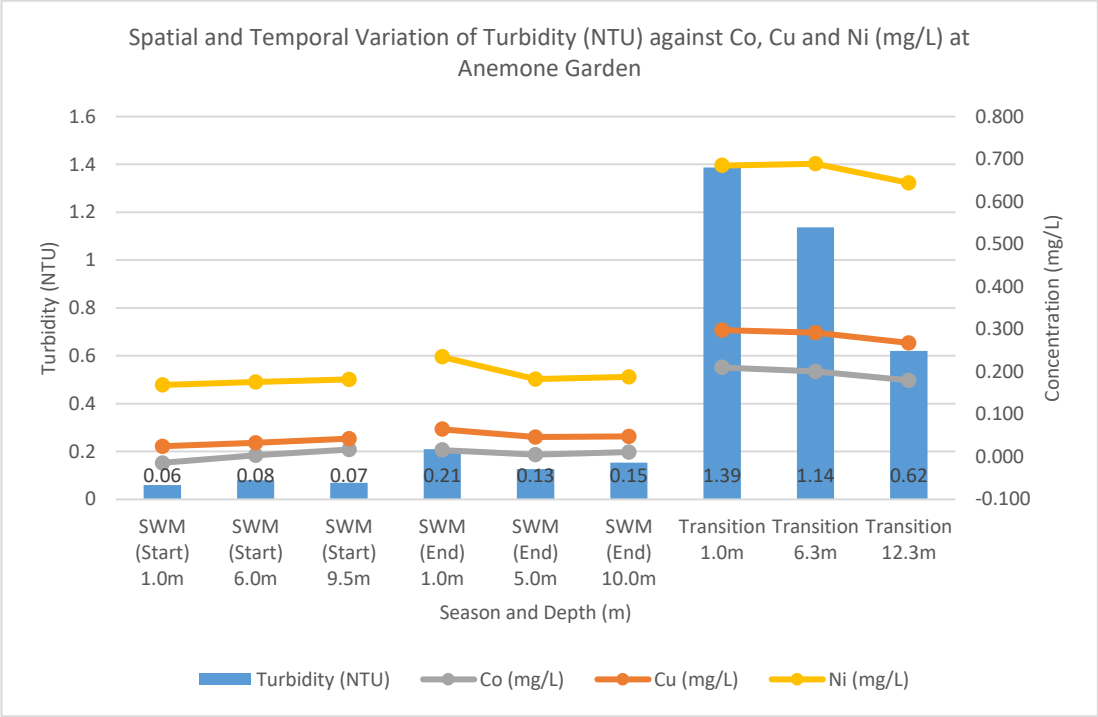

Figure 5.2.48 - Turbidity (NTU) against Co, Cu and Ni (mg/L) at Anemone Garden

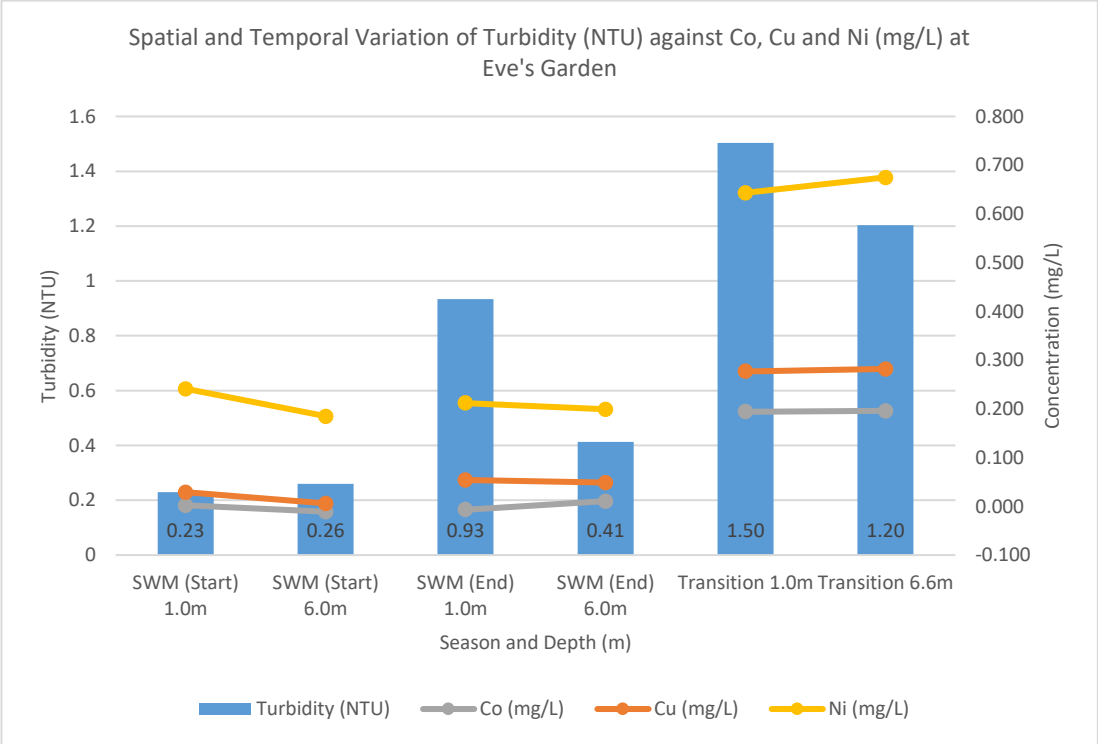

Figure 5.2.49 - Turbidity (NTU) against Co, Cu and Ni (mg/L) at Eve's Garden

Figures 5.2.50 to 5.2.52 show the variation of iron concentration during the three seasons and depths of each site compared to turbidity of the water. The behaviour of iron was similar to that of cobalt, copper and nickel for the beginning and end of SWM but experienced a decrease during NEM transition. It is certain, from the above variations (Figures 5.2.44 to 5.2.49), that Miri river runoff was the key factor for the increase of the trace metal concentrations for cadmium, cobalt, copper and nickel for that season (Mackey et al., 1996; Zaidi, 2006; Cabon et al., 2007). The concentration of iron obtained during the transition was slightly lower than the concentrations at the beginning and end of SWM. However, the average spatial and temporal concentration of iron at the three sites were still higher than the analyses made by Rakestraw (1943) and Anthoni (2006). The spatial and temporal variations indicated a decrease in concentration at North Siwa with increasing turbidity when going deeper, while the opposite was observed at Anemone Garden. Eve's Garden held a rather constant value while the turbidity was lower at the seabed. The concentration of iron was noted to be higher at Eve's Garden and getting less when reaching the further sites. The reason behind the decrease in concentration could be due to the dissolved iron spreading over more area which would explain the similarities of concentrations between North Siwa and Anemone Garden. The concentration of iron is both naturally occurring and through human intervention. Both Sunda (2012) and, Hutchins and Boyd (2016) explain that the concentration of iron in water through Aeolian deposition has increased over the years. The island of Borneo is often shrouded in thick clouds of smoke due to forest fires within the island which can lasts for weeks, during start of SWM (Abram et al., 2003; Then, 2012; "Wildfires flare up in Kuala Baram," 2014, 2015, 2016). However, during transition period, the amount of rainfall as noted in Table 4.5.3, makes it difficult for the fire to persist which would explain the lower concentration of iron during the transition period (Sunda, 2012). The decrease in concentration in iron also means an increase in the algae population as has been observed at Eve's Garden (Figure 5.6.25 – 5.6.27) since iron stimulates plant growth and is an important nutrient for the growth of plankton (Wells et al., 1995; Anthoni, 2006; Nair and Balakrishnan, 2006; Hutchins and Boyd, 2016)

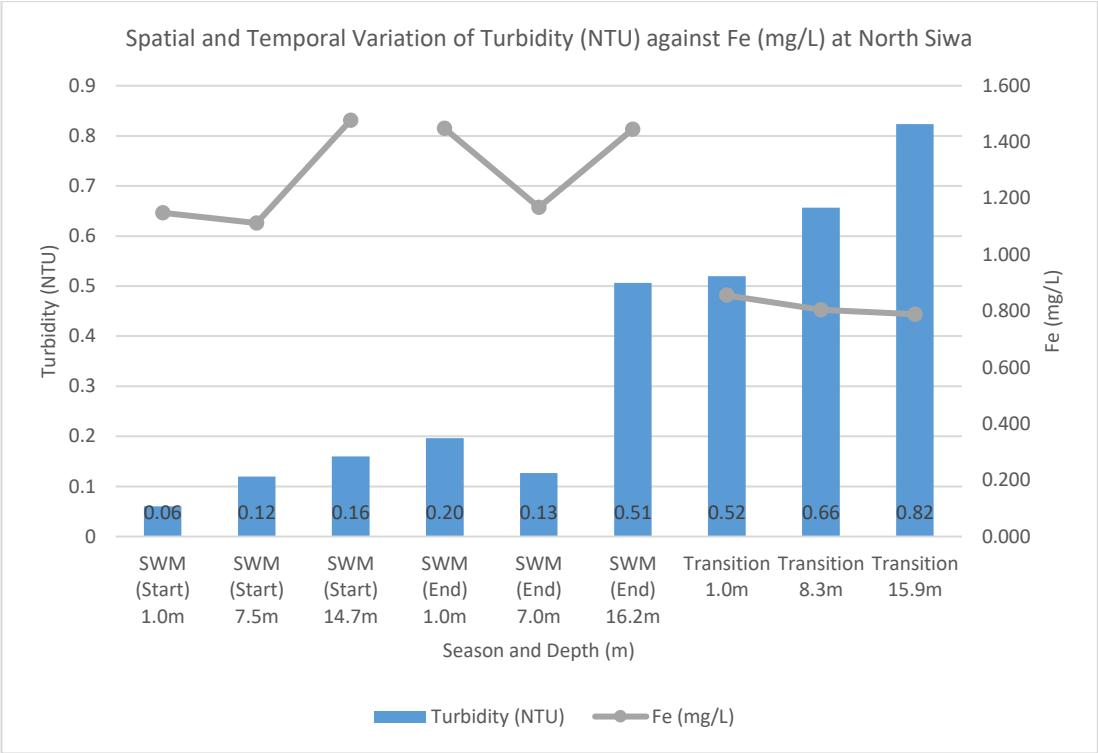

Figure 5.2.50 – Turbidity (NTU) against Fe (mg/L) at North Siwa

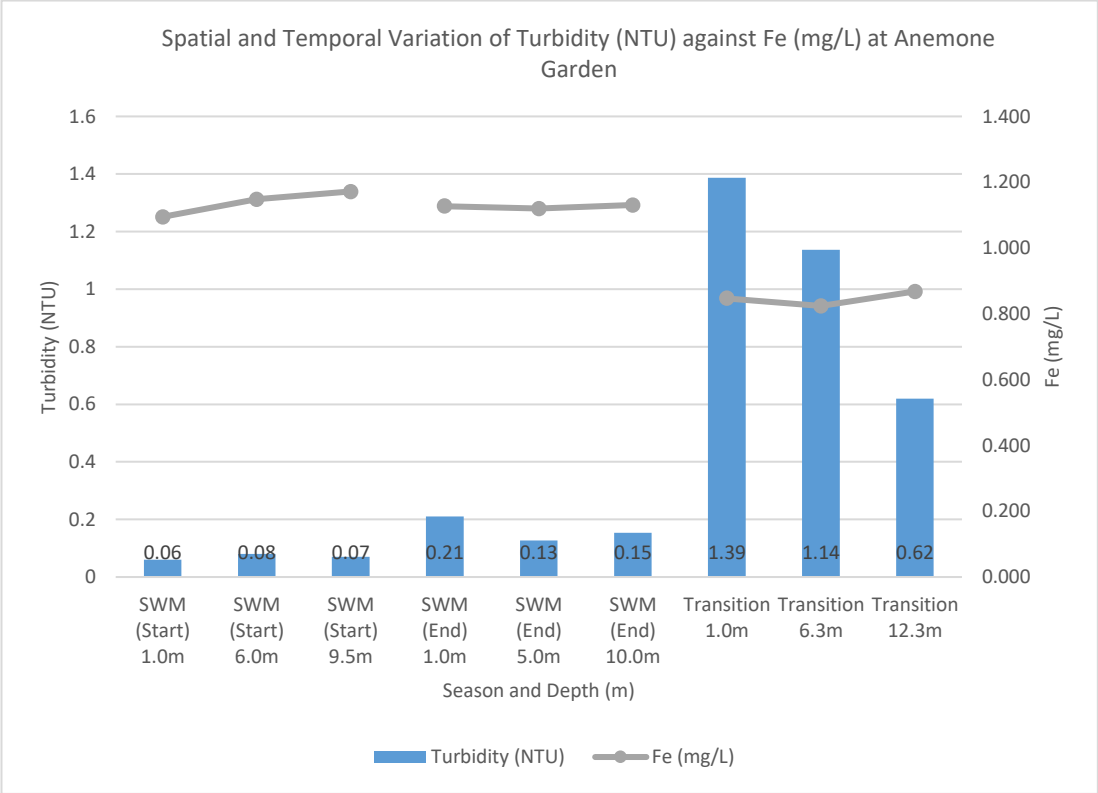

Figure 5.2.51 – Turbidity (NTU) against Fe (mg/L) at Anemone Garden

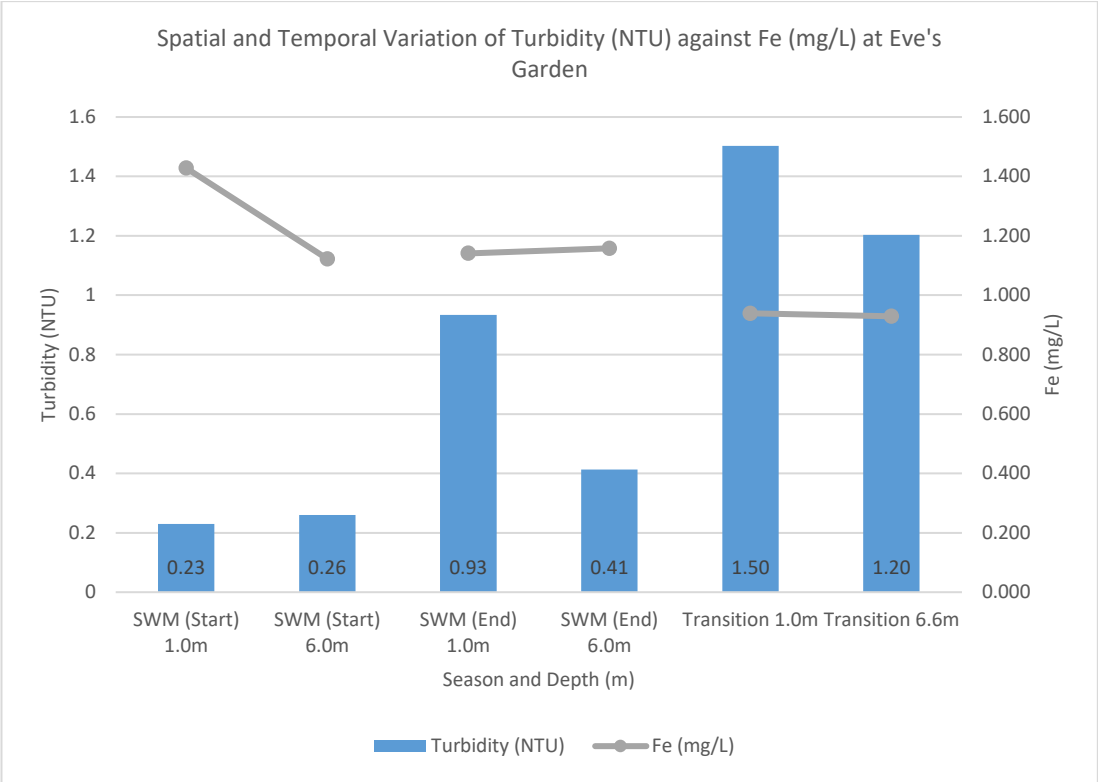

Figure 5.2.52 – Turbidity (NTU) against Fe (mg/L) at Eve's Garden

Figures 5.2.53 – 5.2.55 show the spatial and temporal variations of manganese and zinc with respect to turbidity. At North Siwa, the concentration of manganese observed a depth-wise increase as the turbidity increased, however, the exact opposite was noted at Anemone Garden, where the manganese concentration decreased slightly with increasing turbidity going to the seabed. From surface to seabed, Eve's Garden observed an increase in its concentration during the start of SWM with increasing turbidity and still observed an increase in concentration when the turbidity decreased during the end of SWM. However, during the NEM transition period, a decrease in turbidity was accompanied by a decrease in the concentration of manganese at Eve's Garden. Marine organisms in seawater have an influence on the concentration of manganese present in seawater (Rakestraw, 1943). Along with marine organisms, manganese can be found in seawater through natural sources, river runoffs, fertilisers and other anthropogenic sources (Statham, 1985; Zaidi, 2006; Cabon et al., 2007; Lenntech, 2017h). The fluctuations noticed in the depth-wise concentration could be due to the time taken for manganese to settle, which is usually a few days (Zaidi, 2006; Lenntech, 2017h).

The concentration of zinc was very closely related to the turbidity of the three sites during start of SWM and end of SWM. During NEM transition period, the behaviour of zinc was noted to behave similar to iron which was the concentration of the metal opposite to that of turbidity. The presence of zinc in seawater is attributed to the same factors as the other trace metals, which are mostly river runoff and solid waste disposal (Cabon et al., 2007; Lenntech, 2017l). Zinc and manganese share a common feature whereby they provide essential proteins that are required for cell growth and regeneration (Sunda, 2012).

The concentration of lead was below detection limit during the start and end of SWM. However, a high concentration was observed during the transition to NEM. Owing to the colour of the water and the turbidity values during that period, the high concentration of the metal can only be attributed to strong anthropogenic activities such as industrial discharge and waste disposal. A similar situation was observed by Cuoco et al. (2015) during their study in Southern Italy.

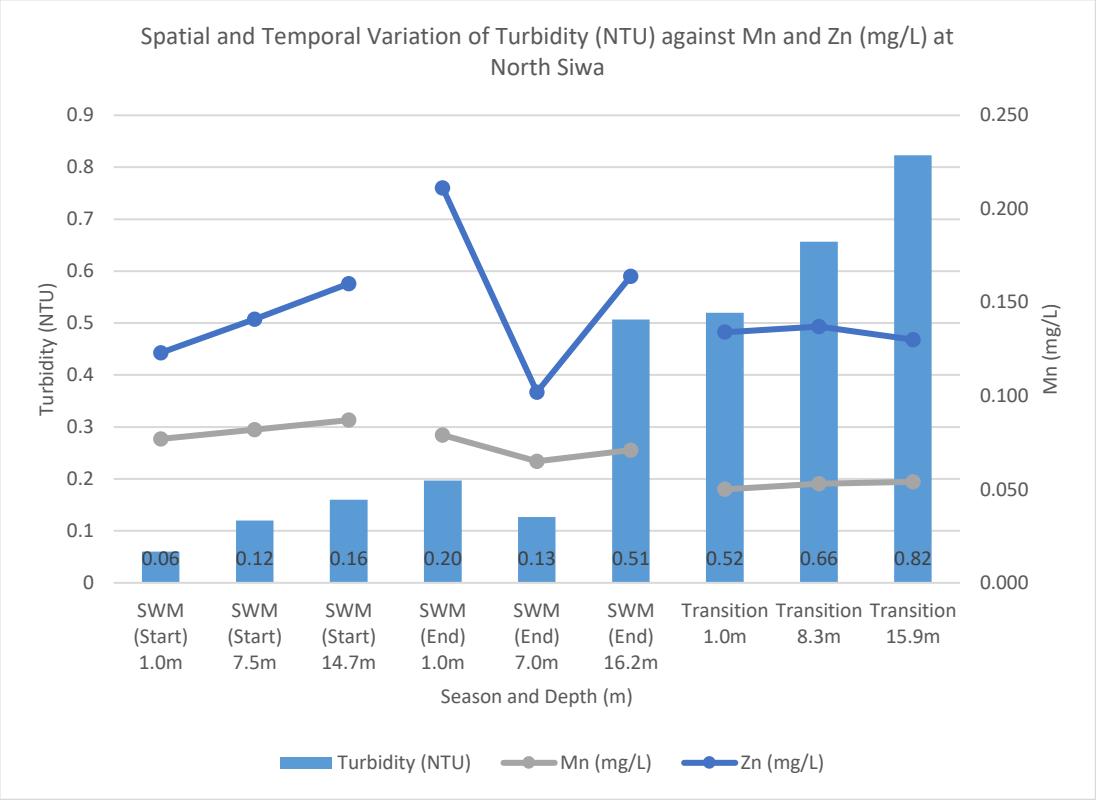

Figure 5.2.53 – Turbidity (NTU) against Mn and Zn (mg/L) at North Siwa

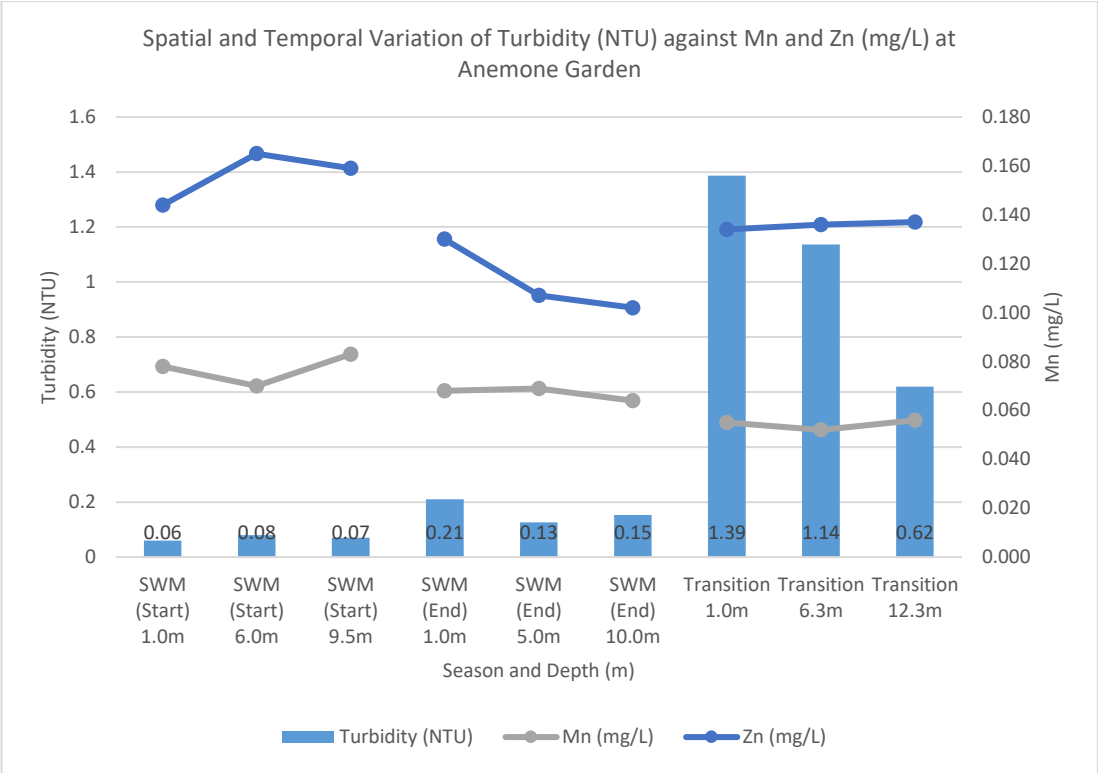

Figure 5.2.54 – Turbidity (NTU) against Mn and Zn (mg/L) at Anemone Garden

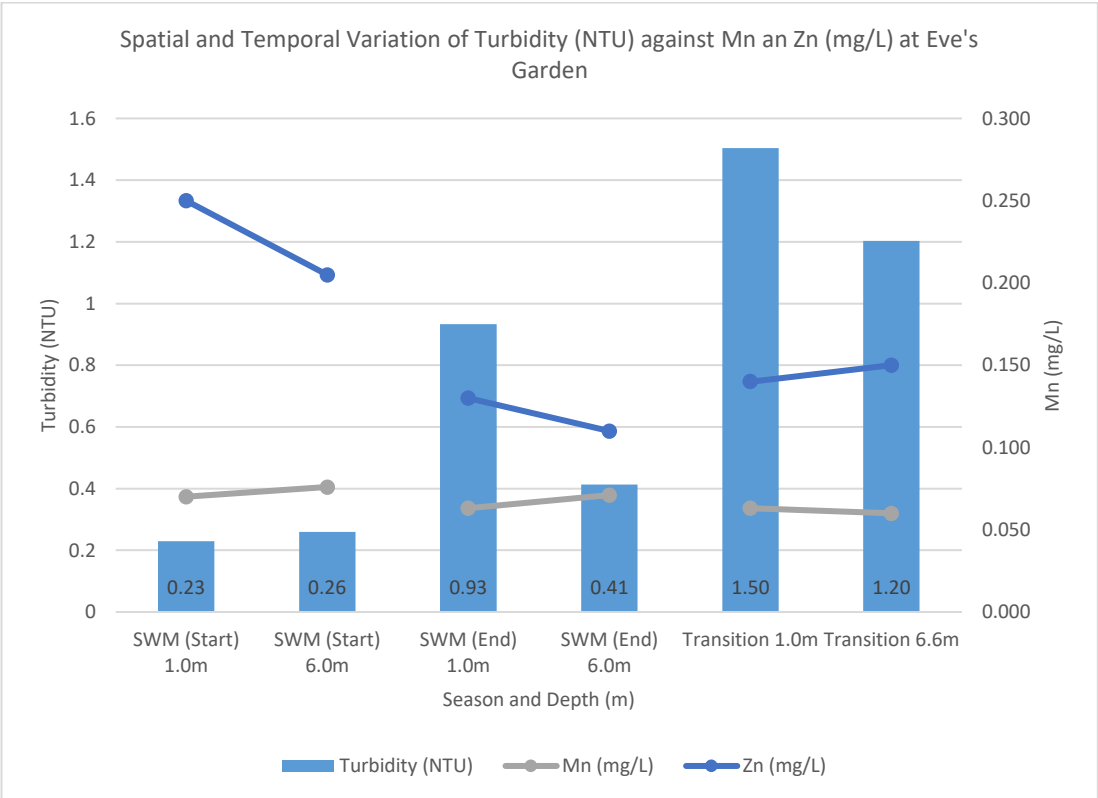

Figure 5.2.55 – Turbidity (NTU) against Mn and Zn (mg/L) at Eve's Garden

5.3 Sipadan Island Park

5.3.1 In-Situ Parameters

A 0.1ppt difference in salinity as well as a 0.1mS/cm difference in EC were observed from the surface and middle layer to the seabed of Barracuda Point. South Point did not have any variations in either EC or salinity values as observed in Figure 5.3.1. Since EC is a measure of salinity (Health, 2016), the correlation between these two parameters showed a linear relationship at both Barracuda point and South Point.

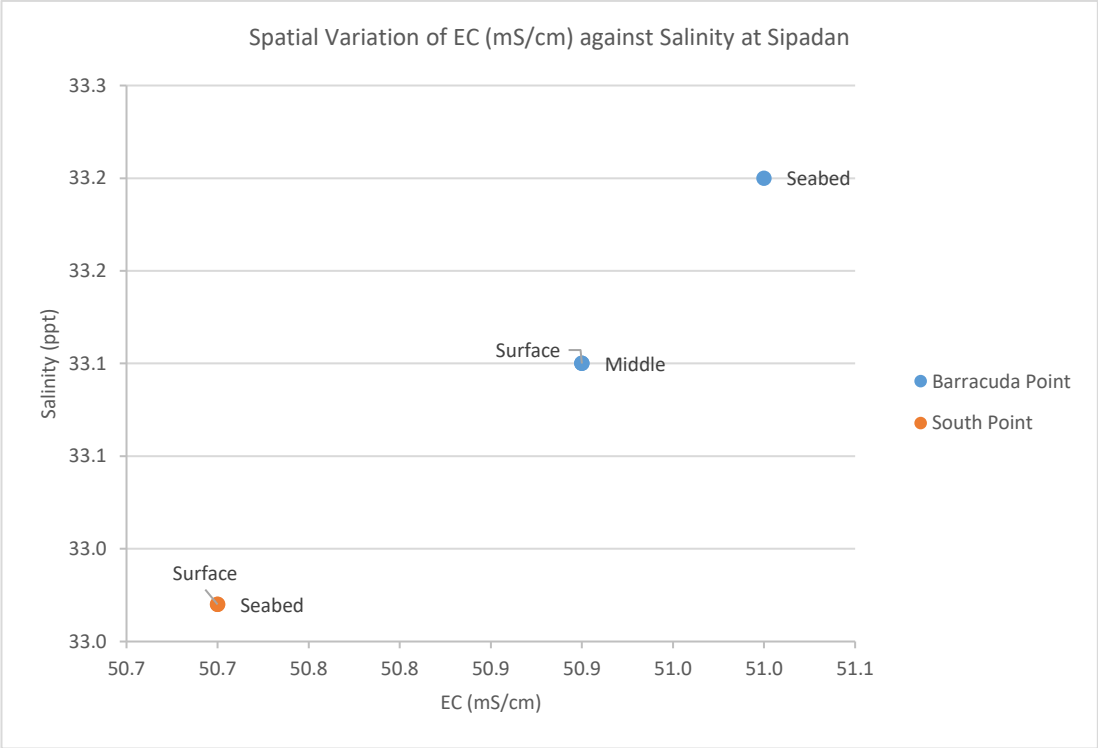

Figure 5.3.1 – EC (mS/cm) against Salinity (ppt)

According to Rakestraw (1943), ORP is associated with the pH and the amount of DO present in the seawater. Comparing the pH values to ORP, Figure 5.3.2 shows an inverse relationship between the two parameters. pH observed an increase while the ORP values decreased from surface to seabed at both sites. The low pH and high ORP values could be due to the rainfall from the previous day because rainwater has a lower pH value due to the presence of carbon dioxide from the atmosphere creating carbonic acid (APHA, 2012).

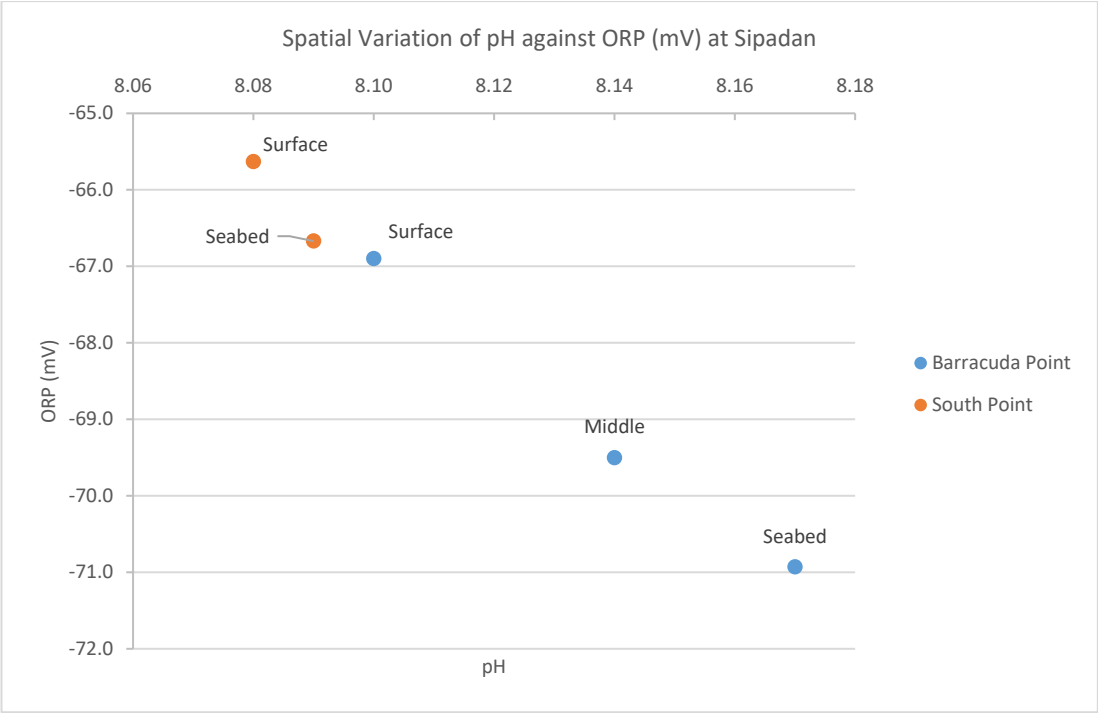

Figure 5.3.2 – pH against ORP (mV)

From Figure 5.3.3, the conductivity of the seawater at Barracuda Point increased with TDS at the seabed. As mentioned in Section 5.2.1, the increase in TDS concentration correlates with increasing conductivity values due to the presence of various salt species (Measurements, 2016a). Though EC was the same value at both surface and seabed at South Point, TDS value observed an increase.

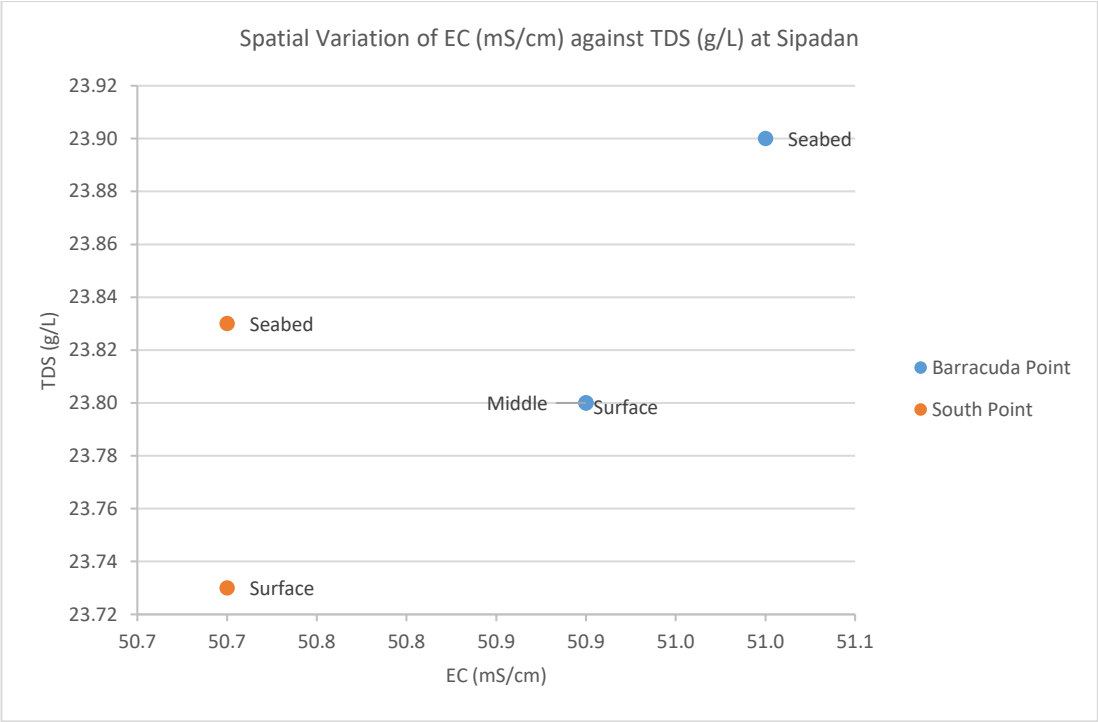

Figure 5.3.3 – EC (mS/cm) against TDS (g/L)

The concentration of DO and the pH values decreased from surface to seabed at both sites as shown in Figure 5.3.4. The surface of Barracuda point observed a higher concentration of DO due to boat activities and the site being the closest to the passenger drop off region. The constant activity at that location help with the absorption of oxygen in the seawater. However, South Point, being further from land had a lower pH and DO concentration which could have been due to the rainfall from the previous day together with less boat activity in that region.

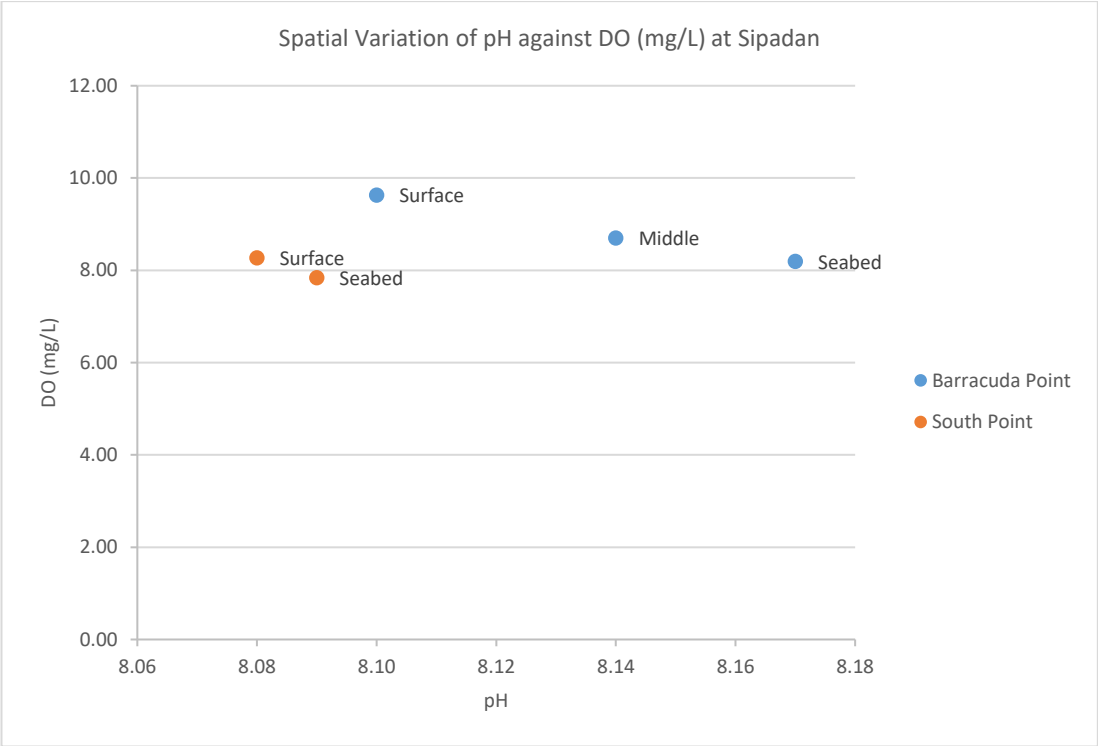

Figure 5.3.4 – DO (mg/L) against pH

5.3.2 Nutrients

The concentration of Nitrate observed at both Barracuda Point and South Point was 0.02mg/L from surface to seabed (Table 4.3.4). Low concentration of nitrate indicates that the amount of algae present at the sites would not be invasive and suffocate the corals (Higuchi et al., 2015)

In Section 5.2.2, it was mentioned that the concentration of sulphate in the ocean was roughly 2700mg/L (Rakestraw, 1943; Anthoni, 2006). The seabed of Barracuda Point observed a value of 2600mg/L, while the surface and middle depth both noted concentrations of 2400mg/L, similar to South Point (Table 4.3.7). The surface and middle values from both sites indicate dilution of the seawater resulting from the rainfall of the previous day (Prasanna et al., 2010).

There was very little variation in the concentration of ammonia-nitrogen at both sites in Sipadan (Table 4.3.7). A higher concentration was observed at the surface of Barracuda Point since it was the closest to the drop off point. South Point had the same concentration at both surface and seabed. These values indicate the presence of divers

and boats which are not equipped with wastewater and sewage systems (Ilter. et al., 2012; Lamb et al., 2014).

Phosphate is an essential constituent of living organisms as mentioned in Section 5.2.2. The presence of a higher level of phosphate at Barracuda Point could be attributed to bottom sediments released from boats landing on the beach to embark and disembark tourists (M. Lee et al., 2008). South Point had lower values as the site was further from the island than Barracuda Point and could also indicate the presence of phytoplankton since phosphate is an important nutrient for these organisms (Rakestraw, 1943).

5.3.3 Major Ions

As shown in Figure 5.3.5, the concentration of bicarbonate decreases as the pH increases. Following Equation [1] from Section 5.2.3, as the pH increases, the bicarbonate ion will go the left of the equation forming carbonic acid, thereby decreasing the concentration of bicarbonate (Measurements, 2016c).

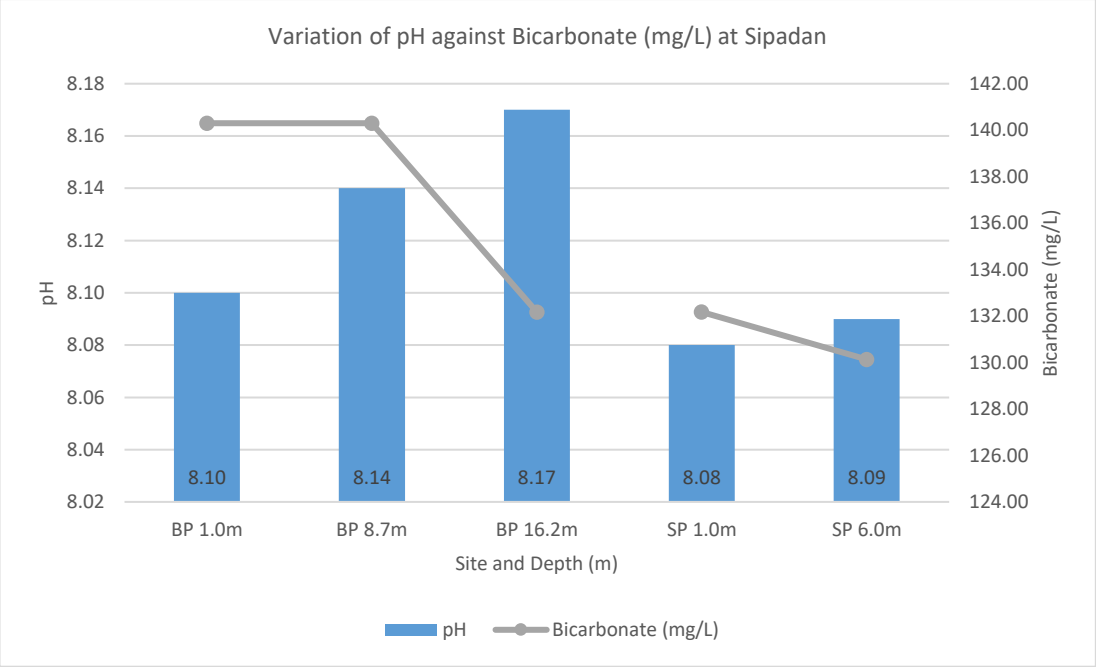

Figure 5.3.5 – pH against Bicarbonate (mg/L)

A decrease in the concentration of calcium was observed from surface to seabed while the pH increased at both sites (Figure 5.3.6) and a similar trend was observed with

bicarbonate from Figure 5.3.4. The change in concentration is a normal behaviour of seawater characteristics (Readman et al., 2013; Lenntech, 2017b).

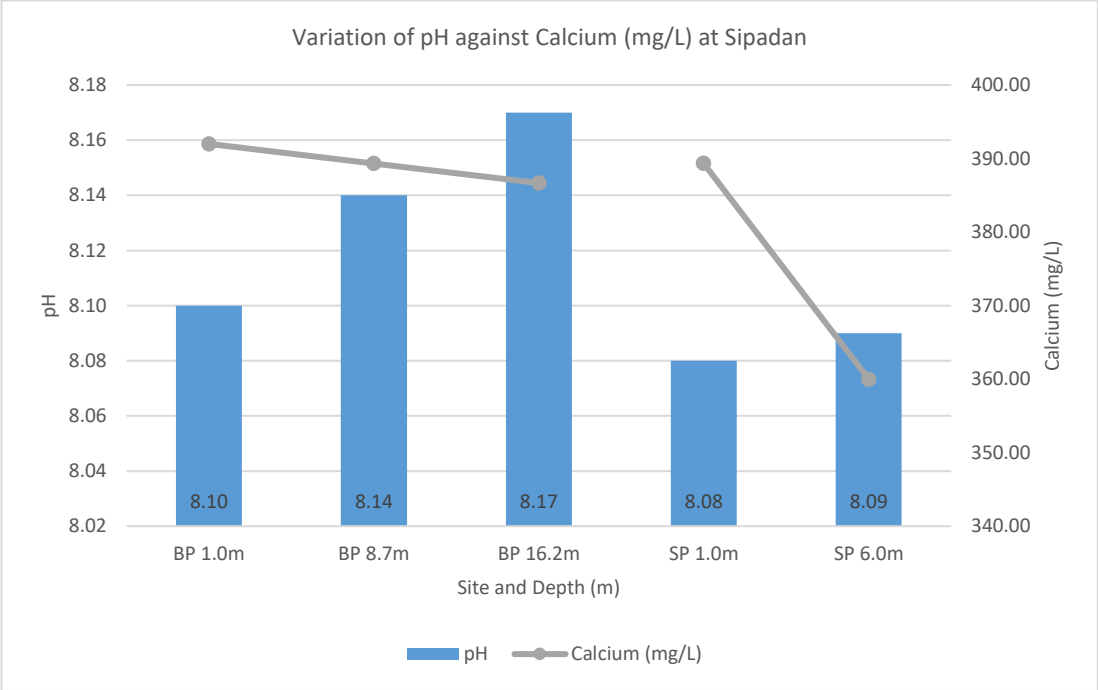

Figure 5.3.6 – pH against Calcium (mg/L)

Figure 5.3.7 shows the concentration of magnesium and pH values at Barracuda Point and South Point. A decrease in the concentration of magnesium was observed from surface to the middle layer and maintained that concentration until the seabed of Barracuda Point. This decreasing in concentration could be attributed to the intrusion of freshwater due to the proximity of the site to the island (Lenntech, 2017g). The increase in concentration from surface to seabed at South Point would indicate the presence of corals and other marine organisms (Rakestraw, 1943; Grasshoff et al., 1999).

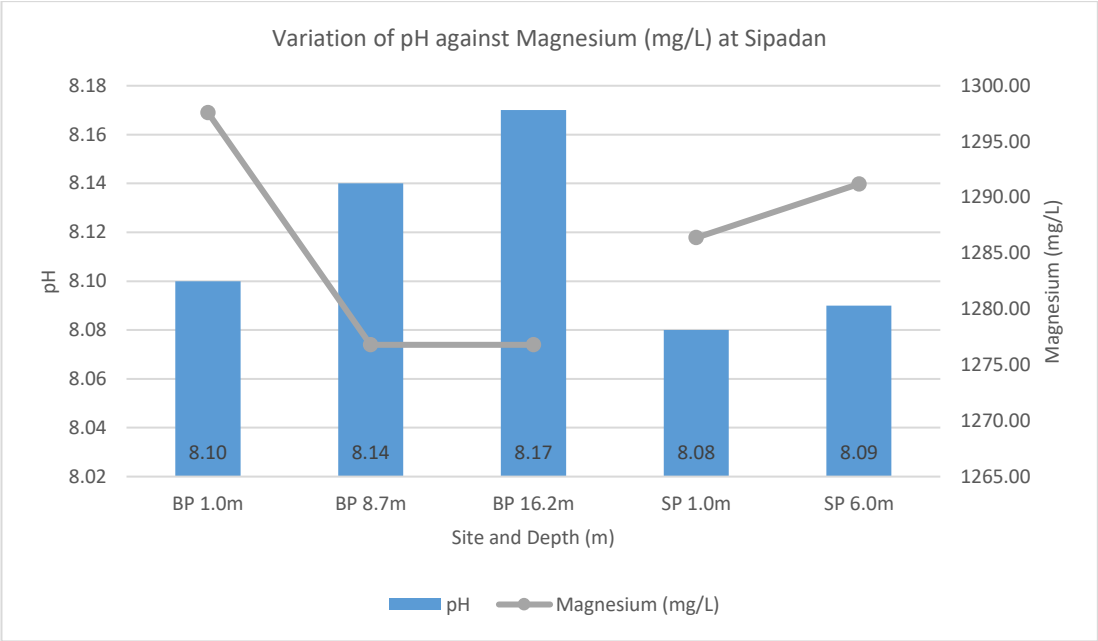

Figure 5.3.7 – pH against Magnesium (mg/L)

An increase in the concentration of potassium along with the pH level was observed from surface to seabed at both Barracuda Point and South Point as shown in Figure 5.3.8. The depth-wise increase in concentration is a normal behaviour of potassium in seawater (Measurements, 2016a).

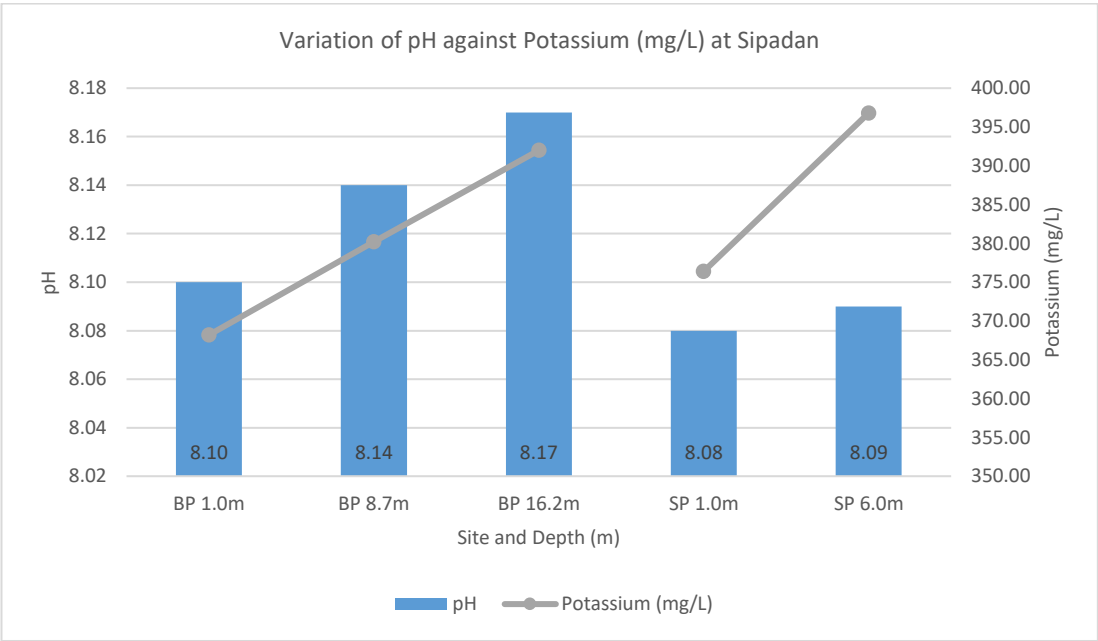

Figure 5.3.8 – pH against Potassium (mg/L)

Figure 5.3.9 shows the depth-wise variation of sodium at Barracuda Point and South Point. The concentration of sodium observed an increase similar to potassium, from surface to seabed. However, a high concentration was observed at the surface of South Point. According to Anthoni (2006), the concentration of sodium in the ocean is around 10,800mg/L. The value recorded at the seabed of South Point was closer to the ocean's average than the surface indicating the effect of human activities like throwing food in the sea to attract fish to the surface (Lenntech, 2017k).

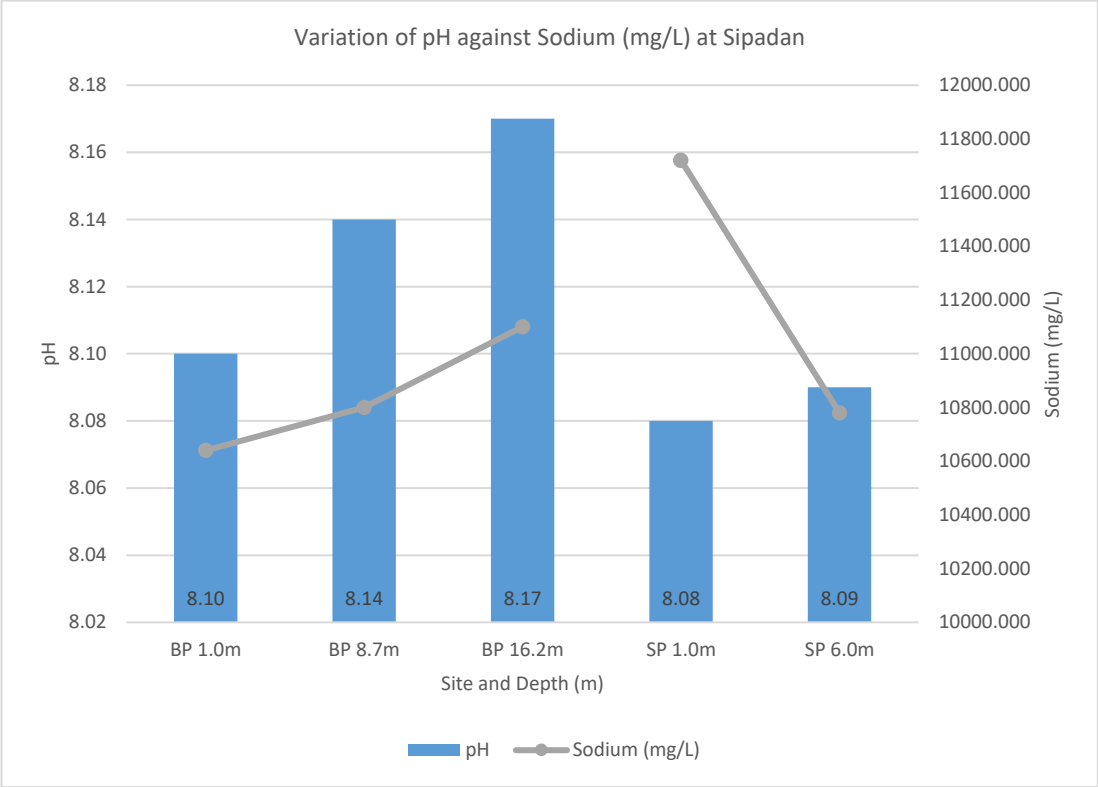

Figure 5.3.9 – pH against Sodium (mg/L)

From Figure 5.3.10, the decrease in chloride concentration from surface to seabed at Barracuda point could be due to the presence of freshwater and vertical mixing of the seawater from the ocean current. The variation in concentration of chloride at South Point was negligible since little change was noted, similar to the value of pH.

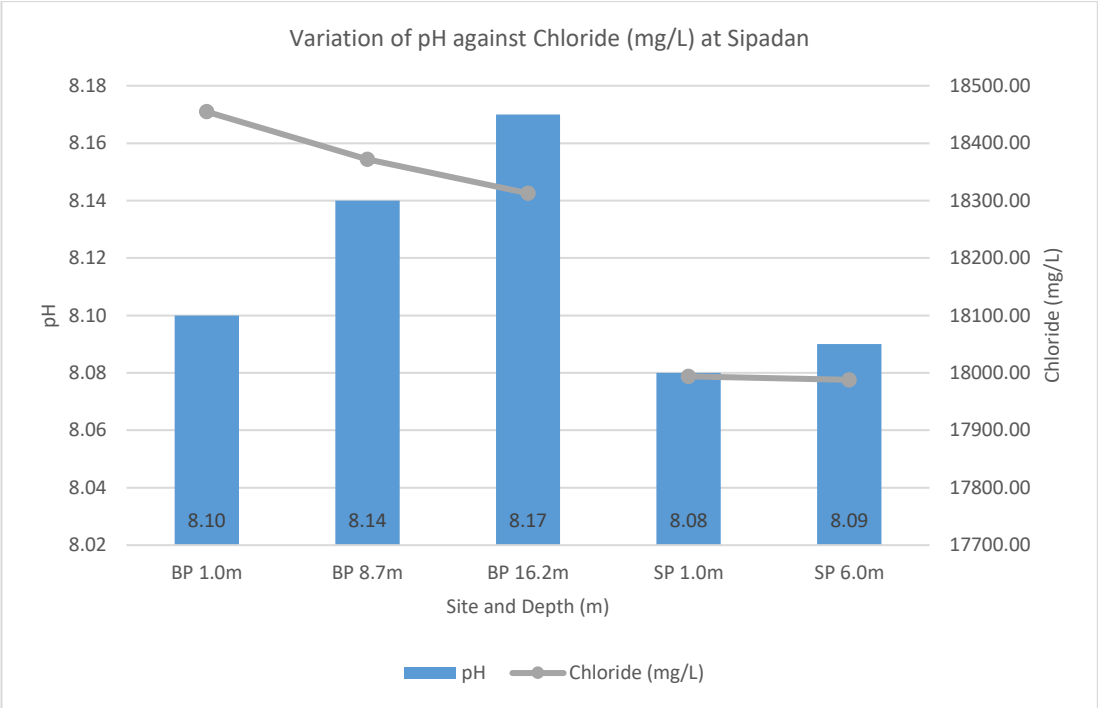

Figure 5.3.10 – pH against Chloride (mg/L)

5.3.4 Trace Metals

The concentrations of copper and zinc had similar patterns but only differed in concentration where that of zinc was higher than copper as observed in Figure 5.3.11. The high concentration of copper at the middle depth, according to J.-M. Lee et al. (2011), comes from the release of copper from surface sediments which sink and are then re-mineralised from biological uptake. Zinc was present from bioaccumulation factor in corals according to the study done by Mokhtar et al. (2012), which was released to the seawater after breaking.

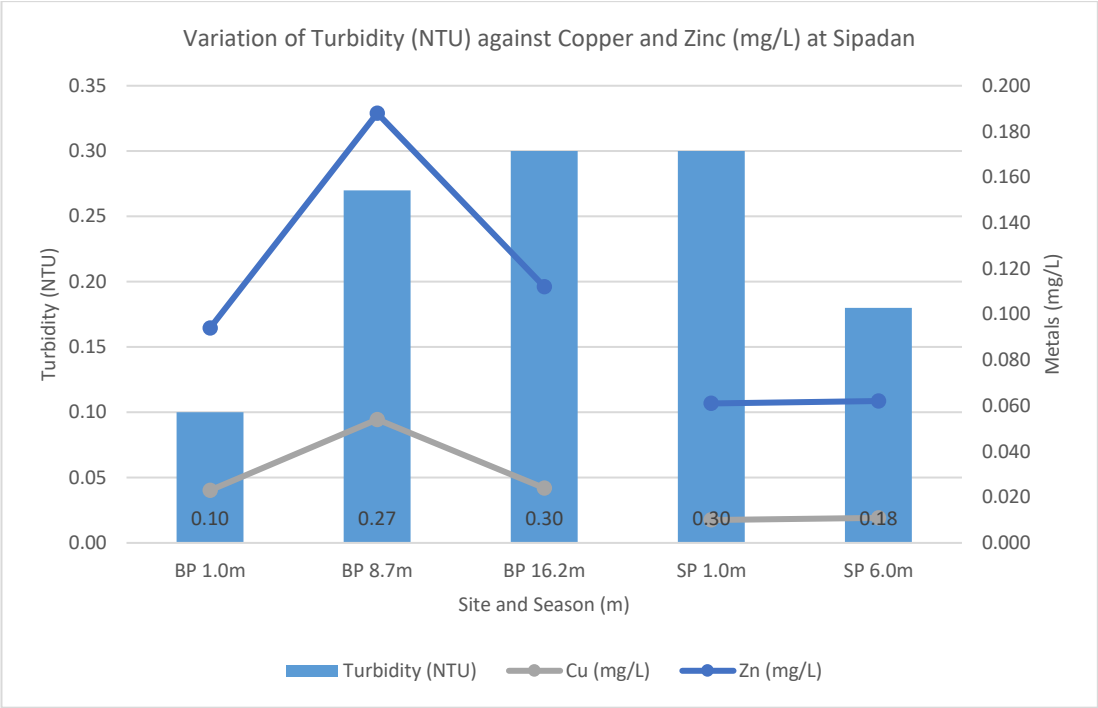

Figure 5.3.11 – Turbidity (NTU) against Cu and Zn (mg/L)

Figure 5.3.12 and 5.3.13 show the variation of iron and manganese from surface to seabed at Barracuda Point and South Point. The concentration of iron observed were over eight times more than previously analysed and that of manganese was close to three times more than in 2012 (Mokhtar et al., 2012). Iron and manganese are naturally occurring elements in seawater, which contributes to the presence of phytoplankton (T. G. Thompson and Wilson, 1935; Mackey et al., 1996; Rodriguez et al., 2016)

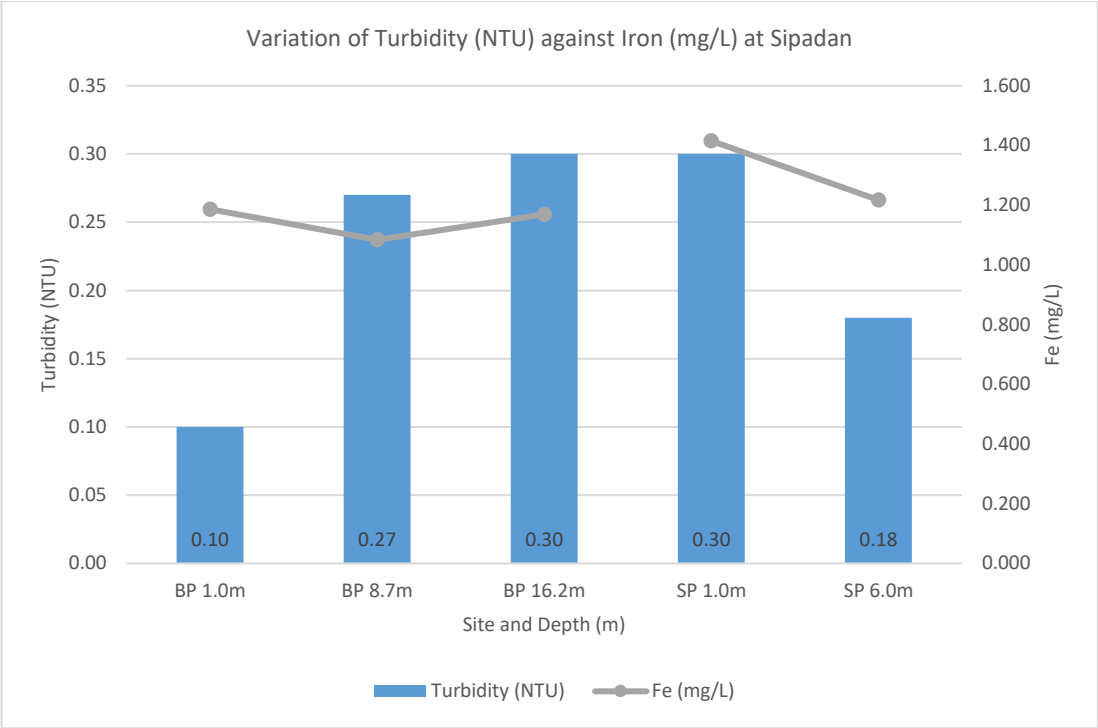

Figure 5.3.12 – Turbidity (NTU) against Fe (mg/L)

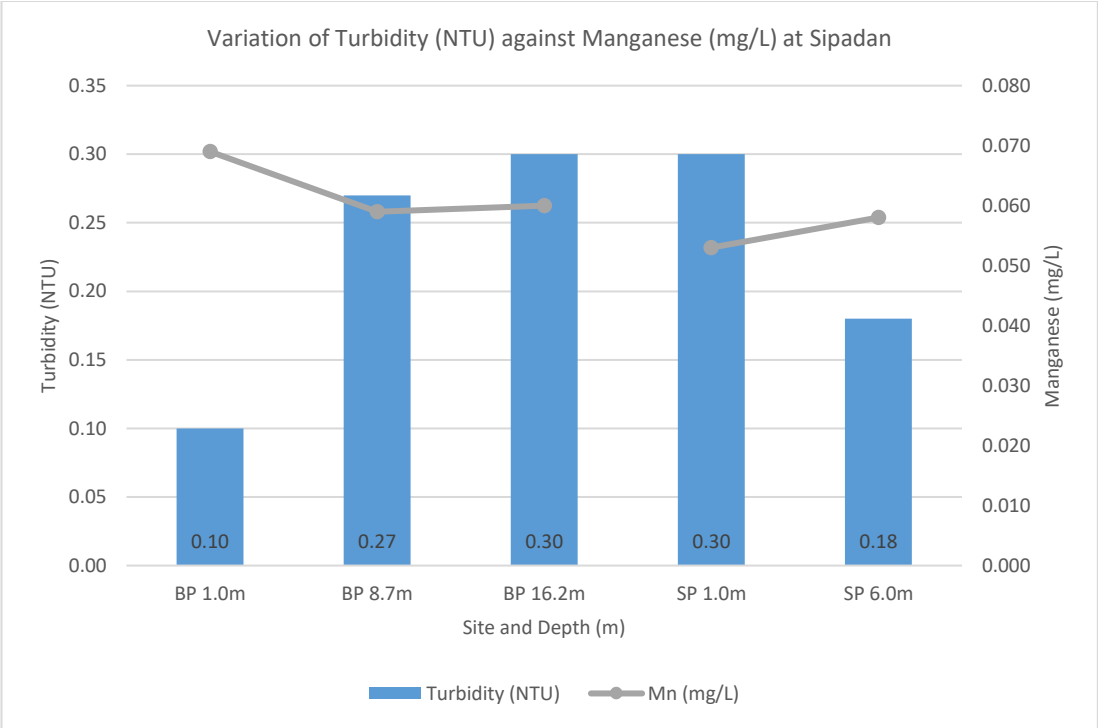

Figure 5.3.13 – Turbidity (NTU) against Manganese (mg/L)

The concentration of nickel decreases from surface to seabed (Figure 5.3.14). Based on the analyses done by Mokhtar et al. (2012), the concentration of nickel in 2012 was 0.02mg/L at Sipadan. The concentration of nickel in 2016 was an average of 0.155mg/L, which is 7.75 times more than 4 years ago. The high concentration at the surface is attributed to the presence of many boats for both fishing and recreational activities as well as weathering effects (Mokhtar et al., 2012).

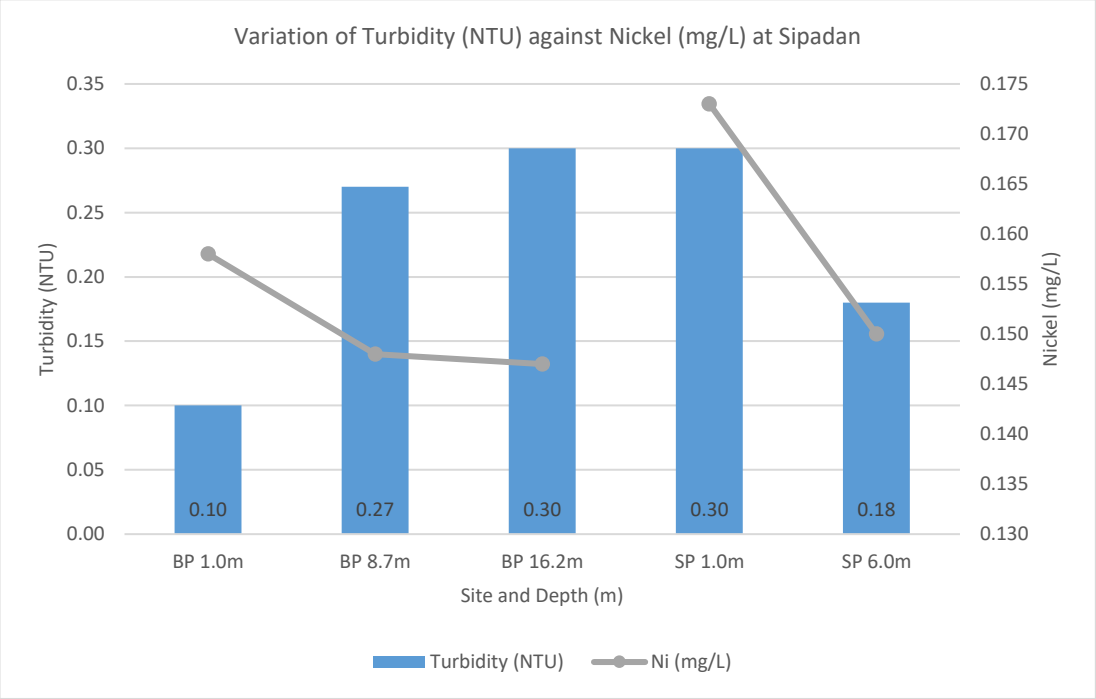

Figure 5.3.14 – Turbidity against Nickel (mg/L)

5.4 Statistical Analysis

Combining all the parameters examined during this research namely, depth, physico-chemical parameters, nutrients, major ions and trace metals along with 29 different seawater samples, came a total of 783 analysis completed. The integration, interpretation, and representation of this amount of data can become challenging. Hence, a reliable interpretation of large data sets was done by applying multivariate statistical analysis. This technique helped in organising large sets of data which was then used to detect the relationship to the quality of the seawater. Numerous research showed its efficacy in linking parameters, for example, the concentration of trace nutrients to river runoffs and other anthropogenic activities (Prasanna et al., 2010;

Mokhtar et al., 2012; Prasanna et al., 2012; Vasanthavigar et al., 2013; Singaraja et al., 2015; Chidambaram et al., 2016). Correlation analyses and factor analyses were carried out by using the Statistical Package of Social Studies (SPSS) version 17 software. The results were used to differentiate the various characteristics of the seawater samples, and to identify geochemical processes controlling the quality of the seawater at different seasons.

5.4.1 Correlation Analysis

This is the first step when conducting multivariate statistical analyses from the data gathered. The computation of a correlation matrix provides the relationship among the data set which then creates pairs with the parameters also known as the Pearson's correlation (Thilagavathi et al., 2017). The correlation matrix (Table 1 to 4) contains various values ranging from negative values to a maximum value of +1. This study will be focusing only on the positive values where high degree correlation values are measured from +0.75 to +1.00, moderate degree correlation are from +0.25 to +0.75 and low degree correlation are from 0.00 to +0.25 (Prasanna et al., 2010; Vasanthavigar et al., 2013; Singaraja et al., 2014; Thivya et al., 2015).

5.4.2 Miri-Sibuti Coral Reef National Park

5.4.2.1 Start of SWM

At the beginning of the SWM season, a high degree correlation exists between depth with EC, ORP and TDS while a moderate degree correlation exists with calcium and manganese, indicating the presence of large coral population at the sites (Lenntech, 2017b, 2017h). Moderate correlation observed between temperature with sulphate and zinc, and pH with salinity, magnesium, copper, potassium and nickel. EC has moderate correlation with salinity, ORP, calcium, magnesium and manganese while having a high correlation with TDS indicating the presence of those ions in the TDS thereby contributing to the conductivity of the ocean (Thivya et al., 2015; Measurements, 2016a). Salinity observed a moderate degree correlation with TDS, calcium and magnesium. ORP had a high correlation with calcium and manganese, and a moderate correlation with TDS. A high correlation was observed between turbidity with chloride, nickel and zinc, and a moderate correlation with potassium. The correlation

with nickel and zinc indicates the presence of phytoplankton and river runoffs respectively (Rakestraw, 1943; Lenntech, 2017l). Moderate correlation of TDS with calcium, magnesium and manganese were noted. When observing the nutrients, nitrate and ammonia-nitrogen had a moderate correlation with phosphate and zinc respectively. This correlation links to anthropogenic activities such as fertilizers, coastal development and river runoff (Abram et al., 2003; Vasanthavigar et al., 2013; Lenntech, 2017l). Bicarbonate had a moderate correlation with cadmium, iron and sodium indicating the presence of phytoplankton and chemical weathering (Wells et al., 1995; Thivya et al., 2015). Calcium was observed to have a high degree correlation with magnesium and manganese, while having a moderate correlation with copper indicating anthropogenic activities (Zaidi, 2006). Magnesium had a moderate correlation with copper and manganese. Chloride had a very high correlation with nickel and moderate correlation with iron and zinc. Copper was the only trace metal that observed a moderate correlation with lead. Iron showed a high correlation with nickel and lastly, nickel showed a high correlation with zinc.

5.4.2.2 End of SWM

The correlation analysis for the end of SWM showed a high positive correlation present between depth with EC, salinity, TDS and cadmium. Moderate correlation was observed between temperature and ORP, turbidity, nitrate, ammonia-nitrogen and lead. pH only had a moderate correlation with EC and salinity. EC showed very high correlation with salinity and TDS, and a moderate correlation with cadmium. A high correlation also existed between salinity and TDS, and a moderate correlation with cadmium, similar to EC. Turbidity observed a high correlation with nitrate and lead, and medium correlation with ammonia-nitrogen, magnesium and copper, indicating the presence of fertilisers, wastewater and coastal development activities (Singaraja et al., 2015). TDS had a high correlation with cadmium indicating the presence of anthropogenic activities (Yılmaz and Sadikoglu, 2011). A moderate correlation was observed between DO with phosphate and sodium. High positive correlation was obtained between nitrate with ammonia-nitrogen and a moderate correlation with copper indicating the use of fertilisers probably from river runoffs (Singaraja et al., 2015). A moderate degree correlation was observed between phosphate with cobalt and sodium. Ammonia-nitrogen and bicarbonate, both observed a moderate correlation

with copper. Calcium only had a moderate correlation with lead. Magnesium observed moderate correlation with cadmium, copper, iron, nickel, lead and zinc. A moderate correlation was observed between chloride with iron, manganese, nickel and zinc, again showing signs of anthropogenic activities. A moderate correlation was obtained between cadmium with iron. Similar to the beginning of SWM, a moderate correlation was observed between copper with lead. A high correlation was obtained between iron with manganese, nickel and zinc. Potassium had a moderate-to-high correlation with sodium. Manganese had a moderate correlation with nickel and a moderate-to-high correlation with zinc. Nickel obtained a very high correlation with zinc. Magnesium showed good correlation with chloride and sodium, and chloride had a good correlation with potassium. Cadmium had high correlation with cobalt, copper, nickel, lead and zinc. Similarly, cobalt and copper showed high correlation with nickel lead and zinc.

5.4.2.3 Transition to NEM

During transition to NEM, the correlation analysis for depth showed moderate correlation with ammonia-nitrogen, magnesium, chloride and sodium. Moderate correlation was also observed between pH with turbidity, sulphate, cadmium, cobalt, copper, nickel and lead. A high correlation was observed for EC with salinity and TDS, while a moderate correlation was obtained with ORP, nitrate, ammonia-nitrogen, magnesium, chloride and potassium. Salinity had a high correlation with TDS and moderate correlation with ORP, nitrate, ammonia-nitrogen, magnesium, chloride and potassium. ORP showed moderate correlation with TDS, DO, ammonia-nitrogen and iron. A moderate correlation was also observed between turbidity with bicarbonate and manganese. TDS showed moderate correlation with nitrate, ammonia-nitrogen, magnesium, chloride and potassium, and DO only had a moderate correlation with zinc. Nitrate observed a moderate correlation with bicarbonate, potassium and sodium. A moderate correlation was noted among phosphate with cadmium, cobalt, copper, nickel and lead; sulphate with manganese; ammonia-nitrogen with magnesium and sodium indicating anthropogenic activities such as river runoffs and waste disposal. The major ions, bicarbonate and calcium observed moderate correlation with iron and manganese, and with potassium respectively. A moderate degree correlation was noted between calcium and potassium, magnesium with chloride and sodium and chloride

with potassium. A high correlation was observed between cadmium and cobalt, copper, nickel, lead and zinc indicate anthropogenic activities in the form of sewage, coastal development and river runoff (Cuoco et al., 2015; Singaraja et al., 2015). A similar phenomenon was observed with cobalt and copper where a high correlation was observed with nickel, lead and zinc. Moderate correlation was observed between iron with manganese and sodium. Nickel and lead were also very strongly associated with zinc showing definite link to anthropogenic activities (Florence and Batley, 1976; Mackey et al., 1996; Abram et al., 2003; Yılmaz and Sadikoglu, 2011; Paraskevopoulou et al., 2014).

5.4.3 Sipadan Island Park

The correlation analysis for Sipadan seawater samples had high correlation of depth with pH, TDS and sulphate, and moderate correlation were observed with EC, salinity, turbidity, potassium and zinc. pH had high correlation with EC, salinity, TDS, and sulphate. A moderate correlation was observed with phosphate, chloride, copper and zinc. EC showed high correlation with salinity, phosphate, sulphate and chloride whereas medium correlation with TDS, bicarbonate, calcium, copper, manganese and zinc. A high correlation was shown between salinity and phosphate, sulphate and chloride. The high correlations with phosphate would indicate the presence of phytoplankton as well as the rise of bottom sediments from boat traffic (M. Lee et al., 2008). Salinity, sulphate and chloride would be the constituents for the normal composition of seawater (Rakestraw, 1943; Zhou et al., 2014). A moderate correlation was observed by salinity with TDS, calcium, copper, manganese and zinc. ORP presented a high correlation with magnesium and nickel which would indicate the presence of boat activities and tourism (Abdullah et al., 1997; Mokhtar et al., 2012), and moderate correlation with ammonia-nitrogen and iron. Turbidity only had a moderate correlation with sodium and lead. TDS observed a high correlation with sulphate, and a moderate correlation with potassium. DO showed a high correlation with bicarbonate, chloride and manganese, and moderate correlation with phosphate and calcium. Phosphate had a high correlation with chloride and manganese, and moderate correlation with sulphate, bicarbonate, calcium and zinc. The high correlation with manganese existing with DO and phosphate indicate anthropogenic activities from waste possibly from tourism in the island (Mokhtar et al., 2012; Zhou

et al., 2014). Sulphate only had a moderate correlation with potassium. Ammonia-nitrogen showed a high correlation with magnesium, and moderate correlation with iron and nickel. A high correlation was observed between bicarbonate and chloride, while maintaining a moderate correlation with calcium, cobalt, copper, manganese and zinc. Only a moderate correlation was observed between calcium and chloride. Chloride showed a high correlation with manganese and moderate correlation with copper and zinc. Cobalt had a moderate correlation with copper, and copper showed a high correlation with zinc. A very high correlation was observed between sodium and nickel while exhibiting a moderate correlation with lead. Potassium also had a moderate correlation with lead. Sodium displayed moderate correlation with nickel and lead. The high correlations observed with bicarbonate can be linked to the mixing of carbon dioxide with seawater, and the high correlations with sulphate and chloride are indicators of basic seawater composition (Rakestraw, 1943; Abdullah et al., 1997; Kura et al., 2015; Measurements, 2016a).

5.4.4 Factor Analysis

After correlation analysis, factor analysis is performed and from which factor scores are derived. Factor analysis, also known as factor loading, measures the closeness between the values (Singaraja et al., 2014). Factor analyses are done through a number of iterations which generates a rotated component matrix containing several factors. These iterations aid in simplifying the quantity of new variables required to reproduce certain parts of the data (Thivya et al., 2015). The first factor contains the highest data variance that help understand the nature of the seawater quality by pointing towards the elements that have more control on the seawater chemistry. The second factor loading has less variance than the first. The sequence continues with the other factors where the data variance decreases with each iteration (Prasanna et al., 2010; Vasanthavigar et al., 2013; Singaraja et al., 2014; Thivya et al., 2015).

Consequently, factor score coefficients are a result of factor loadings which are then computed using a matrix multiplication of the factor score coefficient from the standardised data (Thivya et al., 2015). Factor scores have positive and negative values. The positive factor scores, meaning, parameters that have an influence on the

quality of the seawater. Factor scores can be used to show the spatial and temporal variation of the parameters at each site as noted in Figures 1 to 6

5.4.5 Miri-Sibuti Coral Reef National Park

5.4.5.1 Start of SWM

At the beginning of SWM, seven factors were extracted with 100% of total data variability. The factor scores for these loadings are shown in Figure 5.4.1 and 5.4.2. The first factor contained depth, EC, salinity, ORP, TDS, calcium, magnesium and manganese. These strong salinity factor indicate normal seawater chemistry as well as the presence of phytoplankton (Abram et al., 2003; Vasanthavigar et al., 2013; Lenntech, 2017b). The high factor score was observed at the seabed of North Siwa which had the largest number of hard corals out of all the sites. Factor 2 was turbidity factor represented by turbidity, chloride, iron, nickel and zinc with total variance of 17.88%. The presence of iron accounts for algal growth as well as river runoffs (Mackey et al., 1996; Lenntech, 2017e). Nickel and zinc are both attributed to anthropogenic activities such as coastal development and industrial influence (Rakestraw, 1943; Paraskevopoulou et al., 2014). The high factor score was at the surface of Eve's Garden, closest to the Miri river mouth, which is influenced by river runoff. The third factor was also a salinity factor indicated by pH, salinity, sulphate, magnesium, potassium and sodium which is part of the chemistry of seawater (Singaraja et al., 2014). Factor 4 was the river discharge factor, which included ammonia-nitrogen and cadmium which indicates the presence of industrial discharge and boat traffic (Yılmaz and Sadikoglu, 2011; Readman et al., 2013). The high factor score was observed at the middle layer of Anemone Garden because ships pulling barges coming from oil rigs occasionally go close to that site. The fifth factor was the major ions factor represented by ORP, bicarbonate, manganese and sodium. Figure 5.4.2 indicate the high factor score at the surface of Anemone Garden indicating the presence of marine organisms such as phytoplankton (Sunda, 2012; Lenntech, 2017h). Factor 6 and 7 were both anthropogenic factors containing lead and copper respectively which were both indications of anthropogenic activities (Florence and Batley, 1976). The high factor scores for these two factor loadings were observed at the middle depth and surface of North Siwa respectively.

e

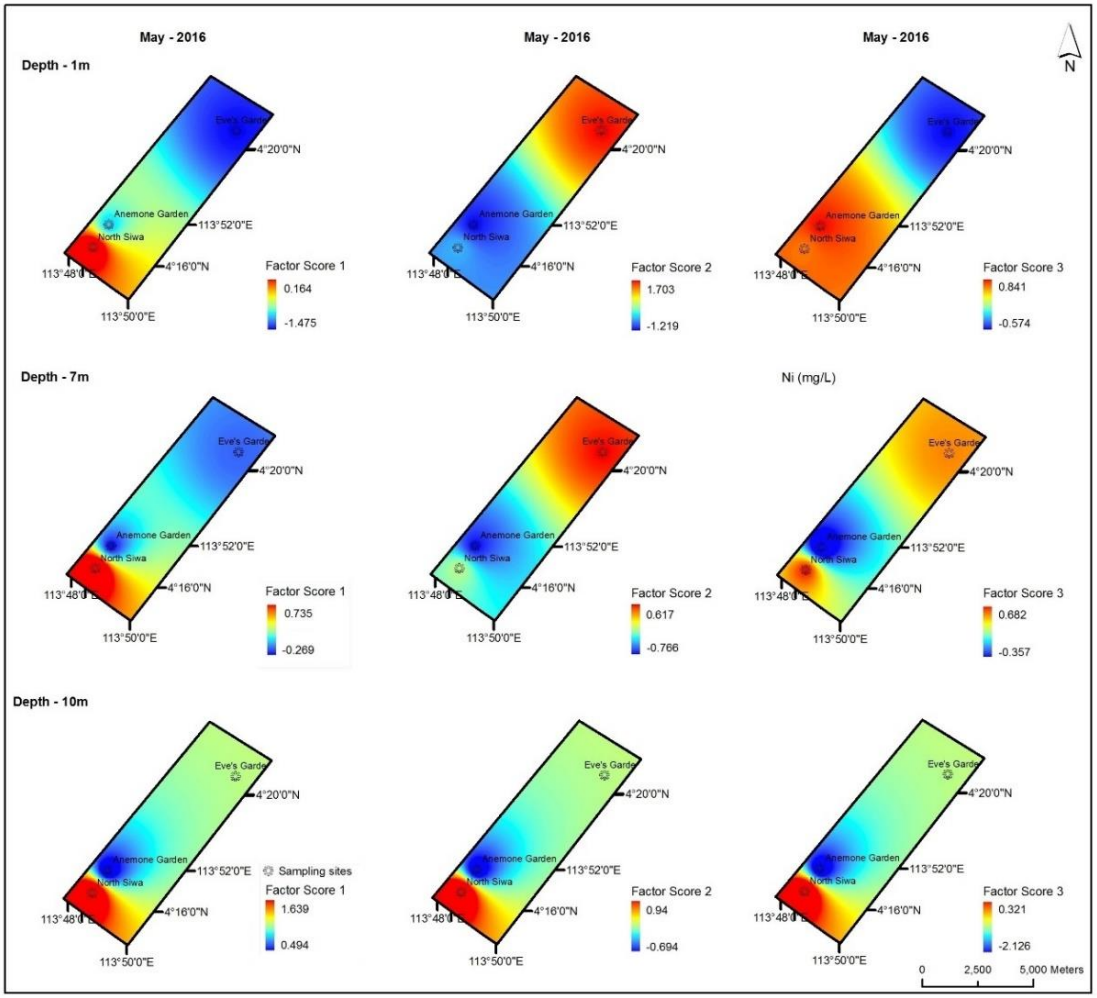

Figure 5.4.9 – Spatial Distribution of Factors 1 to 3 (Start of SWM)

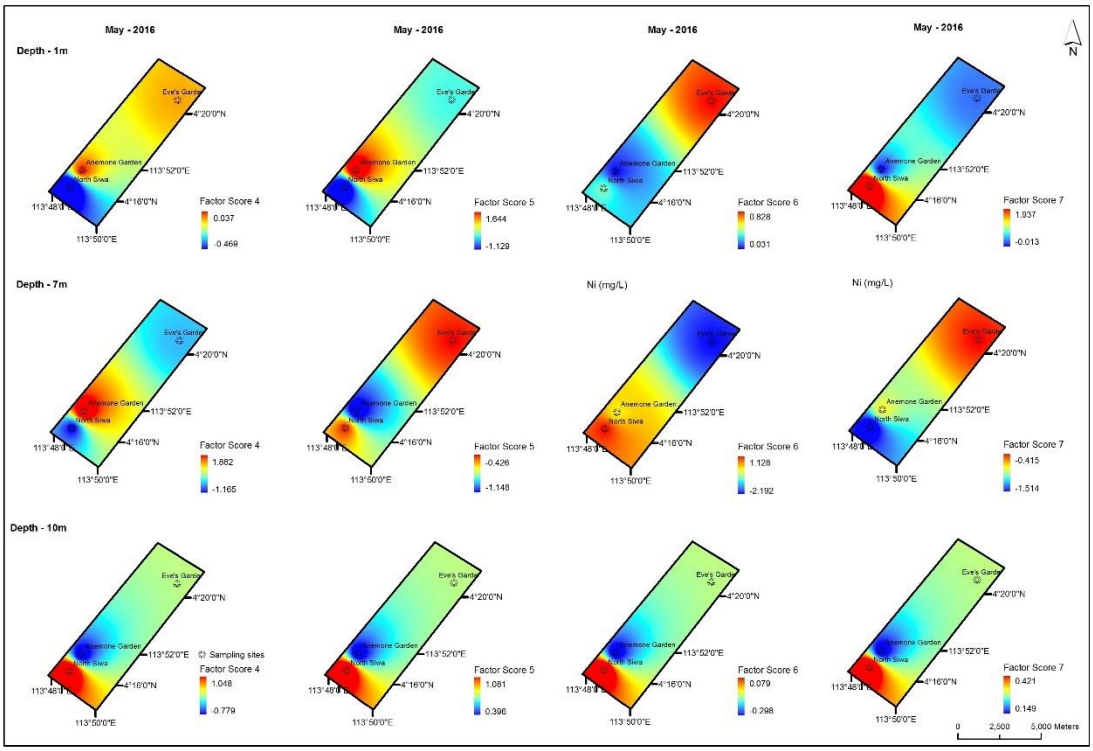

Figure 5.4.10 – Spatial Distribution of Factors 4 to 7 (Start of SWM)

5.4.5.2 End of SWM

Six factors were extracted at the end of SWM with a total data variability of 97.89%. The factor scores are shown in Figures 5.4.3 and 5.4.4. Factor 1 was the river runoff factor contained ORP, chloride, iron, manganese, nickel and zinc. From Figure 5.4.3, the high factor score was noted at the surface of North Siwa. The presence of these trace metals was due to anthropogenic sources linking to boat traffic and weathering effects originating from the decommissioned oil platform located at some distance to the site (Mackey et al., 1996; Zaidi, 2006; Lenntech, 2017e). Factor 2 was the salinity factor, limited to depth, EC, salinity, TDS and cadmium. Based on the high factor score at the seabed of North Siwa, the presence of cadmium at the site could also be industrial discharge being carried by ocean currents. The third factor was turbidity factor represented by temperature, turbidity, nitrate, ammonia-nitrogen and copper. The high factor score at the surface of Eve's Garden and the presence of nitrate and ammonia-nitrogen, along with high turbidity showed the influence of the Miri river input and coastal development. These nutrients promote algal growth, thus suffocating the corals and eventually causing them to bleach (Ilter. et al., 2012; Lamb et al., 2014; Cuoco et al., 2015; Naumann et al., 2015). The presence of copper is associated with coastal

development and industrial activities (Balls, 1985; APHA, 2012). Eve's Garden has already shown strong signs of coral bleaching and algal growth as an evidence (Figures 5.6.22 – 5.6.27). Factor 4 was coastal development factor, which included turbidity, calcium, magnesium, and copper. A high factor was observed at the surface of Eve's Garden. Copper would be linked to coastal development and industrial activities (Rakestraw, 1943; Balls, 1985; APHA, 2012; Mokhtar et al., 2012). Factor 5 had turbidity, sulphate and nickel. The high factor score was attributed to the seabed of North Siwa. Turbidity was shown in factors 3 and 4, and was recorded at Eve's Garden clearly indicating river input. Finally, factor 6 had potassium, sodium and lead. Potassium and sodium form the basic composition of seawater whereas lead was due to influence of the Miri river input.

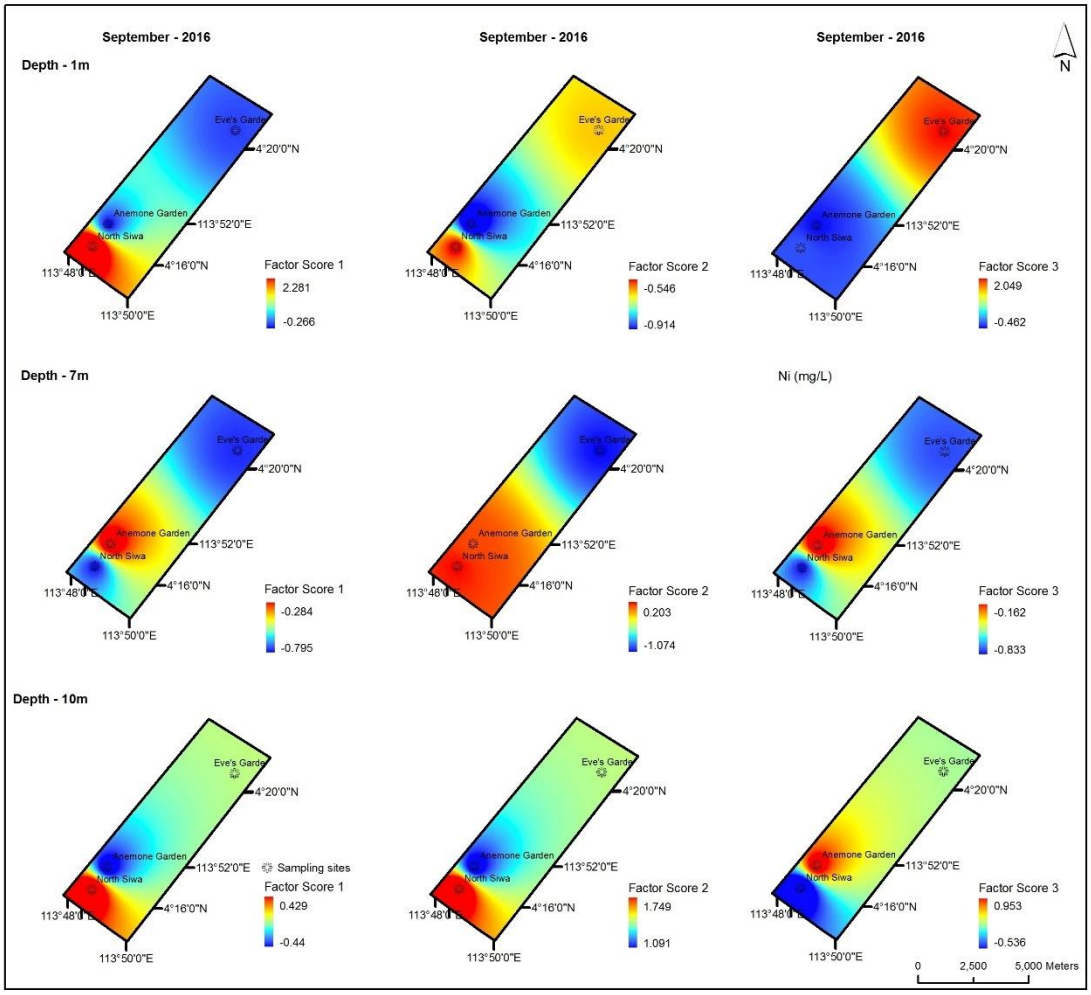

Figure 5.4.11 – Spatial Distribution of Factors 1 to 3 (End of SWM)

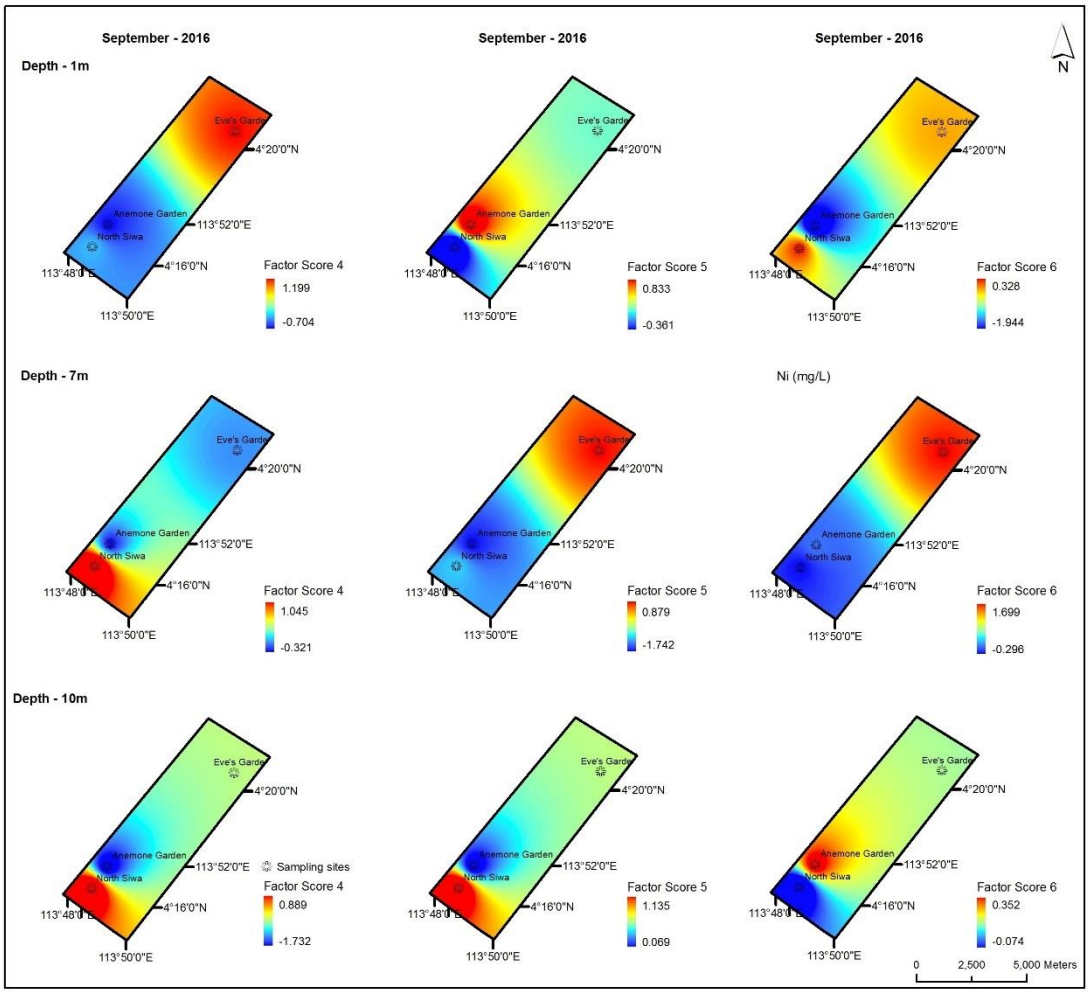

Figure 5.4.12 – Spatial Distribution of Factors 4 to 6 (End of SWM)

5.4.5.3 Transition to NEM

The period of transition to NEM had a total data variability of 95.62% extracted from five factors. The factor scores for the five factor loadings are shown in Figures 5.4.5 and 5.4.6. Factor 1 contained pH, phosphate, cadmium, cobalt, copper, nickel, lead and zinc, which were the anthropogenic factors. The presence of six trace metals and phosphate strongly relate to anthropogenic activities such as river runoffs, industrial discharge, coastal development and sewage disposal and (Mackey et al., 1996; Abram et al., 2003; Yılmaz and Sadikoglu, 2011). The high factor score (Figure 5.4.5) was recorded at the seabed of North Siwa. The second factor was the salinity factor contained EC, salinity, TDS, nitrate, magnesium, chloride and potassium relating mostly to the chemistry of the seawater with a high factor score at the surface of North Siwa. Factor 3 was represented by pH, nitrate and bicarbonate. The high factor score was recorded at the seabed of North Siwa. The presence of nitrate is attributed to river

runoffs and is also a key factor of coral bleaching (Fabricius, 2005; Higuchi et al., 2015). Factor 4 included calcium and zinc and the high factor score was recorded at the surface of North Siwa which could be coming from the boats patrolling the area (Lenntech, 2017l). Factor 5 consisted of only ammonia-nitrogen which is a key nutrient that contributes to coral bleaching (Wagner et al., 2010). The high factor score was at Eve's Garden and Anemone Garden where most of the bleached corals were found as shown in Figures 5.6.16 – 5.6.27.

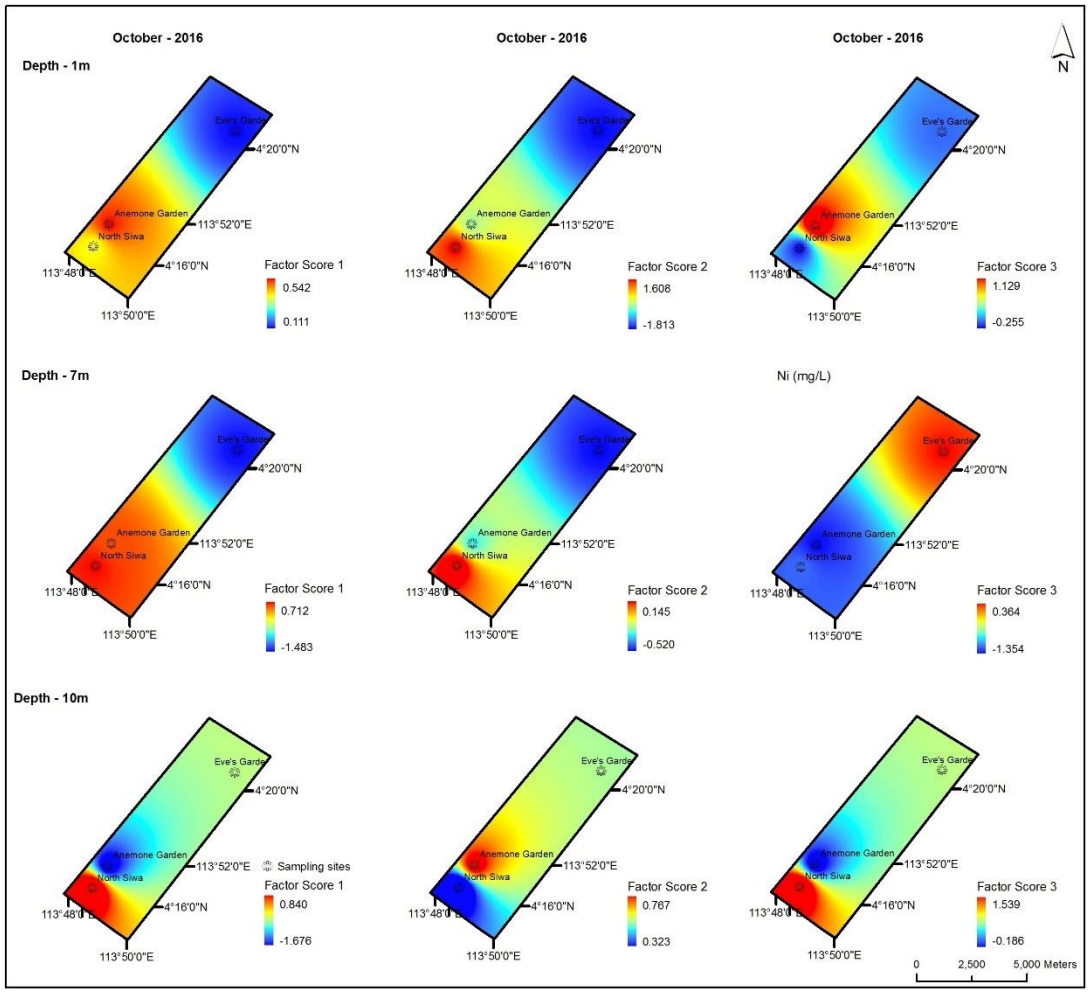

Figure 5.4.13 – Spatial Distribution of Factors 1 to 3 (NEM Transition)

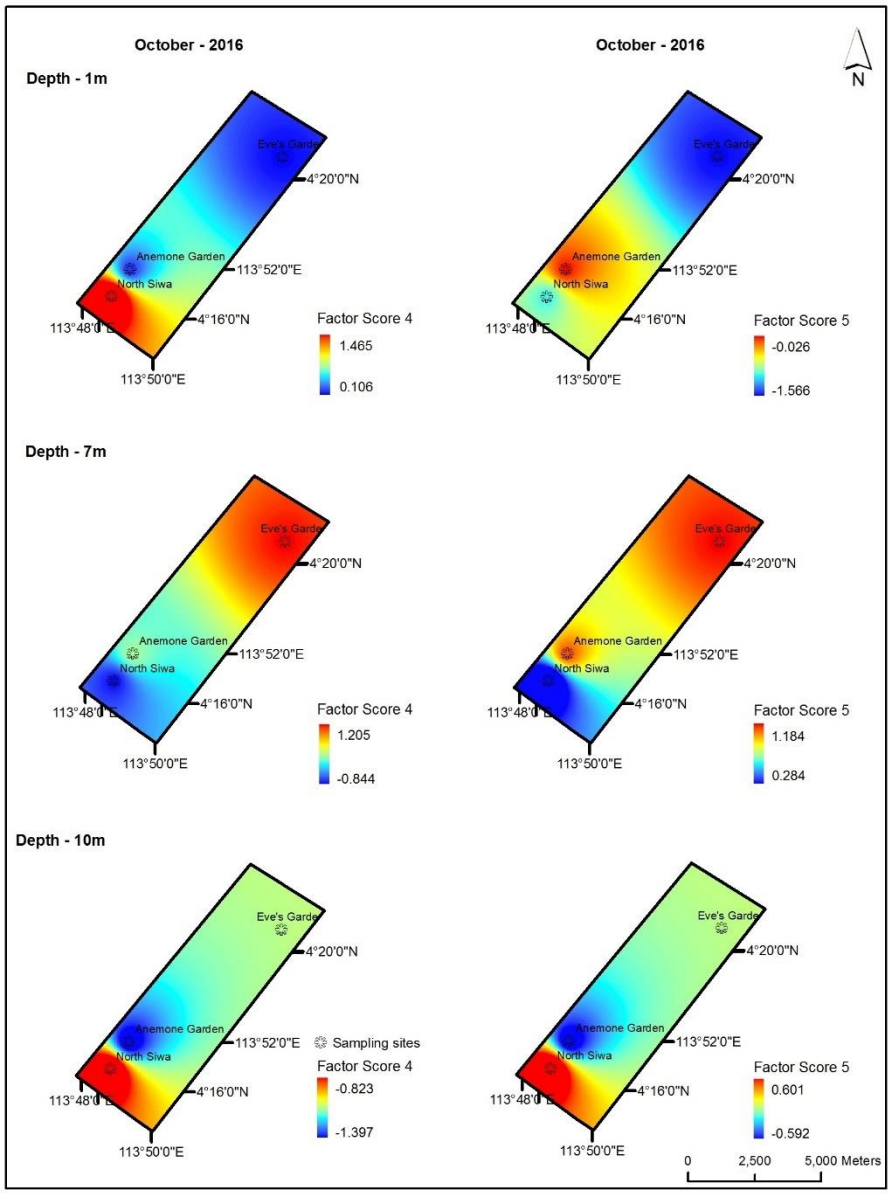

Figure 5.4.14 – Spatial Distribution of Factors 4 and 5 (NEM Transition)

5.4.6 Sipadan Island Park

A total of four factors were extracted from Sipadan Island Park with a total data variability of 100%. Factor 1 consisted of depth, pH, EC, salinity, TDS, phosphate, sulphate and chloride. While sulphate and chloride are part of seawater chemistry, the presence of phosphate originated from bottom sediments released by boat traffic in and out of the beach (M. Lee et al., 2008). Factor 2 was represented by EC, salinity, DO, phosphate, bicarbonate, calcium, chloride, copper and manganese. The presence of copper was due to sediments releasing copper and manganese is naturally found in seawater as a nutrient for phytoplankton (Sunda, 2012; Balch, 2015; Chan, 2016;

Hutchins and Boyd, 2016; Vanar, 2016; Lenntech, 2017h). Factor 3 contained depth, pH, turbidity, copper and zinc. The occurrence of zinc was due to bioaccumulation from corals which were released in the seawater after breaking (Mokhtar et al., 2012). Factor 4, with a data variance of 19.12%, was limited to turbidity, iron, sodium and nickel. Similar to manganese, the presence of iron was also attributed to natural occurrences while nickel was due to the presence of fishing and recreational boats and weathering effects (Mokhtar et al., 2012; Hutchins and Boyd, 2016).

Table 5.4.1 – Correlation Matrix for Start of SWM													
Correlation		**Depth**	**Temperature**	**pH**	**EC**	**Salinity**	**ORP**	**Turbidity**	**TDS**	**DO**	**NO_3^-**	**PO_4^{3-}**	**SO_4^{2-}**	**NH_3-N**
	Depth	1.000												
	Temp	-.529	1.000											
	pH	-.126	-.423	1.000										
	EC	**.766**	-.635	-.081	1.000									
	Salinity	.291	-.606	**.500**	**.526**	1.000								
	ORP	**.781**	-.704	-.136	**.619**	.340	1.000							
	Turbidity	.088	.309	.292	-.304	-.335	-.407	1.000						
	TDS	**.773**	-.632	-.039	**.995**	**.550**	**.584**	-.238	1.000					
	DO	.380	-.085	-.398	.410	.428	.248	-.218	.439	1.000				
	NO_3^-	-.574	.319	-.088	-.462	-.491	-.477	.078	-.449	-.204	1.000			
	PO_4^{3-}	-.132	.222	-.078	.190	-.083	-.362	.080	.218	.052	**.617**	1.000		
	SO_4^{2-}	-.536	**.516**	.025	-.178	-.114	-.800	.145	-.167	-.141	.026	.249	1.000	
	NH_3-N	.113	.300	-.262	-.221	-.058	-.049	.241	-.210	.379	-.543	-.673	.152	1.000
	HCO_3^-	.101	-.031	.241	-.253	-.037	**.**355	.037	-.278	-.463	-.091	-.244	-.571	-.190
	Ca^{2+}	**.581**	-.974	.322	**.649**	**.580**	**.767**	-.331	**.649**	.186	-.218	-.124	-.649	-.358
	Mg^{2+}	.366	-.940	**.575**	**.505**	**.557**	.445	-.108	**.525**	.034	-.143	-.109	-.352	-.326
	Cl^-	.088	-.063	.420	-.244	-.346	-.226	**.841**	-.197	-.413	.079	-.148	.018	.135
	Cd	-.336	.253	.144	-.310	.180	-.081	-.297	-.353	-.300	-.447	-.460	.242	.260
	Co	.426	.016	-.710	.308	-.512	.428	-.168	.247	-.051	-.242	-.207	-.136	.172
	Cu	-.020	-.665	**.603**	.255	.512	.348	-.471	.220	-.447	-.235	-.189	-.160	-.500
	Fe	.361	-.257	.323	-.084	-.209	.330	.445	-.094	-.558	-.409	-.592	-.333	.200
	K	.048	-.147	**.466**	-.148	.182	-.122	**.508**	-.070	.173	.427	.320	-.341	-.218
	Mn	**.715**	-.721	.082	**.638**	.372	**.807**	-.198	**.639**	.221	-.064	.150	-.813	-.472
	Na	-.014	-.151	.290	-.232	.402	.320	-.199	-.227	.110	.007	-.199	-.623	-.088
	Ni	-.056	.062	**.539**	-.420	-.344	-.285	**.821**	-.385	-.639	.018	-.228	.053	.111
	Zn	-.235	**.672**	-.063	-.639	-.695	-.545	**.787**	-.617	-.373	.091	-.168	.325	.479

Table 5.4.1 – Correlation Matrix for Start of SWM (cont.)														
Correlation		HCO_3^-	Ca^{2+}	Mg^{2+}	Cl^-	Cd	Co	Cu	Fe	K	Mn	Na	Ni	Zn
	HCO_3^-	1.000												
	Ca^{2+}	.081	1.000											
	Mg^{2+}	-.135	**.895**	1.000										
	Cl^-	-.022	-.012	.274	1.000									
	Cd	**.449**	-.350	-.398	-.393	1.000								
	Co	-.049	-.012	-.203	-.032	-.108	1.000							
	Cu	.351	**.573**	**.584**	-.160	.382	-.186	1.000						
	Fe	**.526**	.173	.209	**.656**	.137	.305	.239	1.000					
	K	.081	.245	.339	.412	-.541	-.662	-.182	-.058	1.000				
	Mn	.319	**.843**	**.585**	-.094	-.440	.096	.310	.130	.353	1.000			
	Na	**.699**	.252	.042	-.313	.327	-.506	.263	.005	.411	.372	1.000		
	Ni	.270	-.156	.109	**.922**	-.052	-.121	-.005	**.760**	.313	-.204	-.130	1.000	
	Zn	.070	-.724	-.540	**.648**	.059	.122	-.570	.437	.033	-.613	-.297	**.722**	1.000

Table 5.4.2 – Correlation Matrix for the End of SWM													
Correlation		**Depth**	**Temperature**	**pH**	**EC**	**Salinity**	**ORP**	**Turbidity**	**TDS**	**DO**	**NO_3^-**	**PO_4^{3-}**	**SO_4^{2-}**	**NH_3-N**
	Depth	1.000												
	Temp	-.642	1.000											
	pH	.425	-.565	1.000										
	EC	**.880**	-.712	**.616**	1.000									
	Salinity	**.855**	-.716	**.521**	**.987**	1.000								
	ORP	-.426	**.580**	-.998	-.632	-.543	1.000							
	Turbidity	-.061	**.466**	-.020	-.211	-.255	.067	1.000						
	TDS	**.871**	-.562	.161	**.868**	**.910**	-.185	-.293	1.000					
	DO	-.058	-.421	.336	.167	.114	-.341	-.552	-.059	1.000				
	NO_3^-	-.304	**.573**	.050	-.158	-.188	-.026	**.762**	-.323	-.253	1.000			
	PO_4^{3-}	-.354	.267	.435	-.112	-.219	-.429	-.042	-.446	**.526**	.326	1.000		
	SO_4^{2-}	.234	.003	.229	.098	.093	-.229	.322	.067	-.690	.105	-.337	1.000	
	NH_3-N	-.181	**.514**	.074	.037	.015	-.062	**.581**	-.103	-.132	**.939**	.408	-.070	1.000
	HCO_3^-	-.463	.113	.280	-.453	-.502	-.276	.001	-.669	-.002	-.122	.416	.164	-.273
	Ca^{2+}	-.471	.185	-.015	-.625	-.702	.053	.238	-.772	.199	.066	.205	.079	-.208
	Mg^{2+}	.001	.021	-.213	-.284	-.271	.253	**.668**	-.227	-.464	.169	-.577	.312	-.107
	PO_4^{3-}	-.233	-.102	-.665	-.353	-.223	**.643**	-.350	.002	-.184	-.500	-.729	-.006	-.585
	Cd	**.779**	-.423	-.030	**.580**	**.624**	.038	.241	**.749**	-.388	-.129	-.747	.194	-.093
	Co	-.115	-.063	.353	.022	-.008	-.385	-.553	-.102	.181	-.400	**.503**	.056	-.297
	Cu	-.451	.302	-.091	-.370	-.337	.113	**.695**	-.476	-.335	**.713**	-.122	.205	**.496**
	Fe	.324	.004	-.651	-.042	.037	**.655**	.059	.397	-.539	-.368	-.878	.186	-.407
	K	.383	.028	-.079	.172	.087	.111	.102	.225	.302	-.015	.103	-.323	.061
	Mn	-.098	.180	-.749	-.439	-.385	**.748**	-.254	-.019	-.210	-.610	-.467	-.169	-.631
	Na	-.247	.389	-.187	-.258	-.340	.207	-.064	-.270	**.529**	.162	**.564**	-.543	.241
	Ni	.003	.241	-.620	-.321	-.232	**.621**	.258	.055	-.828	-.181	-.785	.433	-.317
	Zn	-.122	.375	-.868	-.412	-.305	**.868**	.176	.054	-.676	-.120	-.758	.159	-.201

Table 5.4.2 – Correlation Matrix for End of SWM (cont.)														
Correlation		**HCO_3^-**	**Ca^{2+}**	**Mg^{2+}**	**Cl^-**	**Cd**	**Co**	**Cu**	**Fe**	**K**	**Mn**	**Na**	**Ni**	**Zn**
	HCO_3^-	1.000												
	Ca^{2+}	.436	1.000											
	Mg^{2+}	.028	.431	1.000										
	Cl^-	-.097	.044	.313	1.000									
	Cd	-.584	-.468	**.457**	.153	1.000								
	Co	**.649**	-.137	-.675	-.197	-.546	1.000							
	Cu	.089	.294	**.630**	.078	-.009	-.540	1.000						
	Fe	-.449	-.167	**.472**	**.634**	**.674**	-.453	-.129	1.000					
	K	-.520	.163	-.016	-.327	.221	-.380	-.404	.217	1.000				
	Mn	.002	.082	.183	**.658**	.125	-.003	-.380	**.744**	.176	1.000			
	Na	-.211	.351	-.351	-.337	-.450	-.077	-.287	-.226	**.739**	.080	1.000		
	Ni	-.008	-.084	**.581**	**.633**	.447	-.239	.178	**.827**	-.251	**.651**	-.515	1.000	
	Zn	-.263	-.101	**.473**	**.718**	.383	-.405	.156	**.875**	-.066	**.738**	-.232	**.914**	1.000

Table 5.4.3 – Correlation Matrix for NEM Transition												
Correlation		**Depth**	**pH**	**EC**	**Salinity**	**ORP**	**Turbidity**	**TDS**	**DO**	**NO_3^-**	**PO_4^{3-}**	**SO_4^{2-}**	**NH_3-N**
	Depth	1.000											
	pH	-.045	1.000										
	EC	.324	-.681	1.000									
	Salinity	.314	-.682	**.998**	1.000								
	ORP	.050	-.999	**.675**	**.677**	1.000							
	Turbidity	-.459	**.473**	-.850	-.865	-.481	1.000						
	TDS	.285	-.672	**.990**	**.980**	**.664**	-.794	1.000					
	DO	-.338	-.545	.291	.295	**.542**	-.369	.282	1.000				
	NO_3^-	.211	-.018	**.452**	**.453**	.029	-.263	**.455**	-.584	1.000			
	PO_4^{3-}	-.677	.245	-.240	-.238	-.251	.128	-.188	.411	-.358	1.000		
	SO_4^{2-}	-.296	**.454**	-.706	-.668	-.438	.380	-.746	-.122	-.355	.443	1.000	
	NH_3-N	**.508**	-.640	**.620**	**.594**	**.619**	-.299	**.638**	.024	.176	-.671	-.795	1.000
	HCO_3^-	-.093	.400	-.404	-.394	-.397	**.588**	-.397	-.862	**.527**	-.309	.232	-.127
	Ca^{2+}	-.296	-.161	.183	.160	.181	-.055	.210	.231	.310	.008	-.443	-.040
	Mg^{2+}	**.683**	-.110	**.571**	**.551**	.087	-.512	**.593**	-.167	.207	-.229	-.459	**.580**
	PO_4^{3-}	**.511**	-.116	**.735**	**.718**	.108	-.787	**.734**	.179	.269	-.096	-.637	.369
	Cd	-.344	**.569**	-.360	-.380	-.576	.174	-.314	.307	-.453	**.696**	.148	-.546
	Co	-.285	**.554**	-.242	-.259	-.559	.026	-.206	.305	-.346	**.688**	.111	-.554
	Cu	-.337	**.485**	-.229	-.247	-.492	.032	-.189	.389	-.415	**.732**	.108	-.530
	Fe	.014	-.450	.036	.062	**.463**	.148	-.006	-.293	.327	-.538	.100	.276
	K	.139	-.189	**.722**	**.728**	.204	-.748	**.699**	.110	**.658**	-.032	-.462	.049
	Mn	-.133	.286	-.725	-.697	-.274	**.671**	-.765	-.479	-.121	-.217	**.669**	-.305
	Na	**.630**	-.302	.379	.377	.306	-.266	.378	-.520	**.542**	-.514	-.135	**.490**
	Ni	-.311	**.535**	-.286	-.305	-.543	.099	-.246	.340	-.430	**.661**	.081	-.503
	Pb	-.306	**.568**	-.305	-.323	-.576	.098	-.264	.305	-.421	**.706**	.149	-.551
	Zn	-.478	.252	-.214	-.230	-.259	.173	-.192	**.498**	-.422	.390	-.161	-.285

Table 5.4.3 – Correlation Matrix for NEM Transition (cont.)															
Correlation		**HCO_3^-**	**Ca^{2+}**	**Mg^{2+}**	**Cl^-**	**Cd**	**Co**	**Cu**	**Fe**	**K**	**Mn**	**Na**	**Ni**	**Pb**	**Zn**
	HCO_3^-	1.000													
	Ca^{2+}	-.098	1.000												
	Mg^{2+}	-.229	-.454	1.000											
	Cl^-	-.537	.124	**.724**	1.000										
	Cd	-.402	.181	-.122	.197	1.000									
	Co	-.437	.214	-.061	.320	**.984**	1.000								
	Cu	-.492	.202	-.072	.295	**.987**	**.994**	1.000							
	Fe	**.556**	-.078	-.275	-.562	-.909	-.936	-.930	1.000						
	K	-.220	**.540**	.200	**.700**	-.014	.147	.105	-.177	1.000					
	Mn	**.691**	-.351	-.518	-.876	-.360	-.452	-.468	**.626**	-.663	1.000				
	Na	.325	-.351	**.547**	.099	-.763	-.719	-.745	**.536**	.076	.119	1.000			
	Ni	-.447	.210	-.088	.274	**.995**	**.990**	**.992**	-.930	.056	-.425	-.774	1.000		
	Pb	-.426	.148	-.064	.260	**.995**	**.994**	**.994**	-.932	.043	-.402	-.731	**.995**	1.000	
	Zn	-.394	.511	-.382	.126	**.787**	**.756**	**.773**	-.643	.067	-.341	-.943	**.814**	**.754**	1.000

Table 5.4.4 – Correlation Matrix for Sipadan Island Park												
Correlation		**Depth**	**pH**	**EC**	**Salinity**	**ORP**	**Turbidity**	**TDS**	**DO**	**PO_4^{3-}**	**SO_4^{2-}**	**NH_3-N**
	Depth	1.000										
	pH	**.916**	1.000									
	EC	**.647**	**.877**	1.000								
	Salinity	**.709**	**.905**	**.993**	1.000							
	ORP	-.925	-.996	-.855	-.880	1.000						
	Turbidity	**.506**	.422	.064	.127	-.399	1.000					
	TDS	**.861**	**.769**	.656	**.709**	-.783	.028	1.000				
	DO	-.413	-.044	.419	.328	.069	-.594	-.214	1.000			
	PO_4^{3-}	.296	**.592**	**.904**	**.869**	-.564	-.315	.472	.728	1.000		
	SO_4^{2-}	**.897**	**.869**	**.782**	**.840**	-.860	.182	**.959**	-.138	**.576**	1.000	
	NH_3-N	-.675	-.684	-.360	-.366	**.715**	-.700	-.271	.348	.017	-.320	1.000
	HCO_3^-	-.218	.159	**.480**	.374	-.163	-.366	-.193	.874	**.647**	-.133	-.109
	Ca^{2+}	-.070	.287	**.540**	**.500**	-.224	.201	-.244	.656	**.588**	.009	-.106
	Mg^{2+}	-.775	-.765	-.433	-.471	**.767**	-.862	-.348	.424	-.023	-.466	**.934**
	Cl^-	.235	.576	**.870**	**.808**	-.564	-.288	.333	**.781**	**.950**	.425	-.154
	Co	-.210	-.133	-.045	-.136	.057	-.588	-.051	.325	.084	-.246	-.099
	Cu	.345	**.587**	**.578**	**.511**	-.617	.160	.130	.339	.440	.175	-.742
	Fe	-.541	-.670	-.688	-.643	**.719**	.214	-.614	-.272	-.603	-.542	**.496**
	K	**.653**	.304	-.100	-.018	-.348	.316	**.627**	-.862	-.387	**.488**	-.354
	Mn	-.083	.155	**.559**	**.498**	-.152	-.785	.310	**.808**	**.834**	.283	.400
	Na	-.123	-.212	-.378	-.316	.269	**.707**	-.448	-.420	-.510	-.279	-.022
	Ni	-.752	-.711	-.574	-.576	**.766**	.074	-.834	.121	-.392	-.719	**.513**
	Zn	**.483**	**.705**	**.655**	**.604**	-.730	.274	.239	.254	**.463**	.305	-.809

Table 5.4.4 – Correlation Matrix for Sipadan Island Park (cont.)

Correlation		HCO_3^-	Ca^{2+}	Mg^{2+}	Cl^-	Co	Cu	Fe	K	Mn	Na	Ni	Zn
	HCO_3^-	1.000											
	Ca^{2+}	**.635**	1.000										
	Mg^{2+}	.069	-.216	1.000									
	Cl^-	**.829**	**.630**	-.103	1.000								
	Co	**.551**	-.286	.255	.294	1.000							
	Cu	**.737**	.414	-.557	**.674**	**.509**	1.000						
	Fe	-.539	-.006	.310	-.714	-.633	-.771	1.000					
	K	-.734	-.772	-.378	-.468	-.075	-.188	-.160	1.000				
	Mn	**.633**	.250	.474	**.789**	.413	.207	-.539	-.415	1.000			
	Na	-.499	.238	-.261	-.575	-.813	-.419	**.829**	-.049	-.761	1.000		
	Ni	-.118	.316	.391	-.423	-.453	-.519	**.900**	-.563	-.325	**.724**	1.000	
	Zn	**.652**	.425	-.670	**.668**	.388	**.986**	-.773	-.098	.156	-.357	-.566	1.000

Table 5.4.5 – Rotated Component Matrix for Start of SWM							
	Component						
	1	2	3	4	5	6	7
Depth	**.858**	.172	-.244	.205	.219	-.141	-.253
Temp	-.817	-.003	-.291	.026	-.061	-.461	-.179
pH	.109	.387	**.815**	.077	.031	.052	.407
EC	**.921**	-.255	-.104	.100	-.199	-.163	.022
Salinity	**.516**	-.365	**.699**	.333	.020	-.012	-.026
ORP	**.747**	-.146	-.236	.178	**.484**	.313	-.034
Turbidity	-.144	**.869**	.102	-.074	-.034	-.404	-.208
TDS	**.927**	-.215	-.045	.078	-.211	-.202	-.021
DO	.315	-.457	.100	.022	-.059	-.108	-.816
NO_3^-	-.423	-.054	.011	-.898	.021	-.042	.099
PO_4^{3-}	.050	-.236	.031	-.650	-.195	-.670	.177
SO_4^{2-}	-.449	-.042	.074	.197	-.799	-.308	.136
NH_3-N	-.240	.209	-.112	**.619**	-.101	.156	-.685
HCO_3^-	-.080	.158	-.014	.196	**.880**	-.040	.393
Ca^{2+}	**.841**	-.068	.250	-.149	.193	.397	.095
Mg^{2+}	**.713**	.157	**.457**	-.187	-.114	.435	.147
Cl^-	.012	**.969**	.082	-.160	-.147	.076	-.025
Cd	-.436	-.247	.096	**.760**	.194	.044	.351
Co	.236	.041	-.944	.135	-.081	.161	.003
Cu	.319	-.161	.353	.194	.099	.362	**.755**
Fe	.169	**.779**	-.178	.350	.294	.254	.245
K	.097	.334	.602	-.551	.297	-.191	-.298
Mn	**.812**	-.082	.016	-.290	**.496**	.016	.045
Na	-.072	-.230	**.456**	.057	**.850**	.079	-.047
Ni	-.176	**.955**	.130	.029	.029	.012	.194
Zn	-.581	**.717**	-.254	.116	-.067	-.193	-.166
Total	7.151	4.827	3.424	3.162	3.126	2.675	2.636
% of Variance	26.484	17.877	12.681	11.710	11.578	9.907	9.763
Cumulative %	26.484	44.361	57.042	68.752	80.330	90.237	100.000

Table 5.4.6 – Rotated Component Matrix for End of SWM						
	Component					
	1	2	3	4	5	6
Depth	-.195	**.882**	-.247	.059	.248	.235
Temp	.410	-.572	**.621**	-.149	.189	.247
pH	-.955	.223	-.095	-.030	.151	-.077
EC	-.425	**.895**	-.067	-.117	.001	-.008
Salinity	-.313	**.931**	-.065	-.128	-.030	-.117
ORP	**.946**	-.239	.104	.073	-.139	.110
Turbidity	-.021	-.120	**.607**	**.590**	**.452**	.142
TDS	.075	**.973**	-.118	-.178	.013	.028
DO	-.477	-.074	-.292	-.114	-.795	.192
NO_3^-	-.182	-.160	**.932**	.258	.065	.011
PO_4^{3-}	-.631	-.454	.283	-.423	-.213	.282
SO_4^{2-}	-.088	.079	-.012	.152	**.832**	-.207
NH_3-N	-.184	.030	**.978**	.014	-.072	.061
HCO_3^-	-.345	-.712	-.282	-.168	.350	-.259
Ca^{2+}	-.173	-.731	-.244	**.515**	-.007	.259
Mg^{2+}	.241	-.089	-.046	**.890**	.318	-.100
Cl^-	**.724**	-.068	-.445	.169	-.167	-.433
Cd	.258	**.820**	-.063	.401	.229	-.002
Co	-.330	-.263	-.325	-.809	.200	-.136
Cu	-.002	-.295	**.539**	**.638**	.049	-.462
Fe	**.812**	.353	-.267	.260	.248	.123
K	.025	.236	-.017	.180	-.213	**.931**
Mn	**.795**	-.157	-.503	-.079	.058	.229
Na	-.028	-.299	.170	-.124	-.479	**.788**
Ni	**.766**	.021	-.131	.206	**.550**	-.212
Zn	**.951**	.013	-.008	.183	.235	-.082
Total	6.752	6.349	4.012	3.724	2.880	2.714
% of Variance	25.006	23.516	14.859	13.791	10.667	10.052
Cumulative %	25.006	48.522	63.381	77.172	87.839	97.891

Table 5.4.7 – Rotated Component Matrix for NEM Transition					
	Component				
	1	**2**	**3**	**4**	**5**
Depth	-.174	.255	.200	-.684	.436
pH	**.564**	-.430	**.660**	-.139	-.175
EC	-.231	**.918**	-.201	-.066	.211
Salinity	-.254	**.917**	-.203	-.067	.169
ORP	-.574	.433	-.650	.153	.158
Turbidity	.041	-.878	.218	.243	.044
TDS	-.193	**.912**	-.194	-.052	.238
DO	.270	.235	-.890	.246	-.094
NO_3^-	-.383	**.549**	**.715**	.167	.039
PO_4^{3-}	**.571**	-.021	-.230	.138	-.675
SO_4^{2-}	.008	-.571	.052	-.149	-.783
NH_3-N	-.420	.310	-.235	-.222	**.765**
HCO_3^-	-.446	-.401	**.748**	.132	-.036
Ca^{2+}	.159	.311	.085	**.842**	.222
Mg^{2+}	.045	**.495**	.060	-.766	.315
Cl^-	.381	**.811**	.026	-.299	.307
Cd	**.975**	-.117	-.047	.099	-.128
Co	**.980**	.034	.003	.085	-.172
Cu	**.972**	.023	-.097	.096	-.180
Fe	-.966	-.178	.045	.168	-.026
K	.086	**.905**	.244	.262	-.054
Mn	-.471	-.804	.229	.009	-.223
Na	-.701	.267	.273	-.514	.061
Ni	**.987**	-.048	-.060	.106	-.087
Pb	**.982**	-.050	-.034	.049	-.165
Zn	**.772**	-.105	-.215	**.522**	.194
Total	8.971	7.260	3.302	2.836	2.494
% of Variance	34.503	27.922	12.699	10.910	9.594
Cumulative %	34.503	62.425	75.124	86.034	95.628

Table 5.4.8 – Rotated Component Matrix for Sipadan Island Park				
	Component			
	1	2	3	4
Depth	**.846**	-.284	**.452**	.019
pH	**.855**	.122	**.504**	-.004
EC	**.827**	**.517**	.212	-.059
Salinity	**.877**	**.436**	.203	.012
ORP	-.842	-.082	-.526	.084
Turbitity	.101	-.269	**.736**	**.612**
TDS	**.944**	-.259	-.016	-.205
DO	-.025	**.934**	-.272	-.228
PO_4^{3-}	**.663**	.722	-.125	-.155
SO_4^{2-}	**.993**	-.099	.063	.014
NH_3-N	-.252	.110	-.956	.098
HCO_3^-	-.051	.884	.186	-.425
Ca^{2+}	.076	**.874**	.234	.418
Mg^{2+}	-.397	.132	-.880	-.227
Cl^-	**.507**	**.800**	.088	-.308
Co	-.226	.131	.080	-.962
Cu	.182	**.474**	**.737**	-.446
Fe	-.558	-.222	-.323	**.732**
K	.394	-.898	.150	-.124
Mn	.385	.614	-.498	-.477
Na	-.323	-.183	.181	**.911**
Ni	-.698	.188	-.266	**.638**
Zn	.304	.421	**.778**	-.354
Total	7.813	6.715	4.882	4.590
% of Variance	32.554	27.980	20.341	19.125
Cumulative %	32.554	60.534	80.875	100.000

5.5 Miri-Sipadan Comparison

5.5.1 In-Situ Parameters

A general comparison of the in-situ parameters between Miri and Sipadan indicated a higher average of all values at Sipadan except for temperature, where the average was 1°C lower than Miri. The average pH of Sipadan was slightly more alkaline with a difference of 0.05. EC had an average difference of 2.6mS/cm and mean salinity had a variance of 2ppt. ORP had a -3.5mV disparity in the average while turbidity, TDS and DO had a difference of 0.75NTU, 0.67mg/L and 0.61mg/L in their respective averages.

Figures 5.5.1 to 5.5.7 show the depth-wise variation of the physico-chemical parameters between Miri and Sipadan. The difference in the average pH values could be attributed to the influence of river runoffs as mentioned in Sections 5.2 and 5.3. A similar pattern in the value of pH was observed at BP, SP and NS (Figure 5.5.1). However, AG and EG followed a different pattern whereby the pH value decreased from surface to seabed. A similar behaviour was observed for the depth-wise variation of ORP (Figure 5.5.4) but the patterns were the opposite to that of pH. The increasing pH and decreasing ORP values from surface to seabed at BP, SP and NS indicate the absorption of carbon dioxide at the surface (Rakestraw, 1943; Measurements, 2016c). However, the decreasing pH and increasing ORP values at AG and EG in Miri would indicate the presence of river runoffs since Turbidity (Figure 5.5.5) was also observed to be the highest at those two sites. The conductivity and salinity values (Figures 5.5.2 and 5.5.3) were highest at Sipadan due to very low influence from any fresh water source. EG had the highest dilution effect since the mouth of the Miri river was around 10km followed by AG which was 20km away. The decreasing salinity and conductivity value at NS could be attributed to the mixing of ocean currents. As mentioned in Section 5.2, concentration of TDS is the combination of the various types of salt present in seawater and the amount of marine organisms in the seawater also plays a role in the increase or decrease of TDS concentration. Sipadan noted a higher concentration of TDS compared to Miri and the concentration was also increasing from surface to seabed. The increase in TDS concentration is due to human activities such as diving, and the presence of over 3000 species of fish as well as hundreds of different types of corals have been identified there. The region is also often visited by whale sharks and manta rays, and the island itself is made of corals (R. C. Malaysia, 2015b).

The concentration of DO was noted to be higher at Sipadan than in Miri. DO concentrations observed a decrease from surface to seabed except for Anemone Garden which increased from surface to the middle depth before declining towards the seabed. This depth-wise variation at AG could be due to stratification as mentioned in Section 5.2.

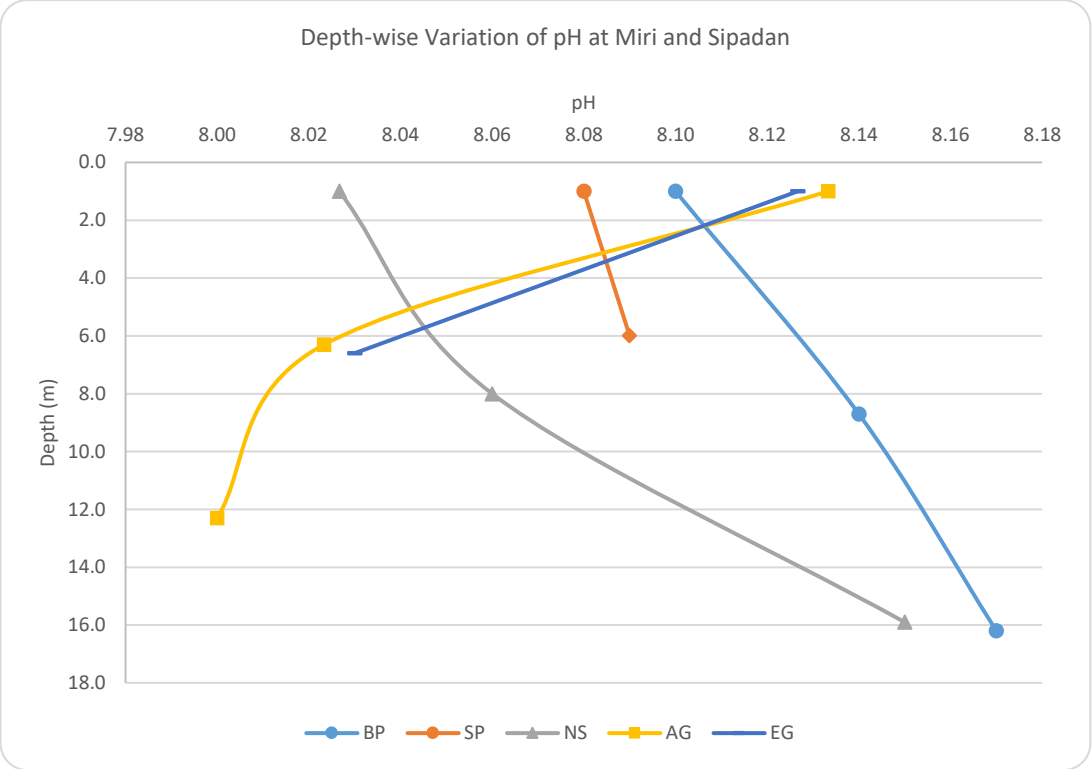

Figure 5.5.1 – Depth-wise Variation of pH at Sipadan and Miri

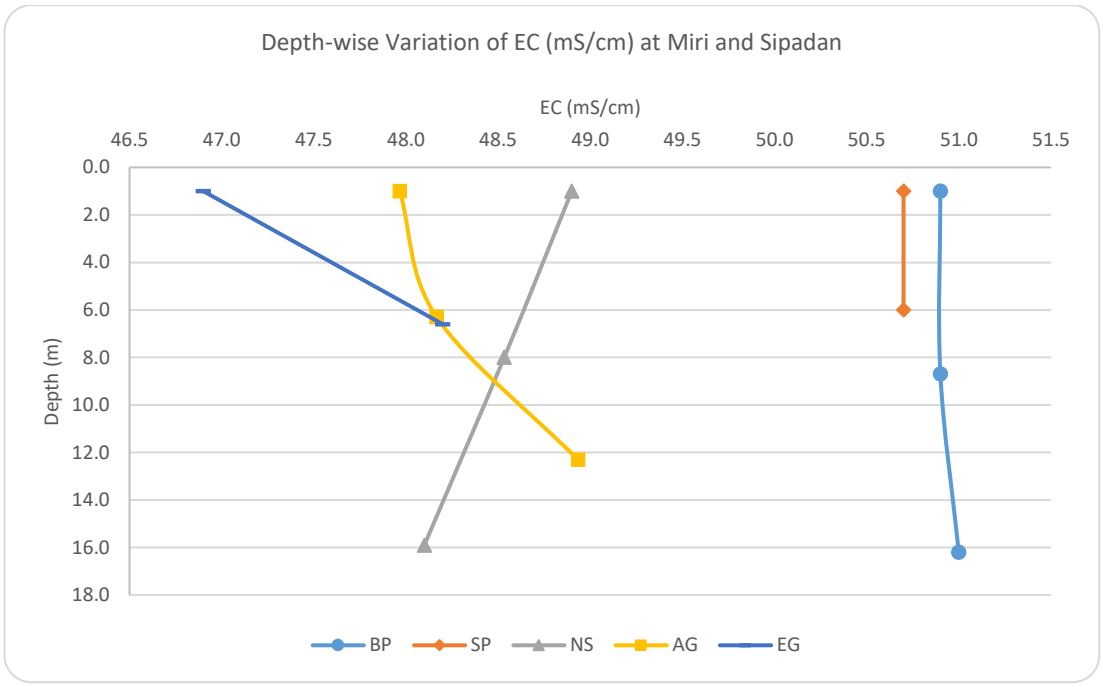

Figure 5.5.2 – Depth-wise Variation of EC (mS/cm) at Sipadan and Miri

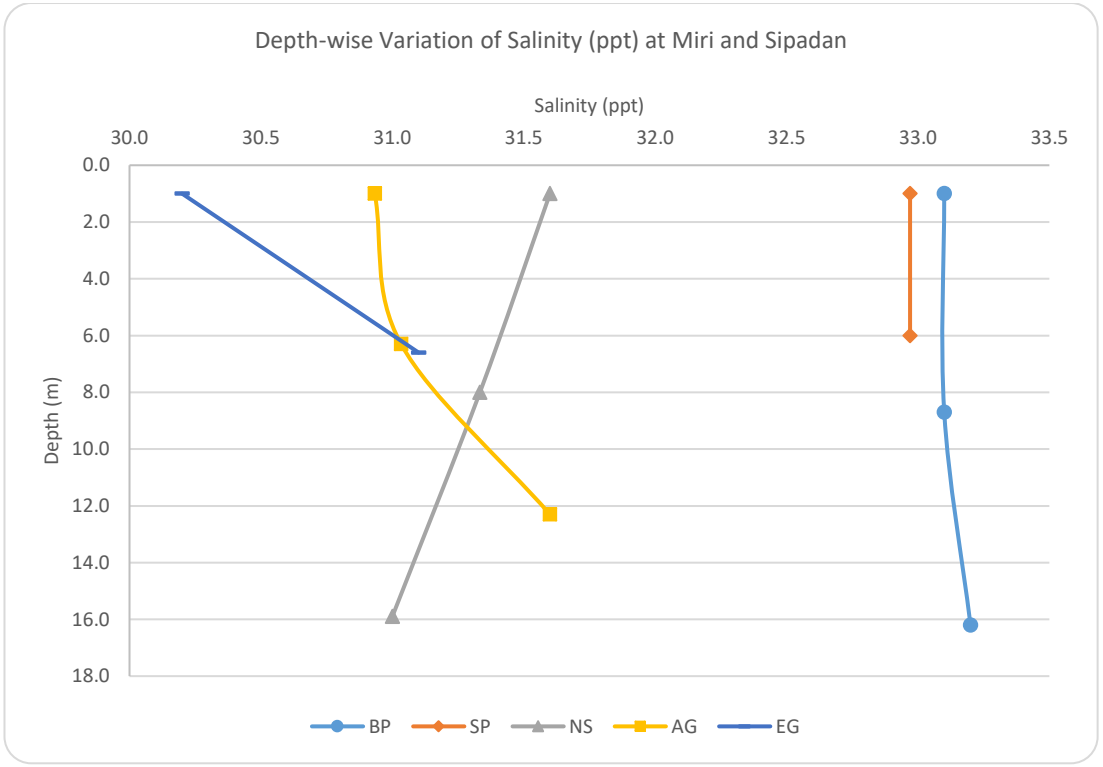

Figure 5.5.3 – Depth-wise variation of salinity (ppt) at Sipadan and Miri

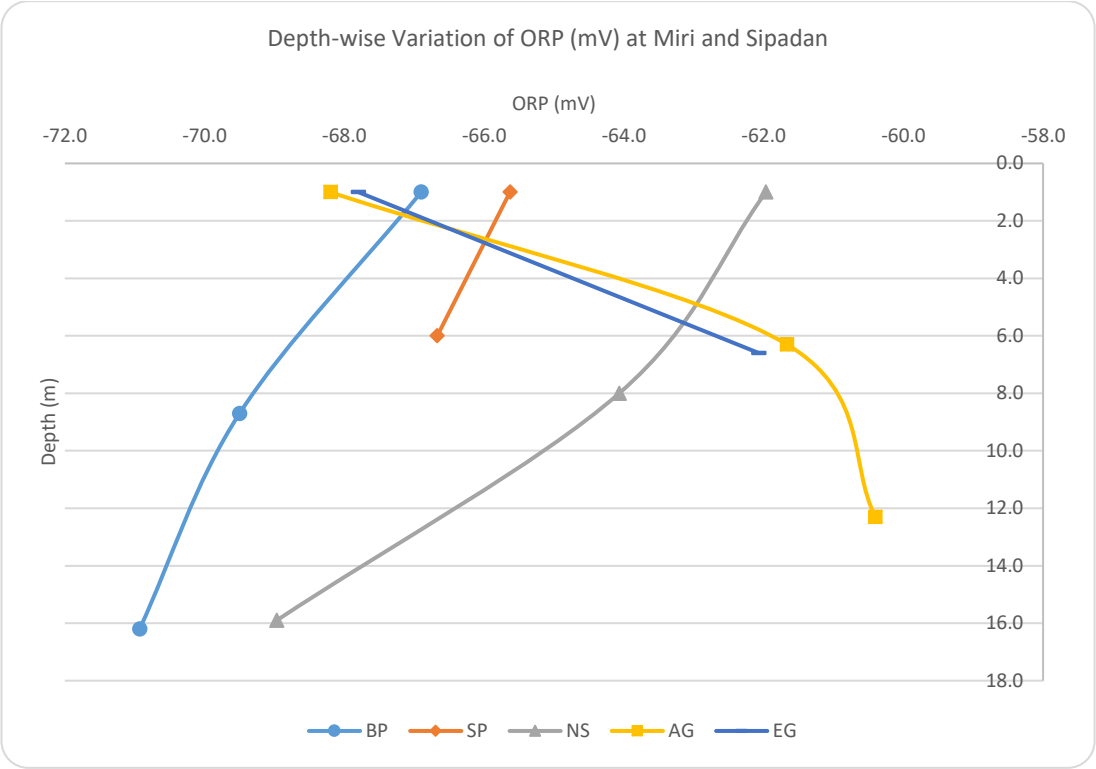

Figure 5.5.4 – Depth-wise Variation of ORP (mV) at Miri and Sipadan

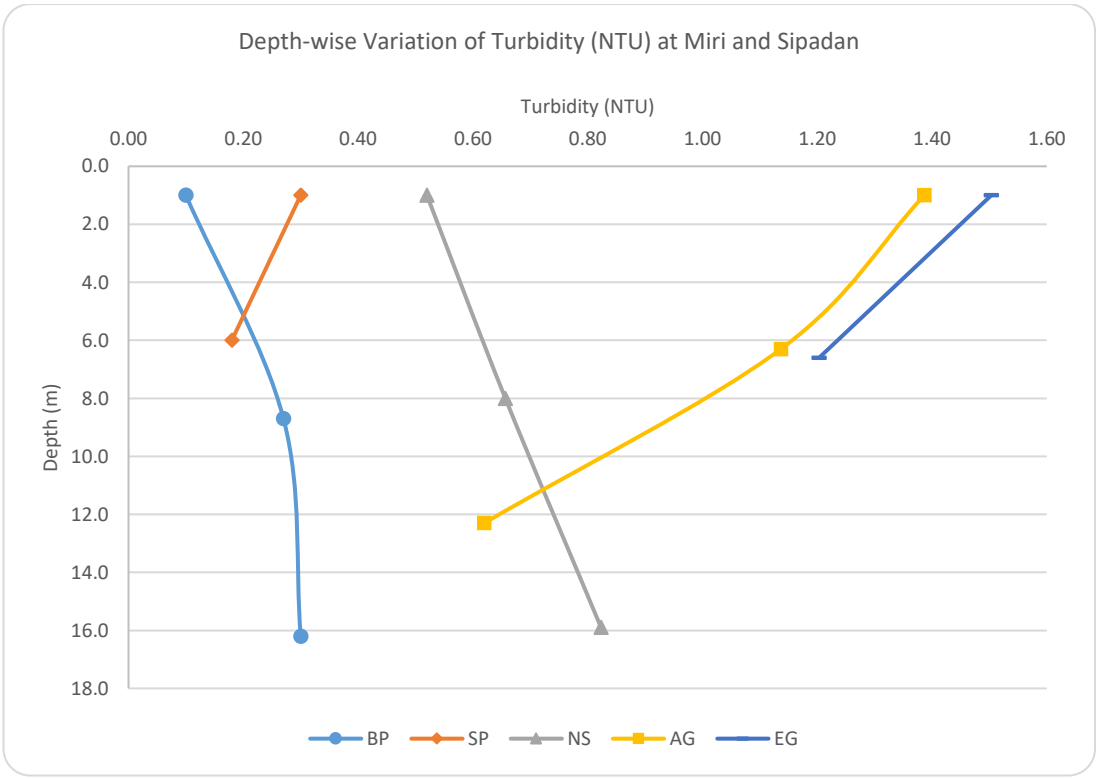

Figure 5.5.5 – Depth-wise Variation of Turbidity (NTU) at Miri and Sipadan

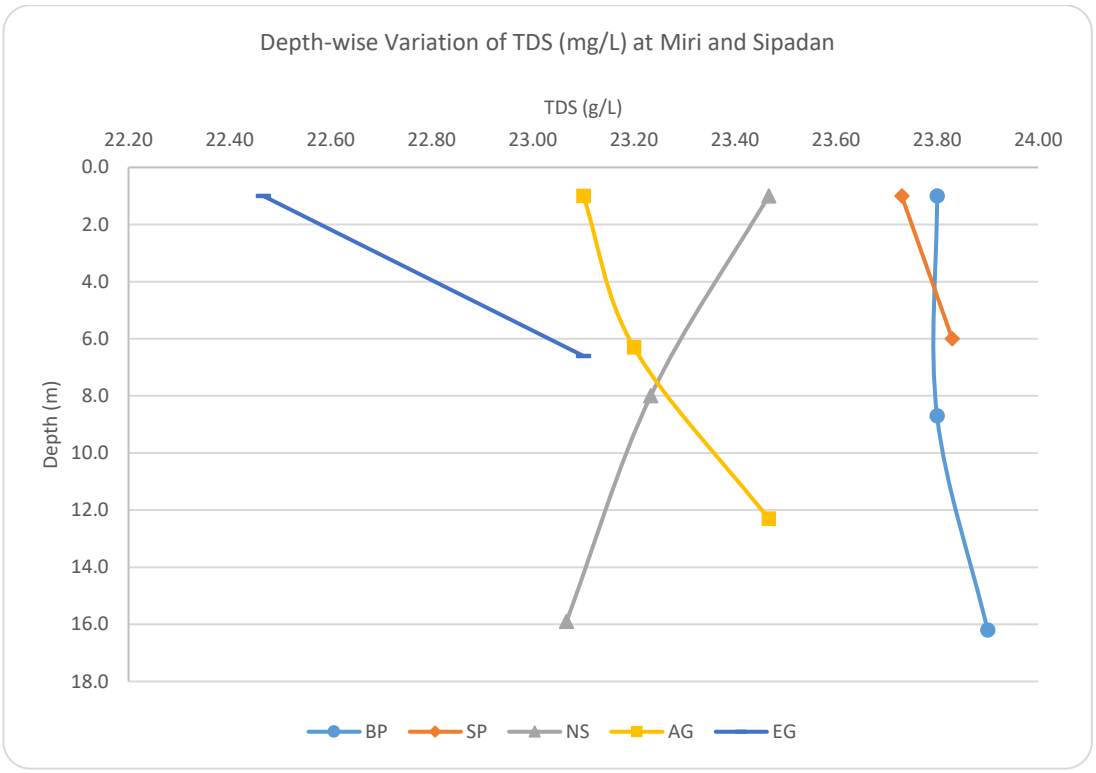

Figure 5.5.6 – Depth-wise Variation of TDS (m/L) at Miri and Sipadan

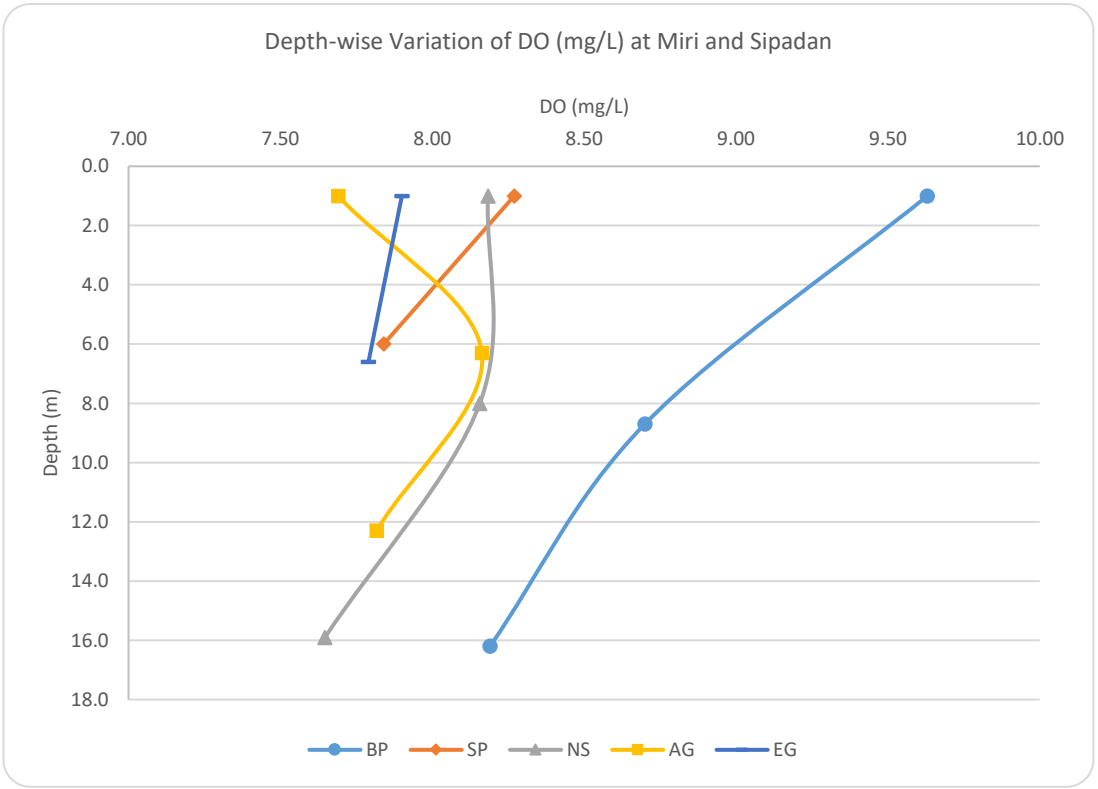

Figure 5.5.7 – Depth-wise Variation of DO (mg/L) at Miri and Sipadan

5.5.2 Nutrients

The variation of nutrients at both Miri and Sipadan is shown in Figures 5.5.8 to 5.5.11. Miri observed a higher phosphate and sulphate concentration as compared to Sipadan, while the average nitrate content at both places averaged to 0.02mg/L. The difference in average values for phosphate and sulphate were 0.09mg/L and 292.5mg/L respectively. The concentration of phosphate observed a decrease from surface to seabed at Miri, whereas a relatively low concentration was found at SP. BP observed a decrease in concentration at the middle depth before increasing again at the seabed. The difference in concentration at both sites indicate less influence of river input at Sipadan as compared to Miri. The concentration of sulphate observed a much higher average at Miri because of the high concentration measured at EG which could have been due to the presence of dynamite fishing as mentioned in Section 5.2. Ammonia-Nitrogen which had a higher average at Sipadan than Miri with a difference of 0.02mg/L. The higher concentration at Sipadan indicates the presence of recreational activities around the island.

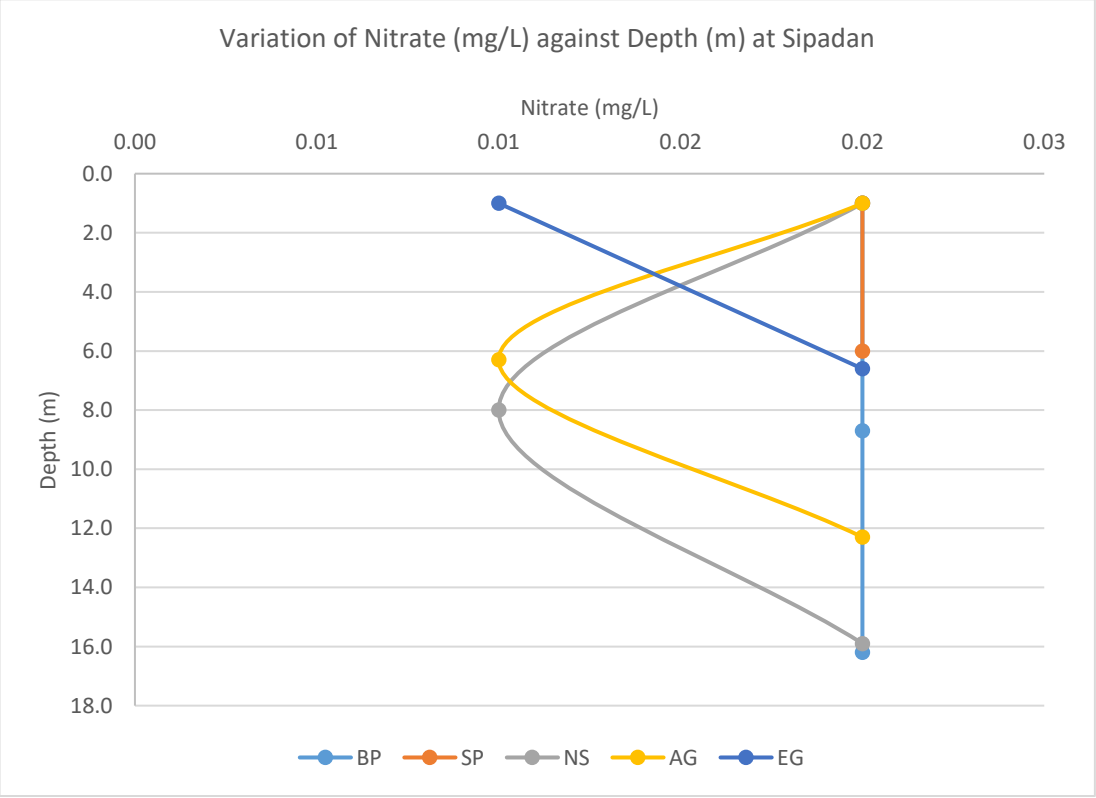

Figure 5.5.8 – Depth-wise Variation of Nitrate (mg/L) at Miri and Sipadan

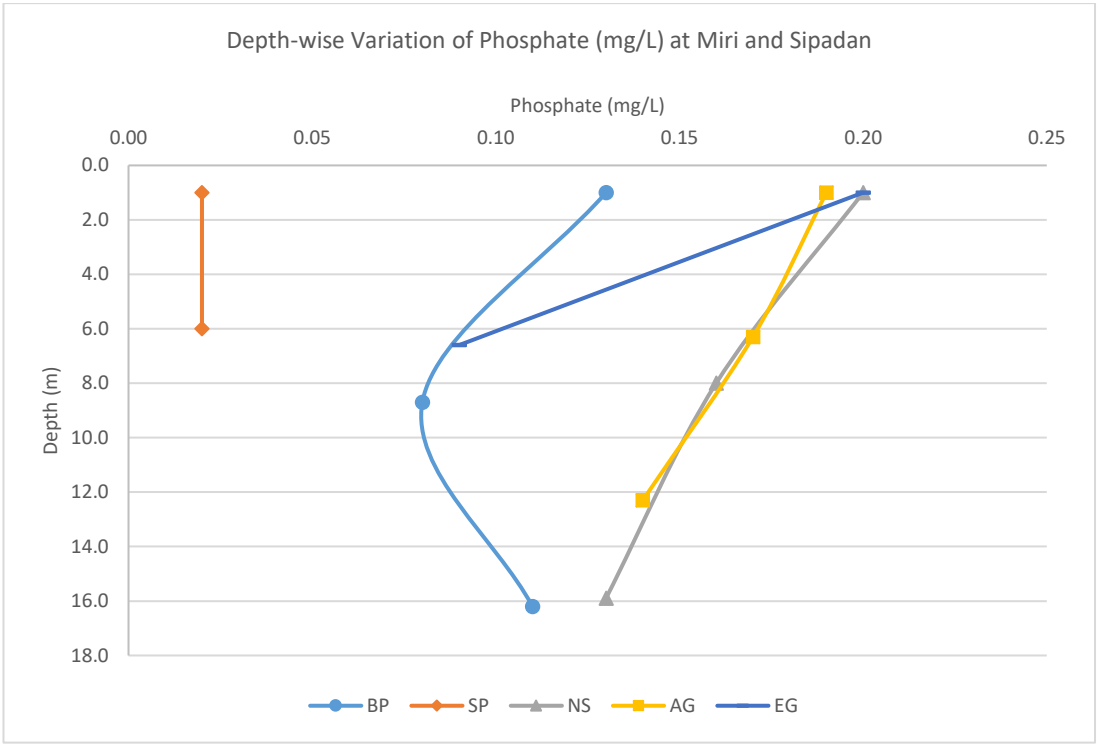

Figure 5.5.9 – Depth-wise Variation of Phosphate (mg/L) at Miri and Sipadan

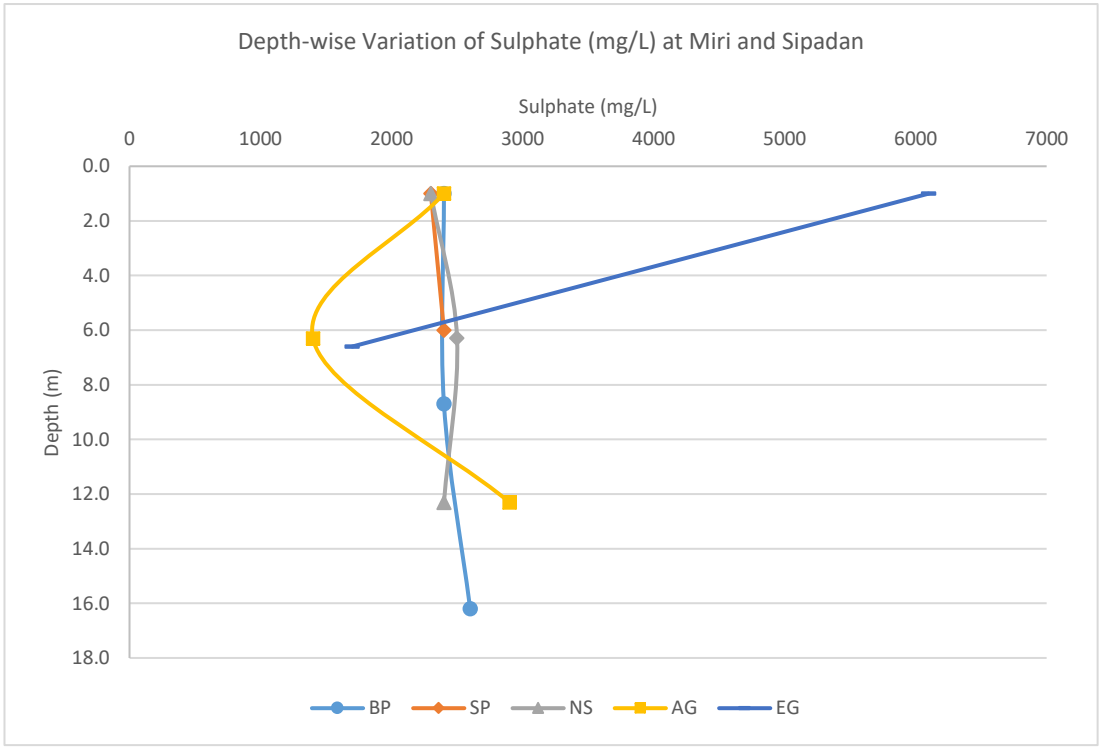

Figure 5.5.10 - Depth-wise Variation of Sulphate (mg/L) at Miri and Sipadan

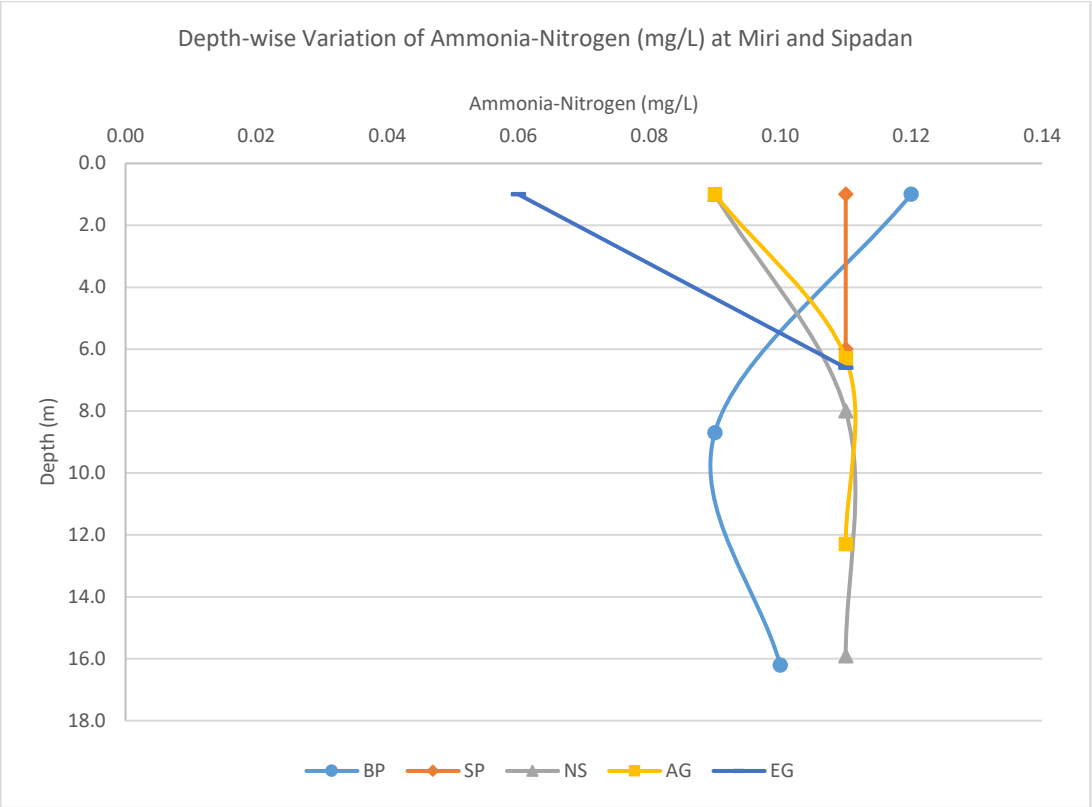

Figure 5.5.11 - Depth-wise Variation of Ammonia-Nitrogen (mg/L) at Miri and Sipadan

5.5.3 Major Ions

The Figures 5.5.12 to 5.5.17 show the variation of major ions from surface to seabed at both Miri and Sipadan. The major ions that had higher average concentrations at Sipadan as compared to Miri were bicarbonate with a difference of 11.99mg/L; magnesium with 117.56mg/L; potassium with 8.67mg/L; sodium with 608mg/L; chloride with 1274.72mg/L. Calcium was the only major ion with a higher average concentration in Miri than in Sipadan with a difference of 70.2mg/L. A decrease from surface to seabed was observed in the concentration of bicarbonate while the opposite was noted in Miri (Figure 5.5.12). While the lower values in Miri could be attributed to the influence of river runoffs, the higher concentration at Sipadan was quite nominal since the average concentration of bicarbonate in seawater has been observed around 140mg/L to 145mg/L (Rakestraw, 1943; Anthoni, 2006). Comparatively, calcium has a lower concentration in Sipadan than in Miri (Figure 5.5.13). While the high values of calcium during the transition to NEM season was attributed to coastal development (Section 5.2.3), that of Sipadan was again observed to remain within normal seawater levels (Rakestraw, 1943; Anthoni, 2006). The lower values of magnesium observed in

Miri, explained in Section 5.2.3, was attributed to the influence of river discharge (Figure 5.5.14). The concentration of magnesium was again observed to remain within normal seawater concentrations at Sipadan. Similarly, the concentration of potassium, sodium and chloride were also within the normal seawater values at Sipadan as indicated by Rakestraw (1943) and Anthoni (2006).

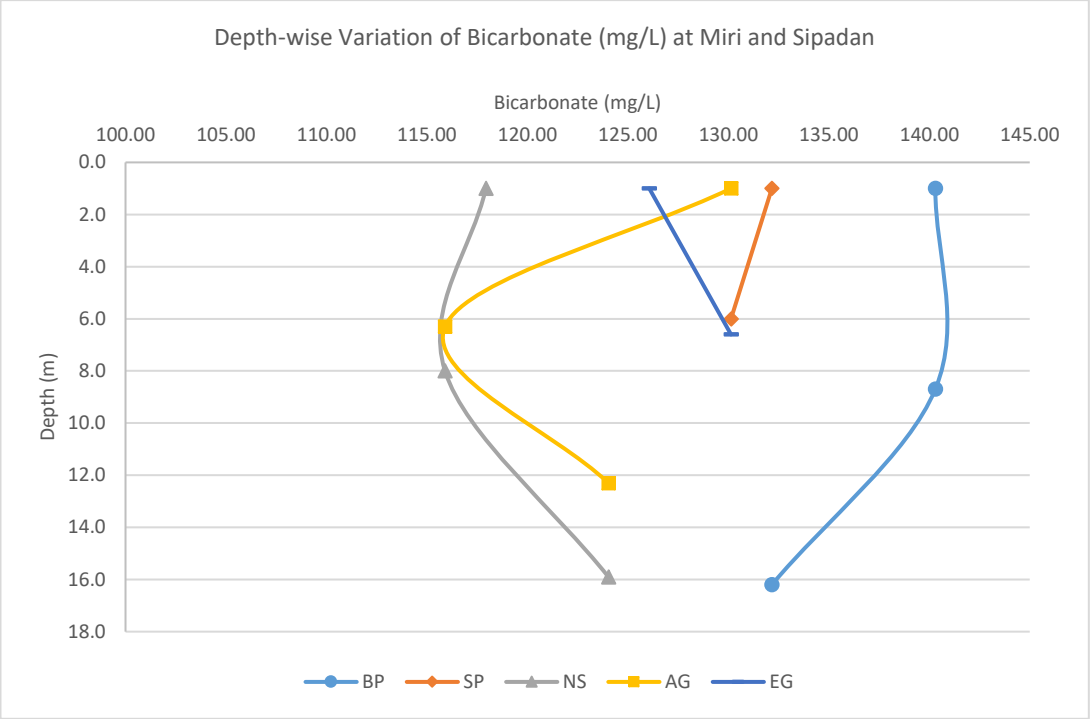

Figure 5.5.12 – Depth-wise Variation of Bicarbonate (mg/L) at Miri and Sipadan

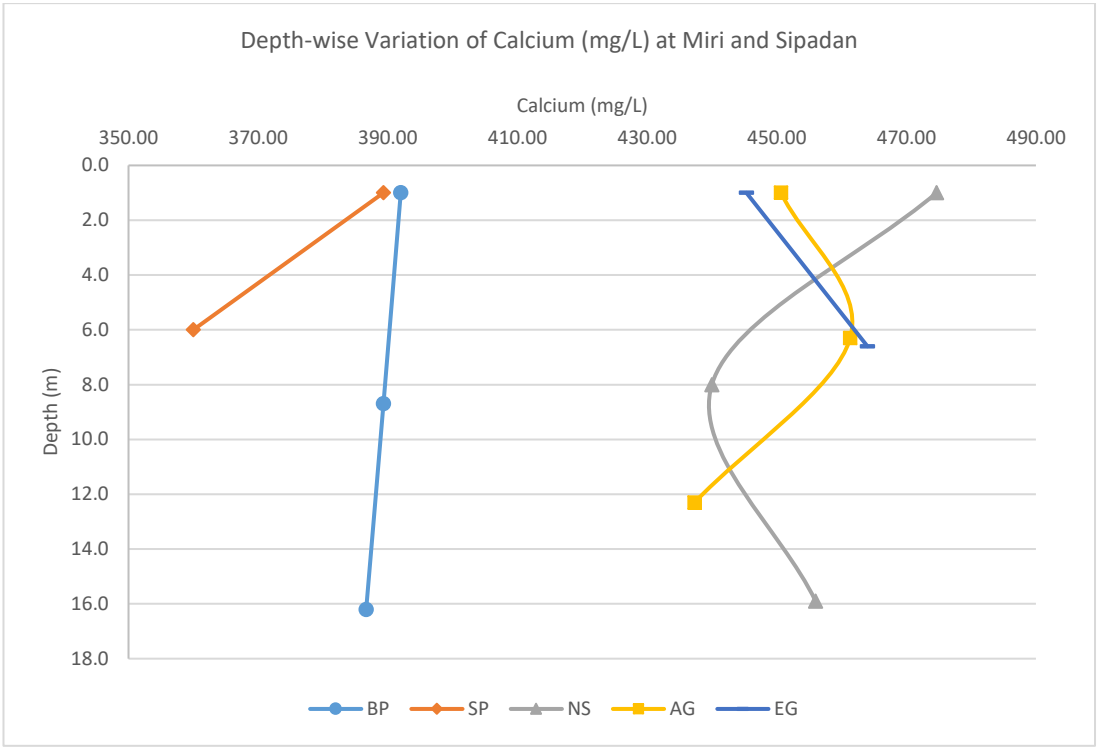

Figure 5.5.13 - Depth-wise Variation of Calcium (mg/L) at Miri and Sipadan

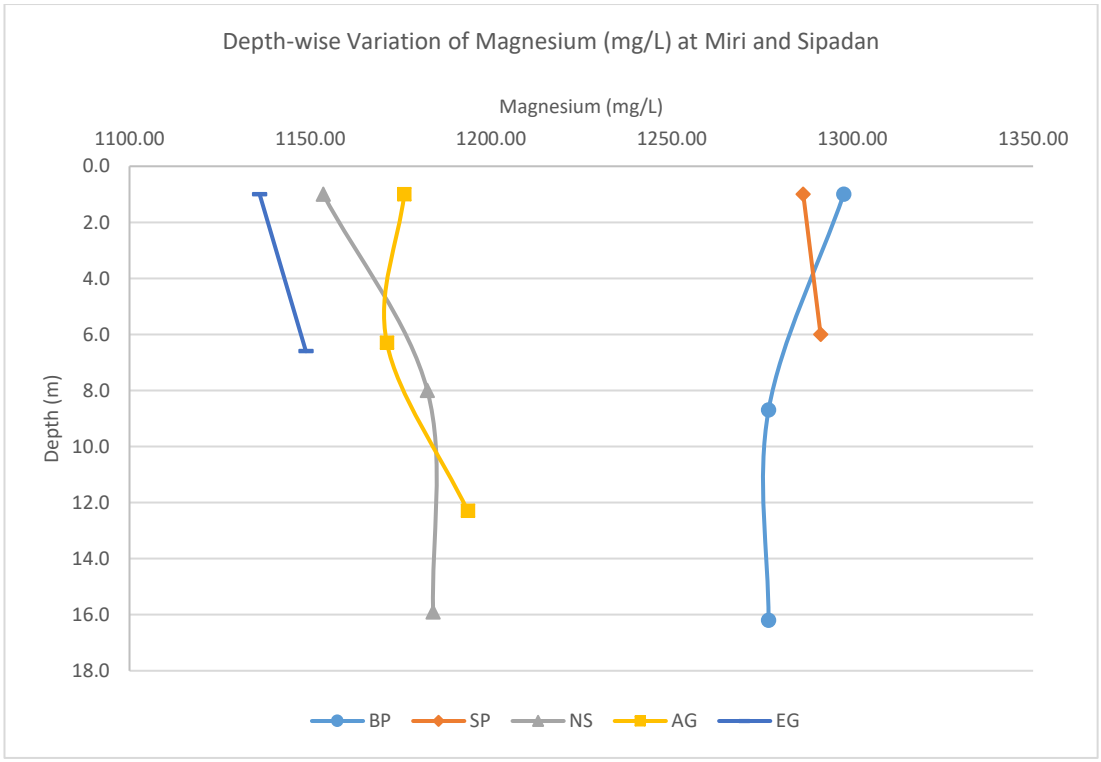

Figure 5.5.14 – Depth-wise Variation of Magnesium (mg/L) at Miri and Sipadan

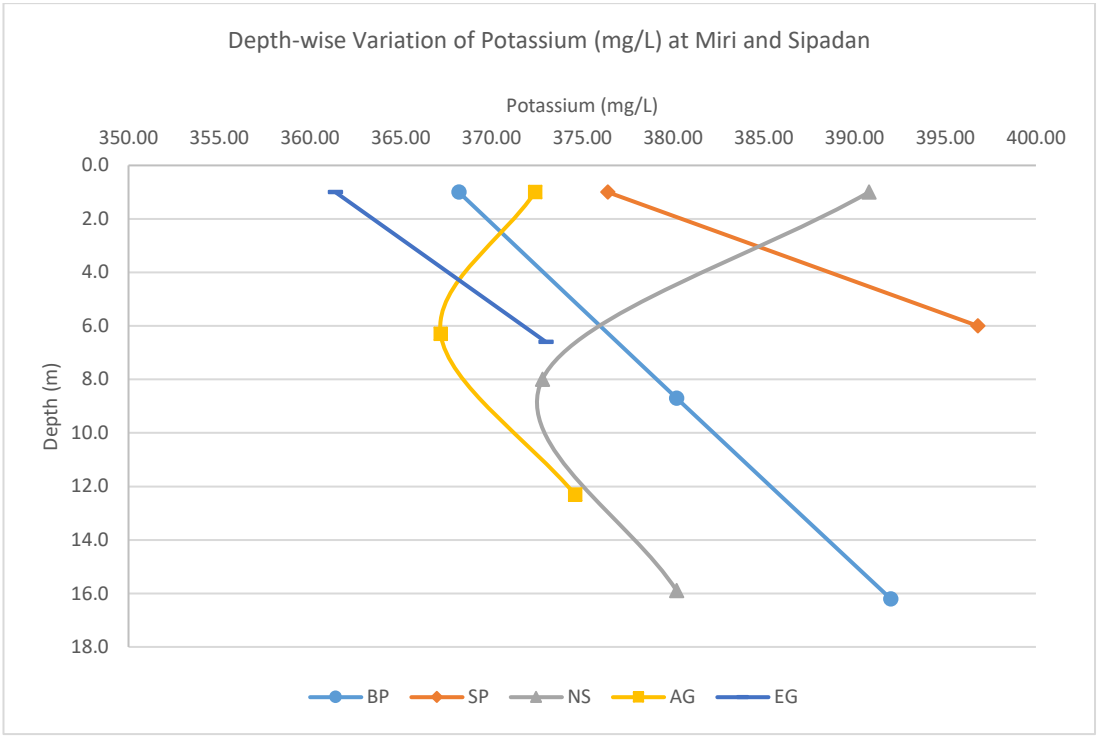

Figure 5.5.15 – Depth-wise Variation of Potassium (mg/L) at Miri and Sipadan

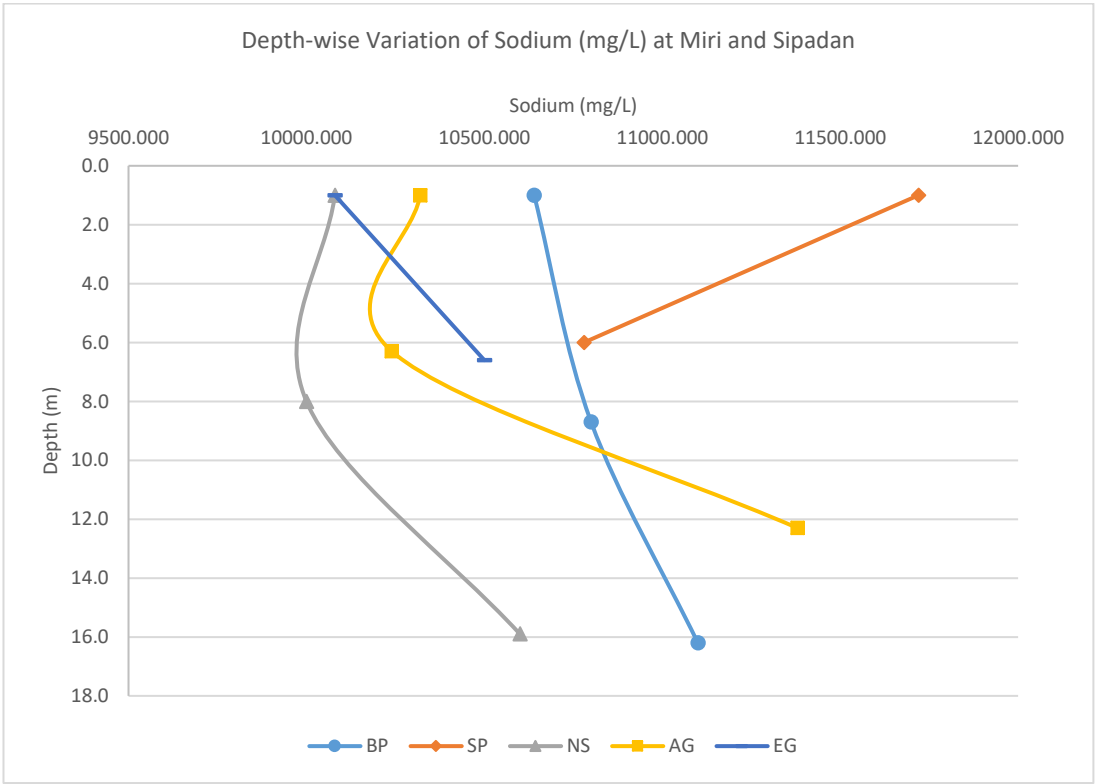

Figure 5.5.16 – Depth-wise Variation of Sodium (mg/L) at Miri and Sipadan

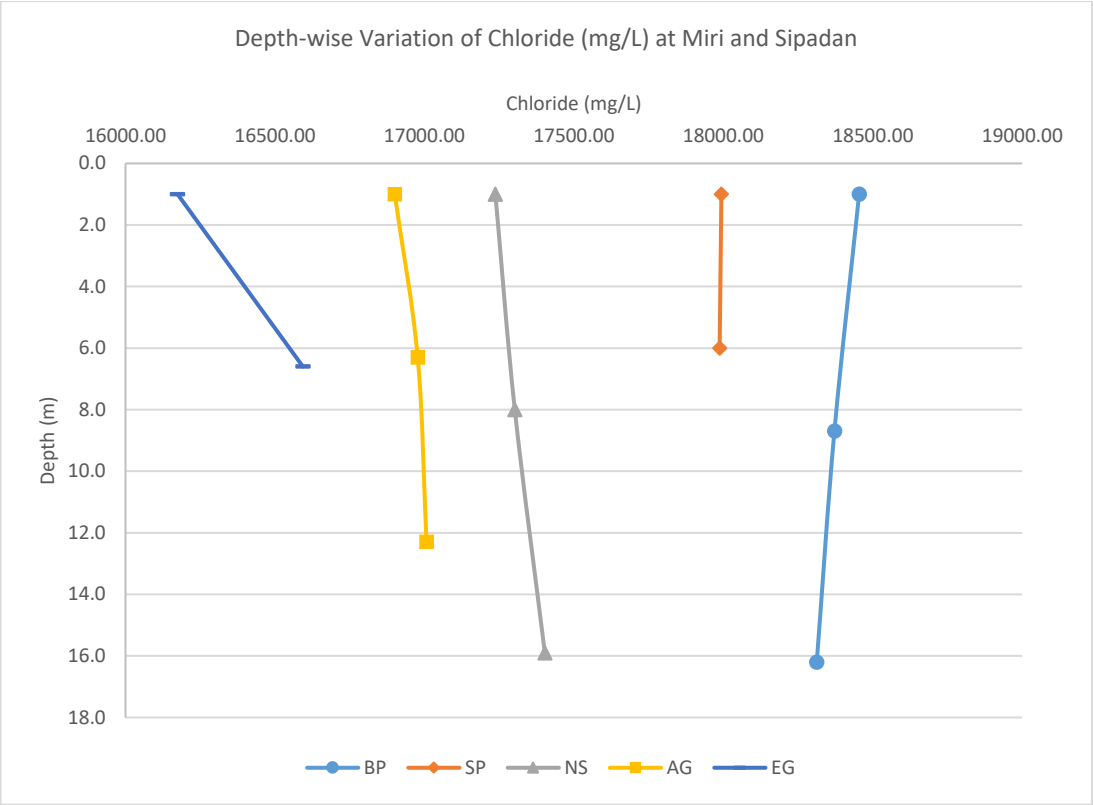

Figure 5.5.17 – Depth-wise Variation of Chloride (mg/L) at Miri and Sipadan

5.5.4 Trace Metals

The comparison of trace metals between Miri and Sipadan omitted cadmium, cobalt and lead because their presence were mostly below detection limit at Sipadan. The trace metals in Figures 5.5.18 to 5.5.22 consist of copper, iron, manganese, nickel and zinc. The average concentration of copper had a difference of 0.065mg/L between Miri and Sipadan where the lower values were observed at Sipadan (Figure 5.5.18). The concentration of iron was higher in Sipadan than in Miri as shown in Figure 5.5.18. The difference in average concentration was 0.357mg/L between the two regions. A similarity was noted in the vertical behaviour of iron between BP and AG. Both sites observed a decrease in iron concentration at the middle depth before increasing at the seabed. This variation could be attributed to the presence of phytoplankton at that depth (Wells et al., 1995). The difference in concentration of manganese between the two sites was 0.005mg/L with a higher value in Sipadan. Figure 5.5.20 shows the depth-wise variation of the metal at both sites. AG, EG and BP observed an increase in manganese concentration from surface to around 6m. Then the concentration started increasing again towards the seabed at both AG and BP. The presence of marine

organisms such as phytoplankton could be the reason for this variation at those two sites (T. G. Thompson and Wilson, 1935; Zaidi, 2006). The concentration of nickel was much lower in Sipadan than in Miri as shown in Figure 5.5.21. The difference in average values was 0.233mg/L. The lower concentration at Sipadan could be attributed to the absence of a river mouth within the close vicinity of the island leaving only boat traffic (Mokhtar et al., 2012). The concentration of zinc was again higher in Miri than at Sipadan. However, the average difference between the two sites was 0.003mg/L, which was relatively small compared to the other metals. In Sipadan, zinc had a similar pattern to copper from surface to seabed (Figures 5.5.18 and 5.5.22), indicating a release of bioaccumulations from corals after breaking (Mokhtar et al., 2012).

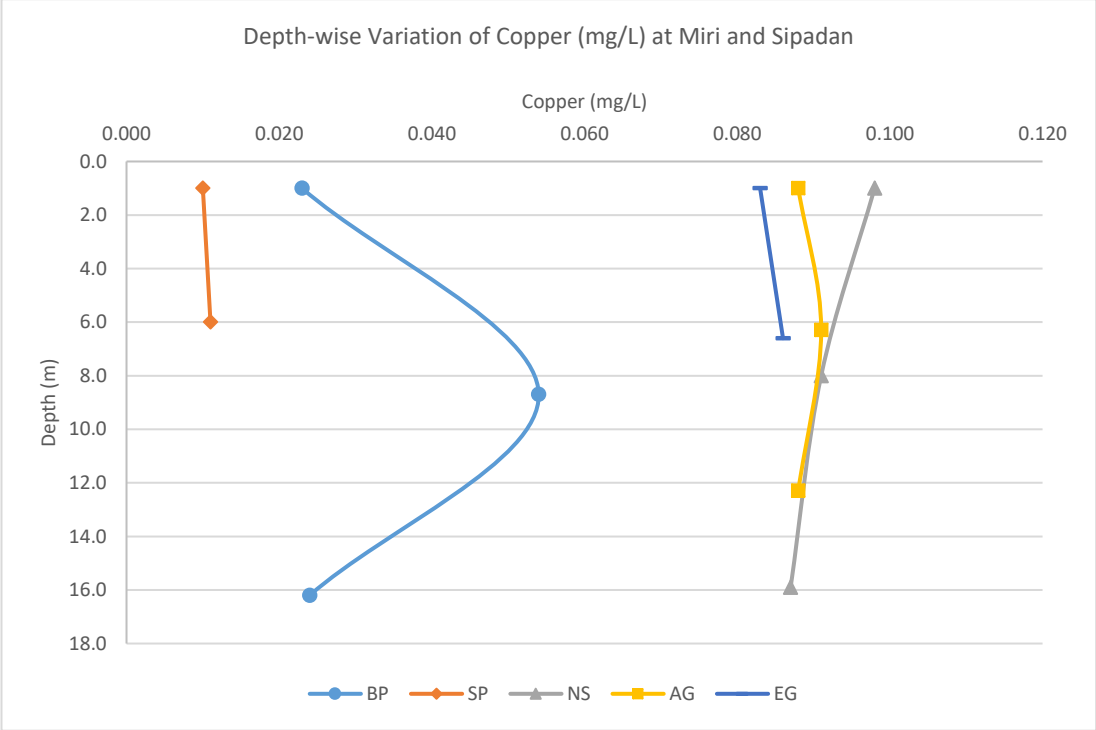

Figure 5.5.18 – Depth-wise Variation of Copper (mg/L) at Miri and Sipadan

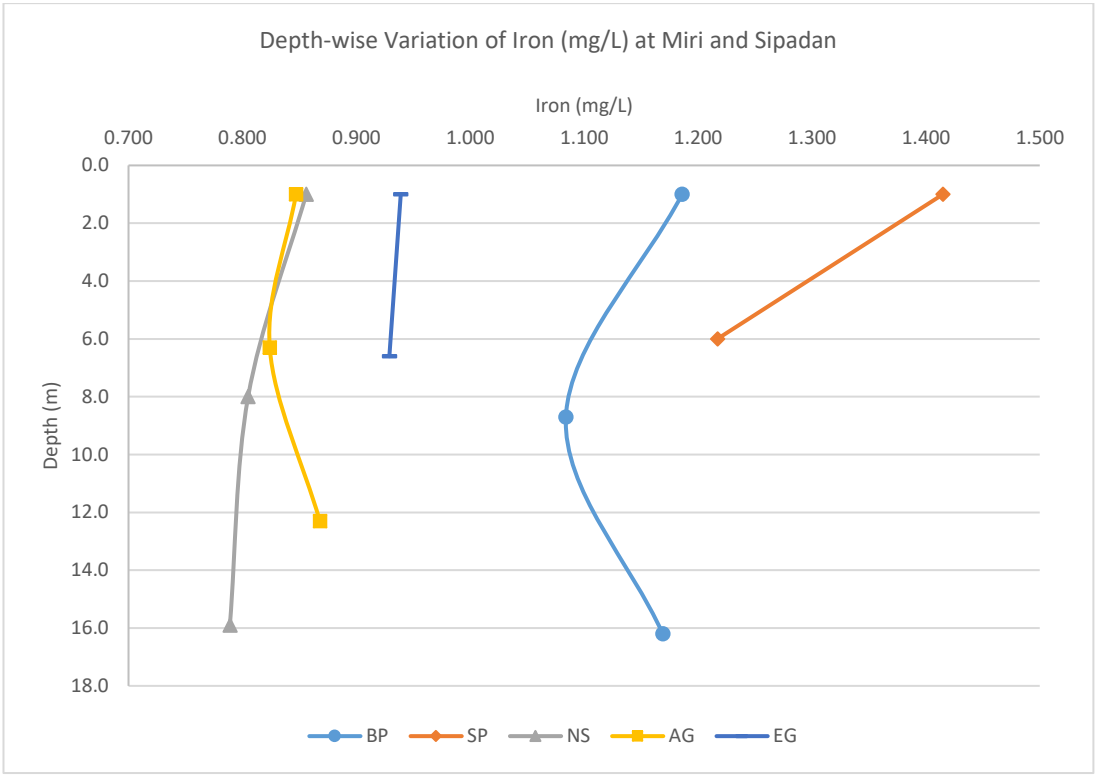

Figure 5.5.19 – Depth-wise Variation of Iron (mg/L) at Miri and Sipadan

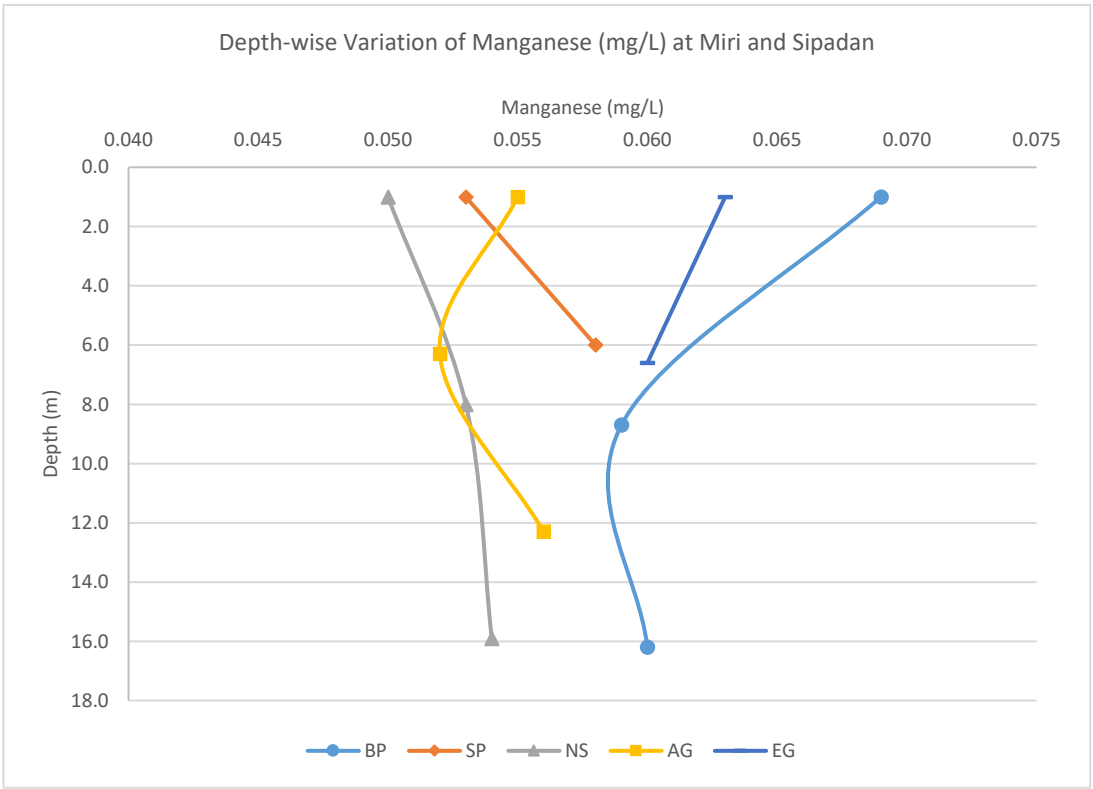

Figure 5.5.20 – Depth-wise Variation of Manganese (mg/L) at Miri and Sipadan

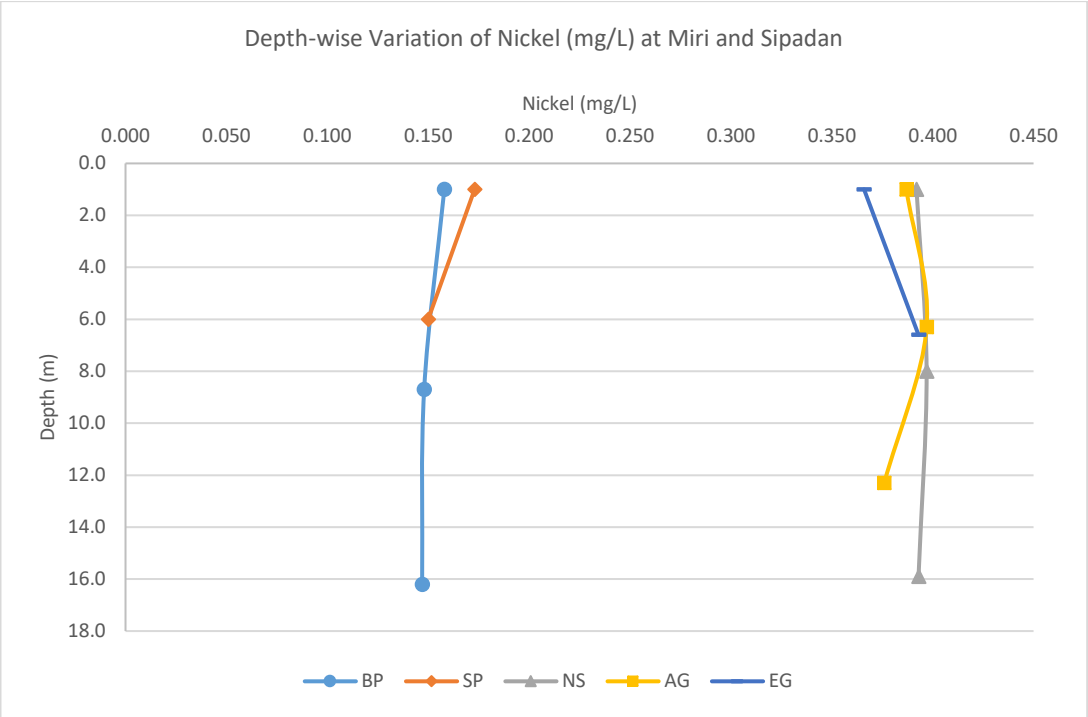

Figure 5.5.21 – Depth-wise Variation of Nickel (mg/L) at Miri and Sipadan

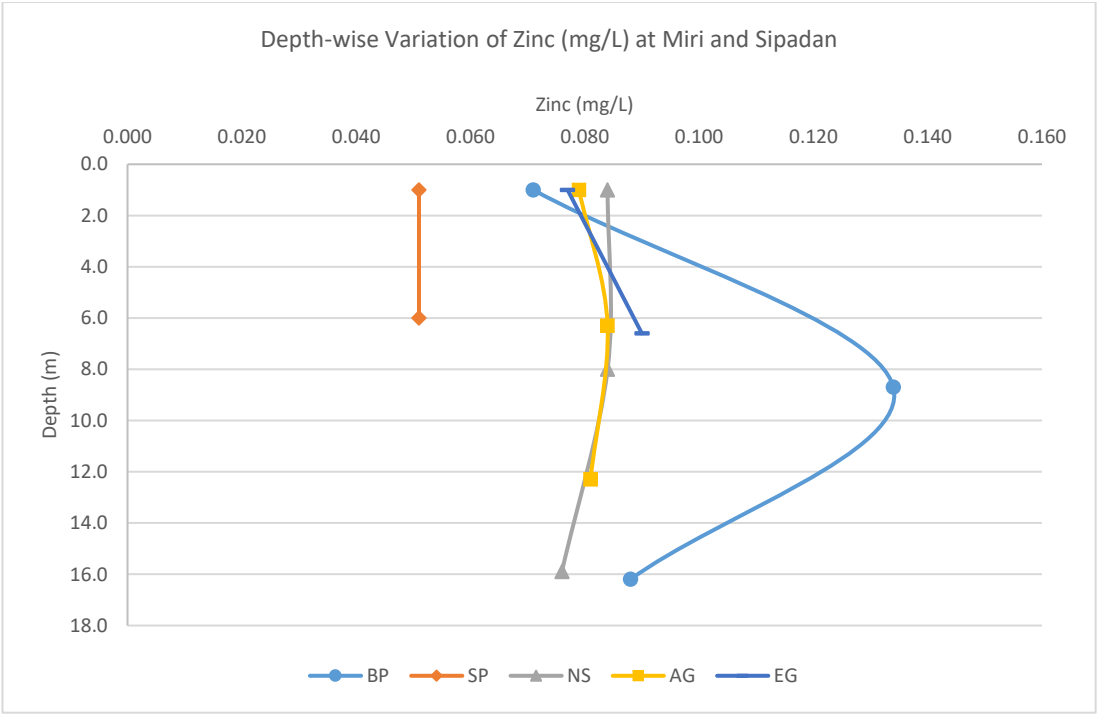

Figure 5.5.22 – Depth-wise Variation of Zinc (mg/L) at Miri and Sipadan

5.5.5 Summary

The elements in Table 5.5.1 to 5.5.4 compare the values from the Miri sites to that of Sipadan and their variances were observed. The in-situ parameters measured which indicated higher values at MSCRNP than Sipadan were temperature, ORP and turbidity. The parameters with lower values were pH, EC, salinity, TDS and DO. MSCRNP observed higher turbidity, and lower pH as well as EC and salinity due to its proximity to Miri river mouth and the presence of coastal development as compared to Sipadan which is over 27km from the mainland of Sabah.

Nitrate was the only nutrient that had a similar concentration at both MSCRNP and Sipadan. The presence of the Miri river was the main reason behind the higher concentration of phosphate and lower concentration sulphate at MSCRNP as compared to Sipadan. The lower concentration of ammonia-nitrogen was mostly attributed to a lower number of tourism activities being practiced during that period at MSCRNP due to declining weather conditions.

The major ions concentrations which were lower in Miri than at Sipadan were bicarbonate, magnesium, potassium, sodium and chloride. The lower concentration is once more attributed to the short distance of Miri river mouth to the sites.

The only trace metal which had a lower concentration at MSCRNP than Sipadan was iron. Miri river carries most of the pollution since it passes through Miri City which explains the higher concentrations of trace metals as opposed to Sipadan which is further in the ocean.

The seawater quality being better at Sipadan means a healthier coral reef system as compared to MSCRNP. However, the presence of coral reefs at such small distance from a major river indicates a better adaptation from the reefs at MSCRNP. The corals have also been observed to make yearly recoveries after being stressed during NEM season which brings high amount of rainfall.

Table 5.5.1 – Comparison of In-Situ Parameters from MSCRNP to Sipadan

Parameter	NS Value	AG Value	EG Value	Sipadan Value	Status
Temperature (°C)	30	30	30	29	*I*
pH	8.08	8.05	8.08	8.12	*D*
EC (mS/cm)	48.5	48.4	47.6	50.8	*D*
Salinity (ppt)	31.3	31.2	30.7	33.1	*D*
ORP (mV)	-65.00	-63.42	-64.93	-67.93	*I*
Turbidity (NTU)	0.67	1.05	1.35	0.23	*I*
TDS (g/L)	23.26	23.26	22.78	23.81	*D*
DO (mg/L)	8.00	7.89	7.85	8.53	*D*

Table 5.5.2 – Comparison of Nutrients from MSCRNP to Sipadan

Nutrients (mg/L)	NS Value	AG Value	EG Value	Sipadan Value	Status
NO_3^-	0.02	0.02	0.02	0.02	-
PO_4^{3-}	0.16	0.17	0.15	0.07	*I*
SO_4^{2-}	2400	2233	3900	2420	*D*
NH_3-N	0.09	0.10	0.09	0.11	*D*

Table 5.5.3 – Comparison of Major Ions from MSCRNP to Sipadan

Major Ions (mg/L)	NS Value	AG Value	EG Value	Sipadan Value	Status
HCO_3^- (mg/L)	119.29	123.36	128.10	135.01	*D*
Ca^{2+} (mg/L)	456.89	449.78	454.67	383.47	*I*
Mg^{2+} (mg/L)	1173.33	1180.27	1142.40	1285.76	*D*
K^+ (mg/L)	381.27	371.40	367.20	382.72	*D*
Na^+ (mg/L)	10226	10646	10290	11008	*D*
Cl^- (mg/L)	17314	16961	16383	18224	*D*

Table 5.5.4 – Comparison of Trace Metals from MSCRNP to Sipadan

Trace Metals (mg/L)	NS Value	AG Value	EG Value	Sipadan Value	Status
Co (mg/L)	0.223	0.197	0.195	0.008	*I*
Cu (mg/L)	0.092	0.089	0.085	0.024	*I*
Fe (mg/L)	0.817	0.846	0.934	1.214	*D*
Mn (mg/L)	0.052	0.054	0.062	0.060	*I*
Ni (mg/L)	0.394	0.387	0.380	0.155	*I*
Pb (mg/L)	0.414	0.411	0.404	0.033	*I*
Zn(mg/L)	0.081	0.081	0.084	0.079	*I*

5.6 Photo-Documentation

The various pictures taken throughout the dive trips gave a good indication of the quality of the coral environment in the Miri-Sibuti Coral Reef National Park. However, the small timeframe was not enough to fully examine the effects of the seawater quality on the corals. The pictures illustrated below do show signs of coral bleaching. The coral environment at North Siwa, Anemone Garden and Eve's Garden were at a depth of 14m, 11m and 6m respectively. From the three sites, North Siwa was observed as the healthiest of them. The presence of algae was not as invasive as noted at Eve's Garden.

The various white patches, as seen in Figures 5.6.3, 5.6.8 and 5.6.9 show the beginning of coral bleaching, and Figures 5.6.1, 5.6.5 and 5.6.7 show healthy Porites and Diploastrea at the North Siwa. Figure 5.6.6 shows a large Porites coral that contains coral borers. Coral borers are worms that eat into the coral and over time, these worms affect the integrity of the reef, weakening it. These coral borers, also known as Christmas worms thrive in nutrient rich environments. Being the furthest reef, at 20.96km from the marina, North Siwa was also the healthiest among the three sites. Even though bleaching was present, most of the hard corals and soft corals looked healthy and less algae was found.

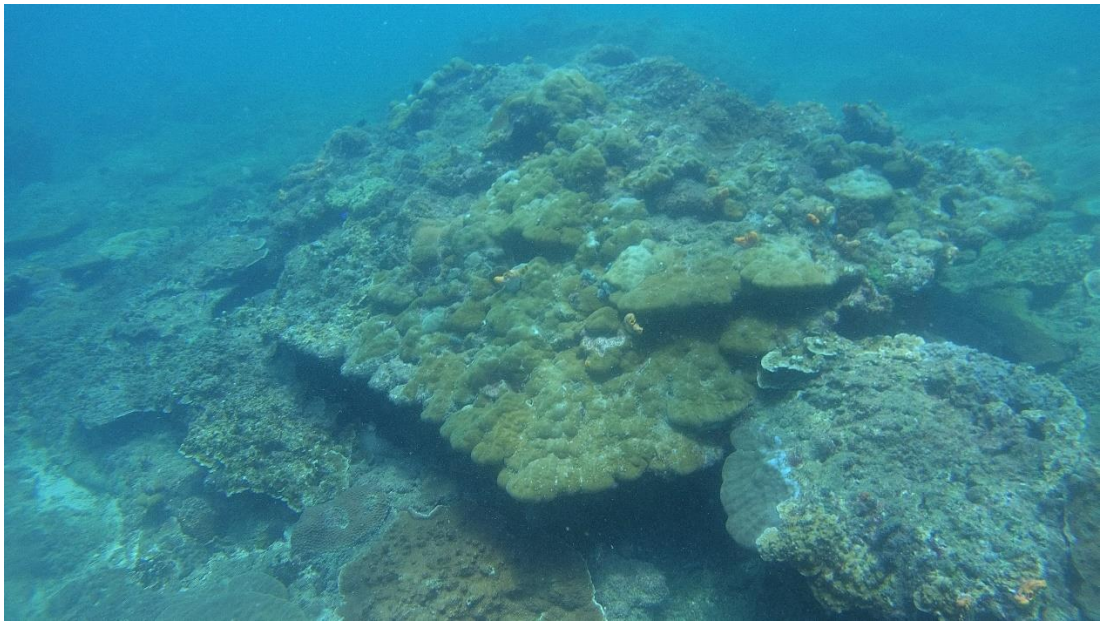

Figure 5.6.1 – Porites at North Siwa (May, 2016)

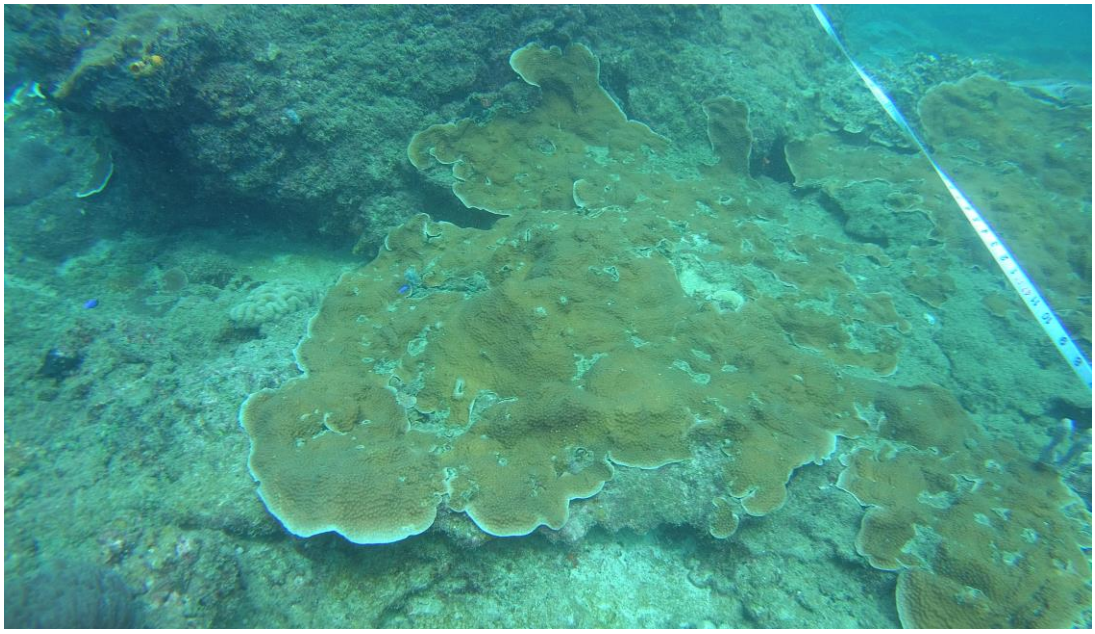

Figure 5.6.2 – Echinopora at North Siwa (October, 2016)

Figure 5.6.3 – Partially bleached Porites at North Siwa (October, 2016)

Figure 5.6.4 – Healthy soft coral at North Siwa (September, 2016)

Figure 5.6.5 – Top view of large healthy Porites at North Siwa (October, 2016)

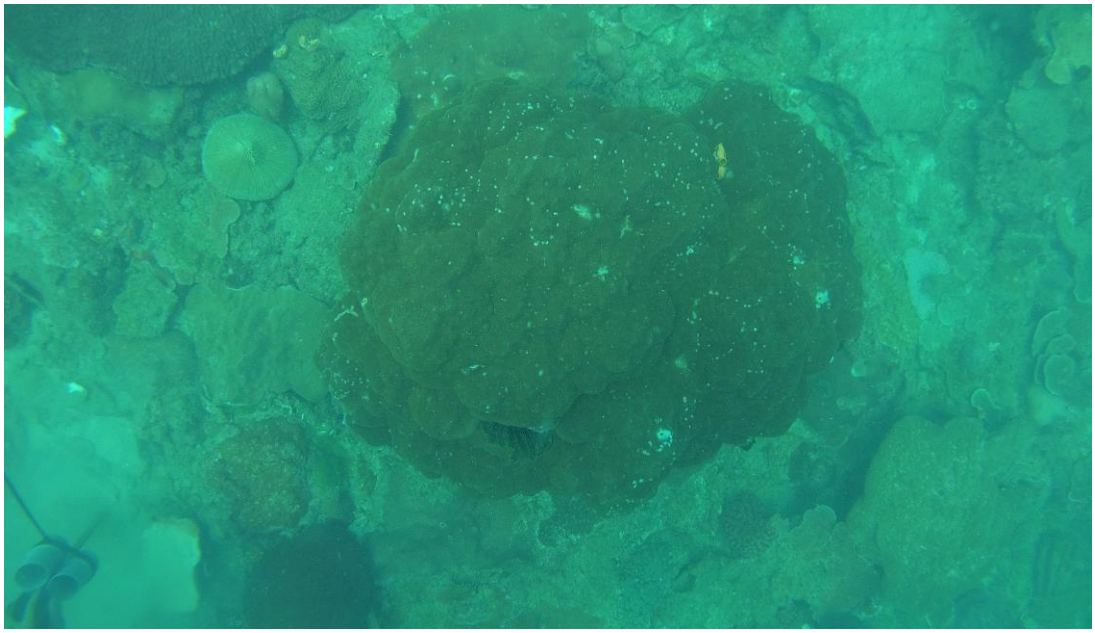

Figure 5.6.6 – Coral borers in Porites at North Siwa (October, 2016)

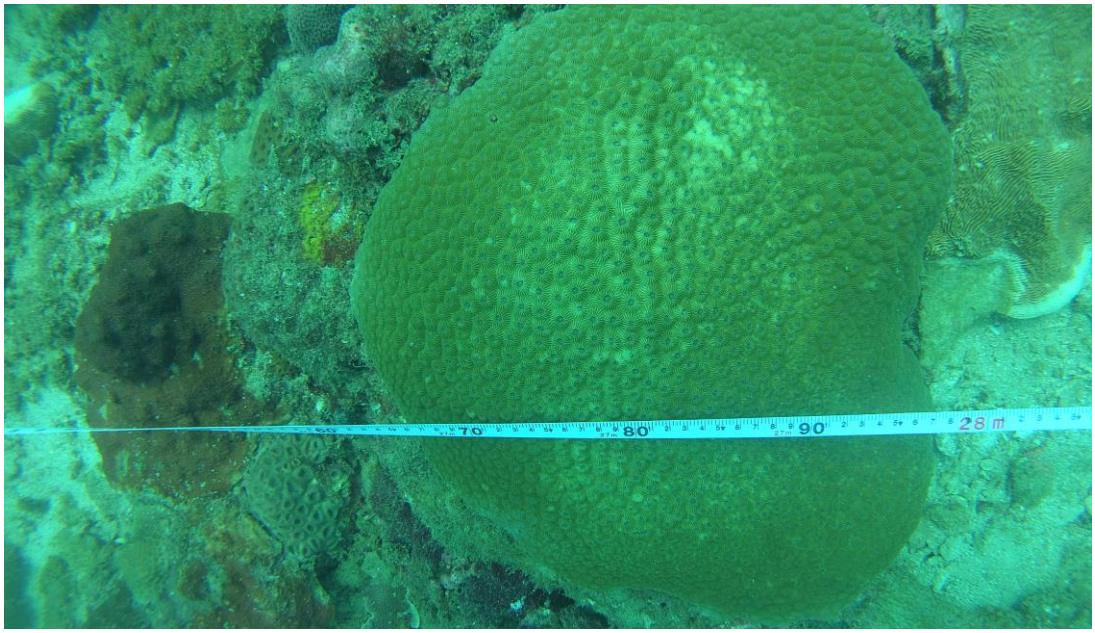

Figure 5.6.7 – Healthy Diploastrea at North Siwa (October, 2016)

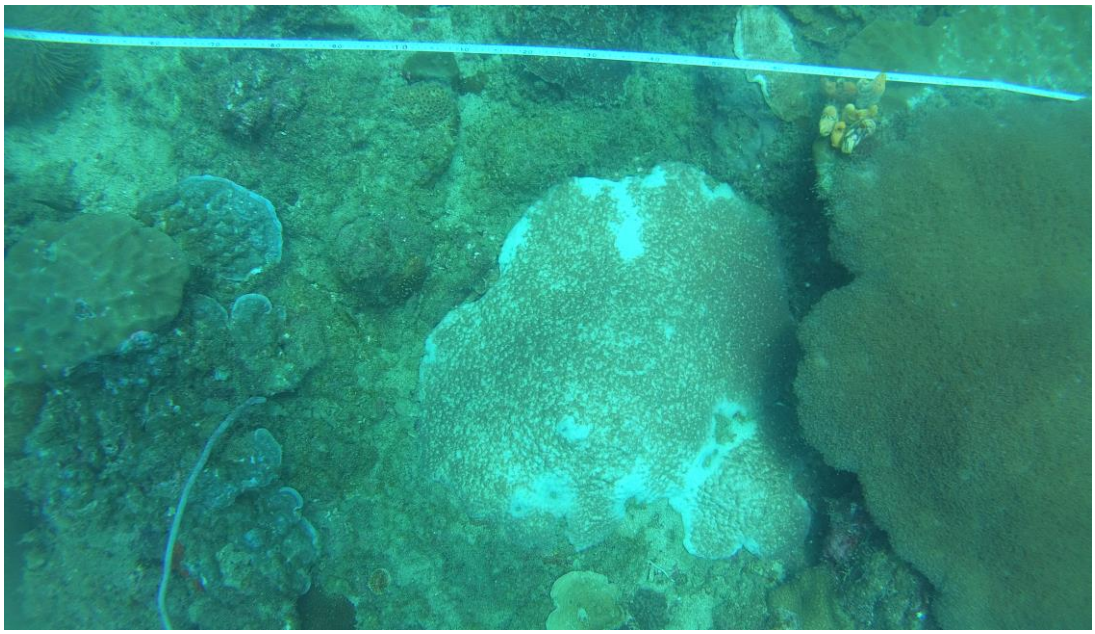

Figure 5.6.8 – Bleached Diploastrea (middle) at North Siwa (October, 2016)

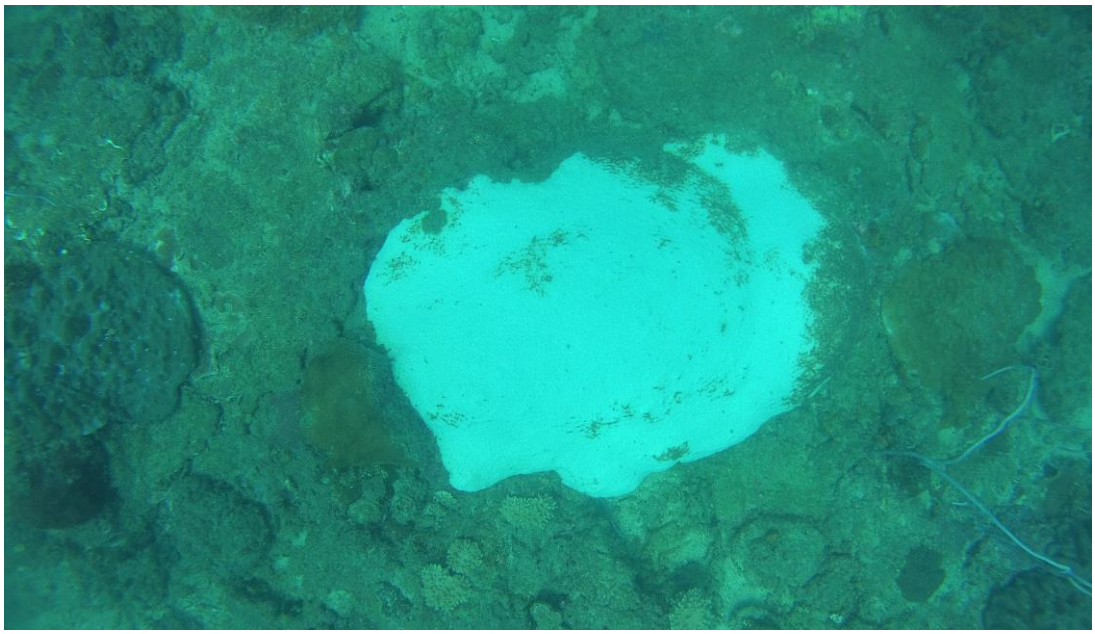

Figure 5.6.9 – Bleached Diploastrea at North Siwa (October, 2016)

Anemone Garden, which is roughly 11km from the shore, is one of the most popular sites among divers and not as deep as North Siwa. This site in particular gave a very good indication of the effect of too many activities being carried out as well as evaluating the more resilient corals to the least ones. Most of the time, the mooring line was cut, lots of nets were found at the seabed indicating illegal fishing activities

and higher concentrations of nutrients when compared to North Siwa. The pictures shown in Figures 5.6.10 to 5.6.15, except 5.6.13, indicate traces of bleaching. The large Porites in Figure 5.6.11 is heavily bleached and is also home to many coral borers similar to Figure 5.6.12 which shows a Porites undergoing partial bleaching.

Figure 5.6.10 – Porites at Anemone Garden (October, 2016)

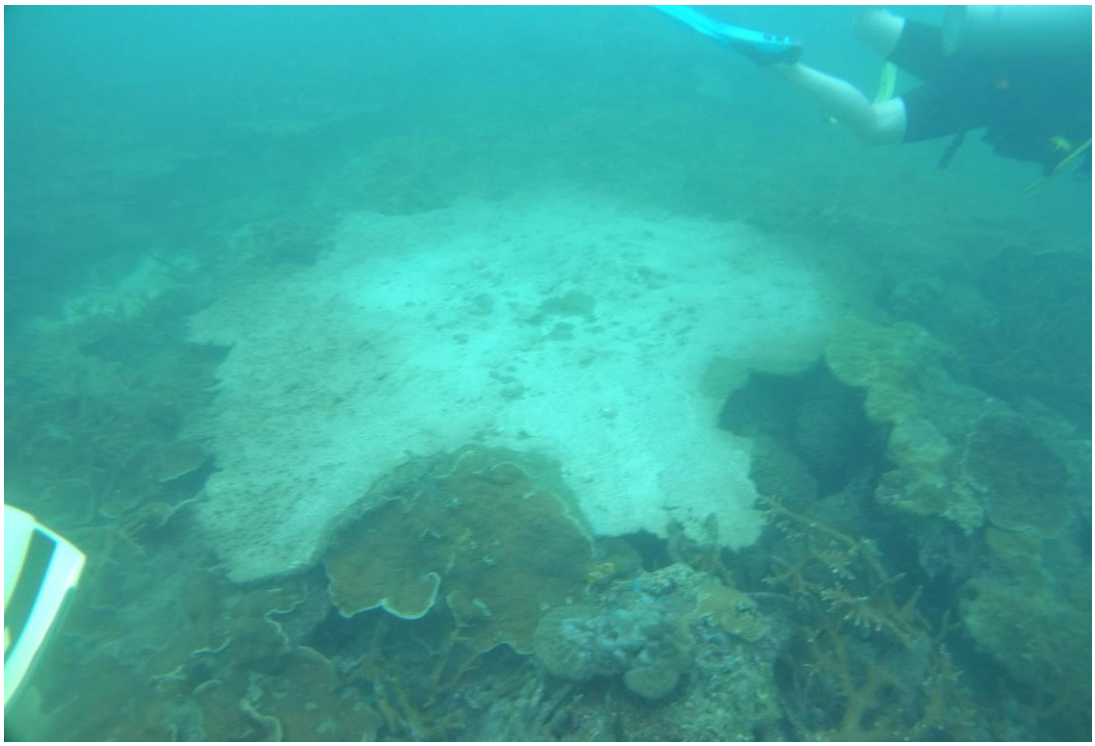

Figure 5.6.11 – Bleached Porites (centre) at Anemone Garden (October, 2016)

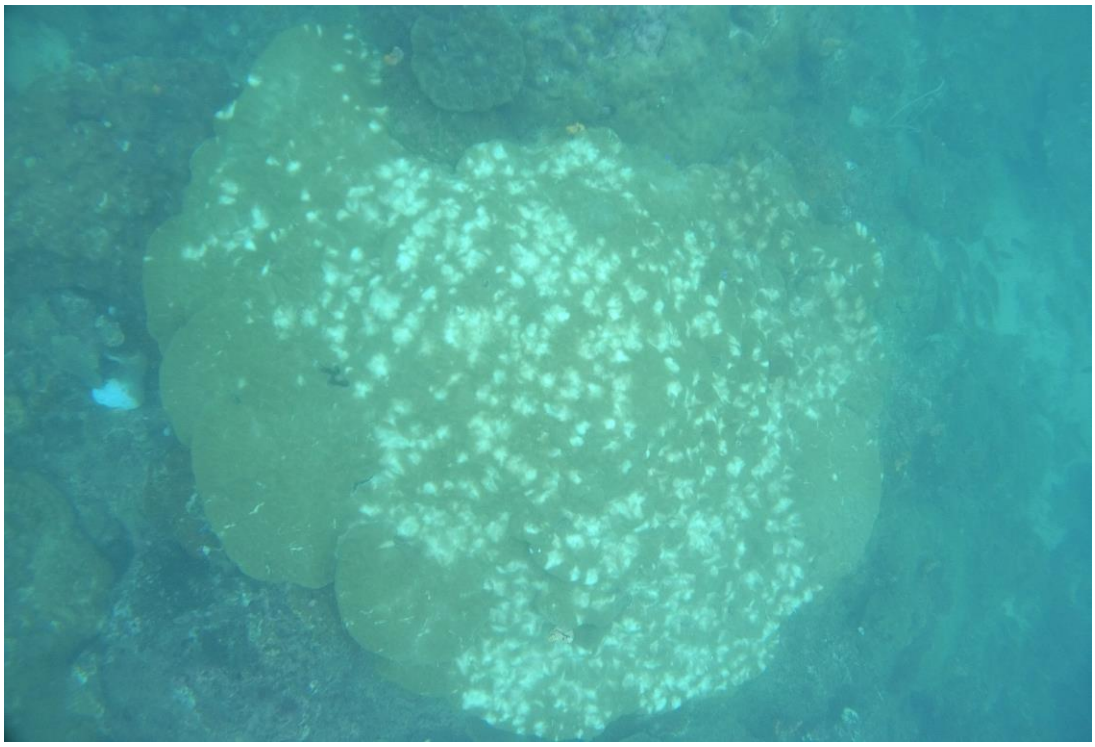

Figure 5.6.12 – Many bleaching spots on Porites at Anemone Garden (October, 2016)

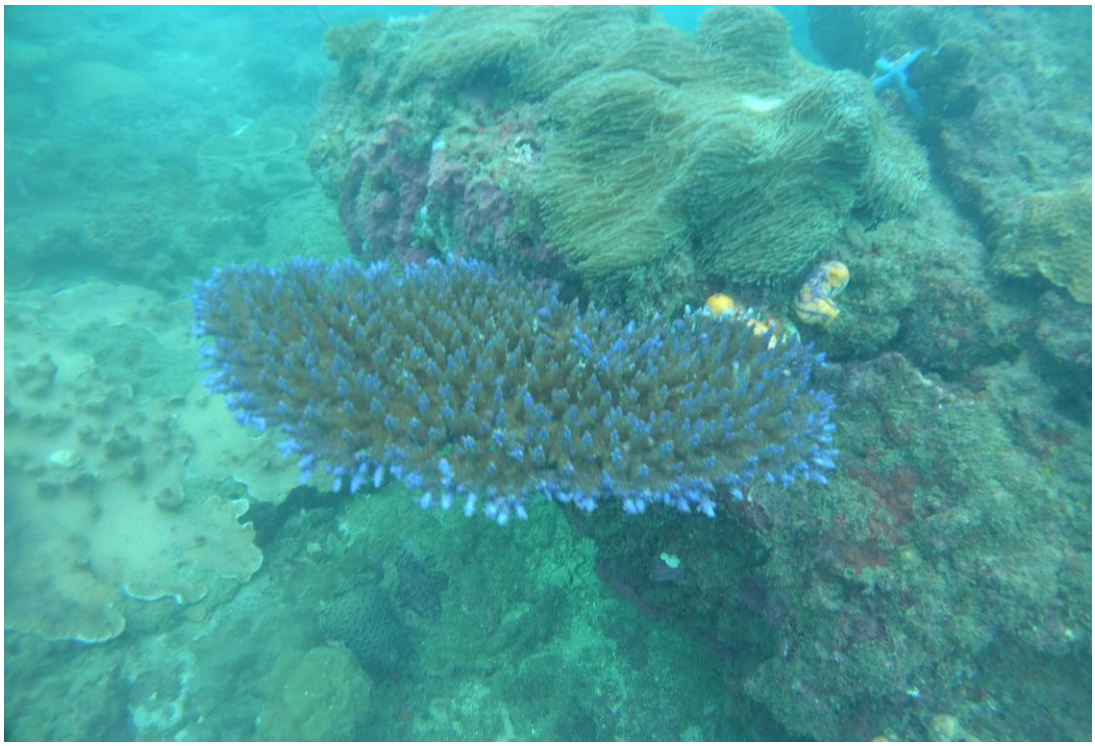

Figure 5.6.13 – Healthy Acropora at Anemone Garden (October, 2016)

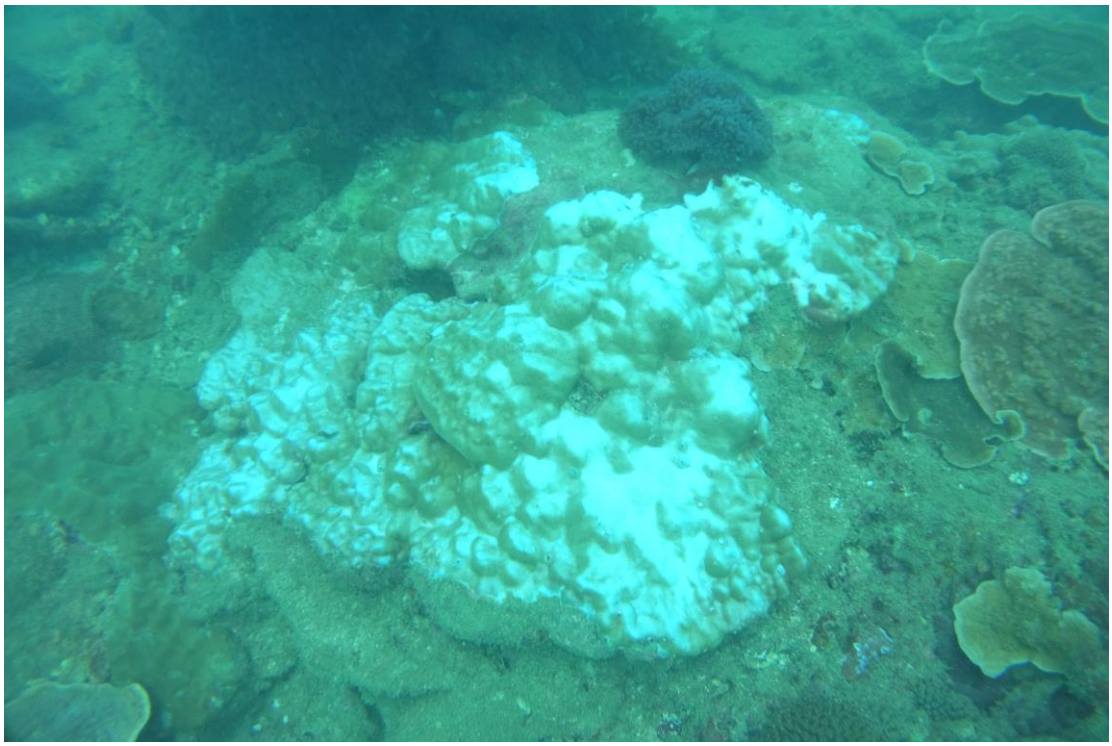

Figure 5.6.14 – Bleaching Porites at Anemone Garden (October, 2016)

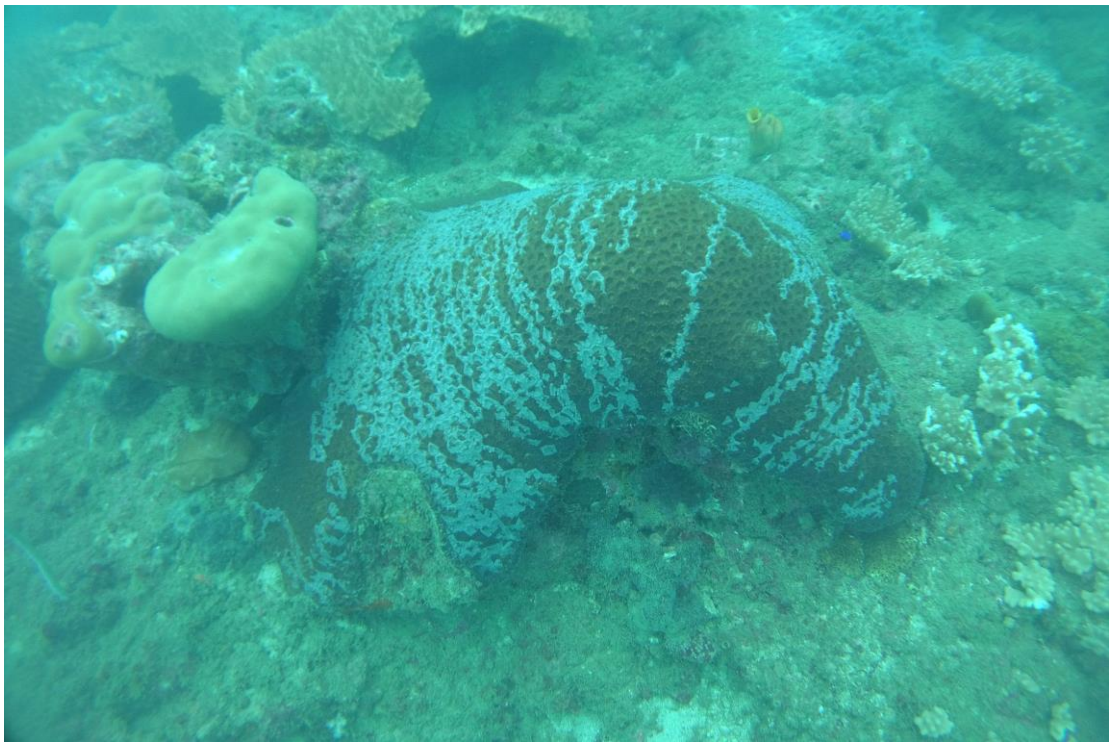

Figure 5.6.15 – Bleaching Favia at Anemone Garden (October, 2016)

Eve's Garden was by far the most affected reef out of all three reefs and had the highest input from the Miri river because of its closeness to its mouth at only 10.70km. Located at around 7km from the shore, it was also the closest and the shallowest at only 6m deep. This site was also the target of dynamite fishing in December 2015 because of the high diversity of corals that was also home to various fish species. The data in Chapter 4 indicates that most nutrients as well as highest turbidity were observed when compared to the other two sites. Figures 5.5.18 to 5.5.23 gives an idea of the level of damage at Eve's Garden. Most of the soft corals are bleached or bleaching and there were also thick layers of algae found all over the seabed. Figure 5.5.18 sums up the state of most of the corals at Eve's Garden, showing the sea floor covered with algae, a bleached soft coral, a bleaching Diploastrea and two Porites filled with coral borers. Figure 5.5.23 shows the level of turbidity present at the site. The last sampling done on 27-10-2016 was even more turbid and visibility at the seabed was less than 1 metre.

Figure 5.6.16 – Acropora at Eve's Garden (May, 2016)

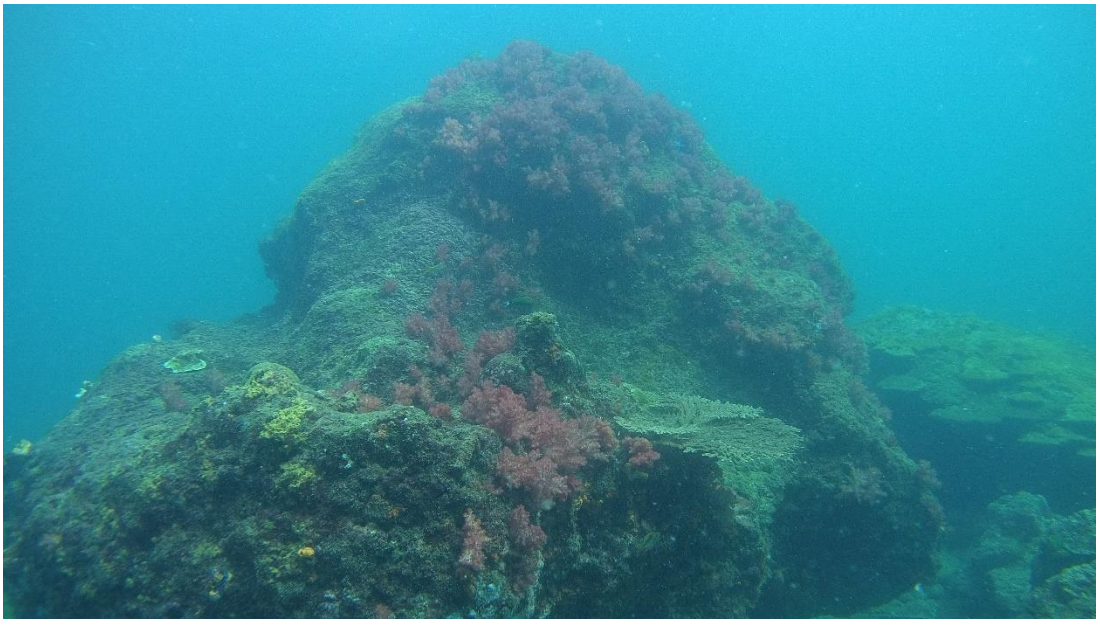

Figure 5.6.17 – Soft Corals at Eve's Garden (May, 2016)

Figure 5.6.18 – Bleached soft coral surrounded by algae at Eve's Garden (October, 2016)

Figure 5.6.19 – Bleached soft coral surrounded by algae at Eve's Garden (October, 2016)

Figure 5.6.20 – Bleached soft corals and algae at Eve's Garden (October, 2016)

Figure 5.6.21 – Bleached Porites, coral borers and algae at Eve's Garden (October, 2016)

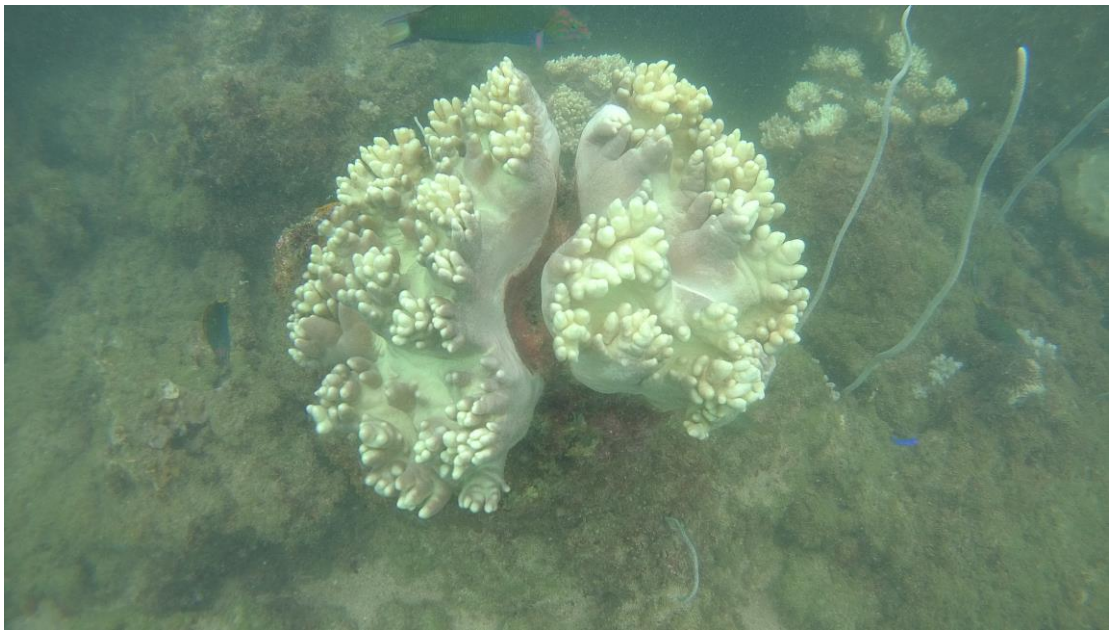

Figure 5.6.22 – Bleached soft coral on an algae-covered seabed at Eve's Garden (October, 2016)

Figure 5.6.23 – Bleached Porites and soft coral in very high turbid water at Eve's Garden (October, 2016)

Figures 5.6.24 to 5.6.30 show some of the coral types at Sipadan out of the hundreds of existing species. The low concentration of nutrients and abundance of ions have shown lower presence of algae and more healthy corals accompanied with many types of fish including white tip sharks, green and leather-back turtles and manta rays to name a few. Figure 5.6.28 shows a broken Acropora table coral. According to the dive

marshal, the coral did not break because of human interference but because of heavy waves from storms crashing into the corals and breaking them. The Porites in Figure 5.6.30 shows many coral borers housed in the coral. These borers, also known as Christmas tree worms are very common in the warm waters of Malaysia and thrive in tropical waters.

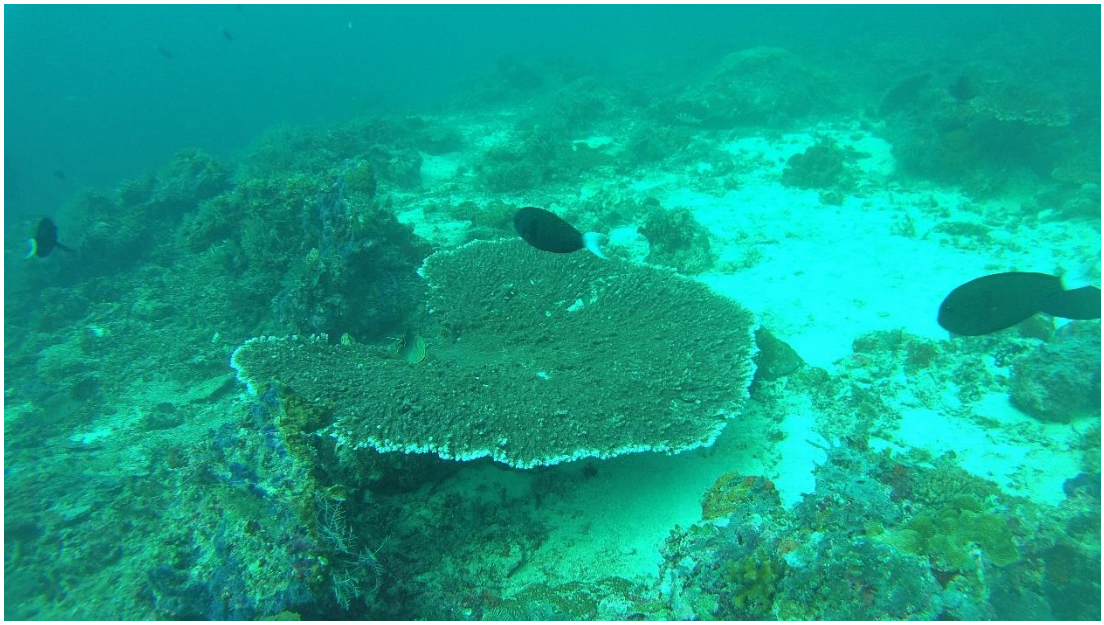

Figure 5.6.24 – Acropora table at Sipadan (October, 2016)

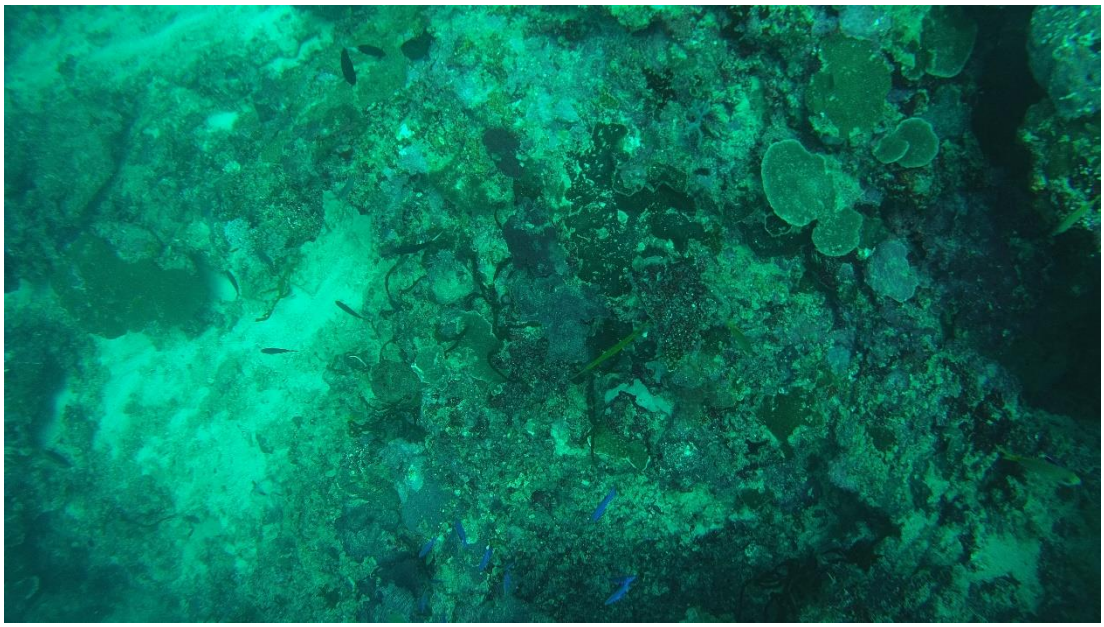

Figure 5.6.25 – Various coral types at Sipadan (October, 2016)

Figure 5.6.26 – Acropora table corals At Sipadan (October, 2016)

Figure 5.6.27 – Acropora Humilis at Sipadan (October, 2016)

Figure 5.6.28 – Broken Acropora table coral (October, 2016)

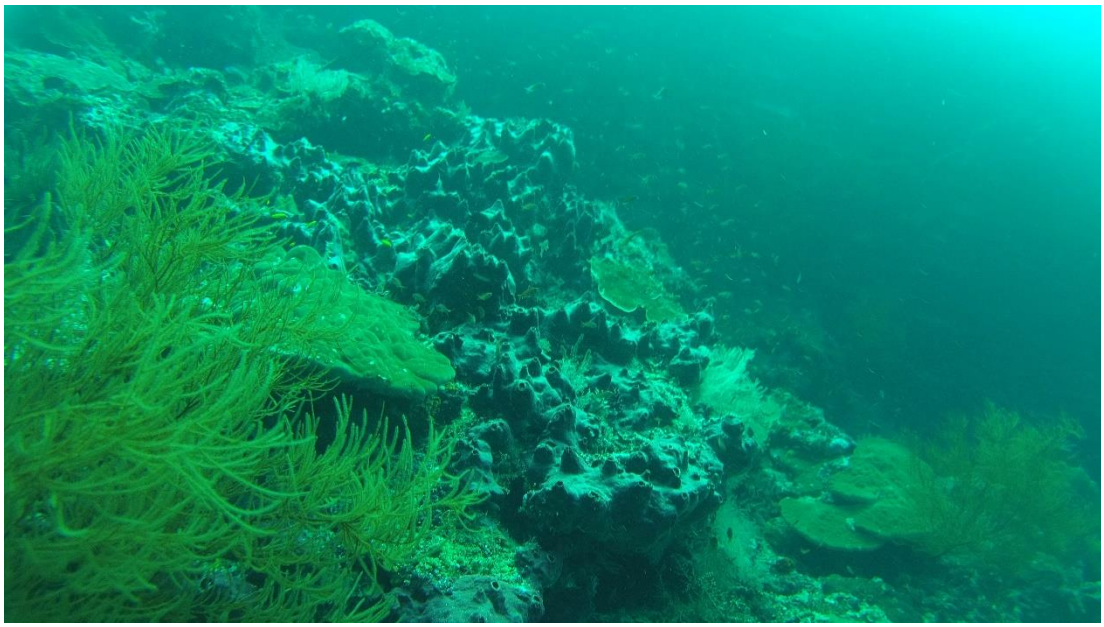

Figure 5.6.29 – Sponge coral and plants at Sipadan (October, 2016)

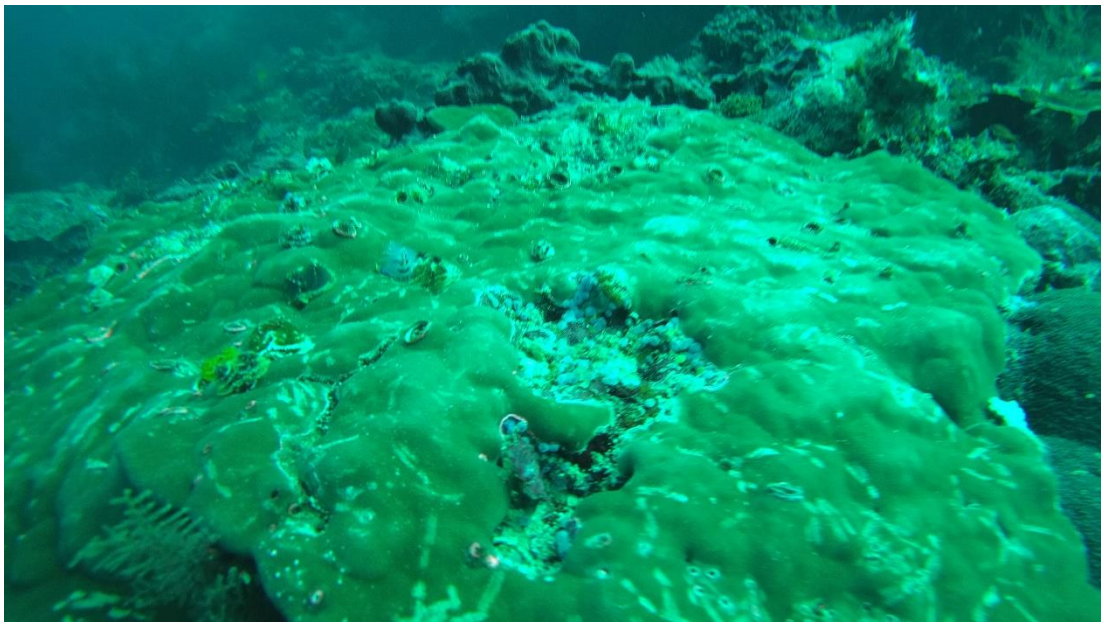

Figure 5.6.30 – Coral borers on a Porites at Sipadan (October, 2016)

A comparison of all three reefs helped identify the coral species which were more resilient to bleaching and the types that would get affected. Diploastrea, Pachyseris and soft corals were more bleached than Favia, Favites, Fungia, and Montipora appeared to be more resistant. Porites are usually more tolerant due to their massive structure and have the ability to resist stormy weathers and heavy waves as opposed to the smaller and more brittle Acropora, Montipora and Favia. North Siwa appeared to be the healthiest which could be mostly due to being the furthest from the shore as well as the Baram and Miri rivers.

Comparatively, the corals in Sipadan appear much healthier than the ones in Miri. The reason behind the better coral health would be mostly due to the strict laws upheld in order to maintain the pristine condition of the park. The rules include capping the number of visitors to the island and diving at the same time to 120 per day, the requirement of a pass given by the Sabah Parks Department before visiting the island, the presence of a dive marshal and a maritime office on the island and lastly, the constant patrolling of maritime officers to guard against poachers, fishermen and other undesirable activities. However, though the corals at MSCRNP are constantly facing high sedimentation, pollution heat stress, they seem to go through the same cycle every year which actually makes them quite resistant.

5.7 Summary and Conclusion

Seawater quality is essential for the survival of the coral environment along with the variety of marine organisms in the ocean. This attempt is the first detailed seawater quality study at Miri-Sibuti Coral Reef National Park (MSCRNP) and the results were compared to that of Sipadan Island Park Coral Reefs. Various parameters were investigated such as the concentration of major ions (HCO_3^-, Ca^{2+}, Mg^{2+}, K^+, Na^+, Cl^-), nutrients (SO_4^{2-}, PO_4^{3-}, NH_3-N, NO_3^-) and trace metals (Cd, Co, Cu, Fe, Mn, Ni, Pb, Zn). In-situ observations (temperature, pH, EC, salinity, ORP, turbidity, TDS and DO) were also conducted as well as the state of the corals at the sites through photo-documentation, direction of the ocean current, and colour of the seawater. The daily, monthly, and yearly rainfall data from 2006 to 2016 were obtained to understand the rainfall pattern and justify the field conditions that would have an influence on the quality of the seawater. Wind speed and direction data from the past eleven years was also obtained because of their importance in influencing the surface ocean currents. Samples at MSCRNP were collected during the start of southwest monsoon (SWM) (May), end of SWM (September), and northeast monsoon transition (NEM) (October) of 2016 from three sites; North Siwa, Anemone Garden and Eve's Garden. Sipadan samples were collected during NEM transition (October 2016) at two sites; Barracuda Point and South Point.

In MSCRNP, the pH, DO and ORP values experienced a decrease from beginning of SWM to NEM transition with the lowest during the end of SWM. The opposite was observed for temperature, EC, salinity and TDS, where the highest value was observed during the transition period. The temperature variation among all the seasons were due to seasonal changes, whereas the influence of the Miri River caused the other parameters such as nutrients, major ions and trace metals to fluctuate. The concentration of phosphate and sulphate were highest during NEM transition and that of nitrate, during the transition period. The higher TDS and turbidity values associated with high nutrient content indicate the presence of anthropogenic sources such as coastal development and river discharge. High concentrations of ammonia-nitrogen during start of SWM were caused by recreational activities such as diving. The variation in the concentration of major ions were due to both river runoffs and the amount of rainfall. Bicarbonate concentration increased from beginning of SWM to NEM transition, whereas magnesium and chloride decreased. Calcium, potassium and

sodium had minimum values during end of SWM. Trace metals that experienced an increase in their concentrations at the start of SWM to NEM transition were cadmium, copper and nickel. Cobalt and lead were below detection limits during beginning and end of SWM but a high concentration of the two metals were observed during transition to NEM, which were attributed to anthropogenic sources.

Depth-wise variations of in-situ parameters, nutrients, major ions and trace metals indicate anthropogenic activities such as river inputs, coastal activities and tourism. Each site was affected differently due to the distance from the mouth of the Miri river, the direction of the ocean current as well as the condition of the sea. At the beginning of SWM, the in-situ parameters that observed an increase from surface to seabed were EC, turbidity, TDS and DO whereas pH, EC and TDS were in transition period. During transition to NEM, the parameters fluctuated more from surface to seabed at each site because of vertical mixing caused by strong waves that had been persisting from transition period. The high concentration of nitrate, at the surface of EG and the seabed of AG during the transition period were due to river runoff, vertical mixing and the current and wind direction. The concentration of phosphate was higher at the seabed during the start and end of SWM period at EG and AG. However, during the end of SWM and NEM transition, phosphate was higher at the surface due to the influence of river runoff. Sulphate also followed the same trend except at EG during the end SWM, where higher values were observed at the surface because of dynamite fishing. Ammonia-Nitrogen had higher values during the beginning of SWM at the middle depth due to the presence of diving activities. The depth-wise decrease in calcium, sodium and chloride, and the increase in magnesium indicated freshwater mixing during the end of SWM and NEM transition. The influence of river runoffs and coastal development were linked to the higher concentrations of the trace metals at the surface.

Statistical analysis also showed a link among the various parameters examined during the study. Higher factor scores relating to anthropogenic activities were more persistent at EG throughout all seasons due to the site's proximity to the Miri river and the constant boat and ship activities around the region. EG, AG and NS had all been exhibiting coral bleaching signs, with EG being the most affected, which were linked to high turbidity during the end of SWM and NEM transition.

From the three sites chosen at MSCRNP, photo-documentation showed EG as the most affected site due to river runoff, coastal development, over fishing, coral bleaching, and an overwhelming presence of algae. The reefs at EG were also very slimy during NEM transition which was a defensive reaction from the corals from being suffocated by a growing population of algae and sponge corals. Most of the soft corals had already bleached at EG and those of AG had also started exhibiting bleached pattern. NS had less soft corals but the hard corals started showing signs of bleaching. NS was also the least affected site and comparatively the healthiest among the three. Photos of the coral reefs at Sipadan showed healthier corals with little algae as compared to MSCRNP. However, the damage observed were because of strong waves during tropical storms as well as human interaction from diving activities.

In Sipadan, the seawater quality indicated very little pollution as compared to MSCRNP. Higher concentration of ammonia-nitrogen was observed at both sites due to the presence of divers and boats, and a slight variation was noted from surface to seabed. The concentration of phosphate at the surface and seabed at BP was also observed to be slightly higher due to tourism on the island. Ni was higher at the surface due to the presence of boat activities. The statistical analysis also confirmed that human interference was higher at Sipadan.

The comparison between MSCRNP and Sipadan indicated higher EC, salinity, TDS and DO values at Sipadan due to the limited presence of freshwater sources. The concentration of ammonia-nitrogen was higher at Sipadan because of the number of divers at the sites and the variation of major ions were also much less as opposed to MSCRNP. In terms of trace metals, Cd, Co and Pb were mostly below detection level and Cu was less at Sipadan than Miri. The overall seawater quality at Sipadan was superior to that of MSCRNP due to strict regulations imposed by the Sabah government to restrict the number of daily tourists. The absence of big ships and oil platforms also contributed to a less affected seawater quality.

As a baseline study of MSCRNP and its comparison to Sipadan Island Park, the reefs in Miri are threatened by coastal development, heavy sedimentation, and other anthropogenic sources than Sipadan Island. Given the constant mixing of seawater through the influence of wind direction and varying ocean currents, the dates during which the samples were taken in 2016 might not have the same results in the future,

therefore to ensure the survival of the reefs, proper management needs to be implemented. Otherwise, the corals would not recover from the heavy amount of nutrients from the river runoff, coastal development, heat stress and decreasing amount of rainfall.

Some recommendations that could be implemented would be to educate the local businesses and industries on the importance of water quality as well as showing them the devastating effects of untreated sewage discharge on the marine fauna. Furthermore, the city council could provide incentives to businesses that opt for wastewater treatment and recycling of solid wastes. A governmental body could also be established in Miri dedicated to the welfare of the marine reserve and enforce its preservation through periodical monitoring and surveying water related activities. The introduction of a limit to the number of tourists in the marine reserve similar to Sipadan would also cause less stress on the coral reefs and seawater quality. This dedicated body could also implement recreational and research areas and rotate some of the sites to monitor the impact on corals which could be further used to research the more resilient corals species. Collaboration between private organisations and governmental bodies to better monitor, protect and conduct research in the reserve could also be established to build a strong data set which could be used to promote the eco-tourism aspect of the city. Working on a feasible fishing alternative could be funded to reduce the stress on the marine reserve. Employing and training people from the fishing villages would also increase awareness of the state of the marine reserve and promote its preservation.

REFERENCES

Abdel Ghani, S. A. (2015). Trace metals in seawater, sediments and some fish species from Marsa Matrouh Beaches in north-western Mediterranean coast, Egypt. *The Egyptian Journal of Aquatic Research, 41*(2), 145-154. http://dx.doi.org/http://dx.doi.org/10.1016/j.ejar.2015.02.006

Abdullah, Mokhtar, M. B., Tahir, S. H. J., and Awaluddin, A. B. T. (1997). Do tides affect water quality in the upper phreatic zone of a small oceanic island, Sipadan Island, Malaysia? *Environmental Geology, 29*(1-2), 112-117. http://dx.doi.org/10.1007/s002540050109

Abdullah, Musta, B., Mokhtar, M., and Aris, A. (2006). Major ions characteristics in a disturbed aquifer of an oceanic island—Sipadan, Malaysia. *Chinese Journal of Geochemistry, 25*(1), 151-152. http://dx.doi.org/10.1007/BF02840033

Abdullah, M. (2017). Authorities asked to probe cause of death of marine life. *Borneo Post Online*,

Abram, N. J., Gagan, M. K., McCulloch, M. T., Chappell, J., and Hantoro, W. S. (2003). Coral reef death during the 1997 Indian Ocean dipole linked to Indonesian wildfires. *Science, 301*(5635), 952-955. Retrieved from https://search.proquest.com/docview/213585570?accountid=10382

Anthoni, F. (2006). The Chemical Composition of Seawater. 2006

APHA. (2012). *Standard Methods for the Examination of Water and Wastewater, 22th Edition*: American Public Health Association, American Water Works Association, Water Environment Federation.

Arakaki, T., Fujimura, H., Hamdun, A., Okada, K., Kondo, H., Oomori, T., . . . Taira, H. (2005). Simultaneous Measurement of Hydrogen Peroxide and Fe Species (Fe(II) and Fe(tot)) in Okinawa Island Seawater: Impacts of Red Soil Pollution. *Journal of Oceanography, 61*(3), 561-568. http://dx.doi.org/10.1007/s10872-005-0064-9

Aronson, R. B., Edmunds, P. J., Precht, W. F., Swanson, D. W., and Levitan, D. R. (1994). Large-Scale, Long-Term Monitoring of Caribbean Coral Reefs: Simple, Quick, Inexpensive Techniques. *NATIONAL MUSEUM OF NATURAL HISTORY, SMITHSONIAN INSTITUTION*, 1-20. http://dx.doi.org/10.5479/si.00775630.421.1

Atkins, J. P., Burdon, D., Elliott, M., and Gregory, A. J. (2011). Management of the marine environment: Integrating ecosystem services and societal benefits with the DPSIR framework in a systems approach. *Marine Pollution Bulletin, 62*(2), 215-226. http://dx.doi.org/http://dx.doi.org/10.1016/j.marpolbul.2010.12.012

Azpurua, M. A., and Ramos, K. D. (2010). A comparison of spatial interpolation methods for estimation of average electromagnetic field magnitude. *Progress In Electromagnetics Research, M*(14), 135-145.

Balch, O. (2015, 11 November 2015). Indonesia's forest fires: everything you need to know. *The Guardian.* Retrieved from https://www.theguardian.com/sustainable-business/2015/nov/11/indonesia-forest-fires-explained-haze-palm-oil-timber-burning

Balls, P. W. (1985). Copper, lead and cadmium in coastal waters of the western North Sea. *Marine Chemistry, 15*(4), 363-378. http://dx.doi.org/http://dx.doi.org/10.1016/0304-4203(85)90047-7

Billah, M. M., Kamal, A. H. M., Hoque, M. M., and Bhuiyan, M. K. A. (2016). Temporal distribution of water characteristics in the Miri estuary, east Malaysia. *Zoology and Ecology*, *26*(2), 134-140. http://dx.doi.org/10.1080/21658005.2016.1148960

Bradshaw, A., and Schleicher, K. (1980). Electrical conductivity of seawater. *IEEE Journal of Oceanic Engineering*, *5*(1), 50-62. http://dx.doi.org/10.1109/JOE.1980.1145449

Briggs, J. (2011). Marine extinctions and conservation. *Marine Biology*, *158*(3), 485-488. http://dx.doi.org/10.1007/s00227-010-1596-0

Brooks, R. R., Presley, B. J., and Kaplan, I. R. (1967). APDC-MIBK extraction system for the determination of trace elements in saline waters by atomic-absorption spectrophotometry. *Talanta*, *14*(7), 809-816. http://dx.doi.org/http://dx.doi.org/10.1016/0039-9140(67)80102-4

Browne, N. K., Tay, J. K. L., Low, J., Larson, O., and Todd, P. A. (2015). Fluctuations in coral health of four common inshore reef corals in response to seasonal and anthropogenic changes in water quality. *Marine Environmental Research*, *105*(0), 39-52. http://dx.doi.org/http://dx.doi.org/10.1016/j.marenvres.2015.02.002

Burgin, S., and Hardiman, N. (2015). Effects of non-consumptive wildlife-oriented tourism on marine species and prospects for their sustainable management. *Journal of Environmental Management*, *151*(0), 210-220. http://dx.doi.org/http://dx.doi.org/10.1016/j.jenvman.2014.12.018

Burrough, P. A., and Mcdonnell. (1998). *Principles of GIS*.

Cabon, J. Y., Burel, L., Jaffrennou, C., Giamarchi, P., and Bautin, F. (2007). Study of trace metal leaching from coals into seawater. *Chemosphere*, *69*(7), 1100-1110. http://dx.doi.org/http://dx.doi.org/10.1016/j.chemosphere.2007.04.018

Cairns, D. (2012). Tourism And The Reef. Retrieved from https://www.divingcairns.com.au/reef_tourism

Chan, F. (2016, 30 August). 60% of forest fires in Kalimantan, Sumatra not on concession land. *The Straits Times Singapore*. Retrieved from http://www.straitstimes.com/asia/se-asia/60-of-forest-fires-not-on-concession-land

Chidambaram, S., Thilagavathi, R., Thivya, C., Karmegam, U., Prasanna, M. V., Ramanathan, A., . . . Sasidhar, P. (2016). A study on the arsenic concentration in groundwater of a coastal aquifer in south-east India: an integrated approach. *Environment, Development and Sustainability*, 1-26. http://dx.doi.org/10.1007/s10668-016-9786-7

Chung, S.-s., Au, A., and Qiu, J.-W. (2013). Understanding the Underwater Behaviour of Scuba Divers in Hong Kong. *Environmental Management*, *51*(4), 824-837. http://dx.doi.org/10.1007/s00267-013-0023-y

Costanza, R., de Groot, R., Sutton, P., van der Ploeg, S., Anderson, S. J., Kubiszewski, I., . . . Turner, R. K. (2014). Changes in the global value of ecosystem services. *Global Environmental Change*, *26*, 152-158. http://dx.doi.org/https://doi.org/10.1016/j.gloenvcha.2014.04.002

Crompton, T. R. (2006). Analysis of Seawater.1 ed.: (Springer-Verlag Berlin Heidelberg).

Cuoco, E., Darrah, T. H., Buono, G., Verrengia, G., De Francesco, S., Eymold, W. K., and Tedesco, D. (2015). Inorganic contaminants from diffuse pollution in shallow groundwater of the Campanian Plain (Southern Italy). Implications

for geochemical survey. *Environmental Monitoring and Assessment, 187*(2), 1-17. http://dx.doi.org/10.1007/s10661-015-4307-y
Dimmock, K., and Musa, G. (2015). Scuba Diving Tourism System: A framework for collaborative management and sustainability. *Marine Policy, 54*(0), 52-58. http://dx.doi.org/http://dx.doi.org/10.1016/j.marpol.2014.12.008
Dive-The-World. (2014). A Brief History of Pulau Sipadan. Retrieved from http://www.dive-the-world.com/reefs-and-parks-malaysia-sipadan-history.php
Drupp, P. S. (2015). *Observations and modeling of the CO2-carbonic acid system on Hawaiian coral reefs: Implications of future ocean acidification and climate change.* 10085580 (Ph.D.). University of Hawai'i at Manoa, Ann Arbor. Retrieved from https://search.proquest.com/docview/1779659769?accountid=10382
Dulvy, N. (2005). Extinction and Threat in the Sea. Retrieved from http://www.ifremer.fr/gascogne/actualite/colloque/atelier-biodiversite/dulvy.pdf
Dygico, M., Songco, A., White, A. T., and Green, S. J. (2013). Achieving MPA effectiveness through application of responsive governance incentives in the Tubbataha reefs. *Marine Policy, 41*, 87-94. http://dx.doi.org/http://dx.doi.org/10.1016/j.marpol.2012.12.031
Edzwald, J. K., and Haarhoff, J. (2011). Seawater pretreatment for reverse osmosis: Chemistry, contaminants, and coagulation. *Water Research, 45*(17), 5428-5440. http://dx.doi.org/http://dx.doi.org/10.1016/j.watres.2011.08.014
Elcee-Instrumentation, S. B. (2002). *An Integrated Approach to a Reef Management Program (ReefMap) for the Miri-Sibuti Reefs, Sarawak.*
Enviroware. (2017). Win Rose Online.
Fabinyi, M. (2008). Dive tourism, fishing and marine protected areas in the Calamianes Islands, Philippines. *Marine Policy, 32*(6), 898-904. http://dx.doi.org/http://dx.doi.org/10.1016/j.marpol.2008.01.004
Fabricius, K. E. (2005). Effects of terrestrial runoff on the ecology of corals and coral reefs: review and synthesis. *Marine Pollution Bulletin, 50*(2), 125-146. http://dx.doi.org/http://dx.doi.org/10.1016/j.marpolbul.2004.11.028
Florence, T. M., and Batley, G. E. (1976). Trace metals species in sea-water—I. *Talanta, 23*(3), 179-186. http://dx.doi.org/http://dx.doi.org/10.1016/0039-9140(76)80166-X
Francis, R., and McIntyre, D. R. (2016). CASE HISTORIES: The Importance of Redox Potential on Corrosion Control. *Materials Performance, 55*(5), 48-54. Retrieved from http://search.proquest.com/docview/1787079206?accountid=10382
Gerhard, K. (2009). Dissolved Organic and Particulate Nitrogen and Phosphorous *Practical Guidelines for the Analysis of Seawater*: CRC Press. http://dx.doi.org/:doi:10.1201/9781420073072.ch9
Grasshoff, K., Kremling, K., and Ehrhardt, M. (1999). *Methods of Seawater Analysis* (3rd ed.): WILEY-VCH.
Griffis, R., and Howard, J. (2013). Oceans and Marine Resources In a Changing Climate. *Sea Technology, 54*(10), 65. Retrieved from https://search.proquest.com/docview/1458210887?accountid=10382
HACH. (2007). DR 2800 Spectrophotometer.
HACH. (2013). HQd Portable Meter.

HACH®. (2015a). Nitrate: Cadmium Reduction Method 8192. 21 Jan 2016 Retrieved from http://www.hach.com/
HACH®. (2015b). Nitrogen, Ammonia: Salicylate Method 8155. 21 Jan 2016 Retrieved from http://www.hach.com/
HACH®. (2015c). Phosphorus, Reactive (Orthophosphate): PhosVer 3® Ascorbic Acid Method 8048. 21 Jan 2016 Retrieved from http://www.hach.com/
HACH®. (2015d). Sulfate: SulfaVer 4 Method 8051. 21 Jan 2016 Retrieved from http://www.hach.com/
Hall, I. R., Hydes, D. J., Statham, P. J., and Overnell, J. (1996). Dissolved and particulate trace metals in a Scottish sea loch: an example of a pristine environment? *Marine Pollution Bulletin, 32*(12), 846-854. http://dx.doi.org/http://dx.doi.org/10.1016/S0025-326X(96)00030-6
Hasan, A. B., Kabir, S., Selim Reza, A. H. M., Zaman, M. N., Ahsan, M. A., Akbor, M. A., and Rashid, M. M. (2013). Trace metals pollution in seawater and groundwater in the ship breaking area of Sitakund Upazilla, Chittagong, Bangladesh. *Marine Pollution Bulletin, 71*(1–2), 317-324. http://dx.doi.org/http://dx.doi.org/10.1016/j.marpolbul.2013.01.028
Health, O. (2016). Chemistry of Seawater. Retrieved from http://oceanplasma.org/documents/chemistry.html
Hearn, A., Acuña, D., Ketchum, J., Peñaherrera, C., Green, J., Marshall, A., . . . Shillinger, G. (2014). Elasmobranchs of the Galapagos Marine Reserve. In J. Denkinger and L. Vinueza (Eds.), *The Galapagos Marine Reserve* (pp. 23-59): Springer International Publishing. http://dx.doi.org/:10.1007/978-3-319-02769-2_2
Higuchi, T., Yuyama, I., and Nakamura, T. (2015). The combined effects of nitrate with high temperature and high light intensity on coral bleaching and antioxidant enzyme activities. *Regional Studies in Marine Science,* http://dx.doi.org/http://dx.doi.org/10.1016/j.rsma.2015.08.012
Hobbs, J.-P. A., Frisch, A. J., Ford, B. M., Thums, M., Saenz-Agudelo, P., Furby, K. A., and Berumen, M. L. (2013). Taxonomic, Spatial and Temporal Patterns of Bleaching in Anemones Inhabited by Anemonefishes. *PLoS ONE, 8*(8), e70966. http://dx.doi.org/10.1371/journal.pone.0070966
Hoey, A. H., E.; Johansen, J.; Hobbs, Jean-Paul; Messmer, V.; McCowan, D.; Wilson, S.; Pratchett, M. (2016). Recent advances in understanding the effects of climate change on coral reefs.
Howard, J., Auer, C., Beard, R., Bond, N., Boyer, T., Brown, D., . . . Xue, Y. (2013). Climate-Driven Physical and Chemical Changes in Marine Ecosystems. In R. Griffis and J. Howard (Eds.), *Oceans and Marine Resources in a Changing Climate: A Technical Input to the 2013 National Climate Assessment* (pp. 7-34). Washington, DC: Island Press/Center for Resource Economics. http://dx.doi.org/:10.5822/978-1-61091-480-2_2
Hutchins, D. A., and Boyd, P. W. (2016). Marine phytoplankton and the changing ocean iron cycle. *Nature Clim. Change, 6*(12), 1072-1079. http://dx.doi.org/10.1038/nclimate3147
Ilter., Kanat, G., and Bayhan, H. (2012). Sea water quality assessment of Prince Islands' Beaches in Istanbul. *Environmental Monitoring and Assessment, 184*(1), 149-160. http://dx.doi.org/10.1007/s10661-011-1954-5
International, C. (2008). *Economic Values of Coral Reefs, Mangroves, and Seagrasses: A Global Compilation*

International, D. (1997). Sipadan, The Problems. Retrieved from http://www.ukdiving.co.uk/conservation/articles/sipadan2.htm

Jakobsen, F., Hartstein, N., Frachisse, J., and Golingi, T. (2007). Sabah shoreline management plan (Borneo, Malaysia): Ecosystems and pollution. *Ocean & Coastal Management, 50*(1–2), 84-102. http://dx.doi.org/http://dx.doi.org/10.1016/j.ocecoaman.2006.03.013

Jones, R., Fisher, R., Stark, C., and Ridd, P. (2015). Temporal Patterns in Seawater Quality from Dredging in Tropical Environments. *PLoS ONE, 10*(10), e0137112. http://dx.doi.org/10.1371/journal.pone.0137112

Joniston, B. (2004, 05/14/2004). Visits to Sipadan Island only by day to protect environs. *New Straits Times.* p. 07. Retrieved from http://search.proquest.com/docview/271812218?accountid=10382

Keith, H., Russell, F., and Sylvia, G. S. (2009). Sampling and Measurements of Trace Metals in Seawater *Practical Guidelines for the Analysis of Seawater*: CRC Press. http://dx.doi.org/:doi:10.1201/9781420073072.ch14

Kitchen-Wheeler, A.-M., Ari, C., and Edwards, A. (2012). Population estimates of Alfred mantas (Manta alfredi) in central Maldives atolls: North Male, Ari and Baa. *Environmental Biology of Fishes, 93*(4), 557-575. http://dx.doi.org/10.1007/s10641-011-9950-8

Komjarova, I., and Blust, R. (2006). Comparison of liquid–liquid extraction, solid-phase extraction and co-precipitation preconcentration methods for the determination of cadmium, copper, nickel, lead and zinc in seawater. *Analytica Chimica Acta, 576*(2), 221-228. http://dx.doi.org/http://dx.doi.org/10.1016/j.aca.2006.06.002

Krieger, J., and Chadwick, N. (2013). Recreational diving impacts and the use of pre-dive briefings as a management strategy on Florida coral reefs. *Journal of Coastal Conservation, 17*(1), 179-189. http://dx.doi.org/10.1007/s11852-012-0229-9

Krupp, F., and Abuzinada, A. H. (2008). Impact of oil pollution and increased sea surface temperatures on marine ecosystems and biota in the Gulf. In A. H. Abuzinada, H.-J. Barth, F. Krupp, B. Böer and T. Z. Al Abdessalaam (Eds.), *Protecting the Gulf's Marine Ecosystems from Pollution* (pp. 45-56). Basel: Birkhäuser Basel. http://dx.doi.org/:10.1007/978-3-7643-7947-6_3

Kura, N., Ramli, M., Ibrahim, S., Sulaiman, W., Aris, A., Tanko, A., and Zaudi, M. (2015). Assessment of groundwater vulnerability to anthropogenic pollution and seawater intrusion in a small tropical island using index-based methods. *Environmental Science and Pollution Research, 22*(2), 1512-1533. http://dx.doi.org/10.1007/s11356-014-3444-0

Lamb, J. B., True, J. D., Piromvaragorn, S., and Willis, B. L. (2014). Scuba diving damage and intensity of tourist activities increases coral disease prevalence. *Biological Conservation, 178*, 88-96. http://dx.doi.org/http://dx.doi.org/10.1016/j.biocon.2014.06.027

Lee, J.-M., Boyle, E. A., Echegoyen-Sanz, Y., Fitzsimmons, J. N., Zhang, R., and Kayser, R. A. (2011). Analysis of trace metals (Cu, Cd, Pb, and Fe) in seawater using single batch nitrilotriacetate resin extraction and isotope dilution inductively coupled plasma mass spectrometry. *Analytica Chimica Acta, 686*(1–2), 93-101. http://dx.doi.org/https://doi.org/10.1016/j.aca.2010.11.052

Lee, M., Bae, W., Chung, J., Jung, H.-S., and Shim, H. (2008). Seasonal and spatial characteristics of seawater and sediment at Youngil bay, Southeast Coast of

Korea. *Marine Pollution Bulletin, 57*(6–12), 325-334. http://dx.doi.org/http://dx.doi.org/10.1016/j.marpolbul.2008.04.038
Lemke, L., and Olech, L. (2011). Dive tourism. In A. Papathanassis (Ed.), *The Long Tail of Tourism* (pp. 105-114): Gabler. http://dx.doi.org/:10.1007/978-3-8349-6231-7_12
Lenntech. (2005). Composition of Seawater. Retrieved from http://www.lenntech.com/composition-seawater.htm
Lenntech. (2017a). Cadmium - Cd. Retrieved from http://www.lenntech.com/periodic/elements/cd.htm
Lenntech. (2017b). Calcium (Ca) and water. Retrieved from http://www.lenntech.com/periodic/water/calcium/calcium-and-water.htm
Lenntech. (2017c). Cobalt - Co. Retrieved from http://www.lenntech.com/periodic/elements/co.htm
Lenntech. (2017d). Copper - Cu. Retrieved from http://www.lenntech.com/periodic/elements/cu.htm
Lenntech. (2017e). Iron - Fe. Retrieved from http://www.lenntech.com/periodic/elements/fe.htm
Lenntech. (2017f). Lead - Pb. Retrieved from http://www.lenntech.com/periodic/elements/pb.htm
Lenntech. (2017g). Magnesium (Mg) and water. Retrieved from http://www.lenntech.com/periodic/water/magnesium/magnesium-and-water.htm
Lenntech. (2017h). Manganese - Mn. Retrieved from http://www.lenntech.com/periodic/elements/mn.htm
Lenntech. (2017i). Nickel - Ni. Retrieved from http://www.lenntech.com/periodic/elements/ni.htm
Lenntech. (2017j). Potassium - K. Retrieved from http://www.lenntech.com/periodic/elements/k.htm
Lenntech. (2017k). Sodium - Na. Retrieved from http://www.lenntech.com/periodic/elements/na.htm
Lenntech. (2017l). Zinc - Zn. Retrieved from http://www.lenntech.com/periodic/elements/zn.htm
Lewis, E. L., and Perkin, R. G. (1978). Salinity: Its definition and calculation. *Journal of Geophysical Research: Oceans, 83*(C1), 466-478. http://dx.doi.org/10.1029/JC083iC01p00466
Lough, J. M., and van Oppen, M. J. H. (2009). Coral Bleaching — Patterns, Processes, Causes and Consequences. In M. J. H. van Oppen and J. M. Lough (Eds.), *Coral Bleaching: Patterns, Processes, Causes and Consequences* (pp. 1-5). Berlin, Heidelberg: Springer Berlin Heidelberg. http://dx.doi.org/:10.1007/978-3-540-69775-6_1
Lü, D., Zheng, B., Fang, Y., Shen, G., and Liu, H. (2015). Distribution and pollution assessment of trace metals in seawater and sediment in Laizhou Bay. *Chinese Journal of Oceanology and Limnology, 33*(4), 1053-1061. http://dx.doi.org/10.1007/s00343-015-4226-3
Mackey, D. J., Butler, E. C. V., Carpenter, P. D., Higgins, H. W., O'Sullivan, J. E., and Plaschke, R. B. (1996). Trace elements and organic matter in a pristine environment: Bathurst Harbour, Southwestern Tasmania. *Science of The Total Environment, 191*(1), 137-151. http://dx.doi.org/http://dx.doi.org/10.1016/0048-9697(96)05255-2

Makkaveev, P. N. (2009). The features of the correlation between the pH values and the dissolved oxygen at the Chistaya Balka test area in the Northern Caspian Sea. *Oceanology, 49*(4), 466-472. http://dx.doi.org/10.1134/s0001437009040043

Malaysia, R. C. (2015a). Reef Check Malaysia. 23 Dec 2015 Retrieved from http://www.reefcheck.org.my/

Malaysia, R. C. (2015b). Reef Check Malaysia Annual Report (2015). 23 Dec 2015 Retrieved from http://www.reefcheck.org.my/

Malaysia, W. (2015). Facts and Details about Malaysia. Retrieved from http://www.wonderfulmalaysia.com/malaysia-facts-and-details.htm

Malaysiaasia. (2014, April 1). Miri Diving Sites Retrieved from http://blog.malaysia-asia.my/2015/02/miri-diving-sites.html

Manikandan, B., Ravindran, J., Vidya, P. J., and Mani Murali, R. (2016). Bleaching and recovery patterns of corals in Palk Bay, India: An indication of bleaching resilient reef. *Regional Studies in Marine Science, 8, Part 1*, 151-156. http://dx.doi.org/http://dx.doi.org/10.1016/j.rsma.2016.07.005

Masud, M. M., and Kari, F. B. (2015). Community attitudes towards environmental conservation behaviour: An empirical investigation within MPAs, Malaysia. *Marine Policy, 52*, 138-144. http://dx.doi.org/http://dx.doi.org/10.1016/j.marpol.2014.10.015

Measurements, F. o. E. (2016a). Algae, Phytoplankton and Chlorophyll. Retrieved from http://www.fondriest.com/environmental-measurements/parameters/water-quality/algae-phytoplankton-chlorophyll/#algae16

Measurements, F. o. E. (2016a). Conductivity, Salinity & Total Dissolved Solids. Retrieved from http://www.fondriest.com/environmental-measurements/parameters/water-quality/conductivity-salinity-tds/#cond1

Measurements, F. o. E. (2016b). Dissolved Oxygen. Retrieved from http://www.fondriest.com/environmental-measurements/parameters/water-quality/dissolved-oxygen/

Measurements, F. o. E. (2016c). pH of Water. Retrieved from http://www.fondriest.com/environmental-measurements/parameters/water-quality/ph/#

Measurements, F. o. E. (2016b). Turbidity, Total Suspended Solids & Water Clarity. Retrieved from http://www.fondriest.com/environmental-measurements/parameters/water-quality/turbidity-total-suspended-solids-water-clarity/

Measurements, F. o. E. (2016d). Water Temperature. Retrieved from http://www.fondriest.com/environmental-measurements/parameters/water-quality/water-temperature/#watertemp1

Mentasti, E., Nicolotti, A., Porta, V., and Sarzanini, C. (1989). Comparison of different pre-concentration methods for the determination of trace levels of arsenic, cadmium, copper, mercury, lead and selenium. *Analyst, 114*(9), 1113-1117. http://dx.doi.org/10.1039/AN9891401113

Mezhoud, N., Temimi, M., Zhao, J., Al Shehhi, M. R., and Ghedira, H. (2016). Analysis of the spatio-temporal variability of seawater quality in the southeastern Arabian Gulf. *Marine Pollution Bulletin, 106*(1–2), 127-138. http://dx.doi.org/http://dx.doi.org/10.1016/j.marpolbul.2016.03.016

Miller, J., Sweet, M. J., Wood, E., and Bythell, J. (2015). Baseline coral disease surveys within three marine parks in Sabah, Borneo. *PeerJ, 3*, e1391. http://dx.doi.org/10.7717/peerj.1391

Miller, L. A., and Bruland, K. W. (1994). Determination of copper speciation in marine waters by competitive ligand equilibration/liquid - liquid extraction: An evaluation of the technique. *Analytica Chimica Acta, 284*(3), 573-586. http://dx.doi.org/http://dx.doi.org/10.1016/0003-2670(94)85062-3

Mograbi, J., and Rogerson, C. (2007). Maximising the Local Pro-Poor Impacts of Dive Tourism: Sodwana Bay, South Africa. *Urban Forum, 18*(2), 85-104. http://dx.doi.org/10.1007/s12132-007-9002-9

Mokhtar, M. B., Praveena, S. M., Aris, A. Z., Yong, O. C., and Lim, A. P. (2012). Trace metal (Cd, Cu, Fe, Mn, Ni and Zn) accumulation in Scleractinian corals: A record for Sabah, Borneo. *Marine Pollution Bulletin, 64*(11), 2556-2563. http://dx.doi.org/http://dx.doi.org/10.1016/j.marpolbul.2012.07.030

Musa, G. (2002). Sipadan: A SCUBA-diving paradise: An analysis of tourism impact, diver satisfaction and tourism management. *Tourism Geographies, 4*(2), 195-209. http://dx.doi.org/10.1080/14616680210124927

Nair, T. M., and Balakrishnan. (2006). Monsoon control on trace metal fluxes in the deep Arabian Sea. *Journal of Earth System Science, 115*(4), 461-472. http://dx.doi.org/http://dx.doi.org/10.1007/BF02702874

National Oceanic and Atmospheric Administration. (2014). Marine Protected Areas. Retrieved from http://oceanservice.noaa.gov/ecosystems/mpa/

Naumann, M., Bednarz, V., Ferse, S. A., Niggl, W., and Wild, C. (2015). Monitoring of coastal coral reefs near Dahab (Gulf of Aqaba, Red Sea) indicates local eutrophication as potential cause for change in benthic communities. *Environmental Monitoring and Assessment, 187*(2), 1-14. http://dx.doi.org/10.1007/s10661-014-4257-9

Noack, C. W., Dzombak, D. A., and Karamalidis, A. K. (2015). Determination of Rare Earth Elements in Hypersaline Solutions Using Low-Volume, Liquid–Liquid Extraction. *Environmental Science & Technology, 49*(16), 9423-9430. http://dx.doi.org/10.1021/acs.est.5b00151

NOS. (2017). Currents. 6 July. *NOS Education* Retrieved from https://oceanservice.noaa.gov/education/tutorial_currents/welcome.html

Oliver, J. K., Berkelmans, R., and Eakin, C. M. (2009). Coral Bleaching in Space and Time. In M. J. H. van Oppen and J. M. Lough (Eds.), *Coral Bleaching: Patterns, Processes, Causes and Consequences* (pp. 21-39). Berlin, Heidelberg: Springer Berlin Heidelberg. http://dx.doi.org/:10.1007/978-3-540-69775-6_3

Paraskevopoulou, V., Zeri, C., Kaberi, H., Chalkiadaki, O., Krasakopoulou, E., Dassenakis, M., and Scoullos, M. (2014). Trace metal variability, background levels and pollution status assessment in line with the water framework and Marine Strategy Framework EU Directives in the waters of a heavily impacted Mediterranean Gulf. *Marine Pollution Bulletin, 87*(1–2), 323-337. http://dx.doi.org/http://dx.doi.org/10.1016/j.marpolbul.2014.07.054

Pitkin, L. (2011). Sipadan Revisited. *Dive Magazine* Retrieved from http://divemagazine.co.uk/go/6590-sipadan-2

Prasanna, M. V., Chidambaram, S., and Srinivasamoorthy, K. (2010). Statistical analysis of the hydrogeochemical evolution of groundwater in hard and sedimentary aquifers system of Gadilam river basin, South India. *Journal of*

King Saud University - Science, *22*(3), 133-145. http://dx.doi.org/http://dx.doi.org/10.1016/j.jksus.2010.04.001

Prasanna, M. V., Praveena, S. M., Chidambaram, S., Nagarajan, R., and Elayaraja, A. (2012). Evaluation of water quality pollution indices for heavy metal contamination monitoring: a case study from Curtin Lake, Miri City, East Malaysia. *Environmental Earth Sciences*, *67*(7), 1987-2001. http://dx.doi.org/10.1007/s12665-012-1639-6

Praveena, S. M., Siraj, S. S., and Aris, A. Z. (2012). Coral reefs studies and threats in Malaysia: a mini review. *Reviews in Environmental Science and Bio/Technology*, *11*(1), 27-39. http://dx.doi.org/10.1007/s11157-011-9261-8

Rakestraw, N. W. (1943). The Oceans: Their Physics, Chemistry, and General Biology (Sverdrup, H. U.; Johnson, Martin W.; Fleming, Richard H.). *Journal of Chemical Education*, *20*(10), 517. http://dx.doi.org/10.1021/ed020p517.1

Ramesh, R., and Anbu, M. (1996). Chemical Methods for Environmental Analysis: Water and Sediment. India: MacMillan Publishers.

Raphael, J. (2013). Miri offers great diving sites. Retrieved from http://www.theborneopost.com/2013/07/28/miri-offers-great-diving-sites/

Readman, J., DeLuna, F., Ebinghaus, R., Guzman, A., Price, A. G., Readman, E., . . . Sheppard, C. C. (2013). *Coral Reefs of the United Kingdom Overseas Territories* (Vol. 4): Springer Netherlands.

Rodriguez, I. B., Lin, S., Ho, J., and Ho, T.-Y. (2016). Effects of Trace Metal Concentrations on the Growth of the Coral Endosymbiont Symbiodinium kawagutii. *Frontiers in Microbiology*, *7*, 82. http://dx.doi.org/10.3389/fmicb.2016.00082

Rose, D. (2013). Corals at diving sites off Miri among healthiest and most beautiful. Retrieved from http://www.thestar.com.my/News/Community/2013/07/21/Offshore-tourism-gold-mine-Corals-at-diving-sites-off-Miri-among-healthiest-and-most-beautiful/

Sabah, G. o. (2007). Diving Sites. Retrieved from http://ww2.sabah.gov.my/pd.sprn/sipadan.html

Salim, N., Bahauddin, A., and Mohamed, B. (2013). Influence of scuba divers' specialization on their underwater behavior. *Worldwide Hospitality and Tourism Themes*, *5*(4), 388-397. http://dx.doi.org/10.1108/WHATT-03-2013-0015

Schintu, M., Marrucci, A., and Marras, B. (2014). Passive Sampling Technologies for the Monitoring of Organic and Inorganic Contaminants in Seawater. In G. Cao and R. Orrù (Eds.), *Current Environmental Issues and Challenges* (pp. 217-237): Springer Netherlands. http://dx.doi.org/:10.1007/978-94-017-8777-2_14

Scientific, T. (2010). Thermo Scientific Orion Star and Star Plus Meter User Guide. (Thermo Fisher Scientific Inc.).

Setianto, A., and Triandini, T. (2015). Comparison of kriging and inverse distance weighted (IDW) interpolation methods in lineament extraction and analysis. *Journal of Applied Geology, 5(1)*

Singaraja, C., Chidambaram, S., Anandhan, P., Prasanna, M. V., Thivya, C., and Thilagavathi, R. (2015). A study on the status of saltwater intrusion in the coastal hard rock aquifer of South India. *Environment, Development and Sustainability*, *17*(3), 443-475. http://dx.doi.org/10.1007/s10668-014-9554-5

Singaraja, C., Chidambaram, S., Prasanna, M. V., Thivya, C., and Thilagavathi, R. (2014). Statistical analysis of the hydrogeochemical evolution of groundwater in hard rock coastal aquifers of Thoothukudi district in Tamil Nadu, India. *Environmental Earth Sciences, 71*(1), 451-464. http://dx.doi.org/10.1007/s12665-013-2453-5

sipadan.com. (2015). Sipadan Dive Map. In S. D. Map (Ed.).

Stanley, G. D., and van de Schootbrugge, B. (2009). The Evolution of the Coral–Algal Symbiosis. In M. J. H. van Oppen and J. M. Lough (Eds.), *Coral Bleaching: Patterns, Processes, Causes and Consequences* (pp. 7-19). Berlin, Heidelberg: Springer Berlin Heidelberg. http://dx.doi.org/:10.1007/978-3-540-69775-6_2

Statham, P. J. (1985). The determination of dissolved manganese and cadmium in sea water at low nmol 1−1 concentrations by chelation and extraction followed by electrothermal atomic absorption spectrometry. *Analytica Chimica Acta, 169*, 149-159. http://dx.doi.org/http://dx.doi.org/10.1016/S0003-2670(00)86217-0

Strickland, J. D. H., and Parsons, T. R. (1972). *A Practical Handbook of Seawater Analysis* (2nd ed. ed.): Ottawa : Fisheries Research Board of Canada, 1972.

Sunda, W. G. (2012). Feedback Interactions between Trace Metal Nutrients and Phytoplankton in the Ocean. *Frontiers in Microbiology, 3*, 204. http://dx.doi.org/10.3389/fmicb.2012.00204

Sykes, S. (2012). Recreational SCUBA Diving. Retrieved from http://www.slideshare.net/shaunsykes/scuba-diving-presentation-13794656

Teh, L. L., Teh, L. L., and Chung, F. (2008). A private management approach to coral reef conservation in Sabah, Malaysia. *Biodiversity and Conservation, 17*(13), 3061-3077. http://dx.doi.org/10.1007/s10531-007-9266-3

Tew, K. S., Leu, M.-Y., Wang, J.-T., Chang, C.-M., Chen, C.-C., and Meng, P.-J. (2014). A continuous, real-time water quality monitoring system for the coral reef ecosystems of Nanwan Bay, Southern Taiwan. *Marine Pollution Bulletin, 85*(2), 641-647. http://dx.doi.org/http://dx.doi.org/10.1016/j.marpolbul.2013.11.022

Then, S. (2012, 1 July). Forest fires start again in Sarawak. *The Star Online.* Retrieved from http://www.thestar.com.my/news/nation/2012/07/01/forest-fires-start-again-in-sarawak/

Then, S. (2015, 24 March). Forest fires giving Kuala Baram residents sleepless nights. *The Star Online.* Retrieved from http://www.thestar.com.my/metro/community/2015/03/24/smoke-gets-in-their-eyes-forest-fires-giving-kuala-baram-residents-sleepless-nights/

Then, S. (2016, 21 February). Forest fires raging in northern Sarawak. *The Star Online.* Retrieved from http://www.thestar.com.my/news/nation/2016/02/21/forest-fires-raging-in-ulu-baram-north-sarawak/

Thilagavathi, R., Chidambaram, S., Thivya, C., Prasanna, M. V., Keesari, T., and Pethaperumal, S. (2017). Assessment of groundwater chemistry in layered coastal aquifers using multivariate statistical analysis. *Sustainable Water Resources Management, 3*(1), 55-69. http://dx.doi.org/10.1007/s40899-017-0078-7

Thivya, C., Chidambaram, S., Thilagavathi, R., Prasanna, M. V., Singaraja, C., Adithya, V. S., and Nepolian, M. (2015). A multivariate statistical approach to identify the spatio-temporal variation of geochemical process in a hard

rock aquifer. *Environmental Monitoring and Assessment, 187*(9), 1-19. http://dx.doi.org/10.1007/s10661-015-4738-5

Thompson, A., Schroeder, T., Brando, V., and Schaffelke, B. (2014). Coral community responses to declining water quality: Whitsunday Islands, Great Barrier Reef, Australia. *Coral Reefs, 33*(4), 923-938. http://dx.doi.org/10.1007/s00338-014-1201-y

Thompson, T. G., and Wilson, T. L. (1935). The Occurrence and Determination of Manganese in Sea Water. *Journal of the American Chemical Society, 57*(2), 233-236. http://dx.doi.org/10.1021/ja01305a001

Tiedgen, N. (2012). Great Barrier Reef. Retrieved from http://www.tourism.australia.com/story-ideas/national-landscapes-3505.aspx

Toh, A. S. (1999, 06/17/1999). Tips on how to save marine ecosystem on Sipadan Island. *New Straits Times.* p. 11. Retrieved from http://search.proquest.com/docview/266452639?accountid=10382

Toolbox, T. E. (2015). pH Definition. *The Engineering Toolbox* Retrieved from http://www.engineeringtoolbox.com/ph-d_483.html

UNEP. (2007). *National Reports on Coral Reefs in the Coastal Waters of the South China Sea.*:

Uyarra, M., Watkinson, A., and Côté, I. (2009). Managing Dive Tourism for the Sustainable Use of Coral Reefs: Validating Diver Perceptions of Attractive Site Features. *Environmental Management, 43*(1), 1-16. http://dx.doi.org/10.1007/s00267-008-9198-z

Vacation, A. D. (2015). About Sipadan Island. Retrieved from https://asiadivingvacation.com/diving/sipadan-island/about

Valdés, J., Román, D., Rivera, L., Ávila, J., and Cortés, P. (2011). Metal contents in coastal waters of San Jorge Bay, Antofagasta, northern Chile: a base line for establishing seawater quality guidelines. *Environmental Monitoring and Assessment, 183*(1), 231-242. http://dx.doi.org/10.1007/s10661-011-1917-x

Vanar, M. (2016, 6 March). Dive marshals to protect Sipadan reefs. *The Star Online.* Retrieved from http://www.asianews.network/content/dive-marshals-protect-sipadan-reefs-10833

Vasanthavigar, M., Srinivasamoorthy, K., and Prasanna, M. V. (2013). Identification of groundwater contamination zones and its sources by using multivariate statistical approach in Thirumanimuthar sub-basin, Tamil Nadu, India. *Environmental Earth Sciences, 68*(6), 1783-1795. http://dx.doi.org/10.1007/s12665-012-1868-8

Wagner, D. E., Kramer, P., and van Woesik, R. (2010). Species composition, habitat, and water quality influence coral bleaching in southern Florida. *Marine Ecology Progress Series, 408*, 65-78. Retrieved from http://www.int-res.com/abstracts/meps/v408/p65-78/

Waheed, Z., and Hoeksema, B. W. (2013). A tale of two winds: species richness patterns of reef corals around the Semporna peninsula, Malaysia. *Marine Biodiversity, 43*(1), 37-51. http://dx.doi.org/10.1007/s12526-012-0130-7

Wells, M. L., Price, N. M., and Bruland, K. W. (1995). Iron chemistry in seawater and its relationship to phytoplankton: a workshop report. *Marine Chemistry, 48*(2), 157-182. http://dx.doi.org/http://dx.doi.org/10.1016/0304-4203(94)00055-I

Wildfires flare up in Kuala Baram. (2014, 1 July). *The Star Online.* Retrieved from http://www.thestar.com.my/news/community/2014/07/01/wildfires-flare-up-in-kuala-baram/

World-Wildlife-Federation. (2015). Coral Triangle. Retrieved from http://www.worldwildlife.org/places/coral-triangle

Yılmaz, S., and Sadikoglu, M. (2011). Study of heavy metal pollution in seawater of Kepez harbor of Canakkale (Turkey). *Environmental Monitoring and Assessment, 173*(1-4), 899-904. http://dx.doi.org/10.1007/s10661-010-1432-5

Zaidi, S. S. A. (2006). Concise International Chemical Assessment Document (CICAD) 63, Manganese and its Compounds: Environmental Aspects. *Indian Journal of Medical Research, 124*(3), 365-366. Retrieved from https://search.proquest.com/docview/195972794?accountid=10382

Zakai, D., and Chadwick-Furman, N. E. (2002). Impacts of intensive recreational diving on reef corals at Eilat, northern Red Sea. *Biological Conservation, 105*(2), 179-187. http://dx.doi.org/http://dx.doi.org/10.1016/S0006-3207(01)00181-1

Zawada, D. G., Ruzicka, R., and Colella, M. A. (2015). A comparison between boat-based and diver-based methods for quantifying coral bleaching. *Journal of Experimental Marine Biology and Ecology*, *467*(0), 39-44. http://dx.doi.org/http://dx.doi.org/10.1016/j.jembe.2015.02.017

Zhou, W., Yuan, X., Long, A., Huang, H., and Yue, W. (2014). Different hydrodynamic processes regulated on water quality (nutrients, dissolved oxygen, and phytoplankton biomass) in three contrasting waters of Hong Kong. *Environmental Monitoring and Assessment, 186*(3), 1705-1718. http://dx.doi.org/10.1007/s10661-013-3487-6

Every reasonable effort has been made to acknowledge the owners of copyright material. I would be pleased to hear from any copyright owner who has been omitted or incorrectly acknowledged.

APPENDIX

Location: North Siwa **Distance from Jetty: 21km** **Date: 31 May 2016**

Sample	Time	Depth (m)	Temp. (°C)	pH (1-14)	Conductivity (mS/cm)	Colour of Water	Total Dissolved Solids (mg/l)	Salinity (ppt)	Oxidation Potential (mV)	Redux Potential (RmV)
1	9:30am	14.7	28.5	8.29	37.6	Blue	18448	23.9	-51.0	202.1
2				8.22	37.6		18429	23.8	-57.0	196.1
3				8.21	37.6		18401	23.7	-58.0	195.2
4		7.5	28.9	8.27	37.5		18366	23.7	-58.4	194.2
5				8.38	37.4		18325	23.7	-59.3	193.8
6				8.39	37.4		18317	23.7	-59.5	193.6
7		1		8.45	37.5		18362	23.7	-61.5	191.7
8				8.34	37.4		18330	23.7	-61.7	191.4
9			29.1	8.43	37.3		18258	23.6	-61.8	191.3

Colour of water: Blue

Sample	Turbidity (NTU)	Dissolved Oxygen (mg/l)	Surrounding Environment (e.g Rigs, fishing and other activities) and/or any river inputs near by the sampling points / Remarks.	Direction of Current (N,S,E,W)	Approx. Distance of Highest Diversity of Corals from Boat (m) (N,S,E,W)
1	0.17	8.04	Bad weather conditions with swells up to 1m.	North	South, Mooring line is at the edge of the reef
2	0.15	8.00	Uniform current from surface to seabed		
3	0.16	7.95			
4	0.11	8.73			
5	0.14	8.68			
6	0.12	8.64			
7	0.06	7.65			
8	0.08	7.63			
9	0.05	7.61			

Assistant: Stephan Ongetta

Coordinates: 4°16'35.76"N, 113°49'0.96"E

Location: Anemone Garden **Distance from Jetty: 19km** **Date: 31 May 2016**

Sample	Time	Depth (m)	Temp. (°C)	pH (1-14)	Conductivity (mS/cm)	Colour of Water	Total Dissolved Solids (mg/l)	Salinity (ppt)	Oxidation Potential (mV)	Redux Potential (RmV)
1	10:45am	9.5	29.8	8.23	37.5	Blue	18384	23.8	-56.6	197.0
2			29.9	8.27	37.5	Blue	18360	23.7	-57.8	195.6
3			29.9	8.24	37.4	Blue	18340	23.7	-58.3	194.8
4		6	30.0	8.33	37.4	Blue	18340	23.7	-60.7	192.3
5			30.1	8.28	37.4	Blue	18316	23.7	-60.8	192.5
6			30.2	8.33	37.4	Blue	18316	23.7	-60.6	192.6
7		1	30.0	8.33	37.0	Blue	18145	23.4	-59.5	193.4
8			30.1	8.36	37.0	Blue	18123	23.4	-60.5	192.7
9			30.1	8.39	36.9	Blue	18088	23.4	-60.8	192.3

Colour of water: Blue

Sample	Turbidity (NTU)	Dissolved Oxygen (mg/l)	Surrounding Environment (e.g Rigs, fishing and other activities) and/or any river inputs near by the sampling points / Remarks.	Direction of Current (N,S,E,W)	Approx. Distance of Highest Diversity of Corals from Boat (m) (N,S,E,W)
1	0.06	8.15	Weather got better but sea conditions remain choppy	North	Mooring line is in the middle of the reef
2	0.06	8.16			
3	0.05	8.16			
4	0.10	8.44			
5	0.07	8.49			
6	0.08	8.50			
7	0.07	7.58			
8	0.07	7.56			
9	0.09	7.55			

Assistant: Stephan Ongetta

Coordinates: 4°17'22.38"N, 113°49'33.00"E

Location: Eve' Garden **Distance from Jetty: 10km** **Date: 31 May 2016**

Sample	Time	Depth (m)	Temp. (°C)	pH (1-14)	Conductivity (mS/cm)	Colour of Water	Total Dissolved Solids (mg/l)	Salinity (ppt)	Oxidation Potential (mV)	Redux Potential (RmV)
1	11:30am	6	30.0	8.37	37.3	Blue	18287	23.6	-64.3	188.5
2			31.0	8.37	37.3		18299	23.6	-63.9	189.3
3			30.5	8.37	37.4		18302	23.7	-63.6	189.5
4		1	30.3	8.35	36.8		18009	23.2	-62.6	190.4
5			30.4	8.39	36.8		18023	23.3	-62.9	190.3
6			30.4	8.34	36.8		18033	23.3	-63.1	190.0

Colour of water: Blue

Sample	Turbidity (NTU)	Dissolved Oxygen (mg/l)	Surrounding Environment (e.g Rigs, fishing and other activities) and/or any river inputs near by the sampling points / Remarks.	Direction of Current (N,S,E,W)	Approx. Distance of Highest Diversity of Corals from Boat (m) (N,S,E,W)
1	0.26	8.22	Sampling was done after passage of a barge	North	Any direction from the Mooring line.
2	0.26	8.23			
3	0.26	8.23			
4	0.22	7.52			
5	0.21	7.49			
6	0.25	7.48			

Assistant: Stephan Ongetta

Coordinates: 4°20'34.62"N, 113°53'54.12"E

Location: North Siwa **Distance from Jetty: 21km** **Date: 14 September 2016**

Sample	Time	Depth (m)	Temp. (°C)	pH (1-14)	Conductivity (mS/cm)	Salinity (ppt)	Redox Potential (mV)	Relative Redox Potential (RmV)	Turbidity (NTU)
1	9:45am	1	30.6	7.52	47.9	31.4	-43.4	203.5	0.19
2			30.6	7.80	48.0	31.5	-54.3	198.8	0.23
3			30.6	7.97	48.2	31.6	-63.3	189.8	0.17
4		7	29.6	8.05	48.9	32.1	-68.1	185.0	0.13
5			29.6	8.08	48.9	32.1	-69.4	183.7	0.11
6			29.6	8.08	48.9	32.1	-68.4	183.7	0.14
7		16.2	29.8	8.02	49.3	32.4	-65.8	187.3	0.51
8			29.5	8.02	49.3	32.4	-65.8	187.3	0.48
9			29.8	8.03	49.4	32.5	-66.5	186.6	0.53

Colour of Water: Blue/Green

Sample	Total Dissolved Solids (g/l)	Dissolved Oxygen (mg/l)	Surrounding Environment (e.g Rigs, fishing and other activities) and/or any river inputs near by the sampling points / Remarks.	Direction of Current (N,S,E,W)	Approx. Distance of Highest Diversity of Corals from Boat (m) (N,S,E,W)
1	23.6	7.49	Rough sea conditions	North to south	
2	23.5	7.52			
3	23.5	7.58			
4	23.6	8.37			
5	23.6	8.40			
6	23.6	8.45			
7	23.9	7.21			
8	23.9	7.29			
9	23.9	7.29			

Assistant: Stephan Ongetta

Coordinates: 4°16'35.76"N, 113°49'0.96"E

Location: Anemone Garden **Distance from Jetty: 19km** **Date: 14 September 2016**

Sample	Time	Depth (m)	Temp. (°C)	pH (1-14)	Conductivity (mS/cm)	Salinity (ppt)	Redox Potential (mV)	Relative Redox Potential (RmV)	Turbidity (NTU)
1	11:35am	1	30.1	8.01	48.4	31.7	-65.9	187.2	0.15
2			30.1	8.05	48.4	31.8	-68.1	185.0	0.28
3			30.1	8.06	48.4	31.8	-68.4	184.7	0.20
4		5	29.9	7.92	48.9	32.1	-60.3	192.8	0.12
5			29.9	8.05	48.7	32.0	-68.1	185.0	0.13
6		10	29.9	8.06	48.7	32.0	-68.7	184.4	0.13
7			30.1	8.06	49.3	32.4	-68.3	184.8	0.17
8			30.2	8.06	49.3	32.4	-68.4	184.4	0.16
9			30.2	8.06	49.3	32.4	-68.8	184.3	0.13

Colour of Water: Blue/Green Assistant: Stephan Ongetta

Sample	Total Dissolved Solids (g/l)	Dissolved Oxygen (mg/l)	Surrounding Environment (e.g Rigs, fishing and other activities) and/or any river inputs near by the sampling points / Remarks.	Direction of Current (N,S,E,W)	Approx. Distance of Highest Diversity of Corals from Boat (m) (N,S,E,W)
1	23.4	7.51	Persistent rough sea conditions	North to South	
2	23.4	7.55			
3	23.5	7.54			
4	23.6	8.60			
5	23.6	8.61			
6	23.6	8.66			
7	23.9	7.84			
8	23.8	7.87			
9	23.8	7.84			

Assistant: Stephan Ongetta

Coordinates: 4°17'22.38"N, 113°49'33.00"E

Location: Eve' Garden **Distance from Jetty: 10km** **Date: 14 September 2016**

Sample	Time	Depth (m)	Temp. (°C)	pH (1-14)	Conductivity (mS/cm)	Salinity (ppt)	Redox Potential (mV)	Relative Redox Potential (RmV)	Turbidity (NTU)
1	12:48	1	30.7	7.93	48.3	31.6	-61.2	191.9	0.76
2			30.8	7.99	48.2	31.6	-64.5	188.7	1.05
3			30.7	8.01	48.4	31.7	-65.7	187.4	0.99
4		6	30.3	8.02	48.4	31.7	-66.1	187.0	0.44
5			30.3	8.03	48.4	31.7	-67.1	186.0	0.37
6			30.3	8.12	48.4	31.4	-69.9	183.2	0.43

Colour of Water: Top layer green; bottom layer green-ish/blue

Sample	Total Dissolved Solids (g/l)	Dissolved Oxygen (mg/l)	Surrounding Environment (e.g Rigs, fishing and other activities) and/or any river inputs near by the sampling points / Remarks.	Direction of Current (N,S,E,W)	Approx. Distance of Highest Diversity of Corals from Boat (m) (N,S,E,W)
1	23.3	7.44	Strong current and conditions are still the same	North to South	
2	23.4	7.45			
3	23.4	7.45			
4	23.4	7.86			
5	23.4	8.03			
6	23.4	8.09			

Assistant: Stephan Ongetta

Coordinates: 4°20'34.62"N, 113°53'54.12"E

Location: North Siwa **Distance from Jetty: 21km** **Date: 27 October 2016**

Sample	Time	Depth (m)	Temp. (°C)	pH (1-14)	Conductivity (mS/cm)	Salinity (ppt)	Redox Potential (mV)	Relative Redox Potential (RmV)	Turbidity (NTU)
1	9:00am	15.9	30	8.02	48.9	31.6	-61.6	191.5	0.54
2			30	8.03	48.9	31.6	-62.0	191.1	0.49
3			30	8.03	48.9	31.6	-62.3	190.8	0.53
4		8.3	30	8.06	48.6	31.4	-64.0	189.1	0.68
5			30	8.06	48.5	31.3	-64.1	189.0	0.67
6			30	8.06	48.5	31.3	-64.1	189.0	0.62
7		1.0	30	8.15	48.1	31.0	-69.1	184.0	0.89
8			30	8.15	48.1	31.0	-68.9	184.2	0.79
9			30	8.15	48.1	31.0	-68.9	184.2	0.79

Colour of Water: Greenish Brown

Sample	Total Dissolved Solids (mg/l)	Dissolved Oxygen (mg/l)	Surrounding Environment (e.g Rigs, fishing and other activities) and/or any river inputs near by the sampling points / Remarks.	Direction of Current (N,S,E,W)	Approx. Distance of Highest Diversity of Corals from Boat (m) (N,S,E,W)
1	23.6	8.16	Low wind, strong current…not much waves	North to South	
2	23.4	8.18	Poor visibility		
3	23.4	8.21			
4	23.3	8.13			
5	23.2	8.17			
6	23.2	8.17			
7	23.2	7.66			
8	23.0	7.64			
9	23.0	7.64			

Assistant: Claire Nixon and Aniqfizwa bin Akmalnizwa

Coordinates: 4°16'35.76"N, 113°49'0.96"E

Location: Anemone Garden **Distance from Jetty: 19km** **Date: 27 October 2016**

Sample	Time	Depth (m)	Temp. (°C)	pH (1-14)	Conductivity (mS/cm)	Salinity (ppt)	Redox Potential (mV)	Relative Redox Potential (RmV)	Turbidity (NTU)
1	10:30am	1	30	8.12	48.0	30.9	-67.6	185.5	1.45
2			30	8.14	47.9	30.9	-68.4	184.7	1.30
3			30	8.14	48.0	31.0	-68.6	184.7	1.41
4		6.3	30	8.01	48.1	31.0	-60.8	192.3	1.20
5			30	8.03	48.2	31.1	-61.9	191.2	1.04
6			30	8.03	48.2	31.1	-62.3	190.8	1.17
7		12.3	30	7.99	49.0	31.6	-60.0	193.1	0.64
8			30	8.00	48.8	31.6	-60.5	192.6	0.62
9			30	8.01	48.9	31.6	-60.7	192.4	0.60

Colour of Water: Brownish Green

Sample	Total Dissolved Solids (mg/l)	Dissolved Oxygen (mg/l)	Surrounding Environment (e.g Rigs, fishing and other activities) and/or any river inputs near by the sampling points / Remarks.	Direction of Current (N,S,E,W)	Approx. Distance of Highest Diversity of Corals from Boat (m) (N,S,E,W)
1	23.2	7.68		North to South	
2	23.1	7.69			
3	23.0	7.70			
4	23.3	8.14			
5	23.2	8.17			
6	23.1	8.18			
7	23.6	7.80			
8	23.4	7.82			
9	23.4	7.83			

Assistants: Claire Nixon and Aniqfizwa bin Akmalnizwa

Coordinates: 4°17'22.38"N, 113°49'33.00"E

Location: Eve' Garden **Distance from Jetty: 10km** **Date: 27 October 2016**

Sample	Time	Depth (m)	Temp. (°C)	pH (1-14)	Conductivity (mS/cm)	Salinity (ppt)	Redox Potential (mV)	Relative Redox Potential (RmV)	Turbidity (NTU)
1	11:30am	1.0	30	8.1	46.9	30.2	-67.6	185.5	1.50
2			30	8.13	46.9	30.2	-67.9	185.2	1.48
3			30	8.13	46.9	30.2	-67.9	185.2	1.53
4		6.6	30	8.02	48.2	31.1	-61.6	191.5	1.14
5			30	8.03	48.2	31.1	-62.1	191.0	1.26
6			30	8.04	48.2	31.1	-62.5	190.6	1.21

Colour of Water: Brown

Sample	Total Dissolved Solids (mg/l)	Dissolved Oxygen (mg/l)	Surrounding Environment (e.g Rigs, fishing and other activities) and/or any river inputs near by the sampling points / Remarks.	Direction of Current (N,S,E,W)	Approx. Distance of Highest Diversity of Corals from Boat (m) (N,S,E,W)
1	22.6	7.87		North to South	
2	22.4	7.91			
3	22.4	7.92			
4	23.1	7.77			
5	23.1	7.77			
6	23.1	7.83			

Assistant: Claire Nixon and Aniqfizwa bin Akmalnizwa

Coordinates: 4°20'34.62"N, 113°53'54.12"E

Location: Barracuda Point **Distance from Jetty: 14km** **Date: 21 October 2016**

Sample	Time	Depth (m)	Temp. (°C)	pH (1-14)	Conductivity (mS/cm)	Salinity (ppt)	Redox Potential (mV)	Relative Redox Potential (RmV)	Turbidity (NTU)
1	9:30am	1.0	29	8.09	51.0	33.1	-66.6	186.5	0.11
2			29	8.10	50.9	33.1	-66.9	182.2	0.10
3			29	8.10	50.9	33.1	-67.1	186.0	0.09
4		8.7	29	8.15	50.9	33.1	-69.9	183.2	0.28
5			29	8.14	50.9	33.1	-69.4	183.7	0.27
6			29	8.14	50.9	33.1	-69.1	184.0	0.27
7		16.2	29	8.19	51.0	33.2	-72.1	181.0	0.35
8			29	8.16	51.0	33.2	-70.6	182.5	0.28
9			29	8.15	51.0	33.1	-70.1	183.0	0.28

Colour of Water: Turquoise Blue

Sample	Total Dissolved Solids (mg/l)	Dissolved Oxygen (mg/l)	Surrounding Environment (e.g Rigs, fishing and other activities) and/or any river inputs near by the sampling points / Remarks.	Direction of Current (N,S,E,W)	Approx. Distance of Highest Diversity of Corals from Boat (m) (N,S,E,W)
1	23.5	9.81	Sipadan Island to the south of location	East to West	
2	23.8	9.74	Many boats and tourists		
3	24.1	9.33			
4	23.6	8.71			
5	23.9	8.70			
6	24.0	8.69			
7	23.7	8.16			
8	23.9	8.21			
9	24.1	8.21`			

Assistant: Freddy Joliver

Coordinates: 4°7'23.15"N, 118°37'50.76"E

Location: South Point **Distance from Jetty: 16km** **Date: 21 October 2016**

Sample	Time	Depth (m)	Temp. (°C)	pH (1-14)	Conductivity (mS/cm)	Salinity (ppt)	Redox Potential (mV)	Relative Redox Potential (RmV)	Turbidity (NTU)
1	12:30pm	1.0	29	8.06	50.6	32.9	-64.5	188.6	0.27
2			29	8.09	50.7	33.0	-66.6	186.5	0.28
3			29	8.08	50.7	33.0	-65.8	187.3	0.34
4		6.0	29	8.09	50.7	33.0	-66.5	186.6	0.15
5			29	8.09	50.7	33.0	-66.6	186.5	0.19
6			29	8.10	50.7	32.9	-66.9	186.2	0.20

Colour of Water: Turquoise Blue

Sample	Total Dissolved Solids (mg/l)	Dissolved Oxygen (mg/l)	Surrounding Environment (e.g Rigs, fishing and other activities) and/or any river inputs near by the sampling points / Remarks.	Direction of Current (N,S,E,W)	Approx. Distance of Highest Diversity of Corals from Boat (m) (N,S,E,W)
1	23.5	8.25	Sipadan Island to the North of location	East to West	
2	23.8	8.28	Many boats and tourists		
3	23.9	8.27			
4	23.6	7.85			
5	23.9	7.84			
6	24.0	7.83			

Assistant: Freddy Joliver

Coordinates: 4°6'15.10"N, 118°37'47.50"E